DYNA3D:

A Nonlinear, Explicit, Three-Dimensional Finite Element Code for Solid and Structural Mechanics

User Manual

Current Developer: Jerry I. Lin
Methods Development Group
Mechanical Engineering

October, 1999

DYNA3D:

A Nonlinear, Explicit, Three-Dimensional Finite Element Code for Solid and Structural Mechanics

User Manual

Preface

DYNA3D has seen wide application to a variety of problems over the past twenty years. As a public code, DYNA3D has been applied to transient dynamic problems from crash dynamics to human artery simulations by analysts both at LLNL and elsewhere. DYNA3D was originated by Dr. John O. Hallquist of the Methods Development Group at LLNL. During the period 1984–1987, he was joined by Dr. David J. Benson, who is now on the Engineering faculty at the University of California, San Diego. Dr. Hallquist continued as Lead Developer on DYNA3D until 1988, when he left LLNL to pursue a career in private business. During his time at the Laboratory, Dr. Hallquist made innumerable contributions to the field of computational mechanics; many of them by demonstration. It is with great respect for these scientific accomplishments embodied in DYNA3D that the authors continue the expansion of DYNA3D's capabilities to meet new challenges as they arise.

Subsequent to Dr. Hallquist, Dr. Bruce E. Engelmann and Dr. Robert G. Whirley served as Lead Developers of DYNA3D, and are responsible for adding many new features, options, and improvements including the YASE shell element. In 1993, both Dr. Engelmann and Dr. Whirley departed for the private sector. Dr. Jerry I. Lin assumed the Lead Developer role for DYNA3D in 1995, and continues to serve this function along with other members of the Methods Development Group.

DYNA3D USER'S MANUAL

ABSTRACT

This report is the User Manual for the 1999 version of DYNA3D, and also serves as a User Guide. DYNA3D is a nonlinear, explicit, finite element code for analyzing the transient dynamic response of three-dimensional solids and structures. The code is fully vectorized and is available on several computer platforms. DYNA3D includes solid, shell, beam, and truss elements to allow maximum flexibility in modeling physical problems. Many material models are available to represent a wide range of material behavior, including elasticity, plasticity, composites, thermal effects, and rate dependence. In addition, DYNA3D has a sophisticated contact interface capability, including frictional sliding and single surface contact. Rigid materials provide added modeling flexibility. A material model driver with interactive graphics display is incorporated into DYNA3D to permit accurate modeling of complex material response based on experimental data. Along with the DYNA3D Example Problem Manual, this document provides the information necessary to apply DYNA3D to solve a wide range of engineering analysis problems.

1.0 INTRODUCTION

DYNA3D is an explicit finite element code for analyzing the transient dynamic response of three-dimensional solids and structures. The element formulations available include one-dimensional truss and beam elements, two-dimensional quadrilateral and triangular shell elements, two-dimensional delamination and cohesive interface elements, and three-dimensional continuum elements. Many material models are available to represent a wide range of material behavior, including elasticity, plasticity, composites, thermal effects, and rate dependence. In addition, DYNA3D has a sophisticated contact interface capability, including frictional sliding and single surface contact, to handle arbitrary mechanical interactions between independent bodies or between two portions of one body. Also, all element types support rigid materials for modeling rigid body dynamics or for accurately representing the geometry and mass distribution of a complex body at minimum cost. A material model driver with interactive graphics display is integrated into DYNA3D to allow computation of the stress response to any prescribed strain history without inertial effects. This feature allows accurate assessment of the representation of complex material behavior by the numerical constitutive model in DYNA3D.

Over the last twenty years, DYNA3D has been used extensively at LLNL and in industry. It has been applied to a wide spectrum of problems, many involving large inelastic deformations and contact. The code has evolved rapidly to meet changing engineering analysis requirements and to fully exploit current technology in computing hardware. Algorithms have been optimized, and nearly all of the code is now vectorized. Versions of DYNA3D are now available for computing on CRAY/UNICOS platforms, and SUN, SILICON GRAPHICS, Hewlett Packard, DEC, and IBM RS/6000 UNIX-based workstations. Besides these platforms, the code has been ported to many other machines. The use of a “single-source” development system assures that all new developments appear simultaneously in all supported code versions.

Recent developments in DYNA3D span many areas, including both code capability and user convenience. Substantial improvements in simulating rotational machinery problems have been made. These include frame-invariant stress/element force calculations (see IORDER) for brick, beam/truss, and shell elements, expanded velocity initialization by material for rotational motion capabilities, and generalized body force loads by material capabilities. In order to better control contact interactions and minimize computational costs, optional activation/deactivation times have been added to all slidesurfaces. Two new Lagrangain-multiplier based algorithms were added to the current slide surface options. These techniques eliminate interpenetration by solving for the

contact forces exactly, instead of using a penalty-based force. These methods have greatly improved the robustness and utility of slide surfaces in many difficult applications, e.g. when bodies of vastly different material properties collide, multiple and simultaneous contact of shell elements, forging problems involving rigid dies, etc. The automatic contact algorithm has been expanded to give the user more control by allowing multiple surfaces within a problem, by including or excluding contact segments by material number, and by defining a domain limiting box. The local search algorithm is now fully vectorized and it robustness has been markedly increased since its original development. A new airbag model has been implemented to track the response of occupants during crashworthiness simulations. The user now has the ability to represent, on the fly, deformable materials as rigid as well as return these rigid structures back to deformable bodies. Control options can now be specified during input via a free format, keyword based, control input section. By default, the data echoed to the printed output file has been reduced to assist the user.

DYNA3D is part of a set of public codes developed in the Methods Development Group at LLNL. Other analysis codes include the three-dimensional implicit NIKE3D code (Maker, 1995), and the two dimensional codes NIKE2D (Engelmann and Hallquist, 1991) for implicit analysis and DYNA2D (Engelmann, Whirley, and Hallquist, 1992) for explicit analysis. TOPAZ2D (Shapiro and Edwards, 1990) and TOPAZ3D (Shapiro, 1985) are finite element codes for nonlinear heat transfer and field problem analysis. PALM2D (Engelmann, Whirley, and Shapiro, 1990) is a rapidly developing code for fully coupled thermomechanical analysis. Interactive graphics pre-processors and postprocessors include MAZE (Sanford, 1996) and ORION (Hallquist and Levatin, 1985) for the two-dimensional codes and INGRID (Christon, Dovey, and Hallquist, 1992), TAURUS (Spelce and Hallquist, 1991), and GRIZ (Dovey and Spelce, 1996) for the three-dimensional codes. All plotting (except in GRIZ) is accomplished using the DIGLIB public domain graphics library developed by Hal Brand at LLNL.

As a public code, the use of DYNA3D by outside firms has been widespread, and this has played an important role in its development. Many code shortcomings have been discovered and remedied as a direct result of dialog with outside users in industry. In addition, many capabilities have been suggested or inspired by feedback obtained from Collaborators outside LLNL. It is hoped that the DYNA3D user community will continue to expand and provide feedback to the author at LLNL, and that improvements made by others will be made available for possible incorporation into future versions of DYNA3D. This active participation provides important information for future development directions of DYNA3D.

2.0 OVERVIEW OF DYNA3D

DYNA3D is an explicit, nonlinear, finite element code for the transient dynamic response of three-dimensional solids and structures. As an explicit code, DYNA3D is appropriate for problems where high rate dynamics or stress wave propagation effects are important. For static and low rate dynamic problems, the implicit NIKE3D code (Maker, 1995) may be more suitable. DYNA3D may be applied to quasi-static problems by either using the dynamic relaxation option or by simply applying the external loads slowly and integrating the dynamics equations until all significant transients have died out. In contrast to NIKE3D, DYNA3D uses a large number of relatively small time steps, with the solution being explicit (and inexpensive) at each step. Thus, DYNA3D does not form and solve the large matrix equation typical of implicit codes such as NIKE3D, and does not require iteration at each time step. This often leads DYNA3D to be compute-bound, with modest memory requirements, whereas NIKE3D is often memory or I/O bound due to the assembly of a large stiffness matrix at each time step.

The algorithms and architecture are designed for speed and robustness. Nearly all of the code is vectorized for optimal performance on vector computers such as the CRAY. DYNA3D has element formulations that include:

- 2-node truss elements
- 2-node integrated beam elements
- 2-node resultant beam elements
- 3-node triangular shell elements
- 4-node quadrilateral shell elements
- 8-node quadrilateral thick shell elements
- 8-node continuum elements.

These element formulations all handle geometric nonlinearities and do not lock for incompressible materials.

DYNA3D has material models that include:

- elasticity and plasticity (isotropic and anisotropic)
- finite elasticity
- volumetric compaction
- rate dependence
- thermal effects
- damage and failure of ductile and brittle solids.

To model nonlinear pressure-volume behavior, DYNA3D has equations of state that include:

- polynomial functions
- high explosive models
- tabulated functions.

A variety of boundary conditions are available, including:

- prescribed velocities
- non-reflecting (transmitting) boundaries
- sliding boundaries along arbitrary planes
- symmetry planes with failure.

Methods of prescribing loads include:

- nodal forces and moments
- follower forces
- surface pressure loads
- body force loads
- loads due to thermal expansion
- loads arising from momentum deposition
- Brode function airblast loads.

DYNA3D has a general interface contact capability which includes:

- frictional sliding
- single surface contact
- nodes impacting on a surface
- tied interfaces
- one-dimensional slidelines
- rigid walls
- material failure along interfaces
- penalty and Lagrangian projection options for constraint enforcement
- fully automatic contact.

The constraint modeling capabilities include:

- single point constraints
- arbitrary nodal constraints.

Several methods for modeling failure are available, including:

- reduction of material stiffness and/or element stresses to zero after reaching a criterion
- element deletion for solid or shell elements based on a failure criterion
- SAND adaptive contact for penetration or material failure on contact surfaces
- tie-breaking shell slidelines to allow the mesh to split along predefined lines
- tied node sets with failure to allow the mesh to split along arbitrary element boundaries.

DYNA3D can be interfaced to the Crash Victim Simulation codes MADYMO and ATB via:

- a rigid body motion link file for uncoupled analysis
- a PVM-based data exchange for fully coupled analysis.

DYNA3D has the ability to model rigid body dynamics using features such as:

- rigid materials for trusses, beams, shells, and solids
- general rigid body joint definitions between rigid bodies
- inertial property specification by rigid body
- automatic calculation of rigid body inertial properties
- material switching between deformable and rigid idealizations
- merging multiple rigid materials to form one rigid body
- nonlinear springs and dampers to connect rigid or deformable bodies.

The analysis capabilities of DYNA3D include:

- transient dynamic analysis
- static analysis using dynamic relaxation
- dynamic analysis with static initialization from a NIKE3D implicit analysis.

The code may be restarted with a variety of modifications to the analysis, including:

- changes in termination time
- deletion of portions of the model by element or by material
- deletion of sliding interfaces
- modification of boundary conditions on deformable or rigid materials.

There are no inherent limits on the size of a DYNA3D analysis model, and storage allocation is dynamic within the code. Problem size is constrained only by the memory available on the computer. Current generation supercomputers have solved DYNA3D problems with more than 500,000 elements, and computing capabilities continue to expand as new generations of hardware

become available. DYNA3D has been parallelized with shared memory parallelization (SMP) and with message passing parallelization (MPI). Massively parallel processing (MPP) versions of DYNA3D have surpassed these capacities by an order of magnitude on select hardware.

The following sections briefly discuss each of these capabilities and its applicability to engineering analysis problems.

2.1 NOMENCLATURE AND NOTATIONAL CONVENTIONS

This section will briefly describe the notational conventions used in the remainder of this manual. Vectors and tensors are denoted by boldface type ($\mathbf{v}$, $\mathbf{s}$), or in components by subscripted italic characters (v_i, s_{ij}), and matrices are generally indicated by boldface capital letters ($\mathbf{M}$, $\mathbf{K}$). The distinction between vectors and matrices or tensors will be clear from the context in which the symbol is used.

A set of typeface conventions is followed throughout this manual to allow the reader to easily distinguish between **commands**, *parameters,* and `computer generated text`. **Commands** appear in bold type, and should be entered verbatim. *Parameters* appear in italics, and should be given values when included in the input. `Computer generated text`, such as error messages or default file names, is printed in a typewriter-like font.

In the descriptions of input format, “column” numbers refer to character positions in the ASCII input file, “field” refers to a group of character positions which contains one item of data, and “format” specifiers suggest the FORTRAN format edit descriptor used to read that item of data. This form of input description is historical in nature, and evolves from the days when paper punch cards where the predominant medium for data input to the computer. Although those days have long past, this notation and general structure of the input definition has proved convenient and are therefore retained. Further, as modern model generation software progresses, the need for the analyst to directly interact with the DYNA3D input file diminishes. Currently, the most common reason for directly editing this file is to adjust an analysis control parameter, and these quantities are easily and quickly located in the current style of input.

In the input definitions described throughout the remainder of this manual, column numbers are sometimes followed by another set of column numbers enclosed in parenthesis: this second set of column numbers applies to input files using the “large” input option. This feature allows the use of node numbers greater than 99,999, and is the default format for DYNA3D input files generated using the INGRID mesh generator.

2.2 UNITS

There is no unit system embedded in DYNA3D. Problems may be defined in any convenient, *consistent* set of units. The units must be consistent in that mathematical operations directly yield the correct units for the result quantity; no units conversion is done internally in the code. For example, Newton's law states that force equals mass times acceleration, so when mass (in the chosen units) is multiplied by acceleration (derived from the chosen units), the resulting quantity must be force in the chosen units. For example, if the force unit is lb_f, the length unit is in, and the time unit is s, then the units of acceleration are $\frac{in}{s^2}$ and the mass unit is $\frac{lb_f \cdot s^2}{in}$. This approach allows complete freedom in the choice of a units system in which to describe a problem.

2.3 GENERAL FORMULATION

DYNA3D is based on a finite element discretization of the three spatial dimensions and a finite difference discretization of time. The explicit central difference method is used to integrate the equations of motion in time. The central difference method is conditionally stable, and stability is governed by the Courant limit on the time step Δt. For solid elements, this limit is essentially the time required for an elastic stress wave to propagate across the shortest dimension of the smallest element in the mesh. Equivalently, this maximum time step may be related to the period of the highest free vibration mode of the finite element mesh. DYNA3D automatically calculates the maximum time step size at each step of the solution, and adjusts the time step accordingly to minimize the number of time steps used in a solution. This feature minimizes the cost of the analysis while assuring that stability is maintained. Time step considerations suggest the use of structural elements (beams and shells) rather than solid elements for modeling structures that are "thin" in some dimension, since this thin direction has been analytically incorporated into the element formulation. The time step for the structural element model is therefore many times larger than it would be for a corresponding solid element model of the same structure.

DYNA3D uses a lumped mass formulation for efficiency. This produces a diagonal mass matrix $\boldsymbol{M}$, which renders the solution of the momentum equation

$$\boldsymbol{M}\mathbf{a}_{n+1} = \mathbf{f}^{ext} - \mathbf{f}^{int} \tag{1}$$

trivial at each step in that no simultaneous system of equations must be solved. In the above equation, $\mathbf{f}^{ext}$ are the applied external forces, and $\mathbf{f}^{int}$ are the element internal forces. The new accelerations $\mathbf{a}_{n+1}$ are easily found, from which the updated velocity and coordinates are calculated using the central difference integration formulas. Additional details on the general formulation of DYNA3D are given in (Whirley and Engelmann, 1991a).

2.4 MATERIAL MODELS

DYNA3D includes a large number of material models to represent a wide range of physical behavior. Some models may be used with an equation-of-state to represent complex pressure-volume-energy behavior in a material; these are termed hydrodynamic models. The material models presently implemented are:

- elastic
- orthotropic elastic
- kinematic/isotropic plasticity
- thermo-elastic-plastic
- soil and crushable foam
- viscoelastic
- Blatz-Ko hyperelastic rubber
- high explosive burn
- fluid
- isotropic-elastic-plastic hydrodynamic
- Steinberg-Guinan high rate elastic-plastic
- isotropic elastic-plastic
- elastic-plastic with failure
- soil and crushable foam with failure
- Johnson/Cook elastic-plastic
- concrete/geological material
- elastic-plastic with oriented cracks
- power law isotropic elastic-plastic
- strain rate dependent isotropic elastic-plastic
- rigid
- thermal orthotropic elastic
- fiber composite with damage
- thermal orthotropic elastic with variable properties
- rate-dependent tabular isotropic elastic-plastic
- extended two invariant geologic cap
- metallic honeycomb
- compressible Mooney-Rivlin hyperelastic rubber
- resultant plasticity
- closed form update elastic-plastic for shells
- Frazer-Nash hyperelastic rubber

- Ramberg-Osgood elastic-plastic
- general orthotropic elastic-plastic
- normal anisotropic elastic-plastic for shells
- elastic-plastic with forming limit diagram
- brittle damage
- three-invariant viscoplastic cap
- Bammann plasticity
- Sandia damage
- Fahrenthold brittle damage
- fabric
- multi-material laminate
- transversely isotropic visco-hyperelasticity
- low density rigid foam
- DTRA concrete/geologic material
- anisotropic elastic
- material interface guide
- visco statistical crack mechanics model (Visco-SCRAM)
- LANL hyperfoam material
- braided composite model
- uni-directional composite

2.5 EQUATIONS OF STATE

A hydrodynamic material model requires an equation-of-state to define the pressure-volume relationship. The equations of state available in this release are:

- linear polynomial
- JWL high explosive
- Sack high explosive
- Gruneisen
- ratio of polynomials
- linear polynomial with energy deposition,
- ignition and growth of reaction in HE
- tabulated compaction
- tabulated
- pore collapse

2.6 FINITE ELEMENT FORMULATION

The finite element formulations used in DYNA3D have been chosen for their accuracy, speed and robustness in large deformation nonlinear problems. In an explicit analysis code, there are many small time steps, so it is important that the number of operations performed at each time step be minimized. This consideration has largely motivated the use of elements with one-point Gauss quadrature for the element integration. This approach gives rise to spurious zero energy deformation modes, or "hourglass modes," within the element. The element must then be stabilized to eliminate the spurious modes while retaining legitimate deformation modes. This stabilization is effectively accomplished in DYNA3D. A selection of stabilization methods is available to handle almost any situation, and the default algorithms have proven effective for most applications. All element operations are fully vectorized, including the assembly of the element force vector (as described in Ginsberg and Johnson, 1989), for optimal performance on vector computers.

The basic continuum finite element in DYNA3D is the eight-node "brick" solid element. This element optionally uses either one-point integration (default) or the constant stress formulation of (Flanagan and Belytschko, 1981) with exact volume integration. Spurious hourglass modes are stabilized using an "hourglass viscosity" or an "hourglass stiffness." Displacements within the element are interpolated using trilinear interpolation functions, and the constitutive equations are evaluated once based on the state at the center of the element. This element is valid for large displacements and large strains. The element may be degenerated to a wedge or tetrahedral element, but at the expense of accuracy. Thus, these degenerated elements should be avoided whenever possible.

DYNA3D fully supports truss, beam, and shell structural elements. For each of these element types, there are several elements available based on different formulations. There is usually no best element formulation for all problems. Some element formulations perform better on certain problem classes, while in other cases the distinguishing feature may be execution speed/cost. Element formulations may be mixed in a single model. The default shell element formulation may be specified in the master control section of the DYNA3D input. Any beam or shell element formulation may be specified for a specific material on the Material Control Card, and this specification overrides any defaults.

The eight-node thick shell element is an experimental capability, and should be used cautiously. It is integrated using one point in the center for the in-plane contribution, and using an arbitrary number of through-thickness integration points. This multi-point integration through the thickness,

with one constitutive evaluation at each point, permits the element to capture complex stress states associated with bending deformations. Hourglass modes are controlled using techniques similar to those for the solid element.

This release of DYNA3D supports five quadrilateral 4-node shell elements, a quadrilateral 4-node membrane element, two triangular 3-node shell elements, two 2-node beam elements, and a 2-node truss element. The shell elements use three-dimensional plane stress constitutive models where the stress component normal to the shell midsurface is zero. One constitutive evaluation is made for each integration point through the shell thickness. All shell elements use one integration point in the center for the in-plane integration, and a pre-defined or user-defined integration rule for the numerical integration through the thickness.

The five quadrilateral shell element formulations are the Hughes-Liu theory, the Belytschko-Tsay theory, the YASE theory (in reduced and fully integrated form), and the Bathe-Dvorkin theory (fully integrated form). The Hughes-Liu formulation is based on degenerate shell theory, as described in (Hughes and Liu, 1981a), (Hughes and Liu, 1981b) and (Hughes, Liu and Levit, 1981). The DYNA3D implementation of the Hughes-Liu shell element is described in (Hallquist, Benson and Goudreau, 1985) and (Hallquist and Benson, 1986), and uses hourglass control procedures based on those reported in (Belytschko and Tsay, 1984). The Hughes-Liu shell uses normal vectors defined at each node for the element calculations. In addition, the Hughes-Liu shell has a user-defined reference surface, which may be specified as the shell midsurface, or the upper or lower surface. This feature is often useful when modeling stiffened shells or shell-beam intersections. The Hughes-Liu shell is the most expensive of the DYNA3D shell elements. The Belytschko-Tsay element formulation is based on resultant shell theory, and is described in (Belytschko and Tsay, 1981), (Belytschko and Tsay, 1983) and (Belytschko and Tsay, 1984). This is currently the default shell element in DYNA3D. The YASE shell element is based on resultant shell theory and a 3-field variational principle, and is described in (Engelmann and Whirley, 1990) and (Engelmann and Whirley, 1991). Additional details of the formulation are given in (Engelmann, Whirley, and Goudreau, 1989). The Bathe-Dvorkin element formualtion (Bathe and Dvorkin, 19884) is based on resultant shell thoery and an assumed transverse shear strain field. The Belytschko-Tsay, YASE, and Bathe-Dvorkin element formulations use element average normals for all computations. Also, the reference surface must always be the midsurface for these formulations. The Belytschko-Tsay, YASE, and Bathe-Dvorkin elements differ substantially in the treatment of the higher order variations in the stress field. The YASE shell is somewhat more accurate on some problems and is more resistant to hourglassing, while the Belytschko-Tsay element is slightly faster. The fully integrated

Bathe-Dvorkin shell does not require hourglass control, but is computionally more expensive to use. The membrane element is a specialization of the Belytschko-Tsay shell element which has only in-plane stiffness, and is slightly faster than the other shell elements.

The two triangular shell elements implemented in this release of DYNA3D are denoted the C^0 element and the BCIZ element. The C^0 triangular shell is based on the work of Belytschko et. al., and is described in (Belytschko and Marchertas, 1974), and (Belytschko, Stolarski and Carpenter, 1984). The BCIZ triangular shell element is described in (Bazeley, Cheung, Irons, and Zienkiewicz, 1965). Although it is possible to collapse a quadrilateral shell element into a triangle, elements in this configuration lock due to excessive transverse shear, and therefore this procedure is strongly discouraged.

The two beam element formulations now available in DYNA3D are the Hughes-Liu beam and the Belytschko-Schwer beam. The Hughes-Liu beam is an extension of the ideas in the Hughes-Liu shell to produce a degenerated beam element. This element uses nodal fiber vectors for orientation, and has a reference surface which may be defined at the midplane, or on the upper or lower beam surface. This feature is frequently useful when modeling stiffened shells or beam-shell intersections. One point integration is used along the length, and a choice of pre-defined or user-defined integration rules is used for numerical integration over the cross section. When used with a user-defined integration rule, this element can model almost any cross section geometry. The Belytschko-Schwer beam is based on a resultant beam theory, and is described in (Belytschko, Schwer, and Klein, 1977). The Belytschko-Schwer beam formulation is based on hermite cubic shape functions with one integration point along the length. No numerical integration is performed over the cross section; constitutive models for this element are formulated directly in terms of forces and moments. One set of element-average orientation vectors is computed and used for all element calculations. The reference surface for the Belytschko-Schwer beam is always the midsurface. The Hughes-Liu beam element is considerably more expensive than the Belytschko-Schwer beam, but may be more accurate for some problems, especially if the cross section is complex in shape.

The DYNA3D truss element is adapted from the Belytschko-Schwer beam element, and is slightly less expensive. The truss element has only axial stiffness, and may be used for large-displacement problems.

2.7 GENERALIZED RAYLEIGH DAMPING

A global damping capability is implemented in DYNA3D based on concepts from Rayleigh damping in linear analysis. In traditional Rayleigh damping, a global damping matrix $\mathbf{C}$ is constructed as a linear combination of the mass matrix $\mathbf{M}$ and stiffness matrix $\mathbf{K}$ as

$$\mathbf{C} = \alpha\mathbf{M} + \beta\mathbf{K}, \tag{2}$$

where α and β are damping coefficients. This approach can be used to introduce a specified fraction of critical damping at two frequencies, since two parameters are available.

The Rayleigh damping concept is extended to apply to nonlinear analysis with large displacements and strains and nonlinear behavior in (Whirley and Engelmann, 1992). The above damping characteristics are preserved in the nonlinear implementation, but no global damping matrix is actually formed. When used with nonlinear material models, the stiffness proportional damping is found using the elastic part of the material stiffness, i.e., the stiffness proportional damping contribution is computed as though the material was linearly elastic with the elastic properties of the nonlinear material. This approach prevents the amount of damping from varying with the material behavior (such as plastic yielding), and allows accurate computation of the degree of damping introduced into the model.

2.8 LUMPED PARAMETER ELEMENTS

DYNA3D contains lumped parameter elements such as discrete springs and dampers and lumped nodal masses. This feature allows DYNA3D to be used to solve simple spring-mass models, or to couple these simple models with complex finite element models. Lumped parameter elements may be used to connect any combination of deformable and rigid elements, and are often useful in building rigid body models.

2.9 INITIAL AND BOUNDARY CONDITIONS

A transient dynamic problem requires the specification of initial conditions in order to be completely defined. In DYNA3D, initial conditions are specified as initial velocities. All initial velocities may be set to zero by setting a flag in the input, or the initial velocity of every node or a subset of nodes may be explicitly defined.

The time variation of quantities in DYNA3D is specified by "load curves." An arbitrary number of load curves may be defined, and any number of boundary conditions or loads may reference one load curve. Each load curve may have an arbitrary number of points.

DYNA3D contains a number of options for modeling the wide range of boundary conditions encountered in engineering analysis. Nodes may be constrained from translation or rotation in the global coordinate system. Alternatively, a local coordinate system may be defined and nodes constrained from translation or rotation in this local system using Single Point Constraints. Any number of local coordinate systems may be defined in a model. Nodes may be constrained to move only along an arbitrary but specified line or only on an arbitrarily oriented plane using "Sliding Boundary Plane" definitions. "Symmetry Planes with Failure" may be defined to constrain a group of nodes to move only in a specified plane. In addition, a tensile failure stress σ_f may be defined such that if the tensile stress normal to the plane exceeds σ_f in an element, the nodes of that element are released from the symmetry plane. These released nodes are allowed to move in arbitrary directions, but may not pass through the Symmetry Plane. This feature is useful for modeling some oblique penetration problems.

Nodes may be given prescribed velocities as a function of time in any global coordinate direction, or in an arbitrary direction specified by a given vector. In cases where prescribed velocities at $t = 0$ are not equal to defined initial velocities, significant dynamic loads are induced in the model due to the incompatibility of boundary and initial conditions.

Nonreflecting boundaries, also called "transmitting boundaries," may be defined to simulate semi-infinite domains and prevent spurious wave reflections due to the finite extent of the mesh. These boundaries are quite effective, but assume essentially linear material behavior. Thus, it is necessary to discretize the domain sufficiently far from the region of interest to contain all significant nonlinear material behavior in the analysis model.

2.10 INITIAL VELOCITIES FOR ROTATING BODIES

The transient dynamic analysis of rotating bodies arises in many areas, including tire and wheel dynamics, turbomachinery, flywheels, and rotating machine tools. For these problems it is often required to initialize velocities for some part of the model to be consistent with rotation about an arbitrary axis. To address this need, DYNA3D allows initial velocities to be computed for a subset of materials composing a model based on a given angular velocity vector through the origin. This feature is activated by specifying the number of materials to receive velocity initialization on Control Card 9 in section 4.1 on page 62, and then giving the angular velocity and list of rotating materials as described in section 4.46 on page 413. If static initialization (via a NIKE3D stress initialization file or via a static dynamic relaxation solution within DYNA3D) has been performed, then the initial velocities computed with this option are evaluated on the statically deformed geometry.

2.11 LOADS

Several types of applied loads may be defined in DYNA3D. Most load definitions include time variation by reference to a load curve, and multiply the load curve value by a scale factor to evaluate the load to be applied. DYNA3D supports surface loads, body force loads, and thermal loads.

Surface loads may be specified as either nodal forces, follower forces, or surface pressures. Nodal forces may be defined in arbitrary directions, and may include both point forces and point moments defined as a function of time. The direction of concentrated nodal loads is fixed throughout the problem and does not evolve with the deformation. Follower forces may be defined which always act normal to a plane defined by three nodes. The direction of this force evolves with the deformation to remain normal to the specified plane throughout the analysis. Surface pressure loads may be defined, and these always act normal to the surface in the current configuration. Pressures may vary linearly over an element surface, and may be an arbitrary function of time. Alternatively, pressures may be defined to follow a Brode airblast time history shifted by a given shock wave arrival time based on the distance from the Brode origin.

Body force loads can be specified to represent physical phenomena such as gravity, electromagnetic forces, or centrifugal loads due to an angular velocity. Body force loads may be specified as arising from translational ‘‘base acceleration’’ or from an angular velocity of the model about any fixed axis of rotation. In DYNA3D, body force loads may be specified by a translational base acceleration $\boldsymbol{a}$, where $\boldsymbol{a}$ has components defined in the global x, y, and z directions. The body force density $\boldsymbol{b}$ is found from

$$\boldsymbol{b} = -\rho\boldsymbol{a}, \tag{3}$$

where ρ is the material mass density. In addition, body force loads arising from rotation about an arbitrary axis through the global origin may be defined by specifying the angular velocity components about the global x, y, and z axes. Body force density $\boldsymbol{b}$ at a point is then found from the angular velocity vector $\boldsymbol{w}$ and the radius vector $\boldsymbol{r}$ (from the origin to the point) by

$$\boldsymbol{b} = \rho\boldsymbol{w} \times (\boldsymbol{w} \times \boldsymbol{r}). \tag{4}$$

The time variation of angular velocity components ω_i may defined using a load curve, but note that the time derivative of the angular velocity is *not* included in the body force density calculation.

Body force loads can be specified for an entire model, or can be specified by material for a subset of a model. This is particularly useful when computing initial stresses in rotating parts which subsequently interact with nonrotating parts, such as the impact of a stationary workpiece on a spinning machine tool.

Loads due to thermal expansion are applied by specifying temperature changes with material models which include thermal expansion. Nodal temperatures may be read from a TOPAZ3D (Shapiro, 1985) plot database file, or may be individually specified and scaled by a load curve in the DYNA3D input file.

Finally, loads may be defined by directly specifying the momentum transferred into the structure by an external entity. Using the Momentum Deposition option, three components of linear momentum may be added to an individual solid element at a specified time. This capability can be used to represent the physical problem of the impact of many small particles onto a larger body, for example.

2.12 GENERAL INTERFACE CONTACT

DYNA3D contains a robust and efficient capability for modeling the mechanical interaction of two bodies or two parts of a single body. Fourteen different options are offered for defining the behavior of “slide surfaces” in a wide variety of situations. Twelve of these options are actually general slide surface definitions, and the other two are special purpose capabilities. These options include facilities for treating interactions between two surfaces, between discrete nodes and a surface, or between a body and a rigid wall. One option allows material failure along the material surface. All DYNA3D slide surfaces accommodate arbitrarily large relative motions, and slide surfaces may be defined between surfaces of differing element types (e. g., a shell structure may interact with a solid body). Beam element contact on shells or solids is modeled by defining the nodes of the beam as discrete nodes impacting a surface, since the beam element itself is mathematically a line and thus has no area with which to define a surface. Interface pressure distributions on a slidesurface may be written to a special TAURUS database, or interface forces for each node on a slidesurface may be written to the ‘‘FORCES’’ output file, as described in section 2.15 on page 32. The interface forces file also contains the total force across the interface at at given time. There are no limits on the type or total number of slide surfaces defined for a DYNA3D model. In the remainder of this section, first each of the thirteen slide surfaces is briefly discussed, and modeling suggestions are given. The two special purpose capabilities, rigid walls and one-dimensional slidelines, are then presented.

The twelve types of slide surfaces supported in this release of DYNA3D are:

1. sliding only
2. tied
3. sliding with separation and friction
4. single surface
5. discrete nodes impacting surface
6. discrete nodes tied to surface
7. shell edge tied to shell surface
8. node spotwelded to surface
9. tied with failure
10. one-pass algorithm for sliding with separation and friction
11. SAND contact (Slidesurfaces with Adaptive New Definitions)
12. automatic contact - generic
13. automatic contact - material and domain limited
14. automatic contact with SAND

Slidesurface types 1 through 11 are ‘‘defined-surface’’ options, wherein the user specifies the nodes or segments on each side of the contact interface. Slidesurface types 12 and 13 are automatic contact, wherein DYNA3D automatically identifies surfaces which may potentially come into contact and treats them accordingly. This is a new capability which constantly being improved and expanded.

A defined-surface sliding interface is defined by specifying one master surface and either a slave surface or a set of slave nodes, as required by the type of slide surface chosen. Slide surfaces are defined by listing groups of triangular or quadrilateral segments, and each segment is defined by three or four corner nodes. These segments are actually element faces which define the surface. Outward normals are internally computed for segments of solid elements, but for segments of shell elements the outward normal is defined by the “right-hand rule” from the list of defining nodes. *Care should be taken in defining slide surfaces on shell elements to ensure that the correct side of the shell element is chosen*. Each slide surface is designated either a “master surface” or a “slave surface.” The importance of this distinction is discussed below.

Sliding interfaces and contact in DYNA3D are formulated using a “node on surface” concept, as described in (Hallquist, 1977) and (Hallquist, Goudreau, and Benson, 1985). *Slave* nodes are restricted from penetrating *master* surfaces. Conceptually, the two-surface algorithms could thus be thought of as looping over all slave nodes, and for each slave node checking that there is no penetration through any of the master segments defined for this sliding interface. In the symmetric treatments, the designation of the two surfaces as slave or master are interchanged, and the algorithm is applied a second time. Thus, each surface goes through the algorithm once as a master surface and once as a slave surface. This symmetric approach has been found to greatly increase the robustness and reliability of slidesurfaces when both surfaces are deformable.

The contact formulations used in single surface (type 4) and SAND (type 11) account for the thickness of a shell element in contact calculations. All other contact options operate using the midplane definition of shell elements for the surface definition. Situations arise in modeling complex objects when both capabilities are needed, and the slide surface type can be chosen to obtain the desired behavior.

The “sliding only” (type 1) and “tied” (type 2) options are based on a nodal constraint formulation, and are not symmetric, as described in (Hallquist, 1976) and (Hallquist, 1978). *For these types of slide surfaces, it is important that the more coarsely meshed side be defined as the master surface.*

All other slide surface types may use either a penalty formulation or a Lagrangian projection formulation and are completely symmetric; the distinction between master and slave surfaces for these types is for convenience only.

When the penalty formulation is chosen to enforce the contact constraint, a restoring force is placed on a penetrating node to return it to the surface. This force is proportional to the depth of penetration, the bulk modulus of the penetrated material, the dimensions of the penetrated element, and a scale factor specified by the user. The amount of penetration observed is inversely proportional to the chosen scale factor. Using a larger penalty scale factor reduces the observed penetration, but may make the problem more difficult to solve. Using a smaller penalty scale factor makes the problem easier to solve, but may lead to unacceptably large interpenetrations. One global penalty scale factor is defined in the Control Section of the DYNA3D input file, and another penalty scale factor may be defined separately for each surface of a slide surface pair. The default value of the global penalty scale factor is 0.10, and the default for the local penalty scale factors is 1.0. These two factors are combined multiplicatively to arrive at the actual penalty scale factor used for computations.

When the Lagrangian formulation is chosen to enforce the contact constraint, a restoring force is again placed on a penetrating node to return it to the surface, but is computed differently. This option computes the force by determining the predicted location of a node on the interface at the end of the current time step, and computing the contact force required to place the node on the surface at the end of the current time step. This method yields exact enforcement of the contact constraint. Although this construct is a new option in this release of DYNA3D, early use at LLNL has shown considerable promise. This option works particularly well for contact between very thin shells, such as sometimes occurs in sheet forming problems. It addition, it is also advantageous in modeling contact betweem materials of widely varying stiffness. For contact problems involing deformable parts impacting rigid bodies, a specialized, inexpensive option is available.

During the initialization phase of DYNA3D, nodes on a slide surface which are initially interpenetrating are put back on the surface before the dynamic calculation is begun. A message is written to the screen and a summary printout is provided in the “hsp” file when this occurs. Initial interpenetration may result from errors in the definition of the model, or simply from curved parts of different mesh densities placed in close proximity to each other. In the latter case, the maximum distance a node was moved should be a small fraction of the minimum element dimension. An exception to this procedure is that nodes which are part of a NIKE3D static initialization model are not moved during DYNA3D initialization.

The **sliding only** (type 1) slide surface is a two-surface method based on a nodal constraint formulation. The two surfaces are allowed to slide arbitrarily large distances without friction, but are not permitted to separate or interpenetrate. This option performs well when extremely high interface pressures are present.

The **tied** (type 2) slide surface is not really a slide surface at all, but is a feature for joining two parts of a mesh with differing mesh refinement. This is also a nodal constraint formulation, so the more coarsely meshed surface should be chosen as the master surface. Tied interfaces may only be defined between surfaces defined from brick elements.

The **sliding with separation and friction** (type 3) slide surface is the most generally applicable option. This implementation is a penalty formulation, and allows two bodies to be either initially separate or in contact. Large relative motions are permitted, and Coulomb friction is included. Surfaces may separate and come together in a completely arbitrary fashion. Contact between shell surfaces and solid body surfaces is permitted.

The **single surface contact** (type 4) slide surface is a penalty formulation used for modeling two portions of the same body which may come into contact. This situation often arises in buckling problems, where one surface often develops folds and comes into contact with itself. This option may be used with either solid or shell element surfaces. Frictional sliding is permitted between surfaces in contact. When used with shell element surfaces, it is only necessary to define *one* side of the surface in the slide surface definition; internal logic accounts for the possibility that contact may occur on either side. Due to the complexity of this algorithm, it is slightly more expensive than the other slide surface options, and therefore should only be used where necessary. The formulation of single surface contact is described in (Benson and Hallquist, 1990).

The **discrete nodes impacting surface** (type 5) slide surface is a penalty formulation which allows separate definition of the slave nodes and master surface. This option is necessarily not symmetric, since no slave segments are defined. This feature can be used to model the impact of beams or shell edges onto a solid or shell surface, for example. The target surface is specified as the master surface, and the nodes of the beams or the shell edge nodes are defined as the slave nodes. Coulomb friction may be defined between the nodes and the master surface.

The **discrete nodes tied to surface** (type 6) slide surface is analogous to the "discrete nodes impacting surface" option described above except that the slave nodes are required to remain rigidly attached to the master surface at their initial location. This feature is sometimes useful in joining two parts of a difficult mesh.

The **shell edge tied to shell surface** (type 7) slide surface is another specialization of the tied slide surface idea, although the implementation is somewhat different. This option allows the easy definition of intersections between a shell edge and a shell surface when the mesh spacing prevents merging nodes.

The **node spotwelded to surface** (type 8) slide surface is a combination of the type 5 and type 6 slide surfaces. Slave nodes are constrained to remain on the master surface until a prescribed failure criterion is satisfied. Once the spotweld has "failed," the node is released and then the slide surface functions as a type 5 slide surface.

The **tied with failure** (type 9) slide surface is an experimental penalty method formulation. This option functions as a tied slide surface until a prescribed failure criterion is satisfied, thereafter the slide surface functions as a type 3 slide surface. This option may only be used between surfaces defined from solid elements.

The **one-pass algorithm sliding with separation and friction** (type 10) slide surface is an unsymmetric implementation of the algorithm described for type 3 above. This option may effectively be used when one surface is defined as part of a rigid body, as often occurs in metal forming problems. This algorithm is somewhat less expensive than the symmetric type 3 algorithm, but may yield poor results if used between two deformable bodies.

The **SAND** (type 11 and 14) slide surfaces provide a way to model progressive material failure with contact. SAND is an acronym for Slidesurfaces with Adaptive New Definitions. A failure criterion is defined for a volume of material adjacent to a SAND contact surface; these volumes of potentially failing material are called *SAND volumes*. As material within an element on (or, for type 14, within) the contact surface fails, the failed element is removed from the calculation and the slidesurface definition adapts to the new exterior boundary of the unfailed material. SAND contact may include solid elements or shell elements or any combination thereof. A SAND volume may be composed entirely of solid elements or shell elements for simple structures, or may include an external layer of shell elements followed by layers of solid elements and shell elements as needed to model a honeycomb or composite structure.

SAND types 11 and 14 differ slightly. For type 11 surfaces, only the outside surface needs to be included in the initial sliding interface definition. SAND volumes are defined by listing the DYNA3D material numbers (not material types) for all materials which comprise the SAND volume. A SAND contact interface may have a SAND volume on only the master side, on only the slave side, or on both the master and slave sides. For type 14 surfaces, SAND volumes are selected from all the brick and shell elements contained in the contact surface and arbitrary contact is captured.

Removal of SAND volumes from the calculation can be triggered by a variety of mechanisms. Select material types, e.g., 10, 11, 13, 24, and 35 for solid elements and 15, 19, 22, 24 and 41 for shells, permit element removal based upon constitutive criteria. Alternatively, SAND volumes can be removed based solely upon the element timestep size. In penetration problems, the later approach permits elenets with failed material to remain in the calculation and provide resistance (e.g., as rubble) until their deformation becomes excessive.

The **automatic** (type 12, 13, and 14) slide surfaces are an expanded in this version of DYNA3D. These slidesurfaces eliminate the need for the user to define any contact surfaces or segments. DYNA3D internally finds the outer boundary of all or a subset bodies in the model, and defines the appropriate contact segments to handle the most general contact conditions, including both multibody and single surface contact. The formulation of automatic contact is described in (Whirley and Engelmann, 1993) and (Whirley and Engelmann, 1993a).

“Rigid walls,” also known as “stonewalls,” may be defined to represent a rigid planar surface. This surface may be stationary, or may be given a mass and a specified initial velocity. Rigid walls permit modeling unilateral contact without requiring discretization of the target surface, and thus are considerably less expensive than defining a type 3 slide surface.

Finally, “one-dimensional slidelines” allow truss or beam elements to slide along predefined lines of nodes. This capability is sometimes useful to represent the pullout of reinforcing bars from a concrete continuum model, for example. Friction coefficients may be specified to incorporate the effect of the stress state in the surrounding material on the required pullout force.

2.13 CONSTRAINT EQUATIONS

Two types of constraint equations may be explicitly defined in DYNA3D: nodal single point constraints, and nodal constraint equations. Nodal single point constraints restrict the translational or rotational motion of a specified node in a specified direction. These constraints may be specified using an arbitrary number of local coordinate system definitions, and many nodes may reference one local coordinate system. General translational or rotational constraints may be defined using this option. Nodal single point constraints enforce the constraint exactly, as do global constraints. This approach is slightly more expensive than constraints defined with respect to global axes, so global constraints should be used whenever possible. Nodal constraint equations simply specify that two or more nodes share a global degree-of-freedom.

2.14 CROSS SECTION FORCES

DYNA3D allows a cross section to be defined through a structural model, and at selected intervals will output the total resultant force on this cross section. This feature is often used to quickly evaluate a global response quantity, such as the total force transmitted from one part of a model to another.

2.15 TOTAL INTERFACE FORCES AND REACTION FORCES

The total force across a slidesurface as a function of time can be optionally output from DYNA3D into either an ASCII print file and/or a binary plot file which can be read by TAURUS or other postprocessing software. This interface force information is available for all types of slidesurfaces, including tied slidesurfaces. Thus, it is possible to easily obtain the total cross-section force in a solid element model by simply defining a tied interface and examining the interface force on this surface. Details on this capability are described in section 3.6 on page 59. Interface force output has proven quite useful in many types of engineering analysis, and has been significantly enhanced in this version of DYNA3D.

Reaction forces at each prescribed velocity degree-of-freedom may be output at the state plot interval into a file `FORRCT`. This feature is activated by an option in the control section.

2.16 HIGH EXPLOSIVE PROGRAMMED BURN MODELS

DYNA3D contains several options for simulating the initiation and burning of high explosives. Beta burn defines a compression criteria for the ignition of HE. Programmed burn options allow the specification of lighting times or detonation points for problems where these are known. An HE ignition and growth equation-of-state allows the study of impact or temperature initiation of energetic materials, and is useful when the existence and location of detonation points must be determined by the solution of the boundary value problem. These features have proved useful on a wide range of problems from explosive metal forming to enhanced oil recovery. Each of the DYNA3D burn options is described below.

There are two options for determining the lighting time of HE materials, including ‘‘beta burn’’ and programmed burn. The beta burn option does not use the concept of a lighting time, and computes a burn fraction F directly from

$$F = \beta(1 - V) = \frac{1 - V}{1 - V_{CJ}}, \tag{5}$$

where V is relative volume and V_{CJ} is the Chapman-Jouguet relative volume. The programmed burn option determines an element lighting time based on specified detonation point locations. Single or multiple detonation points may be defined, and the lighting time of an element is computed based on the distance from the center of the element to the nearest detonation point. These burn options allow considerable flexibility in defining the detonation geometry for high explosive problems.

DYNA3D contains an equations-of-state for modeling the ignition and growth of detonation waves in high explosive materials. Equation-of-state 7, developed by Tarver and coworkers, models the behavior of single component explosives. This equation-of-state allows an analysis to determine whether an explosive will ignite and burn due to pressures and temperatures present in the solution of the boundary value problem. This model is quite complex, and care is urged in their use.

2.17 RIGID BODY DYNAMICS

DYNA3D has the ability to do limited rigid body dynamics modeling. The rigid body formulation is described in (Benson and Hallquist, 1986). Rigid body nodal lumped masses, springs, and dashpots are available. Rigid materials can be defined for all element types. This rigid body feature provides an inexpensive method for modeling portions of a structure that are much stiffer than the regions of interest. This feature is also convenient in many metal forming problems, where the punch and die are often effectively rigid.

Two separate rigid bodies may not share any nodes in common. In other words, no one node may be used in the definition of two elements each of which use a different material if both materials are defined as rigid. In this case, the two rigid materials must be merged to form one rigid body using the Rigid Body Merge feature. Alternatively, Rigid Body Joints may be defined which couple the two rigid bodies leaving specified degrees of freedom unconstrained.

Inertial properties for rigid materials may be defined in one of two ways. By default, the inertial properties are calculated from the geometry of the elements of the rigid material and the density specified in the material properties definition. Alternatively, the inertial properties and initial velocity for a rigid body may be directly specified, and this overrides data calculated from the material property definition and nodal initial velocity definitions.

Analysis results for rigid bodies may be post-processed in the usual way. Displacements, velocities, and accelerations are stored in the plot database for each node of a rigid body. It is not meaningful to plot stresses for elements defining a rigid body, however.

2.18 ANALYSIS OPTIONS

DYNA3D may be used for transient dynamic analysis, or for quasistatic analysis, or for transient dynamic analysis with a quasistatic initialization from NIKE3D. A transient dynamic analysis, using the central difference method, is the default option. A quasistatic analysis may be performed using the dynamic relaxation option. Although this capability has proven its value in production calculations, caution should be exercised in its use since monotonic convergence is not guaranteed. This solution procedure may introduce errors into the solution *if* history dependent materials are present in the model. Alternatively, a quasistatic analysis may be performed by simply applying the loads very slowly and using the transient dynamic analysis option. If the analysis is run until all significant transient oscillations die out, then the remaining solution is the quasistatic solution. This procedure may confidently be used with history dependent materials if dynamic oscillations are kept to a minimum (i.e., loads are applied sufficiently slowly). Finally, a transient dynamic analysis may be performed using stresses and geometry initialized from a NIKE3D analysis.
At the end of an analysis, DYNA3D can also generate a file to be used as an initialization file in a subsequent NIKE3D run. This feature is particularly useful when post transient phase long duration simulation, such as metal forming spring-back, is of interest. Details of this feature are described in the following section.

2.19 DYNA3D-NIKE3D LINK

DYNA3D-NIKE3D link works two ways:

1) Stress/deformation Initialization file from NIKE3D for DYNA3D analysis; activated by inclucing **m**=*sif* in the execution line.
2) Stress/deformation Initialization file generated by DYNA3D for NIKE3D analysis; activated by using the **nikefile** keyword input.

The NIKE3D static initialization option provides a versatile capability for incorporating initial stress and deformation effects in a transient dynamic analysis. Typical applications requiring this capability include failure analysis of rotating disks and transient dynamic analysis of internally pressurized thin-wall vessels. Rotating disks often build up large stresses before failure occurs due to centrifugal forces, and these initial stress fields can influence the post-failure dynamic interactions of the fragments with surrounding structures. Internally pressurized thin-wall tanks experience considerable pressure-stiffening, and therefore it is important to have the correct quasi-static equilibrium stresses in the wall material before initiating any studies of transient dynamic events, such as impact or fracture.

To perform a DYNA3D analysis using static initialization from a NIKE3D analysis, the first step is to run the NIKE3D analysis and request the output of a stress initialization file. This file is then specified on the DYNA3D input line, as described in section 3.2 on page 51. The user also has the option to start the DYNA3D run with a simulation time of 0 or the NIKE3D endtime. This is decided by selecting the proper value for keyword input **irestt** (see page 73). The DYNA3D model may be larger than the NIKE3D model, but the part of the model in common must be the lowest numbered nodes and elements. The portion of the model to be initialized must have the same node numbers and element connectivities in both the NIKE3D and DYNA3D model. Different shell element formulations may be used in the DYNA3D and NIKE3D model, but through-thickness integration rule must be the same in both models.

The ability to enlarge the DYNA3D model above that used for the NIKE3D analysis is quite useful if only a small part of the dynamic model needs to be initialized, as would be the case with an internally pressurized tank incorporated into a large structure, for example. The stress initialization capability is verified only for material type 1 and 3 for NIKE3D generated initialization file at this time. Expansion into other material types will be completed in the future as necessary. There is no such limitation for a continuation DYNA3D run from a DYNA3D generated initialization file.

To create a stress/deformation file at the end of a DYNA3D analysis, users must use the keyword input **nikefile** (see page 73) to assign a root file name. The stress/deformation file contains the nodal displacements, velocities and accelerations for all nodes and stresses and other state/history variables for all elements. This file can then be used as an initialization file for either a subsequent NIKE3D or DYNA3D run. This procedure is very useful in studying the spring-back phenomenon in metal forming and the residual stresses in structures as NIKE3 proves to be more effective in suppressing the excessive high frequency modes after the dynamic analysis.

2.20 ANALYSIS WITH DYNA3D INITIALIZATION DATA

Similar to the NIKE3D static initialization option, previously generated DYNA3D results may be used to initialize a subsequent, but geometrically identical, portion of a DYNA3D analysis. This option provides a general method for chronologically altering boundary conditions, slide surface definitions, load curves, material property coefficients, applied loads, geometry, and other model attributes. It allows dynamic relaxation to be performed on a model after a complex transient analysis. The option also facilitates the multiple reuse of DYNA3D results obtained from a previous dynamic relaxation analysis. Typical uses of this feature include redefining load curves, extracting residual stresses and deformed geometries via dynamic relaxation, chronologically changing boundary conditions, and redefining slide surface definitions and attributes.

The procedure involves two steps. First, DYNA3D stress initialization files are generated from an existing restart file. To do this, a restart input file must be prepared that specifies that either all or some subset of the materials will be used for stress initialization. Next, using an existing standard or running restart file and the restart input file, DYNA3D is restarted. (For information on restarting a DYNA3D analysis see section 3.4 on page 56.) DYNA3D will terminate automatically after it extracts all the necessary data from the restart file and writes the stress initialization data files. The second step merely requires that the stress initialization family file name be specified on the command line using the "**n**=*sdf*" option on the new run. (See section 3.2 on page 51 for additional information.)

DYNA3D stress initialization files contain data for: 1) regular elements of selected materials (deformable or rigid), 2) all discrete elements, and 3) all type 8 nodal constraints (rigid nodal sets). For each regular or discrete element, the element's current nodal positions, nodal velocities, and associated history variables are included. For rigid materials and type 8 nodal constraints (rigid nodal sets), the center of mass's current position, displacement, velocity, and inertia are written in the data file. Explicit node numbers are not included in the file.

Stress initialization is performed only on elements of materials whose old material number is specified in the restart input file. (See section 5.2 on page 446 and section 5.10 on page 456.) When $NMSI = -1$, a one to one correspondence is established between all old and new material numbers. If fewer new material numbers exist than old material numbers, the extraneous element data will be ignored. By manually specifying new material numbers for old materials numbers, material numbers may be changed from their value in the restart file (i.e. old material number) to their value in the new input file or be left intentionally uninitialized.

Use of DYNA3D initialization data does not significantly alter how DYNA3D initializes and executes an analysis. Near the end of the initialization process, the data contained in the DYNA3D initialization files is read in and *overwrites* the previous data in memory. Regular element data and rigid body properties are processed based upon old material numbers and internal element ordering. However, discrete elements and type 8 nodal constraint data is initialized in sequential order. Thus, the history and nodal variables of the new first discrete element (or type 8 nodal constraint) are initialized with those of the old first discrete element (or type 8 nodal constraint). The new second discrete element is initialized with data from the old second discrete element, etc. The sequence is terminated when either all new discrete elements (or type 8 nodal constraints) are initialized or all old data has been used. After initialization, DYNA3D then proceeds into the solution phase. With the exception of the data read in from the initialization files, all model attributes are established by the new input deck.

Several restrictions exist on the new input file. The initial physical location and connectivity of all initialized regular elements, discrete elements, and nodes involved in type 8 nodal constraints must be the same in the new input deck and old input deck. The element ordering, within a single material number, must be preserved. Consequently, no additional elements may be defined or excluded from an initialized material. (Material numbers maybe altered for convenience provided that the mapping from old to new material numbers is specified when generating the initialization files.) Element formulations, material types, and element attributes cannot be altered. Finally, although the user is free to modify any model parameter, including material properties and densities, the validity of the new results will depend upon the appropriateness of such changes.

2.21 DYNAMIC RELAXATION FOR STATIC INITIALIZATION

DYNA3D contains a limited capability for performing quasistatic analysis using a dynamic relaxation algorithm. This feature is primarily intended to be used to generate a static stress solution as an initial condition for a transient dynamic analysis, but it has been applied with some success to the solution of more general static problems.

The dynamic relaxation (DR) method is based on the observation that the long-time limit of a damped dynamic solution is the quasistatic solution. Damping is introduced through a ‘‘dynamic relaxation factor’’ (default value=0.995) which multiplies the velocities computed at each step of a DR solution. This factor can be adjusted by the user if required; increasing the factor decreases the effective damping while decreasing this factor increases the effective damping.

During then DR static solution process, ‘‘time’’ is really just a parameter to describe the solution process, and does not correspond to physical time.The current implementation uses a DR time step equal to the standard dynamic time step. Thus, if it is desired to slowly apply the static loads to minimize overshoot in the solution, then a short trial dynamic run can be made to determine the time step size. The static loads to be applied during the DR solution can then be applied over some number of time steps (typically 2000-5000 but problem dependent), and this determines the time points to be used on the load curve controlling the static loads.

The current implementation of DR in DYNA3D is susceptable to dynamic overshoot if static loads are applied too quickly. If only history-independent material models (such as elasticity) are used, then the resulting solution will still be correct and this overshoot behavior is of little consequence. If history-dependent material models (such as plasticity) are used, however, this dynamic overshoot can cause yielding which is erroneous, and therefore an incorrect static solution is obtained. Thus, the DR static solution capability can be used with confidence for elastic initialization, but must be carefully used with slowly applied loads to prevent overshoot and inaccuracy in history-dependent static problems.

An ‘‘elastic only’’ option is included in DYNA3D for DR. This feature increases the yield parameters of many material models during DR to avoid overshoot in history-dependent materials. The material parameters are then reset at the start of the transient analysis.

The stresses and displacements generated by DR can be used in to initialize other DYNA3D transient analyses. This capability is extremely useful when preforming parameter studies that influence only the transient portion of an analysis since the DR portion of the analysis need only be performed once. A new input deck describing the transient portion of the analysis is required. The only limitation is that the mesh geometry, material model types, and select material coefficients be identical in the original DR and subsequent transient analysis input decks.

A DR static solution is activated by specifying the ‘‘load curve option’’ for a load curve to control the application of the static loads, as discussed in section 4.21 on page 334. The dynamic relaxation factor, the DR time step, and the DR convergence tolerance can be modified from default values on Control Card 8 as described in section 4.1 on page 62.

2.22 DYNAMIC RELAXATION FOR STRESSES IN ROTATING BODIES

In many applications such as flywheel design, machine tool safety, or turbine engine containment, it is important to solve a transient dynamic problem beginning with a stress state induced by rotational motion. This problem is easily solved in this release of DYNA3D using the dynamic relaxation option for computing the initial stresses. The part of the model which is rotating should be identified, by material, as receiving a body force load due to prescribed angular velocity. These body force loads should reference a load curve which begins at zero and increases to a value commensurate with the rotational velocity, and remains constant at that value out to some large time. This load curve should be marked as active for static initialization only. Initial velocities for these rotating bodies, computed on their post-initialization deformed geometry, may be generated by specifying on Control Card 9 the number of materials to initialize for rotational motion, and then listing these materials as described in section 4.46 on page 413. This approach will allow a smooth transition from the body-force-based calculation of the initial stresses into the transient dynamic phase where the bodies actually rotate in space. During the transient portion of the analysis, the rotating bodies may be allowed to rotate freely, or may have rotational velocities prescribed for them using load curves flagged to be active for ‘‘transient dynamic analysis only.’’ Also, other loads may be added to the rotational body during the transient dynamic phase, such as impact with stationary object. The breakaway of part of the rotating body may be easily simulated by various techniques using restart input files to change nodal boundary condition codes or to delete elements which tie the broken fragments to the remainder of the rotating body. This is a new capability for DYNA3D, and it is expected that users will find many innovative ways to use this feature.

2.23 RESTART

DYNA3D supports two types of restart: standard restart and running restart. Standard restart files are written at an interval specified in the input file, and are written sequentially. Standard restart files are never overwritten, and therefore the analysis may be restarted from any standard restart dump state. Since these files accumulate, the frequency of writing standard restart files is often limited by the amount of available disk space. To alleviate this problem, running restart capability was developed. Running restart files are also written at an interval specified in the input file, but each running restart dump overwrites the previous dump. Thus, a running restart dump may be written as often as desired without requiring excessive disk storage.

DYNA3D allows many changes to the model and analysis at a restart. These changes are specified in an optional “restart input file,” which is specified in addition to the binary “restart dump file” which contains the data from the first part of the run. The restart dump file may be either a standard restart file or a running restart file, and all restart options are supported from either choice. The restart input file need not be supplied if nothing is to be changed. Analysis options which can be changed at restart include termination time, plot data dump interval, and restart dump intervals. In addition, the model itself may be changed during a restart, including deletion of any number of materials, elements, or slide surfaces, and alterations of nodal boundary conditions for rigid or deformable materials.

2.24 MATERIAL MODEL DRIVER

DYNA3D incorporates a Material Model Driver to simplify fitting material models to experimental data. The driver computes the stress response to a prescribed strain path, and allows the results to be displayed in an interactive graphics environment. Any stress, strain, or history variable may be plotted against any other component to allow clear insight into the material model behavior. In the Material Model Driver, the stress response is computed without inertial effects, so the true constitutive response is shown. This capability is available for all DYNA3D material models for both shell elements and solid elements, and the material input format is identical to that used for dynamic analysis. The Material Model Driver is described in detail in Chapter 6 of this manual.

2.25 COUPLING WITH CRASH VICTIM SIMULATION (CVS) CODES

Two types of coupling are available between DYNA3D and crash victim simulation (CVS) codes: data link and full coupling.

In the link option, a DYNA3D rigid material representing the occupant compartment is selected, and its displacement or acceleration time history is written to the file `CVS.LNK`. This file can then be easily inserted into a CVS input file to prescribe the motion of the occupant environment for detailed injury studies. The data link option is activated by specifying the DYNA3D material number which represents the occupant cage on Control Card 4.

The full coupling option allows the CVS representation of the occupant to impact interior surfaces in the passenger compartment, and thus yields a more realistic simulation. In the current implementation of this coupling, during a time step the CVS program gives to DYNA3D the positions and orientations of each ellipsoid. DYNA3D then uses its contact algorithms to evaluate the total force and moment arising from impact between the ellipsoid and the occupant environment, and transmits this information back to the CVS code. To use this full coupling, the DYNA3D model should contain a geometric representation of the ellipsoids in the CVS model, and each ellipsoid should be defined as a separate DYNA3D rigid material.

The CVS coupling has been implemented to two specific CVS codes: MADYMO and ATB. MADYMO is a commercial code developed and distributed by TNO, and is described in (TNO, 1992)**.** ATB is a U.S. government-developed CVS code (Obergefell, Gardner, Kaleps, and Fleck, 1983). The coupling between DYNA3D and these CVS codes uses the public domain PVM message passing library to implement the interface, and therefore should allow new versions of either DYNA3D or the CVS code to be used in the coupling with little or no additional effort..

As DYNA3D's use has grown rapidly in the crashworthiness area, it is expected that this CVS link should be useful to analysts in evaluating safety aspects of a variety of vehicles including automobiles, airplanes, and helicopters.

2.26 STRESS INITIALIZATION FOR NIKE3D

DYNA3D can now generate stress initialization data for NIKE3D from any restart file. This new and experimental feature permits the static or long term dynamic solution to be ascertained using NIKE3D. The stress initiialization data files are generated from a DYNA3D restart input file and either a standard or running restart file.

2.27 ELEMENT DELETION

Elements which are severely distorted often indicate that material has failed and supports little load, but these same elements may have very small time steps and therefore control the cost of the analysis. The element based time-step deletion option allows these highly distorted elements to be deleted from the calculation, and therefore the analysis can proceed at a larger time step, and thus at a reduced cost. Deleted elements differ from failed elements in that deleted element do not carry any load while constitutively failed elements may carry load in selected modes, e.g., as rubble.

All brick, beam, shell, and thick shell elements may now be selectively removed from the calculation based upon several criteria. Many material models contain failure criteria which can be used to trigger element deletion. The user can also input a timestep size based criteria. For each or all materials, an absolute timestep size as well as a fraction of the initial timestep size may be prescribed. When an element's maximum stable timestep size falls below the timestep criteria, the element is deleted from the calculation. Clearly, this option must be judiciously used to obtain accurate results at a minimum cost.

Element deletion and slide surfaces are not fully compatible. While facets of deleted shell elements are automatically removed from all slidesurface types, facets of solid elements are only deleted from SAND slide surface definitions.

2.28 DYNA3D-PENCRV3D link

PENCRV3D is a target resistance predicting program for penetration simulation. It is developed by Mark Adley et. al. (Adley, Berger, Cargile and White, 1999) of the U.S. Army Engineer Waterways Experiment Station. Given the projectile characteristics and the descriptions of the target media and their surrounding environment, PENCRV3D employs a series of empirical formulas and cratering algorithms to calculate the projectile surface pressures caused by the target resistance. The main objective of this target resistance approach is to avoid modeling the target media, which sometimes expand to half-space in 3D analysis, with costly finite elements.

PENCRV3D is integrated into DYNA3D as a pressure load generating module. The link between these two codes was established by following the guidelines desribed in (Danielson and Adley, 2000). To use this feature in a penetration analysis, the projectile usually is modeled by finite elements, and the descriptions of the target structure, along with additional projectile characteristics, are included in a separate auxiliary file. Keyword input **pencfile** must be used to designate the auxiliary PENCRV3D input file, and keyword option **pencvmat** must be used to assign the projectile materials. The data in PENCRV3D input file and their format are described in the UCRL report by Jerry Lin (Lin, 2000).

Other optional keyword input relevant to DYNA3D-PENCRV3D link are **pennose** and **pentail**, which designate the node numbers for the nose tip and the tail centroid of the projectile. The nose tip of the projectile must be at the origin of the global coordinate at the beginning of the simulation. Nodes must be assigned to the nose tip and the centroid of the projectile tail so that the orientation of the projectile can be properly updated in every time integration step. If **pennose** and **pentail** are not defined by the user, DYNA3D will sort through the material list provided by the keyword option entry **pencvmat** for these nodes. The analysis will be terminated and a error message issued if no nodes can be identified as the nose tip and the centroid of the tail.

To activate the DYNA3D-PENCRV3D link, **pencfile** and **pencvmat** must be included in the DYNA3D keyword and keyword option input. In the PRESSURE LOADS section in the DYNA3D input, segments subject to pressure generated by PENCRV3D must have a -3 as the load curve entry. This feature is currently available only to DYNA3D users affiliated with LLNL and selected U.S. federal agencies.

3.0 ANALYSIS WITH DYNA3D

The typical engineering analysis process begins with a physical description of some problem or system to be studied. First, a pre-processor or mesh generator is used to construct the model. This program writes a DYNA3D input file. This input file is a standard ASCII text file, so it may be edited or modified at this stage, if desired. Next, the DYNA3D analysis is run, which generates the ASCII printout file and a number of binary plot and restart files. The analysis may be conducted all in one run, or there may be multiple DYNA3D terminations and restarts in this part of the process. Finally, a post-processor is used to read the binary plot files and create display and hardcopy graphics output of desired quantities. Each of these steps is described in the sections that follow.

3.1 PRE-PROCESSING AND MODEL GENERATION

DYNA3D does not contain any significant model generation capability, and relies totally on external software for this task. The LLNL mesh generator INGRID (Christon, Dovey, and Hallquist, 1992) is widely used at LLNL and provides full support for all DYNA3D analysis options. In addition, many of the widely-used commercial pre/post-processing codes are now supporting DYNA3D**.** The format of the DYNA3D input file is described in Chapter 4 of this manual. Since the DYNA3D input file is in ASCII text format, many users find it convenient to do all model generation on an engineering workstation, and then transfer the DYNA3D input file to a larger computer to run the analysis.

3.2 STARTING A NEW DYNA3D ANALYSIS

The execution line for DYNA3D varies slightly depending on the computing platform. On all systems except VAX/VMS, the execution line is:

dyna3d i=*inf*, **o**=*otf*, **g**=*ptf*, **d**=*dpf*, **f**=*thf*, **t**=*tpf*, **a**=*rrd*, **m**=*sif*, **s**=*iff*, **u**=*isf1*, **v**=*isf2*, **b**=*rlf*

where

inf=input file name
otf=printed output file name
ptf=binary state data plot file name (for post-processing)
dpf=binary standard dump file name (for restarting)
thf=binary time history data plot file name (for post-processing)
tpf=binary TOPAZ3D plot file name (for temperature profiles)
rrd=binary running dump file name (for restarting)
sif=binary NIKE3D initialization file name (for static initialization)
sdf=binary DYNA3D initialization file name
iff=binary interface force plot file name (for post-processing)
isf1=binary interface save segment file name for writing data
isf2=binary interface save segment file name for reading data
rlf=binary plot file name for dynamic relaxation data (for post-processing)

On VAX/VMS systems, the execution line is:

run dyna3d

The user then types the file name specifications when prompted:

i=*inf*, **o**=*otf*, **g**=*ptf*, **d**=*dpf*, **f**=*thf*, **t**=*tpf*, **a**=*rrd*, **m**=*sif*, **n=***sdf***, s**=*iff*, **u**=*isf*1, **v**=*isf2*, **b**=*rlf*

File names must be unique and can have up to sixty-four characters. When starting an analysis, the input file name must be specified. For example,

dyna3d i=*inf*

is a valid execution line. The specification of other file names is optional, except as noted below.

A TOPAZ3D plot file name, **t**=*tpf*, must be specified if nodal temperatures are to be read from a TOPAZ3D plot file. A stress initialization file name, **m**=*sif* or **n**=*sdf*, must be specified if it is desired to initialize the DYNA3D model using the stresses and deformations from a NIKE3D or a previous DYNA3D analysis. DYNA3D creates an interface force plot file for post-processing when an interface force plot file name, **s**=*iff*, is specified on the command line. Similarly, DYNA3D only creates an interface save segment file when an interface save segment file name, **u**=*isf1*, is given on the command line. An interface save segment file name for reading, **v**=*isf2*, must be specified when stored data is to be read from an existing interface save segment file.

Due to the large volume of data generated by a typical DYNA3D analysis, printed results output is of limited use and is not generated by default. Printed results may be obtained for nodes and elements selected in time history blocks by specifying **f**=**hsp** on the DYNA3D execution line. This flag will signal DYNA3D to write the results for the selected nodes and elements into the printed output file instead of into a binary time history data plot file.

The default file names for DYNA3D files are given in Table 1. It is expected that all file names will have a file extension of `.DAT` on VAX/VMS systems, however, this extension should never be specified in defining a file name. No file name extensions are expected on non-VMS systems.

identifier	default file name	purpose
inf	(none)	input file
otf	`d3hsp`	printed output file
ptf	`d3plot`	binary plot state data file
dpf	`d3dump`	binary standard restart dump file
thf	`d3thdt`	binary time history plot data file
tpf	(none)	TOPAZ3D plot file containing temperature data
rrd	`runrst`	binary running restart dump file
sif	(none)	stress initialization file from NIKE3D
sdf	`d3sint`	stress initialization file fromDYNA3D
iff	(none)	interface force plot data file
isf1	(none)	interface segment save file to be created
isf2	(none)	interface segment save file to be used
rlf	`d3drlf`	binary plot data file for dynamic relaxation

Binary file sizes are set depending on the computing platform being used. Like the other codes in the MDG set, DYNA3D uses a familied file system to control the length of individual files. In this system, a root file is augmented by additional “family members” when data to be written exceeds the set file length. New family members are named by appending a two digit number to the root name. For example, following an analysis with several state dumps written to the plot state database, the resulting family of binary files might be

```
d3plot
d3plot01
d3plot02
d3plot03.
```

If, instead of the default, the binary state data plot file name **g**=*pltdat* had been given on the command line, the resulting file family would be

```
pltdat
pltdat01
pltdat02
pltdat03.
```

Note that file families are specified by their root name, and that there is a maximum of 100 files in a family.

3.3 INTERACTIVE ANALYSIS STATUS QUERY AND EDITING

DYNA3D offers several "sense switches" to allow the brief interruption of an analysis to request a status report, request that a plot state or restart file be written at the current time, or to cleanly terminate the run. To use sense switches on CRAY/NLTSS, simply type the desired switch while DYNA3D is executing. On CRAY/UNICOS, VAX/VMS, and SUN/UNIX machines, first interrupt execution by typing <ctrl>c, and then enter the desired sense switch at the prompt. The following four sense switches are available:

Type	Response
edit	DYNA3D pauses to allow user to interactively edit control card parameters.
stop	DYNA3D terminates with out writing a restart file.
sw1.	A restart file is written and DYNA3D terminates.
sw2.	DYNA3D responses with time and cycle numbers.
sw3.	A restart file is written and DYNA3D continues.
sw4.	A plot state is written and DYNA3D continues.
sw5.	Force dynamic relaxation convergence and start transient analysis.
time	DYNA3D responses with CPU & wall timing information.

The **edit** sense switch permits user to pause an active DYNA3D run, interactively edit the control card options, e.g. time interval between complete plot files, and resume the run. After interrupting the run with <ctrl>c and entering the switch **edit**, a "Enter edit command:" promt will be displayed. Commands are entered exactly the same way free format control card data is prescribed. To end the edit session and resume the run, the **endfree** keyword command must be issued. For example, an interactive edit command session to change the plot interval would look like:

```
<ctrl>c
.enter sense switch: edit

Edit phase initiated. Enter "endfree" to terminate edit phase and
continue execution.

Enter edit command: pltc 1.0e-6
```

```
Enter edit command: endfree

Edit phase complete. Execution continued.

time= 2.0786E-02   dt= 6.6944E-06 k.e.= 1.2954E-01
i.e.= 0.0000E+00   te= 1.2954E-01 e.w.= 0.0000E+00
rbvx=-5.5357E-01 rbvy=-5.5357E-01 rbvz= 1.7210E+00

dt of time step    3110 is controlled by   solid element       1

time per element-step=   872 microseconds
```

During an edit session, only run time control card parameters such as print, plot, restart and dump intervals should be modified. Geometry (e.g., number of nodes and elements) and problem defintion parameters (e.g., number of slide surface) should never be altered.

3.4 RESTARTING A DYNA3D ANALYSIS

The execution line for restarting a DYNA3D analysis from either a standard restart dump file or a running restart dump file is

dyna3d i=*irf*, **r=***rtf***, o**=*otf*, **g**=*ptf*, **d**=*dpf*, **f**=*thf*, **t**=*tpf*, **a**=*rrd***, s**=*iff*, **u**=*isf1*, **v**=*isf2*, **b**=*rlf*

where

rtf=binary restart dump file name, including the full family name (e.g., d3dump03)

irf=optional restart input file name

and the other file designations are as given in Section 3.2. The restart file name specified by **r**=*rtf* may be either a standard restart file or a running restart file. In either case, care must be taken to specify the entire name of the file, and not just the root name (e.g., d3dump03, not just d3dump). This is necessary since family members in a standard restart dump sequence represent different points in an analysis, and it is necessary to specify which restart dump is to be used as the starting point for the current restart run. Some very large problems require two standard restart dump file family members to store the required data for one restart dump. This case is easily recognized since DYNA3D writes to the screen the name of the first file in which a specific restart dump is written. In most cases, the first three restart dumps would produce messages to the screen like

```
 restart file d3dump01 written, 186350 words
 restart file d3dump02 written, 186350 words
 restart file d3dump03 written, 186350 words
```

For very large problems, the first three restart dumps would produce messages to the screen like

```
restart file d3dump01 written, 1586232 words
restart file d3dump04 written, 1586232 words
restart file d3dump07 written, 1586232 words
```

When restarting these very large problems, the restart dump file name specified by **r**=*rtf* on the command line should name the first restart file family member for the desired restart dump. For example, to restart the very large problem above from the second restart dump state, a valid execution line might be

dyna3d r=`d3dump04`

Specifying the name of restart files is the *only* time a family file member name should be specified including the two digit suffix.

3.5 POST-PROCESSING AND RESULTS DISPLAY

DYNA3D writes up to three binary plot databases. The state data plot file family contains information for complete states at relatively infrequent intervals; 50 to 100 states of data are typical in a state database. The time history data plot file family contains information for only selected nodes and elements, but at much more frequent intervals; 1000 to 10,000 states of data are typical in a time history database. The interface force plot file family, if requested, contains information about the normal and shear forces on DYNA3D slide surfaces.

There are two LLNL codes which can be used to visualize results from DYNA3D: TAURUS (Spelce and Hallquist, 1991) and GRIZ (Dovey and Spelce, 1993). In addition, there are several commercial pre/post-processors which can read and display the DYNA3D database, and more are coming. The LLNL TAURUS and GRIZ codes are briefly described below.

TAURUS is the older of the two LLNL post-processing codes, and uses a command-line based user interface with X-Windows graphics for portability. TAURUS can read any of the three binary plot databases produced by DYNA3D. TAURUS allows plotting of color contours, fringes, deformed shapes, and time histories in an interactive graphics environment. TAURUS fully supports unstructured meshes with arbitrary combinations of beam, shell, and solid element classes. TAURUS can compute a variety of strain measures, momenta, and other response quantities of interest. An interactive help package describes new commands and provides assistance to new or infrequent users. TAURUS is supported for the same computing platforms as DYNA3D: CRAY, VAX/VMS, SUN, SILICON GRAPHICS, and the IBM RS/6000. TAURUS uses the public domain graphics library DIGLIB, developed by Hal Brand at LLNL. DIGLIB supports a large number of display and hardcopy graphics devices, including X-Windows and Postscript (black and white or color) for hardcopy output.

GRIZ is a ground-up new LLNL code for visualization of finite element results. It is under intensive development at the time of this writing, so the following information is subject to change. GRIZ is currently oriented toward hardware-based graphics systems and uses the GL library, although future versions may remove this requirement. GRIZ provides support for modern 3-D visualization techniques such as isosurface display, cutting planes, and display of vector data, all within a menu-driven graphical user environment. GRIZ also provides support for animating data over time and for storing animation frames to a video disk. Initial GRIZ development is aimed at supporting the DYNA3D state database, with time history database and interface force database support to follow in subsequent releases.

3.6 INTERFACE FORCES AND NODAL REACTION FORCES

The total force across a slidesurface as a function of time can be optionally output from DYNA3D into either an ASCII print file and/or a binary plot file which can be read by TAURUS or other post-processing software. This interface force information is available for all types of slidesurfaces, including tied slidesurfaces. Thus, it is possible to easily obtain the total cross-section force in a solid element model by simply defining a tied interface and examining the interface force on this surface. Details on this capability are described in section 3.6 on page 59. Interface force output has proven quite useful in many types of engineering analysis, and has been significantly enhanced in this version of DYNA3D.

Interface forces can be written to an ASCII printout file called FORCES if flags are set on the Slide-surface Control Card described in section 4.28 on page 351. This FORCES file contains interface force data at the time interval specified for state plot output. At each output time, a block of interface force data is written for each side (slave/master) of each slidesurface for which output has been requested. For each block of slidesurface data, the total force acting on the side of the interface is first written in global components. Next, if requested, three lines of data are given for each node on the interface. The first line is the interface force at that node in global coordinates. The second line is the same interface force in a local coordinate system oriented with a local normal $\boldsymbol{n}$ to the surface and two local basis vectors $\boldsymbol{v}$ and $\boldsymbol{c}$ in the plane of the interface. The third line gives the global coordinates of this interface node. It is hoped that this data format in the FORCES file will be convenient for users who want to import this data into another program for display or plotting.

Interface force data can also be written to a binary plot file by specifying a file name using the **s**=*filename* on the command line, as described in section 3.2 on page 51. This option writes contact segments into the database as though they were shell elements, and they can therefore be viewed as a surface at a fixed time in the analysis. Time history plots of total force on an interface, in global components, can be generated with the TAURUS post-processor, and possibly with other codes as well.

In TAURUS Phase 2, time history plots of interfaces are generated using the

FTIME *c n s1 s2 ... sn*

command, where *c* is the interface component number, *n* is the number of interface sides to plot, and *s1* to *sn* are the interface sides to be plotted. Interface component numbers are 1 for x-force, 2 for y-force, and 3 for z-force, and may be displayed using the **FCOMP** command. Interface sides are numbered by beginning with the slave side of slidesurface one as interface side one, the master

side of slidesurface one as interface side two, and proceeding sequentially through all slidesurfaces in the DYNA3D model. Thus, the slave side of DYNA3D slidesurface k is numbered 2k-1, and the master side has interface side number 2k. Note that only a slave side exists for single surface contact, and thus this numbering scheme must be modified if single-surface slidesurfaces are present. Caution should be exercised in determining interface side numbers as no internal validity checking is done in TAURUS, and erroneous plots will be generated if invalid interface side numbers are requested.

4.0 INPUT FORMAT

The following sections describe the input for DYNA3D. Notational conventions are described in section 2.1 on page 9. Numerous notes and explanations are given to describe the purpose and application of specific features. The DYNA3D input file is entirely ASCII, and is completely portable across all computer platforms.

4.1 CONTROL CARDS

Following is the input description for the ten control cards. A set of notes on control card entries follows at the end of this section.

Card 1

Columns	Quantity	Format
1-72	Heading or problem title	A72
73-74	Code input format EQ.87: input follows format of User Manual, Rev. 3, 1987 EQ.88: input follows format of User Manuals since 1988	A2
76-80	Large format option (default in INGRID, use if node numbers exceed 99999); input “large”	A5

Card 2

Columns	Quantity	Format
1-5	Number of materials, *NMMAT*	I5
6-15	Number of nodes, *NUMNP*	I10
16-25	Number of solid (brick) elements, *NUMELH*	I10
26-35	Number of 2-node beam and truss elements, *NUMELB*	I10
36-45	Number of 4-node shell elements, *NUMELS*	I10
46-55	Number of 8-node thick shell elements, *NUMELT*	I10
56-65	Number of interface segments for linking, *NUMIFS*	I10
66-75	Output interval for interface segment save file (Δt), *OPIFS*	E10.0
76-80	Scale factor for minimum shell element time step, *TSLIMT*	E5.0

Card 3

Columns	Quantity	Format
1-5	Number of node time history blocks (maximum of 2000), *NDTH*	I5
6-10	Number of solid element time history blocks (maximum of 2000), *NSTH*	I5
11-15	Number of beam element time history blocks (maximum of 2000), *NSTB*	I5
16-20	Number of shell element time history blocks (maximum of 2000), *NSTS*	I5
21-25	Number of thick shell element time history blocks (maximum of 2000), *NSTT*	I5
26-30	Number of steps between problem status reports, *IKEDIT* EQ.0: default set to 1000	I5
31-35	Reaction forces print flag, *IFCRCT* I5 EQ.0: no printing EQ.1: reactions at nodes with prescribed velocities are written to the file FORRCT	
36-40	Discrete (lumped parameter) element forces print flag, *IFCDIS* I5 EQ.0: no printing EQ.1: forces in all discrete element are written to the file FORDIS	
41-45	Element deletion (SAND database flag) & automatic contact debug, I5 *ISANDB* EQ.0: failed elements not deleted, no SAND info in plot database EQ.1: failed elements are deleted, SAND info in plot database EQ.2: automatic contact database and debug option EQ.10: same as 0, except the failed shell element information is not printed in the *d3hsp* file. EQ.11: same as 1, except the failed shell element information is not printed in the *d3hsp* file. EQ.12: same as 2, except the failed shell element information is not printed in the *d3hsp* file.	

Card 4

Columns	Quantity	Format
1-5	Unused at this time	
6-10	Number of sliding boundary planes, *NUMRC*	I5
11-15	Number of symmetry planes with failure, *NUMRCF*	I5
16-20	Number of points in density vs. depth curve, *NUMDP*	I5
21-25	Brode function flag, *IBRODE* EQ.0: Brode functions are not used. EQ.1: Brode function parameters are defined in input. EQ.2: HE function parameters are defined in input.	I5
26-30	Number of rigid body merge cards, *NRBC*	I5
31-35	Nodal coordinate format: either E10.0 or E20.0, *NIF*	A5
36-40	Number of cross section definitions for force output, *NUMCSD*	I5
41-50	Time interval between output of cross section forces, *CSDINC*	E10.0
51-55	ATB/MADYMO rigid body code link flag, *MATATB* EQ.0: No link file is written. EQ.N: Link file containing displacements is written for rigid material N. EQ.-N: Link file containing accelerations is written for rigid material N.	I5
56-60	Number of ellipsoids for coupled CVS analysis, *NMADEL*	I5
61-65	Number of air-bag gas flow models, *NUMAIR*	I5
66-70	Number of delamination elements, *DELAM*	I5
71-75	Number of slide surface activation/deactivation cards, *NUMSVT*	I5
76-80	Neglect plastic response during dynamic relaxation, *MATDRE* EQ.0:Material properties are unaltered. EQ.1:Material yield strengths are increased by 10^3 during dynamic relaxation and are reset to the inputted values for the transient analysis.	I5

Card 5

Columns	Quantity	Format
1-5	Number of load curves, *NLCUR*	I5
6-10	Number of concentrated nodal loads, *NUMCL*	I5
11-15	Number of element faces having pressure loads applied, *NUMPC*	I5
16-20	Number of prescribed velocity/acceleration cards, *NUMVC*	I5
21-25	Number of rigid walls, *NUMRW*	I5
26-30	Number of nodal constraint cards, *NUMCC*	I5
31-35	Initial condition flag, *INITV* EQ.0: initialize velocities to zero EQ.1: initial velocities are read from the input file	I5
36-40	Number of sliding interfaces, *NUMSV*	I5
41-45	Base acceleration in x-direction, *NTHPX* EQ.0: no EQ.1: yes	I5
46-50	Base acceleration in y-direction, *NTHPY* EQ.0: no EQ.1: yes	I5
51-55	Base acceleration in z-direction, *NTHPZ* EQ.0: no EQ.1: yes	I5
56-60	Angular velocity about x-axis, *NTHSX* EQ.0: no EQ.1: yes	I5
61-65	Angular velocity about y-axis, *NTHSY* EQ.0: no EQ.1: yes	I5
66-70	Angular velocity about z-axis, *NTHSZ* EQ.0: no EQ.1: yes	I5
71-75	Number of solid elements for momentum deposition, *NELMD*	I5
76-80	Number of detonation points, *NDTPTS*	I5

Card 6

Columns	Quantity	Format
1-10	Termination time, *ENDTIM*	E10.0
11-20	Time interval between writes of time history plot data, *PRTC*	E10.0
21-30	Interval between state plot data and interface force data writes, *PLTC* GT.0.0:Time interval between data writes LT.0.0: The absolute value of the load curve number that specifies the plot time interval as a function of analysis time.	E10.0
31-35	Number of time steps between writes of restart file, *IRDECK*	I5
36-40	Number of time steps between writes of running restart file, *NCBRRF*	I5
41-50	Initial time step size, *DT2OLD* EQ.0.0:DYNA3D determines initial step size	E10.0
51-60	Global scale factor for sliding interface penalty stiffness, *SLSFAC* EQ.0.0: default =.10	E10.0
61-65	Thermal effects option, *ITEMP* EQ.0: no thermal effects EQ.n: temperature-time history is defined by load curve n EQ.-1: nodal temperatures are defined in TOPAZ3D generated plot files EQ.-2: nodal temperatures use Temperature Data Option 2 EQ.-3: real-time DYNA3D-TOPAZ3D coupling, available to LLNL users only at this time. EQ.-4: use Temperature Data Option 2 as initial nodal temperature; subsequent temperature history are defined in TOPAZ3D generated plot files. EQ.-9999: nodal temperatures use Temperature Data Option 1	I5
66-70	Reset default hourglass and bulk viscosities flag *IRQ* (Defaults may be reset via keywords without setting *IRQ* = 1) EQ.1: new defaults are read on Control Card 10	I5
71-80	Time step scale factor, *TSSFAC* Negative scale factor indicates a constant time step for the entire analysis. The absolute value of the scale factor will be used as the constant time step. (Default =.90, if high explosive materials are used, the default is lowered to.67)	E10.0

Card 7

Columns	Quantity	Format
1-5	Number of rigid body joint definitions, *NJT*	I5
6-10	Number of rigid bodies for which extra nodes are defined, *NXTRA*	I5
11-15	Number of shell-solid element interface definitions, *NBLK*	I5
16-20	Number of tie-breaking shell slidelines, *NTBSL*	I5
21-25	Number of tied node sets with failure, *NTNWF*	I5
26-30	Load curve number that limits maximum time step size (optional), *LCTM*	I5
31-35	Flag for lumped parameter springs, dampers, and mass input, *INPSD* EQ.0: no discrete springs, dampers, or masses EQ.1: discrete springs, dampers, or masses are input	I5
36-40	Number of rigid bodies for which optional inertial properties are defined, *NUMRBI*	I5
41-45	Flag for output shell-strain tensors at inner and outer gauss points, *ISTRN* EQ.0: no additional data written EQ.1: data written to plot database	I5
46-50	Number of material groups for deformable-rigid switching, *NMSWCH*	I5
51-55	Number of mass proportional damping sets, *MDAMP*	I5
56-60	Hughes-Liu shell normal update option, *IRNXX* EQ.-2: unique nodal fibers EQ.-1: compute normals each time step EQ.0: default set to -1 EQ.1: compute on restarts EQ.n: compute every n time steps	I5
61-65	Shell thickness change option, *ISTUPD* EQ.0: no change EQ.1: membrane straining causes thickness change	I5
66-70	Default shell element formulation, *IBELYT* EQ.1: Hughes-Liu EQ.2: Belytschko-Tsay (default) EQ.3: BCIZ (triangle) EQ.4: C^0 (triangle) EQ.5: Membrane EQ.6: YASE	I5
71-75	Number of nonreflecting boundary segments, *NNRBS*	I5

Card 8

Columns	Quantity	Format
1-5	Number of nodal single point constraints, *NODSPC*	I5
6-10	Number of coordinate systems for single point constraints, *NSPCOR*	I5
11-20	Reduction factor for initial time step size to determine minimum time step size (*TSMIN*). $\Delta t_{min} = \Delta t_{initial} \times TSMIN$ where $\Delta t_{initial}$ is the initial step size determined by DYNA3D. When Δt_{min} is reached, DYNA3D terminates with a restart dump.	E10.0
21-25	Number of user specified beam integration rules, *NUBIR*	I5
26-30	Maximum number of integration points required in the user specified beam integration rules, *MPUBR*	I5
31-35	Number of user specified shell integration rules, *NUSIR*	I5
36-40	Maximum number of integration points required in the user specified shell integration rules, *MPUSR*	I5
41-45	Number of iterations between convergence checks for dynamic relaxation option (default=250), *NRCYCK*	I5
46-55	Convergence tolerance for dynamic relaxation option (default=0.001), *DRTOL*	E10.0
56-65	Dynamic relaxation factor (default=.995), *DRFCTR*	E10.0
66-75	Scale factor for computed time step during dynamic relaxation, *TSSFDR*; if zero, the *TSSFDR* is set to *TSSFAC* defined on Control Card 6. After converging, the scale factor is reset to *TSSFAC*.	E10.0
76-80	Basis of time step size calculation for 4-node shell elements, *ISDO* EQ.0: characteristic length=area/(longest side) EQ.1: characteristic length=area/(longest diagonal) EQ.2: based on bar wave speed and max (shortest side, area/longest side)	I5

Card 9

Columns	Quantity	Format
1-5	Plane stress plasticity algorithm option for shell elements, *MITER* EQ.1: iterative plasticity with 3 secant iterations (default) EQ.2: full iterative plasticity EQ.3: stress scaling noniterative plasticity	I5
6-10	Printout flag for element time step sizes on the first cycle, *IETSPF* EQ.1: the governing time step size for each element is printed. When a non-zero initial time step size is specified, elements whose time step size are smaller than the prescribed initial size are flagged as well.	I5
11-15	Number of one-dimensional slideline definitions, *N1DSL*	I5
16-20	Dynamic relaxation database flag, *IDRINT* EQ.1: write plot database at every convergence check during dynamic relaxation into the DR database	I5
21-30	Not currently used	
31-35	No. of materials with stiffness proportional Rayleigh damping, *NDAMP*	I5
36-40	No. of material sets to initialize for rotational motion, *NMROT*	I5
41-45	No. of material sets with body force loads, *NMBDF*	I5
46-50	Geometry and integration order for stress updates, *IORDER* EQ.0: default=1 EQ.1: first order accurate and end-step geometry (default) EQ.2: second order accurate and mid-step geometry EQ.3: exponential map (exact) and mid-step geometry	I5
51-60	Ratio of current to initial energy for abort, *STPFAC*	E10.0
61-70	Initial minimum time step for mass augmentation, *TSLMAI*	E10.0
71-80	Sustained minimum time step for mass augmentation, *TSLMAS*	E10.0

Card 10
Optional Default Viscosity Reset Card
(define only if IRQ=1)

Columns	Quantity	Format
1-5	Hourglass stabilization method, IHQ, **For hexahedral elements** EQ.0: default=2 EQ.1: standard DYNA3D (viscous form) EQ.2: Flanagan-Belytschko (viscous form) EQ.3: Flanagan-Belytschko with exact volume integration (viscous form) EQ.4: stiffness form of type 2 (Flanagan-Belytschko) EQ.5: stiffness form of type 3 (Flanagan-Belytschko exact volume) EQ.6: selective-reduced 8-point hexahedral element (B-bar) EQ.7: physical stablization (models 1, 2, 3, 18, & 56 only) EQ.8: total displacement physical stablization (models 2 & 46 only) EQ.9: physical stablization - exact volume (models 1, 2, 3, 18, & 56 only) EQ.10: total displacement physical stablization - exact volume (models 2 & 46 only) EQ.12: fully integrated, 8-pt. hexahedral element **For shell, thick shell and beams** EQ.0: default=2 EQ.1: standard DYNA3D (viscous form) EQ.2: Flanagan-Belytschko (viscous form) EQ.3: Flanagan-Belytschko with exact volume integration (viscous form) EQ.4: stiffness form of type 2 (Flanagan-Belytschko) EQ.5: stiffness form of type 3 (Flanagan-Belytschko exact volume) EQ.6: viscous form type 2 and stiffness form type 3 (shells only)	I5
5-15	Hourglass stabilization coefficient (QH, default=.10) Values of QH that exceed .15 may cause instabilities. The recommended default applies to all options and element types. The stiffness forms can stiffen the response, especially if deformations are large, and therefore should be used with care.	E10.0
16-20	Bulk viscosity type for shock capture, IBQ EQ.0: default=1 EQ.1: standard DYNA3D	I5
21-30	Quadratic bulk viscosity coefficient, $BQS1$, (default=1.5)	E10.0
31-40	Linear bulk viscosity coefficient, $BQS2$, (default =.06)	E10.0

For all 4-node shell elements except YASE, $IHG \leq 3$ gives the viscous form of Belytschko-Tsay hourglass stabilization, and $IHG = 4$ or 5 gives the stiffness form. Currently, only these two stabilization algorithms are available for 4-node Belytschko-Tsay and Hughes-Liu shell elements and membrane elements. The above stabilization algorithms do not apply to the 4-node YASE shell element formulation.

A bulk viscosity method is used to smear shock fronts across a small number of solid elements. This procedure improves numerical behavior and minimizes spurious oscillations which may appear in the vicinity of strong shocks in numerical models.

4.2 KEYWORD-BASED CONTROL FEATURES

Keyword-based control information is inserted immediately following the last fixed-format control card (either control card 9 or card 10). Keyword control features and parameters are free-formatted and space delimited. Upper or lower alphabetic characters are permitted, and multiple keywords and parameters may be specified on a single line. Keyword control information overrides any values previously specified in either the control card section or keyword section. The general syntax for keyword input is:

keyword *parameter1 parameter2 ... parameterN*

Here the bold-type **keyword** is the control keyword and is immediately followed by its N parameters. Multiple keyword definitions may be defined on a single line or a single definition may span multiple lines. However, neither keywords nor individual parameters may span more than one line. In the 97 input format, the keyword-based control section must be terminated by the keyword ***"endfree" when ever any keyword-based control information is specified.*** For example, a keyword input might simply look like:

```
endfree
```

or like:

```
iorder 2 isandb 1 endtim 5.0 nrben 7
tssfac 0.5
endfree
```

This later input would set the integration order to 2, turn on the sand database flag, set the termination time to 5.0, indicate that 7 rigid bodies have extra nodes, and reset the time step scale factor to 0.5. The keyword input provides a convenient way to define control information and utilize new features without excessive editing.

The keyword for any control option defined on cards 2 to 10 is the variable name. It is generally shown in italics near or at the end of the line. These control card keywords contain only one parameter, and it is the value of the particular variable.

Keywords may also be used to define auxiliary files that contain bulky sections of input. Currently, nodal data, element definitions, initial velocities, material definitions, sliding interface definitions, and extra keyword inputs may be defined in separate “auxiliary” files. Data should be defined in the auxiliary file exactly as if it were to be included in the main input file. With the exception of the keyword input, the corresponding definitions should be entirely included in the auxiliary file and completely absent from the main input file. While neither the main or auxiliary files should include blank lines, comment lines may be included as desired.

When an auxiliary keyword file is used, the keyword section of the main input deck need only define the auxiliary file name and be terminated with the **endfree** keyword; however, additional keyword definitions are permitted. The auxiliary keyword file must be terminated with the **endfree** command. Commands after the **endfree** keyword in the auxiliary keyword file will not be read

Keyword/Parameters Quantity

General Control and Option Features

drstep *ndrstp* Maximum time steps allowed in dynamic relaxation phase. Execution ends or switches to transient phase after this step limit is reached regardless of convergence. (default=9999999)

drtime *drtime* Maximum time allowed in dynamic relaxation phase. Execution ends or switches to transient phase after this time limit is reached regardless of convergence. (default=9.9e+20)

endfree End keyword input

irestt *irestt* User's option for start time designation (default=0)

- EQ.0: Simulation start time is set to 0. This is used for most cases.
- EQ.1: Simulation start time is set to the time recorded in the stress/deformation initialization file. The initialization file must be assigned by **m**=*sif* in the execution line. This is used for a continuation run from a previous analysis.
- EQ.2: Same as 1, but also read the initial time step from the stress/deformation initialization file. This is usually necessary when continue an earlier DYNA3D analysis.

pressure_display *1* Activate the external pressure display for segments listed in the Pressure Loads section (section 4.23 on page 339). DYNA3D groups all segments under pressure loads into an additional shell material. While postprocessing with GRIZ, choosing any stress quantity for the last material number will display the pressure loads at a given time.

normck *normck* Check for consistent slide surface normals (default=1)

- EQ.0: Slide surface normals are not checked.
- EQ.1: Consistency check is performed and warning is printed if inconsistent normals are detected
- EQ.2: Consistency check is performed and program terminates if inconsistent normals are detected

smp_dynamic *smp_dynamic*

Assign number of SMP processors used statically or dynamically (default=0) (Active for SMP versions on SMP platforms only.)

- EQ.0: Static - always use *threads* number of processors during run
- EQ.1: Dynamic - use *threads* or less number of processor during run

to instantaneously maximize use of system resources. (Provides better scheduling on busy machines, but uses more wall time since, potentially, fewer processors may be used.)

threads *threads* Number of shared-memory processors to use (default= system limit) (Active for SMP versions on SMP platforms only.)

nzip *nzip* Number of zipper elements (default=0)

Keyword/Parameters	Quantity

Time-Step Size Element Deletion

ptsming *ptsming* Default time-step size factor for element deletion (default=0.0)
- EQ.0: Option inactive
- GT.0: Elements with non-zero *ptsmin*s will be deleted when their time-step size becomes less than *ptsmin* times the initial global time-step size.

tsming *tsming* Default time-step size for element deletion (default=0.0)
- EQ.0: Option inactive
- GT.0: Elements with non-zero *tsmin*s will be deleted when their time-step size becomes less than *tsmin*.

HSP and Auxiliary Output Control

rigid_wall *irigid* Print all rigid-wall normal forces to `FORCES` file. Print interval controlled by *PRTC*.
- EQ.0: No forces print to file (default).
- EQ.1: Forces printed to file.

verbose_hsp Generate verbose input and initialization data in hsp file (`d3hsp`)

DYNA3D-PENCRV3D Link Control and Option

pencfile *file_name* Designate *file_name* as the PENCRV3D input file in a DYNA3D-PENCRV3D analysis. This keyword input is limited to selected users.

pennose *node_num* Designate *node_num* as the nose of the projectile in a DYNA3D-PENCRV3D analysis. This keyword input is limited to selected users.

pentail *node_num* Designate *node_num* as the centroid of the projectile tail in a DYNA3D-PENCRV3D analysis. This keyword input is limited to selected users.

Keyword/Parameters	Quantity

Auxiliary Input Files

Auxiliary input file names are limited to a maximum of 80 characters.

beamfile *file_name* Name of the file that contains beam element definitions

brickfile *file_name* Name of the file that contains hex element definitions

infree *file_name* Name of the file that contains auxiliary keyword definitions. The auxiliary file must be terminated with the **endfree** keyword.

loadcurvefile *file_name*
Name of the file that contains the load curve definitions

matfile *file_name* Name of the file that contains material definitions

nikefile *file_name* Name of the stress/deformation file to be created at the end of either a regular or restart analysis. This file can then be used as a initialization file for another NIKE3D or DYNA3D run. Note that a *m=file_name* option on the execution command for a subsequent job should be used to read this file.

nodefile *file_name* Name of the file that contains nodal definitions

pressurefile *file_name*
Name of the file that contains pressure definitions

shellfile *file_name* Name of the file that contains shell element definitions

slidefile *file_name* Name of the file that contains the sliding interface definitions

tshellfile *file_name* Name of the file that contains thick shell element definitions

velofile *file_name* Name of the file that contains the initial nodal velocity definitions

Problem Definition Notes

(card):(field)	Comments
1 : 2	Although many new features have been added, the input format has remained unchanged in the DYNA3D manuals of 1988, 1989, 1991, and 1993.
1 : 3	When specifying the LARGE format option, “large” must be input in lower case.
2 : 1	Materials are defined as described in section 4.4 on page 92.
2 : 2	Nodal coordinates and attributes are defined as described in section 4.7 on page 306.
2 : 3	Solid (brick) element connectivities and attributes are defined as described in section 4.8 on page 308.
2 : 4	Beam and truss element connectivities and attributes are defined as described in section 4.9 on page 310.
2 : 5	Shell element connectivities and attributes are defined as described in section 4.10 on page 313.
2 : 6	Thick shell element connectivities and attributes are defined as described in section 4.11 on page 315.
2 : 7	Interface save segments are defined as described in section 4.12 on page 317.
2 : 8	Time interval between writes of the interface segment save file.
2 : 9	If nonzero, this option allows the specification of a minimum time step size for thin shell elements using material types 3, 19, or 24. When a shell element controls the time step, element material properties will be modified such that the time step does not fall below this factor times the initial time step size.
3 : 1	Node time history blocks are defined as described in section 4.16 on page 325.
3 : 2-5	Element time history blocks are defined as described in section 4.17 on page 326.
3 : 6	Sense switch “sw2.” data summarizing current problem time, time step, energies, and momenta are written to the hsp file at this interval. This is often useful for monitoring the status of a run in batch mode.

Problem Definition Notes (continued)

(card):(field)	Comments
3 : 7	If set, this flag writes the total reaction forces at all degrees-of-freedom with prescribed velocities into the file `FORRCT` at the state plot interval. Note that reactions at nodes with nodal boundary conditions (specified on the node cards) are *not* included.
3 : 8	If set, this flag writes the internal force in each discrete (lumped parameter) element into the file `FORDIS` at the state plot interval.
3 : 9	This flag controls: 1) what happens when ‘‘failure’’ is detected in a material for which SAND contact is supported, or 2) when an automatic contact debug run is made. SAND - If this flag is input as ‘‘1’’ and then the element is deleted from the calculation and marked as deleted in the plot database once failure has occurred regardless of whether or not the element is actually in a SAND volume. If this flag is input as ‘‘0’’ then the element remains in the calculation and is marked active in the plot database, and the subsequent post-failure mechanical behavior is as described for that particular material. AUTOMATIC CONTACT - If this flag is input as “2” and an automatic contact slidesurface is defined, then an automatic contact debug run is executed. The run terminates automatically after two steps and a state plot database is written after each step. The first state in the plot database contains only elements that are involved “in contact” during initialization. An element is included in the plot database if and only if one of its facets is a master segment for which contact is detected during initialization. The second state in the plot database contains all the elements and nodes defined in the problem.
4 : 2	Sliding boundary planes are used to constrain a node to move on an arbitrarily oriented line or plane. These are defined as described in section 4.14 on page 321.
4 : 3	Symmetry planes with failure are used to constrain a node to move on a plane until a critical tensile stress is reached, after which the constraint is released. This feature is frequently used to model oblique penetration. Symmetry planes with failure are defined as described in section 4.15 on page 322.
4 : 4	Density vs. depth curves are used to permit initialization of a hydrostatic stress state due to overburden and gravity. These curves are defined as described in section 4.18 on page 328.

Problem Definition Notes (continued)

(card):(field)	Comments
4 : 5	This option is used to define a pressure time history using the Brode function definition. Define the Brode parameters as described in section 4.19 on page 330, and the surfaces to receive the pressure loading as described in section 4.23 on page 339.
4 : 6	Two distinct materials which each use the rigid material model may not share nodes in common. These two materials may be merged into one rigid body using the rigid body merge feature described in section 4.31 on page 384.
4 : 7	Defines the format in which nodal coordinates are read from the input file. Use of the E20.0 format is recommended when high precision is required in the geometry definition.4 : 8To obtain cross section forces for structural elements, define as described in section 4.20 on page 331.
4 : 10	When a nonzero rigid body material number is specified, the time, followed by the rigid body center-of-mass translational and rotational displacements or accelerations are written to the file named ‘‘`CVS.LNK`’’ in the current directory.
4 : 11	A kinetic interface coupling between DYNA3D and the crash victim simulation codes MADYMO or ATB may be defined. Rigid representations of the CVS ellipsoids should be defined in the DYNA3D model as described in section 4.46 on page 413.
5 : 1	Define load curves as described in section 4.21 on page 334.
5 : 2	Define concentrated nodal loads and follower forces as described in section 4.22 on page 337.
5 : 3	Define pressure loads on element faces as described in section 4.23 on page 339.
5 : 4	Define prescribed velocity (or acceleration) boundary conditions as described in section 4.24 on page 341.
5 : 5	Rigid walls are used to define unilateral contact, such as the impact of a body into a large, rigid object. Define rigid walls as described in section 4.25 on page 344.
5 : 6	Nodal constraints are used to constrain two or more nodes to move together (i.e., share a common degree of freedom). Define nodal constraint sets as described in section 4.26 on page 348.

Problem Definition Notes (continued)

(card):(field)	Comments
5 : 7	Specify nonzero initial velocities as described in section 4.27 on page 350.
5 : 8	Sliding interfaces allow general contact between bodies or parts of bodies. Define sliding interfaces as described in section 4.28 on page 351.
5 : 9-11	Prescribed base acceleration may be used to apply load to an entire structure. Define the three translational acceleration components as described in section 4.35 on page 390. Base acceleration may alternatively be applied to only a subset of the model, as described in section 4.46 on page 413.
5 : 12-14	Prescribed angular velocities about any axis through the origin may be used to apply loads to an entire structure. Define the three angular velocity components as described in section 4.36 on page 391. Prescribed angular velocity may alternatively be specified for only a subset of the model, as described in section 4.46 on page 413.
5 : 15	Momentum may be deposited directly into solid elements. Define momentum deposition as described in section 4.37 on page 393.
5 : 16	Detonation points may be specified for the “programmed HE burn” options described in section 2.16 on page 33. Specify detonation points as discussed in section 4.38 on page 394.
6 : 1	Termination time is the simulation time at which the run is to terminate.
6 : 2	The time history database allows plotting information to be stored frequently for a selected group of nodes and elements, thus allowing resolution of high frequency response components. Alternatively, nodes and elements selected for the time history database may be printed into the hsp file by specifying **f=hsp** on the DYNA3D execution line, as described in section 3.2 on page 51. Nodes and elements are selected for inclusion in the time history database as described in section 4.16 on page 325.
6 : 3	The state plot database contains data for all nodes and elements of a model. The interface force plot database is optional (specified as described in section 3.6 on page 59), and contains interface forces, pressures and shear tractions for all sliding interfaces of a model. The time interval between writes can be constant for the entire analysis by using $PLTC > 0$ or variable by using $PLTC < 0$. In the latter case, the absolute value of $PLTC$ is the load curve number that defines the time interval between writes as a function of analysis time.

Problem Definition Notes (continued)

(card):(field)	Comments
6 : 4	Restart files are written consecutively and are not overwritten, thus allowing restart from any point in an analysis at which a restart file was written. The use of restart is described in section 3.4 on page 56.
6 : 5	Running restart files are continuously overwritten to conserve disk space and allow frequent updates. The use of running restart is described in section 3.4 on page 56.
6 : 7	This factor is used in computing penalty stiffnesses for sliding interface calculations, and is global. Local penalty scale factors may be specified on the sliding interface control card described in section 4.28 on page 351. In general, increasing this factor decreases interpenetration, but may adversely affect stability if the time step scale factor is not also reduced. NIKE3D uses a softer default penalty factor than DYNA3D, so in order to achieve force equilibrium when slidesurfaces are involved in a model in which initial stresses are computed in NIKE3D, the penalty scale factor should be set to 0.046, which is about a factor of two softer than the DYNA3D default of 0.10.
6 : 8	Temperatures must be defined if temperature-dependent material properties are used. Several options are available for specifying temperatures for DYNA3D. Care should be taken in the definition of the reference, or stress-free temperature.
6 : 9	This flag allows the global default values of the hourglass viscosity and shock viscosities to be reset. These values may also be altered for a specific material in the Material Cards, as described in section 4.4 on page 92.
6 : 10	This factor is multiplied by the maximum stable time step to determine the time step size actually used by DYNA3D. This is useful for the (rare) situations in which the time step size is chosen based on other than stability considerations.
7 : 1	Rigid body joints allow the connection of multiple rigid bodies with specified degrees-of-freedom remaining free at the connection. Define rigid body joints as described in section 4.34 on page 388.
7 : 2	Extra nodes can be defined and placed anywhere on a rigid body. This is often useful for defining rigid body joints. Define extra nodes for rigid bodies as described in section 4.32 on page 385.

Problem Definition Notes (continued)

(card):(field)	Comments
7 : 3	One technique for transitioning between shell elements and solid elements in a mesh is the shell-solid interface. This is an experimental capability which enforces appropriate constraints on solid element nodes to provide moment resistance at the interface with a 4-node shell element. Define shell-solid interfaces as described in section 4.39 on page 395.
7 : 4	Tie-breaking shell slidelines allow shell edges to separate once a critical effective plastic strain is exceeded. Define tie-breaking shell slidelines as described in section 4.29 on page 380. Note that tie-breaking shell slidelines may not cross.
7 : 5	Tied node sets allow arbitrary failure and separation of nodes for 4-node shell elements once a critical plastic strain is exceeded. Tied node sets are similar to tie-breaking shell slidelines except that they are defined purely on a nodal level, and there is no restriction on the topology. Define tied node sets with failure as described in section 4.30 on page 382.
7 : 6	If desired, define a load curve giving the maximum time step size as a function of time. DYNA3D will use the smaller of this value or the internally computed time step size. This feature is useful when the time step size must be limited to provide adequate time resolution of an externally applied load.
7 : 7	Set this flag to 1 if discrete springs, dampers, and masses are specified as described in section 4.40 on page 397.
7 : 8	This option allows rigid body inertial properties to be specified directly rather than calculated from the given geometry and mass density. Define rigid body inertial properties as described in section 4.41 on page 405.
7 : 9	The through-thickness location of shell result quantities in TAURUS is selected using the **SHELL INNER**, **SHELL MIDDLE**, and **SHELL OUTER** commands.
7 : 10	The Hughes-Liu shell element formulation uses normal vectors defined at each node. Several algorithms are provided for the definition and evolution of these nodal normal vectors. The ‘‘unique nodal fibers’’ algorithm (nodal normal update option -2) is most nearly the procedure described in the original papers, but is somewhat more expensive than the default option.

Problem Definition Notes (continued)

(card):(field)	Comments
7 : 11	Generalized Rayleigh damping may be used to introduce global dissipation into a model. The mass proportional damping coefficient is global, but may be changed with time. The stiffness proportional coefficients may be defined on a material basis. All damping computations use only the elastic part of the material constitutive response. Generalized Rayleigh damping is described in section 4.46 on page 413 and section 4.47 on page 414.
7 : 12	This option sets the default shell element formulation to be used for 4-node shell elements. The shell element formulation may also be specified by material on the material control card as described in section 4.4 on page 92.
7 : 13	Nonreflecting boundaries prevent artificial stress wave reflections arising from a finite model of an infinite domain. Define nonreflecting boundary segments as described in section 4.42 on page 407.
8 : 1,2	Nodal single point constraints are used to specify a nodal boundary condition in a local coordinate system. Define nodal single point constraints and single point constraint local coordinate systems as described in section 4.13 on page 319.
8 : 3	This options terminates DYNA3D when a minimum time step size is reached, and prevents the code from consuming large amounts of computer time if the time step falls to a very small value.
8 : 4,5	In addition to predefined Gauss and Lobotto integration rules, arbitrary integration rules may be specified for integration over the cross section in the Hughes-Liu beam element. These are mainly useful in describing complex cross section shapes. Define user-specified beam integration rules as described in section 4.5 on page 303.
8 : 6,7	In addition to predefined Gauss and Lobotto integration rules, arbitrary integration rules may be specified for integration through the thickness of shell elements. These are mainly useful for describing laminated composite shells where material properties (such as fiber orientation) vary by lamina. Define user-specified shell integration rules as described in section 4.6 on page 304.
8 : 8	Dynamic relaxation may be used for the static solution of some problems. This feature is activated by the flag on the load curve definition card as described in section 4.21 on page 334. This an experimental capability and caution should be exercised in its use.
8 : 10	The dynamic relaxation factor is the factor by which velocities are reduced at each time step in a dynamic relaxation static analysis.

Problem Definition Notes (continued)

(card):(field)	Comments
8 : 12	This option permits alternative algorithms to be used for approximating the maximum stable time step for shell elements.
9 : 1	Several algorithms are available for performing the plane stress constitutive integration for elastoplastic shell analysis. These options only apply to the elastoplastic shell material models.
9 : 2	This option is useful for determining which elements in a model control the time step and thus the cost of the solution.
9 : 3	One-dimensional slidelines allow beam elements to slide along a predefined row of nodes. Define one-dimensional slidelines as described in section 4.45 on page 410.
9 : 4	This flag controls the output of successive unconverged states into the dynamic relaxation plot file during a dynamic relaxation solution. The name of this binary plot file may be chosen by the user, as described in section 3.2 on page 51.
9 : 6	Generalized Rayleigh damping may be used to introduce global dissipation into a model. The mass proportional damping coefficient is global, but may be changed with time. The stiffness proportional coefficients may be defined on a material basis. All damping computations use only the elastic part of the material constitutive response. Generalized Rayleigh damping is described in section 4.46 on page 413 and section 4.47 on page 414.
9 : 7	Materials are initialized for rotational motion by computing initial velocities from $\mathbf{v} = \boldsymbol{w} \times \mathbf{r}$ for all nodes of all elements using the listed materials. If static initialization is used (via either input from NIKE3D or dynamic relaxation in DYNA3D), $\mathbf{r}$ is evaluated using the post-initialization geometry. Define materials to be initialized for rotational motion as described in section 4.46 on page 413.
9 : 8	Body forces arising from base acceleration (gravity) or from rotational motion may be specified for a selected set of materials using this option. This capability is especially useful for static initialization of stresses in rotating bodies prior to a transient analysis. Define materials to receive body force loads as described in section 4.46 on page 413.

Problem Definition Notes (continued)

(card):(field)	Comments
9 : 9	For computational efficiency, all DYNA3D hex and shell elements are based upon strain rates that are calculated from the geometry at the end of the time step. Additionally, hypo-elastic constitutive variables for hex elements are integrated between configurations using a first order approximation. For rotational motions involving many revolutions, these default approximations can result in large errors even if the amount of rotation during one time step is small, e.g. less than one hundredth of a degree. Although more computationally expensive, second order accurate or exponential map (exact) integration, along with mid-step geometry, should be used for all rotational motion problems that involve one or more revolutions. *IORDER* is not supported for beam, thick shells, and Hugh-Liu shell elements.
9 : 10	Energy abort terminates the analysis when the ratio of current energy to initial energy exceeds the inputted value. This feature is activated by specifying a non-zero value and is useful in terminating analyses that are no longer physical.
9 : 11,12	Mass augmentation is used to maintain a user prescribed minimum time step size and is activated by specifying non-zero values. It increases the density of individual elements to achieve the desired time step, and, thus, ***adds mass to the problem***. The initial minimum time step size is used only during the first cycle, and is a convenient why to normalize a mesh's time step size. During the analysis, element time step sizes are check every ten cycles and mass augmentation is preformed as needed to keep the time step size at (or above) the sustained minimum time step size. A summary of the total mass added to each material is printed in `d3hsp` at each status report and at the end of the analysis.
10 : 1,2	Several algorithms are available for the stabilization of hourglass modes in the solid and shell elements. The standard DYNA3D mode is not longer the default hourglass control. Although cheaper, the standard DYNA3D mode damps out rigid body rotations and should be used with caution. These algorithms do not apply for the YASE shell element formulation.
10 : 3-5	Bulk viscosity methods are used for added stability and resolution when shock waves are present.

4.3 KEYWORD-BASED OPTIONS

Following is the input description for the keyword based OPTIONS section. This new section immediately follows the control card input (either control card 9, card 10, or keyword input) and proceeds the material definitions. The keyword and associated parameters are prescribed follow the same free-formatted convention used to define the analysis control cards (see section 4.2 on page 73). *This section must be initiated with the* **options** *keyword and terminated with the* **endfree** *keyword.*

Keyword/Parameters	Quantity

Option Keywords

options Start options input. This keyword is required at the beginning of this section.

endfree End keyword input. This keyword is required at the end of this section.

Time-Step Size and Inverted Element Deletion

Elements can be optionally deleted from the calculation based upon their time-step size or if they invert. This option can be specified for all brick, beam, shell, or thick shell materials by specifying the control card keywords **tsming** or **ptsming**, or can be selectively applied to individual material numbers or groups of material numbers using the **ptsmin_ex**, **ptsmin_in**, **tsmin_ex,** or **tsmin_in** option keywords. These commands can be used individually or can be combined. (Note, values entered with the **ptsmin_ex** or **ptsmin_in** and **tsmin_ex** or **tsmin_in** option keywords override values entered with the global keywords **ptsming** and **tsming**, respectively. Furthermore, material model inputted values override global or option based tsmin values.) The *tsmin* options permit the user to specify an absolute time-step size for element deletion. The *ptsmin* options determine the deletion time-step size by multiplying the initial time-step size by a user specified factor - *ptsmin*. If both a *tsmin* and *ptsmin* are specified, element deletion is based upon the smaller criteria.

For material with a prescribed deletion value, the associated elements will be deleted from the calculation if and when they invert. This feature is extremely useful when modeling material that is prone to entanglement, but whose removal has little consequence on the remaining calculation, e.g., a foam mitigation part.

SAND slide surfaces should always be used when ever a material associated with the slide surface has a non-zero time-step deletion value.

Caution should be used when employing this feature since element removal can have a large impact on the solution.

ptsmin_ex *ptsmin mat#1 mat#2 mat#3 ... mat#n*

Set *ptsmin* for all other material numbers except these *n* material numbers. Elements with non-zero *ptsmin*s will be deleted when their time-step size becomes less than *ptsmin* times the initial global time-step size.

ptsmin_in *ptsmin mat#1 mat#2 mat#3 ... mat#n*

Set *ptsmin* for only these *n* material numbers. Elements with non-zero *ptsmin*s will be deleted when their time-step size becomes less than *ptsmin* times the initial global time-step size.

tsmin_ex *tsmin mat#1 mat#2 mat#3 ... mat#n*

Set *tsmin* for all other material numbers except these *n* material numbers. Elements with non-zero *tsmin*s will be deleted when their time-step size becomes less than *tsmin*.

tsmin_in *tsmin mat#1 mat#2 mat#3 ... mat#n*

Set *tsmin* for only these *n* material numbers. Elements with non-zero *tsmin*s will be deleted when their time-step size becomes less than *tsmin*.

Plotfile Control Features (Milli Not Yet)

rigid_wall *irigid* Print all rigid-wall normal forces to `FORCES` file. Print interval controlled by *PRTC*.

EQ.0: No forces print to file (default).
EQ.1: Forces printed to file.

verbose_hsp Generate verbose input and initialization data in hsp file (`d3hsp`)

Maximum Material Pressure History Output

maxpfile *file_name mat#1 mat#2 mat#3 ... mat#n*

Write the maximum pressure for the materials in the list at the time history output frequency to a text file. The text file will be named as *file_name*. Only materials associated with hexahedral continuum elements can be included in the list. If no material list is provided, maximum pressure for all materials, shell and beam materials included, will be written to the file. However the maximum pressures associated with shell or beam materials are not accurate and should be ignored.

DYNA3D-PENCRV3D Link

pencvmat *lst mat#1 mat#2 mat#3 ... mat#n*

Provide a list of materials that are included in the projectile in a DYNA3D-PENCRV3D analysis. Listed materials must only be associated with elements that are part of the projectile. The material list is controlled by the character variable *lst*

EQ.list: List of materials must be provided.

EQ.all: No list of materials is needed. All materials are considered as part of the projectile.

This keyword input is limited to selected users.

4.4 MATERIALS

Repeat the following set of cards for each material definition until $NUMMAT$ materials have been defined. Materials may be input in any convenient order, but all materials must be defined. Materials are referenced by their material number, which is used for identification only. Material type refers to the material model number, such as Material Type 1 for elastic behavior. Note that a material number can only apply to one type of element (beam, shell, thick shell, or solid).

A material model typically requires 8 cards for input, and exceptions are noted as appropriate. Not all material models are available for all element types. Valid element types are shown for each material model on the Material Control Card (Material Card 1) description. A brief list of notes follows the description of the Material Control Card.

Some material models, called ‘‘hydrodynamic’’ models, define only the deviatoric behavior of the material. An equation of state must be defined in conjunction with these hydrodynamic models to specify the volumetric behavior of the material. Following the material cards of a hydrodynamic material, the equation of state is defined. Note that different equations of state may require a different number of input cards. Also note that an equation of state is required by some material models and is not permitted by others. Equations of state are applicable to solid elements *only,* and are not used with beam or shell elements.

For structural elements, the cross sectional properties are defined following the material definition using the last 3 cards in this section. Cross sectional properties are defined differently depending on the element type (truss, beam, or shell) and element formulation (Hughes-Liu, Belytschko-Tsay, etc.). Many structural element formulations also permit cross sectional properties to be defined uniquely for each element on the element card. In this case, the cross sectional properties specified in the material cards define default cross section properties for that material, and are overridden by cross sectional property values specified on the element cards.

Card 1

Columns	Quantity	Format
1-5	Material identification number	I5
6-10	Material type. The numbers in brackets indicate the element types for which the material is available: 0-solid, 1-beam, 2-shell, and 3-thick shell. An asterisk * indicates that an equation of state is required *when that model is used with solid elements*. EQ. 1: elastic [0,1,2,3] EQ. 2: orthotropic elastic [0,2,3] EQ. 3: kinematic/isotropic elastic-plastic [0,1,2,3] EQ. 4: thermo-elastic-plastic [0,2] EQ. 5: soil and crushable foam [0] EQ. 6: viscoelastic [0] EQ. 7: Blatz-Ko hyperelastic rubber [0] EQ. 8: high explosive burn* [0] EQ. 9: fluid* [0] EQ.10: isotropic elastic-plastic hydrodynamic* [0] EQ.11: Steinberg-Guinan high rate elastic-plastic* [0] EQ.12: isotropic elastic-plastic [0,2] EQ.13: isotropic elastic-plastic with failure [0] EQ.14: soil and crushable foam with failure [0] EQ.15: Johnson/Cook elastic-plastic* [0,2] EQ.16: concrete/geologic material* [0] EQ.17: isotropic elastic-plastic with oriented cracks* [0] EQ.18: power law isotropic elastic-plastic [0,2] EQ.19: strain rate dependent elastic-plastic [0,2] EQ.20: rigid [0,1,2,3] EQ.21: thermal orthotropic elastic [0,2] EQ.22: fiber composite with damage [0,2] EQ.23: thermal orthotropic elastic with variable properties [0,2] EQ.24: rate dependent tabular isotropic elastic-plastic [0,2] EQ.25: extended two invariant geologic cap [0] EQ.26: metallic honeycomb [0] EQ.27: compressible Mooney-Rivlin hyperelastic rubber [0] EQ.28: resultant plasticity [1,2] EQ.29: mechanical threshold model [0] EQ.30: closed form update elastic-plastic for shells [2] EQ.31: Frazer-Nash hyperelastic rubber [0] EQ.32: Ramberg-Osgood elastic-plastic [0] EQ.33: general orthotropic elastic-plastic [0,2] EQ.34: normal anisotropic elastic-plastic for shells [2] EQ.35: elastic-plastic with forming limit diagram [0,2] (*list of material models continued on next page*)	I5

Columns	Quantity	Format
	Material type. The numbers in brackets indicate the element types for which the material is available: 0-solid, 1-beam, 2-shell, and 3-thick shell. An asterisk * indicates that an equation of state is required *when that model is used with solid elements*. (list of material models continued from previous page) EQ.36: brittle damage [0] EQ.37: 3-invariant viscoplastic cap [0] EQ.38: Bammann plasticity [0,2] EQ.39: Bammann plasticity with damage [0,2] EQ.40: Fahrenthold brittle damage [0] EQ.41: Fabric [2] EQ.42: multi-material laminate [2] EQ.43: transversely isotropic visco-hyperelasticity[2] EQ.44: low density rigid foam [0] EQ.45: DTRA concrete/geologic material* [0] EQ.46: anisotropic elastic [0,2] EQ.47: material interface guide (MIG) [0] EQ.48: visco statistical crack mechanics model (Visco-SCRAM) [0] EQ.49: LANL hyperfoam material [0] EQ.50: braided composite model [2] EQ.56: uni-directional composite [0] EQ.57: reserved for an uncoming LANL material model	
11-20	Mass density, ρ	E10.0
21-25	Equation of state type. Define only for material types 8, 9, 10, 11, 15, 16, and 17 *when these materials are used with solid elements*. EQ. 1: linear polynomial EQ. 2: JWL high explosive EQ. 3: Sack high explosive EQ. 4: Gruneisen EQ. 5: ratio of polynomials EQ. 6: linear polynomial with energy deposition EQ. 7: ignition and growth of reaction in HE (2-term) EQ. 8: tabulated compaction EQ. 9: tabulated EQ.10: not currently used EQ.11: pore collapse EQ.13: ignition and growth of reaction in HE (3-term)	I5

Columns	Quantity	Format
26-30	Hourglass stabilization method (IHQ) **For hexahedral elements** EQ.0: default=2 EQ.1: standard DYNA3D (viscous form) EQ.2: Flanagan-Belytschko (viscous form) EQ.3: Flanagan-Belytschko with exact volume integration (viscous form) EQ.4: stiffness form of type 2 (Flanagan-Belytschko) EQ.5: stiffness form of type 3 (Flanagan-Belytschko exact volume) EQ.6: selective-reduced 8-point hexahedral element (B-bar) EQ.7: physical stabilization (models 1, 2, 3, 18, & 56 only) EQ.8: total displacement physical stabilization (models 2 & 46 only) EQ.9: physical stabilization - exact volume (models 1, 2, 3, 18, & 56 only) EQ.10: total displacement physical stabilization - exact volume (models 2 & 46 only) EQ.12: fully integrated, 8-pt. hexahedral element	I5
	For shell, thick shell and beams EQ.0: default=2 EQ.1: standard DYNA3D (viscous form) EQ.2: Flanagan-Belytschko (viscous form) EQ.3: Flanagan-Belytschko with exact volume integration (viscous form) EQ.4: stiffness form of type 2 (Flanagan-Belytschko) EQ.5: stiffness form of type 3 (Flanagan-Belytschko exact volume) EQ.6: viscous form type 2 and stiffness form type 3 (shells only)	
31-40	Hourglass stabilization coefficient (QH, default = 0.10). Values of QH above 0.15 may cause instabilities if the time step is not decreased. The default value applies to all options and element types. The stiffness forms can stiffen the response, especially if deformations are large, and therefore should be used with care.	E10.0
41-45	Bulk viscosity type for shock capture (IBQ) EQ. 0: default=1 EQ. 1: standard DYNA3D	I5
46-55	Quadratic bulk viscosity coefficient, Q1 (default = 1.5)	E10.0
56-65	Linear bulk viscosity coefficient, Q2, (default = 0.06)	E10.0
66-70	Element type for which this material model is valid EQ. 0: solid (brick)	I5

EQ. 1: beam
EQ. 2: shell
EQ. 3: thick shell

Columns	Quantity	Format
71-75	Material initialization for gravity loading EQ. 0: all materials are initialized EQ. 1: only current material is initialized	I5
76-80	Element formulation if other than default **For beam elements:** EQ. 0: default=1 EQ. 1: Hughes-Liu EQ. 2: Belytschko-Schwer EQ. 3: Truss **For shell elements:** EQ. 0: default=2 EQ. 1: Hughes-Liu EQ. 2: Belytschko-Tsay EQ. 3: BCIZ (triangle) EQ. 4: C^0 (triangle) EQ. 5: membrane EQ. 6: YASE EQ. 7: YASE (fully-integrated inplane) EQ. 8: Bathe-Dvorkin (fully-integrated inplane)	I5

Material Control Card Notes

field	Comments
1	The material identification number should be between 1 and *NUMMAT*, the number of materials in the problem. Materials may be input in any order, but all materials must be defined. It is permissible to have unused materials defined in the input.
2	The material type defines the mathematical model used to evaluate the material stress-strain behavior. Note that not all material types are available for all element types.
3	Define the mass density for the material in consistent units. No unit conversions are done internally in DYNA3D (see discussion in section 2.2 on page 10).
4	If a hydrodynamic material model is selected, then an equation-of-state must be selected to define the material pressure-volume behavior.
5, 6	The default hourglass stabilization algorithm and parameters may be modified for this material, if desired. The standard DYNA3D mode is no longer the default hourglass control. Although cheaper, the standard DYNA3D mode damps out rigid body rotations and should be used with caution. These options do not apply to truss or beam elements, the YASE shell element, or the 8-point hexahedral elements.
7-9	Bulk viscosity methods are used for added stability and resolution in solid elements when shock waves are present.
10	A material definition may only be used for one element type.
11	If density vs. depth curves are used to initialize materials with hydrostatic stresses due to overburden, all materials or selected materials may be chosen for initialization. If only selected materials are to be initialized, this flag indicates whether the current material is to be initialized.
12	Element formulations for an element type may be arbitrarily mixed in an analysis. The default shell element formulation is Belytschko-Tsay, and the default beam element formulation is Hughes-Liu. A non-default element formulation applies only to elements using the current material.

Card 2

Columns	Quantity	Format
1-72	Material identification	A72

This material title will appear in the printed output. It is often helpful to use this heading to identify the physical material for which the DYNA3D material model was constructed.

Cards 3, . . . , 8

Define material cards 3, . . . , 8 as described below for the desired material type.

MATERIAL DEFINITION

Material Type 1 (Elastic)

Columns		Quantity	Format
1-10	Card 3	Young's modulus, E	E10.0
1-10	Card 4	Poisson's ratio, ν	E10.0
	Card 5	Blank	E10.0
	Card 6	Blank	E10.0
	Card 7	Blank	E10.0
	Card 8	Blank	E10.0

This model produces linear elastic material behavior.

Material Type 2 (Orthotropic Elastic)

Columns		Quantity	Format
1-10	Card 3	Elastic modulus, E_a (see Figure 1 and Figure 2)	E10.0
11-20		Elastic modulus, E_b	E10.0
21-30		Elastic modulus, E_c	E10.0
1-10	Card 4	Poisson's ratio, ν_{ba}	E10.0
11-20		Poisson's ratio, ν_{ca}	E10.0
21-30		Poisson's ratio, ν_{cb}	E10.0
1-10	Card 5	Shear modulus, G_{ab}	E10.0
11-20		Shear modulus, G_{bc}	E10.0
21-30		Shear modulus, G_{ca}	E10.0
1-10	Card 6	Material axes definition option, AOPT	E10.0

EQ.0.0: locally orthotropic with material axes determined by element nodes n_1, n_2, and n_4 as shown in Figure 1. Cards 7 and 8 must be blank with this option.

EQ.1.0: locally orthotropic with material axes determined by a point in space P and the global location of the element center, as shown in Figure 1. Note that $\boldsymbol{d}$ is parallel to the global z-axis. Card 8 below is blank.

EQ.2.0: globally orthotropic with material axes determined by vectors defined on Cards 7 and 8. (See Figure 2).

EQ.3.0: applicable to shell elements only. This option determines locally orthotropic material axes by offsetting the material axis $\boldsymbol{a}$ by an angle β from a line in the plane of the shell determined by taking the cross product of the vector $\boldsymbol{v}$ defined on Card 7 with the shell normal vector (See Figure 2). The angle β is defined on Card 8, and may be overridden by specifying a value on the element card.

EQ.4.0: locally orthotropic with cylindrical material axes determined by a point P, located on the axis of revolution, and the vector $\boldsymbol{d}$, which parallels axis of revolution. (See Figure 2.)

Columns		Quantity	Format
1-10	Card 7	x_p, define only if AOPT = 1.0 or 4.0	E10.0
11-20		y_p, define only if AOPT = 1.0 or 4.0	E10.0
21-30		z_p, define only if AOPT = 1.0 or 4.0	E10.0
1-10	Card 7	a_x, define only if AOPT = 2.0	E10.0
11-20		a_y, define only if AOPT = 2.0	E10.0
21-30		a_z, define only if AOPT = 2.0	E10.0
1-10	Card 7	v_x, define only if AOPT = 3.0	E10.0
11-20		v_y, define only if AOPT = 3.0	E10.0
21-30		v_z, define only if AOPT = 3.0	E10.0
1-10	Card 8	d_x, define only if AOPT = 2.0 or 4.0	E10.0
11-20		d_y, define only if AOPT = 2.0 or 4.0	E10.0
21-30		d_z, define only if AOPT = 2.0 or 4.0	E10.0
1-10	Card 8	Material angle β, define only if AOPT=3.0 (may be overridden on the element card)	E10.0

The constitutive matrix $\boldsymbol{C}$ that relates increments in global components of stress to increments in global components of strain is defined as:

$$\mathbf{C} = \mathbf{T}^T \mathbf{C}_L \mathbf{T}, \tag{6}$$

where $\mathbf{T}$ is the transformation matrix between the local material coordinate system and the global coordinate system, and $\mathbf{C}_L$ is the constitutive matrix defined in terms of the material constants of the local orthogonal material axes $\boldsymbol{a}$, $\boldsymbol{b}$, and $\boldsymbol{c}$.

$$C_L^{-1} = \begin{bmatrix} \frac{1}{E_a} & -\frac{\nu_{ba}}{E_b} & -\frac{\nu_{ca}}{E_c} & 0 & 0 & 0 \\ -\frac{\nu_{ab}}{E_a} & \frac{1}{E_b} & -\frac{\nu_{cb}}{E_c} & 0 & 0 & 0 \\ -\frac{\nu_{ac}}{E_a} & -\frac{\nu_{bc}}{E_b} & \frac{1}{E_c} & 0 & 0 & 0 \\ 0 & 0 & 0 & \frac{1}{G_{ab}} & 0 & 0 \\ 0 & 0 & 0 & 0 & \frac{1}{G_{bc}} & 0 \\ 0 & 0 & 0 & 0 & 0 & \frac{1}{G_{ca}} \end{bmatrix} \tag{7}$$

Note that symmetry of the elastic compliance $\mathbf{C}_L^{-1}$ implies

$$\frac{\nu_{ab}}{E_a} = \frac{\nu_{ba}}{E_b}, \quad \frac{\nu_{ca}}{E_c} = \frac{\nu_{ac}}{E_a}, \text{ and } \frac{\nu_{cb}}{E_c} = \frac{\nu_{bc}}{E_b}. \tag{8}$$

Further, positive definiteness of $\mathbf{C}_L$ yields the following restrictions on the elastic constants:

$$\nu_{ba} < \left(\frac{E_b}{E_a}\right)^{\frac{1}{2}}, \quad \nu_{ca} < \left(\frac{E_c}{E_a}\right)^{\frac{1}{2}}, \text{ and } \nu_{cb} < \left(\frac{E_c}{E_b}\right)^{\frac{1}{2}}. \tag{9}$$

Nonphysical energy growth may appear in the solution if these restrictions on the elastic constants are not observed.

Note that the values of Poisson's ratio are defined as

$$\nu_{ij} = \frac{-\varepsilon_j}{\varepsilon_i} \tag{10}$$

where ε_j is the strain in the j^{th} direction and ε_i is the strain in the i^{th} direction in a uniaxial stress test in the i^{th} direction.

In hexahedral elements, the model is implemented with a hyperelastic formulation while in shell and thick-shell elements, a hypoelastic formulation is used.

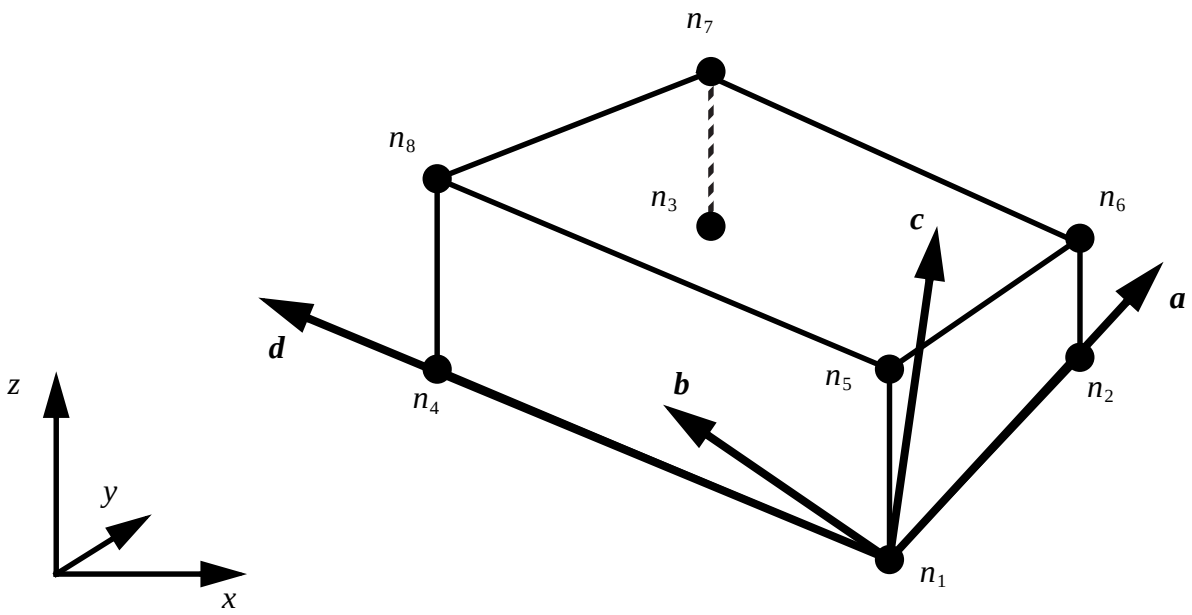

AOPT = 0

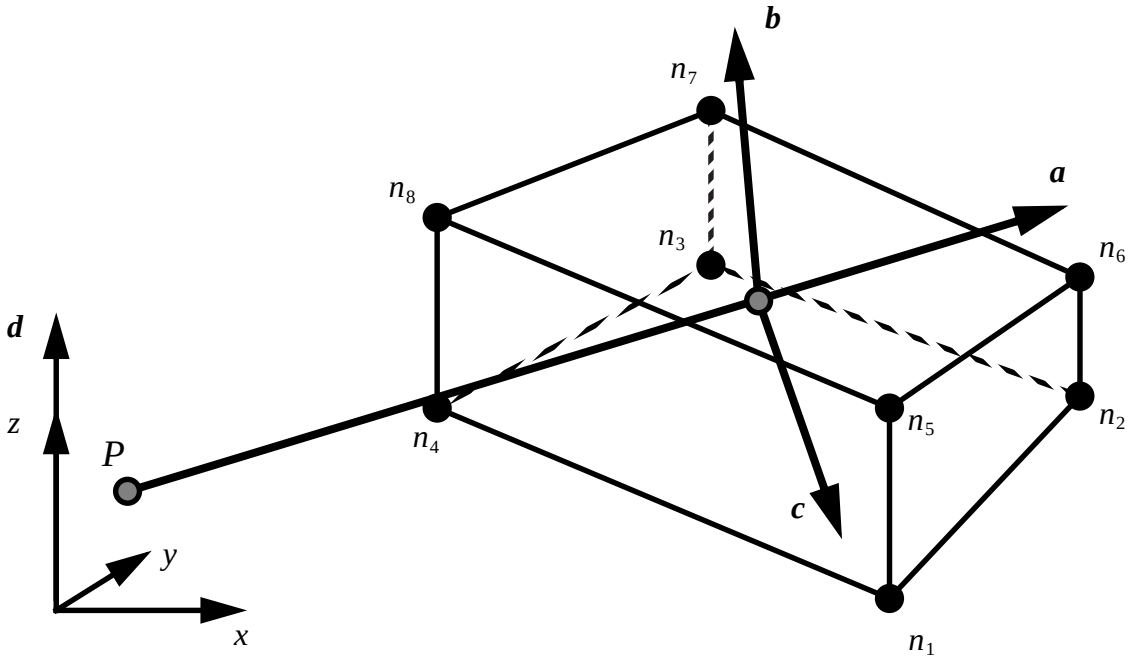

AOPT = 1

Figure 1

Definition of orthotropic material axes for options AOPT=0 and AOPT=1. Note that $\boldsymbol{c} = \boldsymbol{a} \times \boldsymbol{d}$ and $\boldsymbol{b} = \boldsymbol{c} \times \boldsymbol{a}$, where $\boldsymbol{a}$ and $\boldsymbol{d}$ are determined as depicted above.

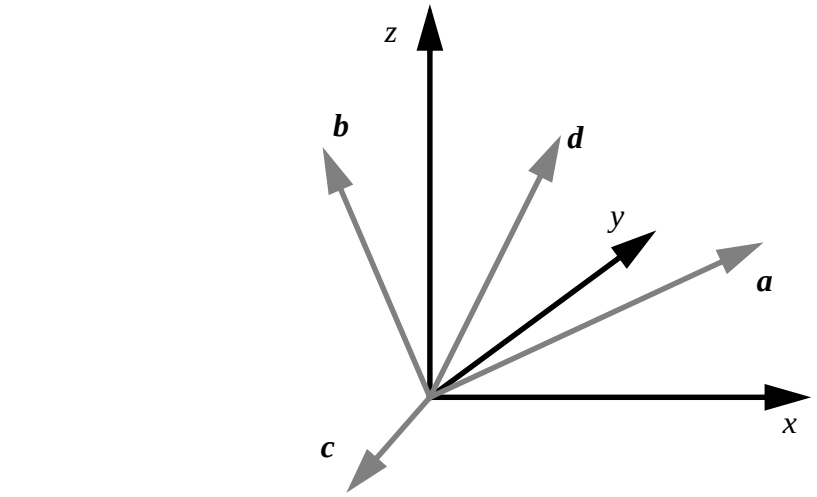

AOPT = 2

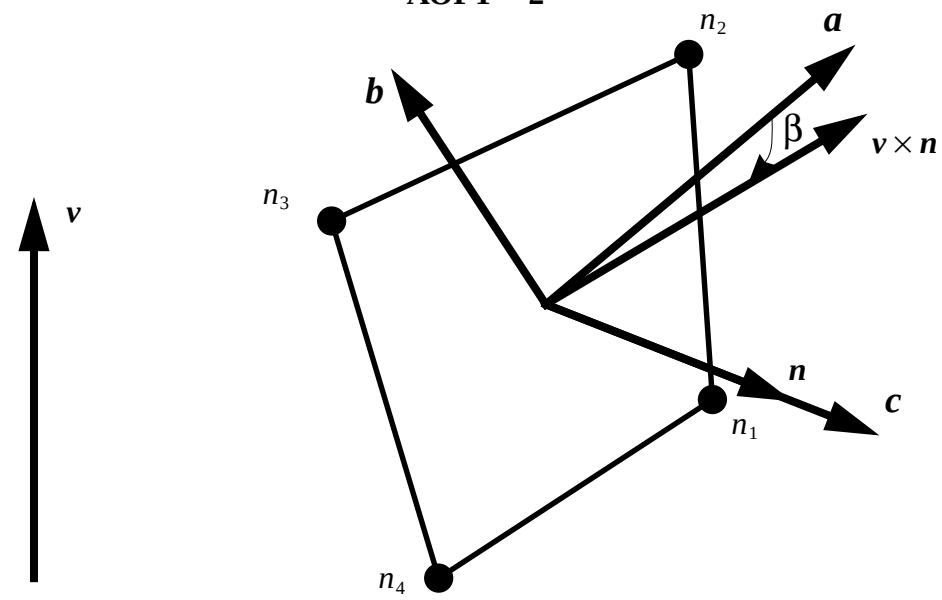

AOPT = 3

Figure 2
Definition of orthotropic material axes for options AOPT=2 and AOPT=3. Note that for AOPT=2 $\boldsymbol{c} = \boldsymbol{a} \times \boldsymbol{d}$ and $\boldsymbol{b} = \boldsymbol{c} \times \boldsymbol{a}$, and for AOPT=3 $\boldsymbol{c} = \boldsymbol{n}$ and $\boldsymbol{b} = \boldsymbol{c} \times \boldsymbol{a}$.

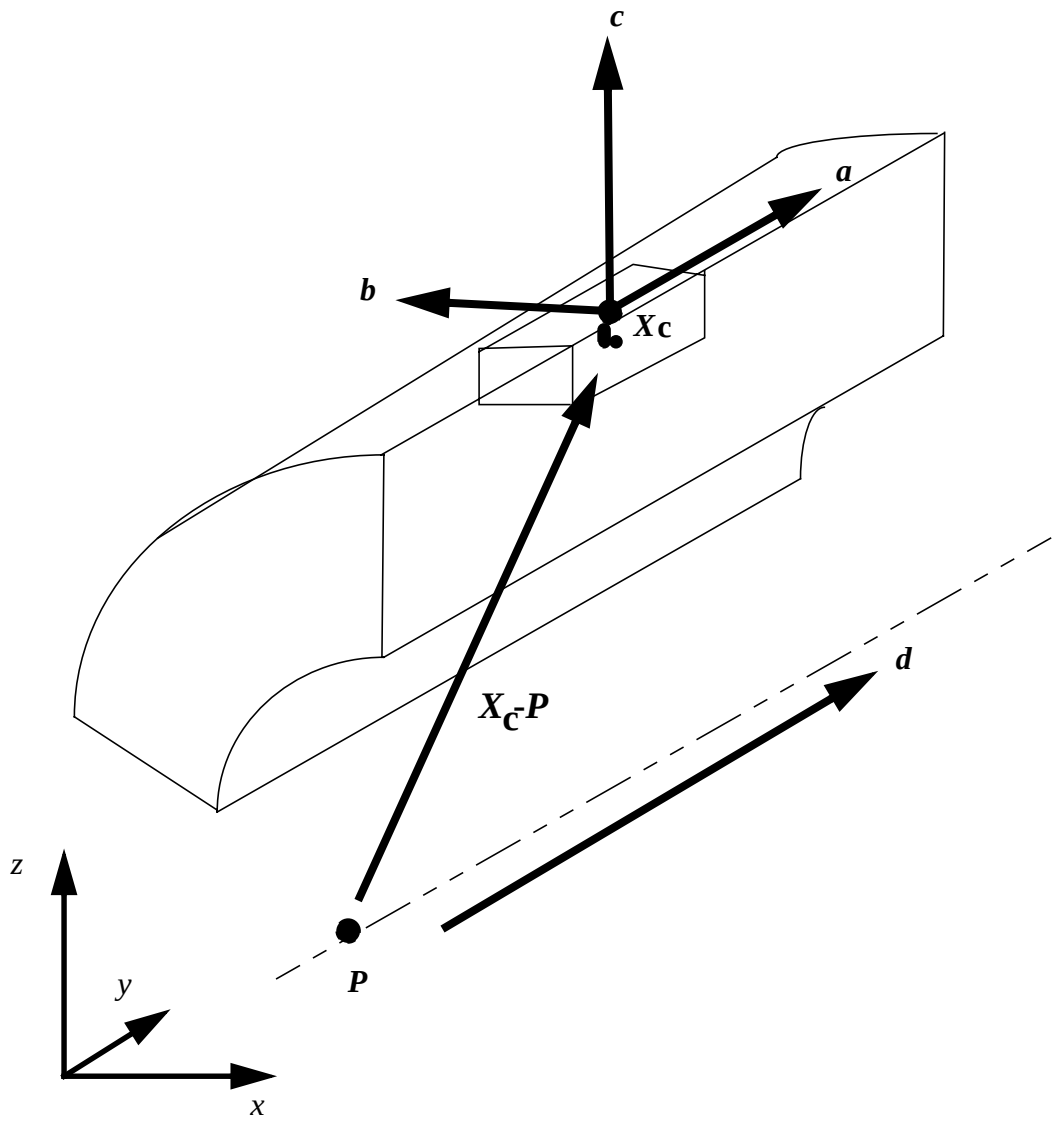

AOPT = 4

Figure 3

Definition of orthotropic material axes for option AOPT=4. Note that $\boldsymbol{b} = (\boldsymbol{X}_c - \boldsymbol{P}) \times \boldsymbol{d}$, $\boldsymbol{c} = \boldsymbol{d} \times \boldsymbol{b}$, $\boldsymbol{a} = \boldsymbol{b} \times \boldsymbol{c}$, and that $\boldsymbol{a}$ and $\boldsymbol{d}$ are parallel. The axis of revolution contains point $\boldsymbol{P}$ and parallels vector $\boldsymbol{d}$.

Material Type 3 (Kinematic/Isotropic Elastic-Plastic)

Columns		Quantity	Format
1-10	Card 3	Young's modulus, E	E10.0
1-10	Card 4	Poisson's ratio, ν	E10.0
1-10	Card 5	Yield stress, σ_0	E10.0
1-10	Card 6	Tangent modulus, E_T	E10.0
1-10	Card 7	Hardening parameter, β	E10.0
	Card 8	Blank	

The material behavior is elastoplastic and includes linear strain hardening. The hardening parameter β specifies an arbitrary combination of kinematic and isotropic hardening; $\beta = 0.0$ yields purely kinematic hardening, while $\beta = 1.0$ gives purely isotropic hardening. Figure 4 illustrates the effect of β on the uniaxial stress-strain curve. For modeling elastoplastic material behavior with purely isotropic hardening, Material Type 12 requires less storage and is somewhat more efficient while producing exactly the same behavior as Material Type 3 with $\beta = 1.0$. The numerical algorithms used in this model are adapted from (Krieg and Key, 1976).

The yield condition can be written

$$\phi = \bar{\sigma} - \sigma_y(\bar{\varepsilon}^p) , \tag{11}$$

where $\bar{\sigma}$ is the effective stress and σ_y is the current yield stress, which may be a function of the effective plastic strain $\bar{\varepsilon}^p$ if strain hardening is included. For isotropic hardening, the effective stress $\bar{\sigma}$ is given by

$$\bar{\sigma} = \left(\frac{3}{2} s_{ij} s_{ij}\right)^{\frac{1}{2}} , \tag{12}$$

where s_{ij} is the deviatoric stress tensor. For kinematic hardening,

$$\bar{\sigma} = \left(\frac{3}{2} \eta_{ij} \eta_{ij}\right)^{\frac{1}{2}} \tag{13}$$

where the translated stress η_{ij} is defined as

$$\eta_{ij} = s_{ij} - \alpha_{ij} , \tag{14}$$

and α_{ij} is the (deviatoric) back stress tensor.

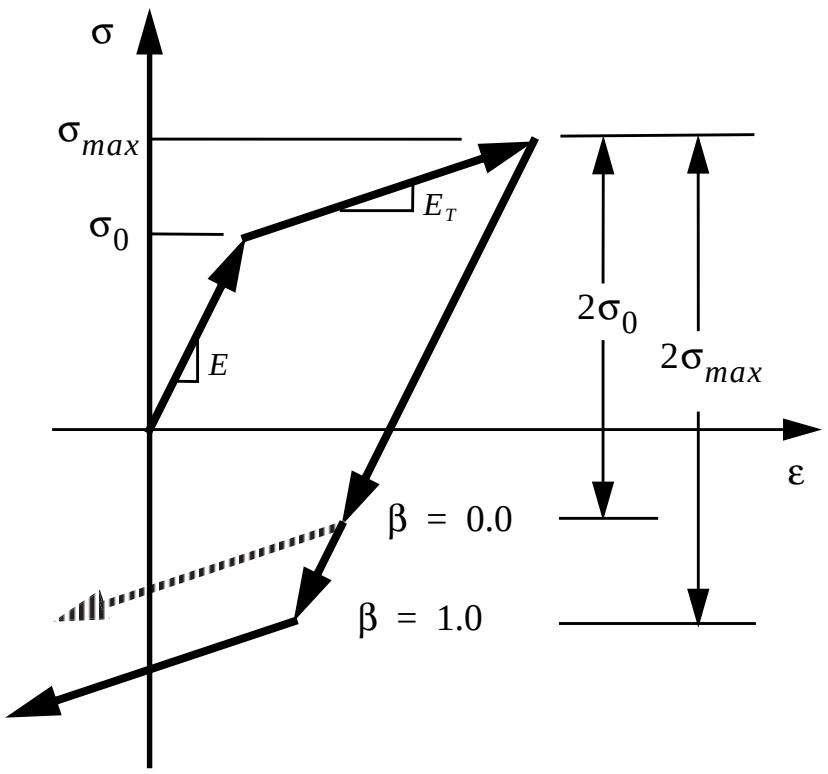

Figure 4
Uniaxial stress-strain curve showing elastic-plastic material behavior for kinematic hardening ($\beta = 0$) and isotropic hardening ($\beta = 1.0$).

The linear isotropic hardening law has the form

$$\sigma_y = \sigma_0 + \beta E_p \bar{\varepsilon}^p , \tag{15}$$

where σ_y is the current yield stress, σ_0 is the initial yield stress, and E_p is the plastic modulus.

The effective plastic strain $\bar{\varepsilon}^p$ is given by

$$\bar{\varepsilon}^p = \int_0^t d\bar{\varepsilon}^p , \tag{16}$$

where the incremental effective plastic strain $d\bar{\varepsilon}^p$ is found from the incremental plastic strain tensor $d\varepsilon_{ij}$ as

$$d\bar{\varepsilon}^p = \left\{ \frac{2}{3} d\bar{\varepsilon}^p_{ij} d\bar{\varepsilon}^p_{ij} \right\}^{\frac{1}{2}} . \tag{17}$$

The plastic modulus is found from Young's modulus E and the tangent modulus E_T using

$$E_p = \frac{EE_T}{E - E_T}. \tag{18}$$

The plastic hardening modulus E_p is the slope of the inelastic portion of the effective stress $\bar{\sigma}$ vs. effective plastic strain $\bar{\varepsilon}^p$ curve. Similarly, the tangent modulus E_T is the slope of the inelastic part of a uniaxial stress vs. strain curve (or equivalently, the effective stress vs. effective strain curve).

Kinematic and isotropic hardening elastoplastic models yield identical behavior under monotonic loading. Under reversed loading from a maximum stress σ_{max}, kinematic hardening predicts reverse yielding when the stress has unloaded by an amount $2\sigma_0$, and isotropic hardening predicts that reverse yielding occurs when the stress reaches $-\sigma_{max}$. Thus, under cyclic loading conditions where many stress reversals may occur, kinematic hardening predicts a hysteretic energy dissipation, while isotropic hardening predicts no energy dissipation after the first cycle. The isotropic model is slightly faster in computation speed, however.

Material Type 4 (Thermo-Elastic-Plastic)

Columns		Quantity	Format
1-10	Card 3	First temperature, T_1	E10.0
11-20		Second temperature, T_2	E10.0
.		.	.
.		.	.
.		.	.
71-80		Eighth temperature, T_8	E10.0
1-10	Card 4	Young's modulus at first temperature, E_1	E10.0
11-20		Young's modulus at second temperature, E_2	E10.0
.		.	.
.		.	.
.		.	.
71-80		Young's modulus at eighth temperature, E_8	E10.0
1-10	Card 5	Poisson's ratio at first temperature, ν_1	E10.0
11-20		Poisson's ratio at second temperature, ν_2	E10.0
.		.	.
.		.	.
.		.	.
71-80		Poisson's ratio at eighth temperature, ν_8	E10.0
1-10	Card 6	Secant coefficient of thermal expansion, $\overline{\alpha_1}$	E10.0
11-20		Secant coefficient of thermal expansion, $\overline{\alpha_2}$	E10.0
.		.	.
.		.	.
.		.	.
71-80		Secant coefficient of thermal expansion, $\overline{\alpha_8}$	E10.0
1-10	Card 7	Yield stress at first temperature, σ_{y1}	E10.0
.		Yield stress at second temperature, σ_{y2}	E10.0
.		.	.

Columns		Quantity	Format
.		.	.
.		.	.
71-80		Yield stress at eighth temperature, σ_{y8}	E10.0
1-10	Card 8	Plastic modulus at first temperature, E_{p1}	E10.0
11-20		Plastic modulus at second temperature, E_{p2}	E10.0
.		.	.
.		.	.
.		.	.
71-80		Plastic modulus at eighth temperature, E_{p8}	E10.0

At least two temperatures and their corresponding material properties must be defined. The analysis will be terminated if a material temperature falls outside the range defined in the input. If a thermo-elastic material is desired (i.e., no plasticity effects), leave Cards 7 and 8 blank.

The plastic hardening modulus E_p is the slope of the effective stress vs. effective plastic strain curve (or equivalently, the uniaxial stress vs. effective plastic strain curve). The plastic hardening modulus may be found from the tangent modulus E_T as

$$E_p = \frac{EE_T}{E - E_T}, \tag{19}$$

where the tangent modulus E_T is the slope of the post-yield portion of the uniaxial stress - strain curve.

Thermal expansion due to temperature change is included when nonzero values of $\bar{\alpha}$ are specified. The *secant* coefficient of thermal expansion $\bar{\alpha}$ can also be a function of temperature, and is defined with respect to the reference temperature at the beginning of the calculation for that material. Total thermal strain ε_{ij}^{T} is defined in terms of the secant thermal expansion coefficient $\bar{\alpha}$ as

$$\varepsilon_{ij}^{T} = \bar{\alpha}(T - T_{ref})\delta_{ij}, \tag{20}$$

where T is the current temperature and T_{ref} is the reference temperature. Therefore, temperature dependent secant coefficients of thermal expansion should be defined as the value *to* that temperature, not the value *at* that temperature. The secant coefficient $\bar{\alpha}$ is related to the tangent coefficient of thermal expansion α by

$$\bar{\alpha} = \frac{1}{T - T_{ref}} \int_{T_{ref}}^{T} \alpha(T)dT . \quad (21)$$

For temperature independent coefficients of thermal expansion, $\bar{\alpha}$ is identical to α, and the classical definition of thermal expansion is valid.

Since this model is temperature dependent, the thermal effects option on Control Card 6 must be nonzero. Care should be taken to define a reference temperature consistent with the specified secant coefficients of thermal expansion. In general, the reference temperature is the element temperature at the beginning of the analysis.

This model is applicable to materials exhibiting elastic or elastoplastic behavior where thermal effects are important. Both thermal strains and temperature-dependent material properties are included.

Material Type 5 (Soil and Crushable Foam)

Columns		Quantity	Format
1-10	Card 3	Shear modulus, G	E10.0
11-20		Bulk unloading modulus, K_u	E10.0
21-30		First yield function constant, a_0	E10.0
31-40		Second yield function constant, a_1	E10.0
41-50		Third yield function constant, a_2	E10.0
51-60		Pressure cutoff for tensile fracture, p_{cut}	E10.0
1-10	Card 4	First (most tensile) tabulated volumetric strain, ε_{v1} (see Figure 5)	E10.0
11-20		First tabulated pressure, p_1 ($p_1 < 0$)	E10.0
21-30		Second tabulated volumetric strain, ε_{v2}	E10.0
31-40		Second tabulated pressure, p_2	E10.0
1-10	Card 5	Third tabulated volumetric strain, ε_{v3}	E10.0
11-20		Third tabulated pressure, p_3	E10.0
21-30		Fourth tabulated volumetric strain, ε_{v4}	E10.0
31-40		Fourth tabulated pressure, p_4	E10.0
1-10	Card 6	Fifth tabulated volumetric strain, ε_{v5}	E10.0
11-20		Fifth tabulated pressure, p_5	E10.0
21-30		Sixth tabulated volumetric strain, ε_{v6}	E10.0
31-40		Sixth tabulated pressure, p_6	E10.0
1-10	Card 7	Seventh tabulated volumetric strain, ε_{v7}	E10.0
11-20		Seventh tabulated pressure, p_7	E10.0
21-30		Eighth tabulated volumetric strain, ε_{v8}	E10.0
31-40		Eighth tabulated pressure, p_8	E10.0
1-10	Card 8	Ninth tabulated volumetric strain, ε_{v9}	E10.0
11-20		Ninth tabulated pressure, p_9	E10.0
21-30		Modified elliptical surface flag, *AMOD*	E10.0
31-40		Unloading factor, α (UOPT=2 only)	E10.0

Columns	Quantity	Format
41-50	Initial relative volume EQ.0.0: no initial relative volume specified (default) GT.0.0: default initial relative volume	E10.0
51-60	Unloading option, UOPT EQ.0.0: volumetric crushing upon unloading EQ.1.0: no volumetric crushing upon unloading EQ.2.0: limited volumetric crushing - variable slope EQ.3.0: limited volumetric crushing - fixed slope	E10.0
61-70	Load curve number for time-dependent relative volume EQ.0.0: no load curve included (default) GT.0.0: load curve number describing relative volume	E10.0
71-80	Hysteresis factor, γ (UOPT=2,3 only)	E10.0

This model is based on the formulation suggested in (Key, 1974).

Pressure is positive in compression, and volumetric strain is negative in compression. Volumetric strain is given by the natural logarithm of the relative volume, $\varepsilon_v = ln\left(\frac{V}{V_0}\right)$. The tabulated pressure-volumetric strain data may contain up to nine pairs of points, and must be given in order of *increasing* compression. If the pressure drops below (i.e., becomes more tensile than) the cutoff value p_{cut}, then the pressure is reset to the cutoff value.

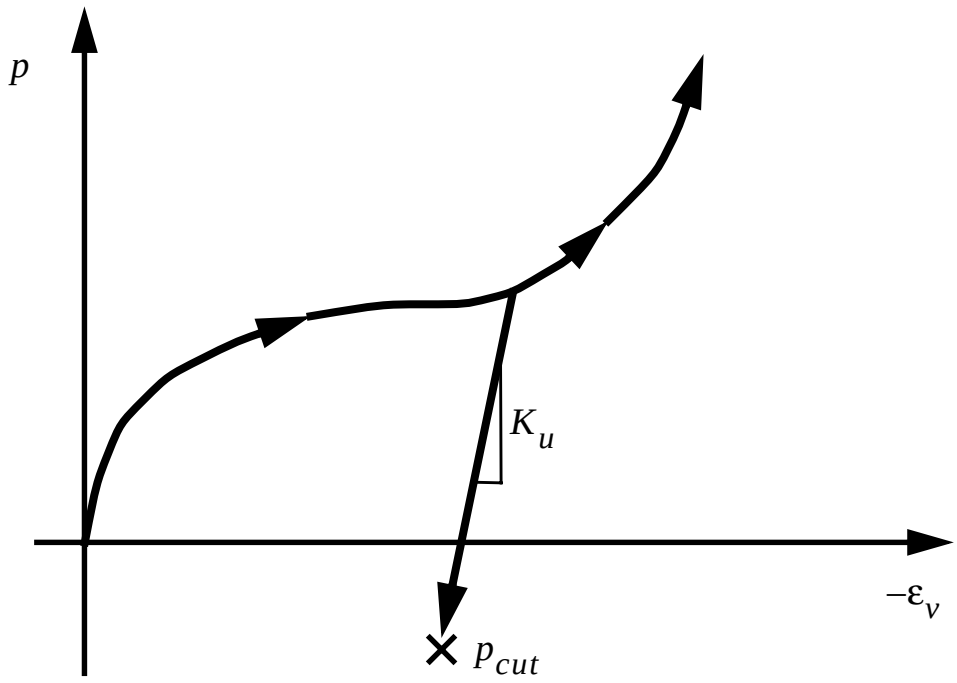

Figure 5
Pressure vs. volumetric strain curve for soil and crushable foam model.

The deviatoric perfectly plastic yield function ϕ is defined as

$$\phi = J_2 - [a_0 + a_1 p + a_2 p^2], \tag{22}$$

where a_0, a_1, and a_2 are constants, p is pressure, and J_2 is the second invariant of the deviatoric stress tensor $\boldsymbol{s}$ given by

$$J_2 = \frac{1}{2} s_{ij} s_{ij}. \tag{23}$$

The variation of σ_{yt} as a function of p has three conical forms which depend on the parameter a_2: elliptic ($a_2 < 0$), parabolic ($a_2 = 0$), or hyperbolic ($a_2 > 0$). These three forms are shown in Figure 6 in terms of J_2 vs. p. Figure 7 shows the corresponding forms in a more familiar engineering form of σ_{yt} vs. p. The elliptic yield function curves back toward the p axis at higher pressures and predicts a softening behavior which is not often observed in test data. If the modified elliptical yield surface flag $AMOD$ is nonzero, then the elliptical yield surface is used up to the point of maximum J_2. For higher pressures, the yield surface is extended as a von Mises surface.

The resulting yield surface is depicted in Figure 6 and Figure 7. This modification yields much improved agreement with a test data for many geologic materials such as concrete, as discussed in (Schwer, Rosinsky, and Day, 1988).

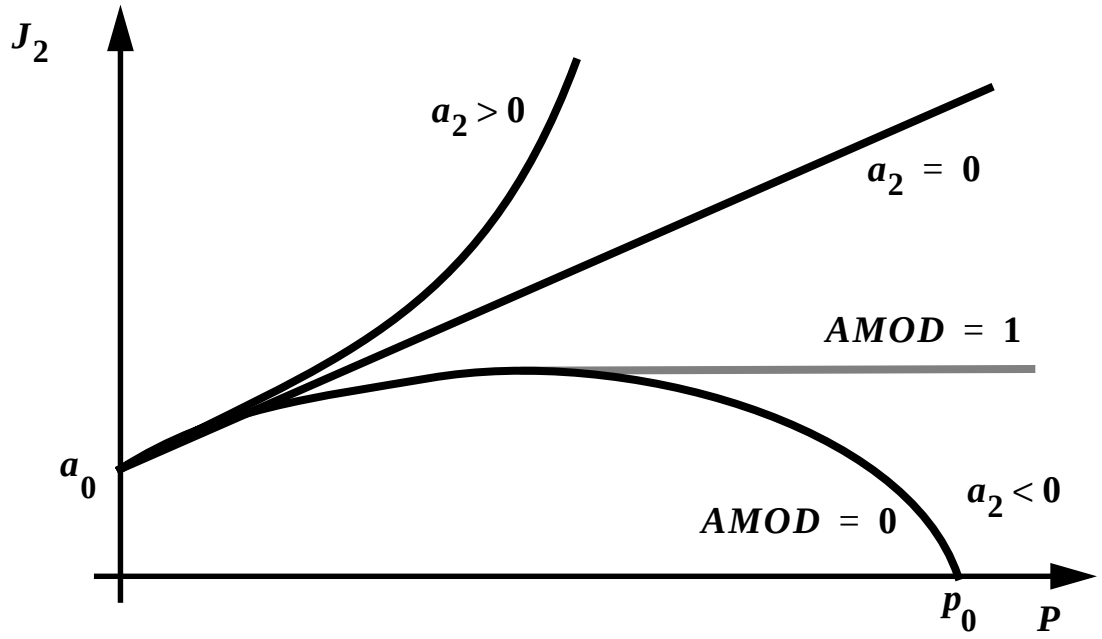

Figure 6
Material type 5 failure surface forms in J_2 vs. p space.

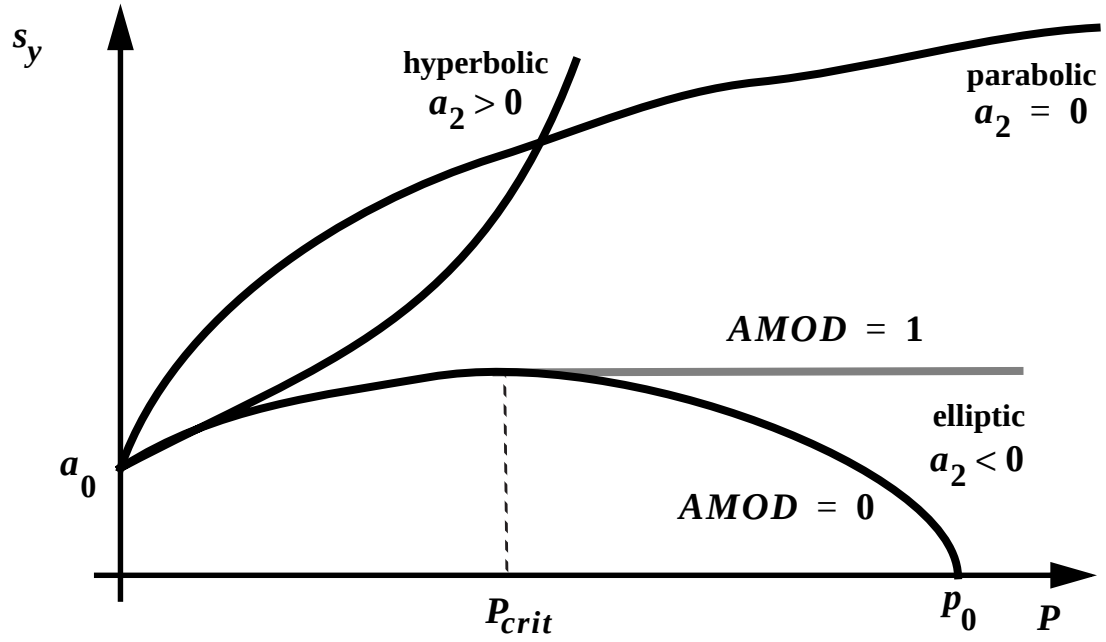

Figure 7
Material type 5 failure surface forms in σ_y vs. p space.

The unmodified elliptic yield surface crosses the $\sigma_y = 0$ at a pressure p_0, as shown in Figure 7. Thus, p_0 is the maximum pressure at which the unmodified elliptic failure surface may be used. It is easily shown that

$$p_0 = \frac{-a_1 + \sqrt{a_1^2 - 4a_0a_2}}{2a_2}. \tag{24}$$

The modified elliptic yield surface transitions to a von Mises surface at pressures greater than p_{crit}, where

$$p_{crit} = -\frac{a_1}{2a_2}. \tag{25}$$

Plastic flow is nonassociative if a_1 or a_2 are nonzero.

On the yield surface, $J_2 = \frac{1}{3}\sigma_y^2$, where σ_y is the uniaxial yield stress. Thus, the yield stress at any pressure p is given by

$$\sigma_y = [3(a_0 + a_1p + a_2p^2)]^{\frac{1}{2}}. \tag{26}$$

There is no strain hardening in this model, so the yield stress is completely determined by the pressure.

To eliminate the pressure dependence of the yield strength, set $a_1 = a_2 = 0$ and $a_0 = \frac{1}{3}\sigma_y^2$. This approach is useful when a von Mises type elastic-plastic model is desired for use with tabulated volumetric data.

This material model is useful as a simple representation of pressure hardening, where the deviatoric yield strength of a material increases as the hydrostatic pressure increases. At any constant pressure, the deviatoric behavior is elastic perfectly-plastic. This model permits a general representation of the material volumetric behavior via a tabulated pressure-volumetric strain curve. This flexibility makes this model useful for representing materials with a stiffening pressure-volume curve, such as porous materials like wood or foam. This model is also often used as a simplified model for concrete or soil.

If the material is pre-stressed, an initial relative volume can be input on the 8th card. This value may be overwritten or prescribed on an element by element basis by specifying an initial relative volume on the element definition card (see SOLID ELEMENTS on page 308). When an initial relative volume is present, a corresponding pressure is internally calculated from the pressure-volumetric strain curve. The element's effective relative volume is the sum of the deformation induced relative volume, any prescribed initial relative volume, and an optionally included user-imposed complementary relative volume. The user-imposed complementary relative volume is defined as a function of time and specified with a load curve. It is useful for phasing in an initial volumetric deformation or cushioning the instantaneous high stresses that arise from some pre-stressing conditions.

A hysteresis effect, as shown in Figure 8, may be introduced into the volumetric response by using *UOPT*=2 or 3. Here the saturation portions of the unload pressure versus volumetric strain curve is given by $\gamma P(\varepsilon_v)$. The slope of the transition between the loading and unloading curves, K_{unload}, can be set proportional to the $P(\varepsilon_v)$ curve as

$$K_{unload} = \alpha \frac{dP(\varepsilon_v)}{d\varepsilon_v} \tag{27}$$

with *UOPT*=2, or be fixed as

$$K_{unload} = K_u \tag{28}$$

with *UOPT*=3.

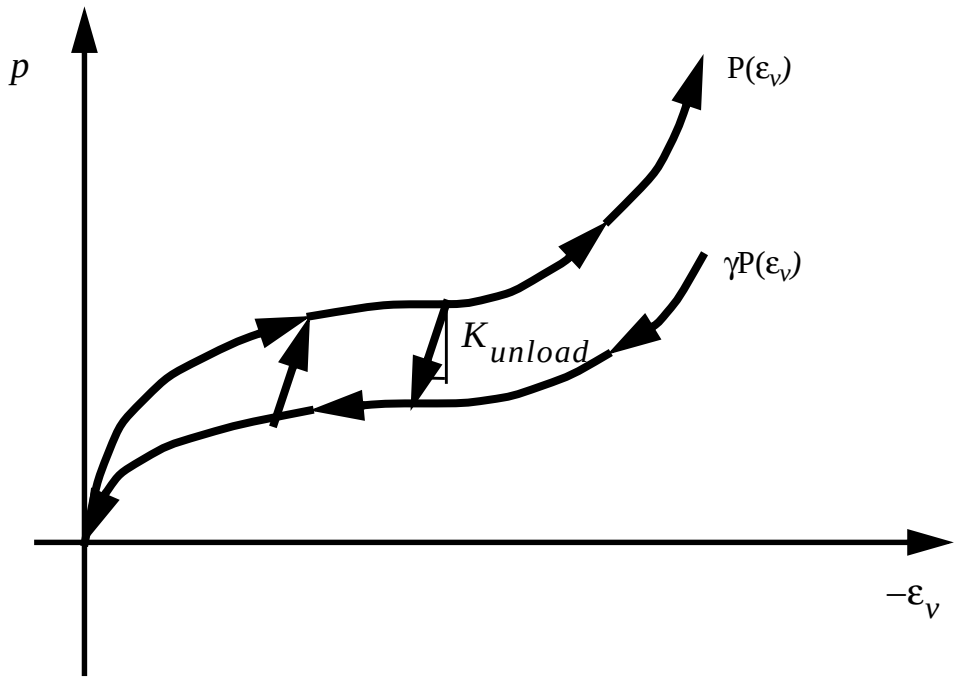

Figure 8
Pressure vs. volumetric strain curve for soil and crushable foam model. *UOPT*=2,3

Material Type 6 (Viscoelastic)

Columns		Quantity	Format
1-10	Card 3	Elastic bulk modulus, K	E10.0
1-10	Card 4	Short-time shear modulus, G_0	E10.0
1-10	Card 5	Long-time shear modulus, G_∞	E10.0
1-10	Card 6	Time parameter MFLAG.EQ.0.0: decay constant, β MFLAG.EQ.1.0: time relaxation constant, τ	E10.0
1-10	Card 7	Model formulation flag, MFLAG EQ.0.0: standard DYNA3D formulation EQ.1.0: Kelvin viscoelastic formulation	E10.0
	Card 8	Blank	

Two formulations of viscoelasticity are available. In the standard DYNA3D model (Key, 1974), the deviatoric stresses are found from

$$s_{ij} = 2\int_0^t G(t-\tau)\dot{e}_{ij}\,d\tau\,, \tag{29}$$

where the shear relaxation behavior is described by

$$G(t) = G_\infty + (G_0 - G_\infty)e^{-\beta t} \tag{30}$$

and $\dot{e}_{ij}$ is the deviatoric strain rate. In the Kelvin viscoelastic formulation, the evolution of deviatoric stress is governed by

$$\dot{s}_{ij} + \frac{1}{\tau}s_{ij} = (1+\delta_{ij})G_0\dot{e}_{ij} + (1+\delta_{ij})\frac{G_\infty}{\tau}\dot{e}_{ij} \qquad \text{(no sum)}, \tag{31}$$

followed by a projection back into deviatoric stress space. The model parameters may be related to shear stiffness and damping properties over a frequency range of interest. This model is primarily intended as a simple viscous shear model for use in seismic studies.

The volumetric response is elastic in both formulations, so the pressure is computed from the current volumetric strain using

$$p = -K\varepsilon_v, \tag{32}$$

where K is the elastic bulk modulus. The viscoelastic model is useful for modeling rate-dependent elastic materials. It is also effectively used whenever viscous dissipation is desired with deviatoric (shear) deformations.

Material Type 7 (Blatz - Ko Hyperelastic Rubber)

Columns		Quantity	Format
1-10	Card 3	Shear modulus, G	E10.0
	Card 4	Blank	
.			.
.			.
.			.
	Card 8	Blank	

This model is a hyperelastic model based on the implementation in (Key, 1974), and is appropriate for materials undergoing moderately large strains. In this formulation, the second Piola-Kirchhoff stress $\mathtt{t}$ is computed as

$$\tau_{ij} = G\left(\frac{1}{\nu}C_{ij} - V^{\frac{-1}{1-2\nu}}\delta_{ij}\right), \tag{33}$$

where V is the relative volume, C_{ij} is the right Cauchy-Green strain tensor, and ν is Poisson's ratio which is set to 0.463 internally. The Cauchy stress $\mathtt{s}$ is then found from $\mathtt{t}$ using

$$\mathtt{s} = \frac{1}{J}\boldsymbol{F}\mathtt{t}\boldsymbol{F}^{T}, \tag{34}$$

where $\boldsymbol{F}$ is the deformation gradient and J is the Jacobian of the deformation.

The Blatz-Ko hyperelastic model is often used to represent the behavior of rubber at moderately large strains. The Blatz-Ko formulation yields a slightly compressible material. Only one input parameter is required, and therefore this model may be useful when detailed test data is not available for the material of interest. For more sophisticated hyperelastic models for rubber, see the Compressible Mooney-Rivlin Rubber model (Material Type 27) or the Frazer-Nash Rubber model (Material Type 31).

Material Type 8 (High Explosive Burn)

An equation of state must be used with this model.

Columns		Quantity	Format
1-10	Card 3	Detonation velocity, D	E10.0
11-20		Chapman-Jouget pressure, P_{CJ}	E10.0
21-30		Lighting time option, $ILOPT$ EQ.0.0: Programmed burn EQ.1.0: Beta burn	E10.0
	Card 4	Blank	
	.		.
	.		.
	.		.
	Card 8	Blank	

This model is based on work described in (Giroux, 1973), and is used to model the burning of explosives. The detonation velocity D is the velocity of a detonation or burn front. The Chapman-Jouguet pressure P_{CJ} is the maximum pressure realizable in a constant volume adiabatic burn.

During DYNA3D initialization, the lighting time of each element is computed from specified detonation points using the programmed burn option. If detonation points are defined, then the lighting time t_L for an element is computed based on the distance from the center of the element to the nearest detonation point, divided by the detonation velocity D.

Burn fractions are computed to control the release of chemical energy for simulating high explosive detonations. If the ‘‘beta burn’’ option ($ILOPT = 1$) is selected, then the burn fraction F is computed from

$$F = \beta(1 - V) = \frac{1 - V}{1 - V_{CJ}}, \tag{35}$$

where V is the current relative volume, V_{CJ} is the Chapman-Jouguet relative volume, and

$$\beta = \frac{1}{1 - V_{CJ}}. \tag{36}$$

This model is useful to detect initiation due to shock compression of HE.

For the programmed burn option, the burn fraction is computed from

$$F = max(F_1, F_2), \tag{37}$$

where

$$F_1 = ((t - t_L)D)/(1.5h) \tag{38}$$

if $t > t_L$, and $F_1 = 0$ if $t < t_L$, and h is a characteristic dimension of the element under consideration. F_2 is computed from

$$F_2 = \beta(1 - V) = \frac{1 - V}{1 - V_{CJ}}. \tag{39}$$

If the above equations produce a burn fraction that is greater than one, then it is reset to one.

The burn front propagates by multiplying the pressure computed from an equation-of-state by the current burn fraction,

$$p = F p_{EOS}(V, E), \tag{40}$$

where $p_{EOS}(V, E)$ is the pressure computed from the equation-of-state at the current relative volume V and energy E. High explosives typically have large initial internal energies, E_0, which yield large pressures as $F \rightarrow 1$.

Material Type 9 (Fluid)

An equation of state must be used with this model.

Columns		Quantity	Format
1-10	Card 3	Pressure cutoff, p_{cut} (positive in compression)	E10.0
11-20		Viscosity coefficient, μ	E10.0
	Card 4.	Blank	
	.		.
	.		.
	.		.
	Card 8	Blank	

The fluid material has no stiffness, and must be used with an equation-of-state. A viscous stress is computed from

$$s_{ij} = \mu \dot{e}_{ij}, \tag{41}$$

where $\dot{e}_{ij}$ is the deviatoric strain rate and s_{ij} is the deviatoric stress.

Materials with no viscosity may reach large distortions under very small shear loads, so a nonzero viscosity should always be used.

The pressure cutoff, p_{cut}, is negative in tension. If the pressure becomes more tensile than p_{cut}, then it is reset to that value. Thus, the pressure cutoff can be interpreted as an approximate model of cavitation. The deviatoric stresses arising from viscous effects are unaffected by the tensile pressure cutoff.

This model is most useful for analyzing structures with contained fluids. Large distortions in the fluid make some free-surface and fluid flow problems more amenable to analysis using other analysis codes employing an Eulerian formulation. Caution should therefore be used when applying this material model in situations where large distortions are expected.

Material Type 10 (Isotropic-Elastic-Plastic-Hydrodynamic)

An equation of state must be used with this model.

Columns		Quantity	Format
1-10	Card 3	Shear modulus, G	E10.0
11-20		Yield stress, σ_0	E10.0
21-30		Plastic modulus, E_p	E10.0
31-40		Pressure cutoff, p_{cut} (positive in compression) EQ.0.0: cutoff of $-\infty$ is assumed (no cutoff)	E10.0
41-50		Linear pressure hardening coefficient, a_1	E10.0
51-60		Quadratic pressure hardening coefficient, a_2	E10.0
61-70		Spall model, $ISPALL$ EQ.0.0: default set to 1.0 EQ.1.0: Pressure limit model EQ.2.0: Maximum principal stress spall criterion EQ.3.0: Hydrostatic tension spall criterion	E10.0
1-10	Card 4	Effective plastic strain at failure, $\bar{\varepsilon}_f^p$ EQ.0.0: no failure	E10.0
11-20		Element deletion flag for plastic strain EQ.0.0: No element removal upon failure EQ.1.0: Element deleted when $\bar{\varepsilon}^p = \bar{\varepsilon}_f^p$	E10.0
21-30		Element deletion flag for spall ($ISPALL = 2, 3$ only) EQ.0.0: No element removal upon spall EQ.1.0: Element deleted by spall criterion	E10.0
1-10	Card 5	First tabulated effective plastic strain, $\bar{\varepsilon}_1^p$	E10.0
11-20		$\bar{\varepsilon}_2^p$	E10.0
.		.	.
.		.	.
.		.	.
71-80		$\bar{\varepsilon}_8^p$	E10.0
1-10	Card 6	$\bar{\varepsilon}_9^p$	E10.0
.		.	.
.		.	.
.		.	.

Columns		Quantity	Format
71-80		$\bar{\varepsilon}^p_{16}$	E10.0
1-10	Card 7	First tabulated yield stress, σ_{y1}	E10.0
.		.	.
.		.	.
71-80		σ_{y8}	E10.0
1-10	Card 8	σ_{y9}	E10.0
.		.	.
.		.	.
.		.	.
71-80		σ_{y16}	E10.0

If a tabulated yield stress vs. effective plastic strain curve is not given (Cards 5-8 are blank), then the initial yield stress σ_0, plastic hardening modulus E_p, and pressure hardening coefficients a_1 and a_2 are taken from Card 3. In this case, a pressure hardening bilinear stress-strain curve similar to that shown in Figure 4 is obtained with linear isotropic strain hardening ($\beta = 1.0$).

The yield condition can be written

$$\phi = \bar{\sigma} - \sigma_y(\bar{\varepsilon}^p, p), \tag{42}$$

where $\bar{\sigma}$ is the effective von Mises stress and σ_y is the current yield stress, which may be a function of the effective plastic strain $\bar{\varepsilon}^p$ and pressure p. The effective stress $\bar{\sigma}$ is given by

$$\bar{\sigma} = \left[\frac{3}{2} s_{ij} s_{ij}\right]^{\frac{1}{2}}, \tag{43}$$

where s_{ij} is the deviatoric stress tensor.

The hardening law has the form

$$\sigma_y = \sigma_0 + E_p \bar{\varepsilon}^p + (a_1 + a_2 p)\hat{p}, \tag{44}$$

where p is the pressure (positive in compression), and $\hat{p}$ is the tension-limited pressure found from

$$\hat{p} = max(p, 0). \tag{45}$$

The effective plastic strain $\bar{\varepsilon}^p$ is given by

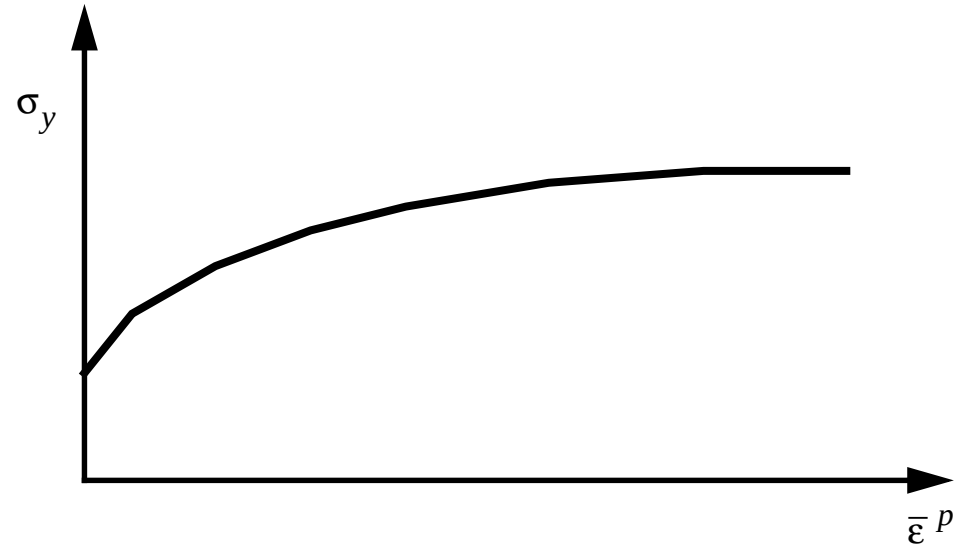

Figure 9
Tabulated yield stress vs. effective plastic strain curve.

$$\bar{\varepsilon}^p = \int_0^t d\bar{\varepsilon}^p, \tag{46}$$

where the incremental effective plastic strain $d\bar{\varepsilon}^p$ is found from the incremental plastic strain tensor $d\varepsilon_{ij}$ as

$$d\bar{\varepsilon}^p = \left\{ \frac{2}{3} d\bar{\varepsilon}^p_{ij} d\bar{\varepsilon}^p_{ij} \right\}^{\frac{1}{2}}. \tag{47}$$

The plastic modulus can be related to Young's modulus E and the tangent modulus E_T using

$$E_p = \frac{E E_T}{E - E_T}. \tag{48}$$

The plastic modulus E_P is the slope of the inelastic portion of the effective stress $\bar{\sigma}$ vs. effective plastic strain $\bar{\varepsilon}^p$ curve, and the tangent modulus E_T is the slope of the inelastic part of a uniaxial stress vs. strain curve (or equivalently, the effective stress vs. effective strain curve).

If tabulated values of yield stress vs. effective plastic strain are specified on Cards 5-8, a nonlinear strain hardening curve like that shown in Figure 9 may be defined. In this case the plastic hardening modulus and pressure hardening coefficients input on Card 3 are not used, and the yield stress is given as

$$\sigma_y = f(\bar{\varepsilon}^p), \tag{49}$$

where $f(\bar{\varepsilon}^p)$ is interpolated from the specified yield stress vs. effective plastic strain curve. Any number of points, from 2 to 16, may be used to define the hardening curve. This option permits additional detail to be included in the nonlinear strain hardening law, but pressure hardening is not modeled with this approach.

A choice of three spall models is offered to represent material splitting, cracking, and failure under tensile loads. The pressure limit model, $(ISPALL = 1)$, limits the hydrostatic tension to the specified value, p_{cut}. If pressures more tensile than this limit are calculated, the pressure is reset to p_{cut}. This option is not strictly a spall model, since the deviatoric stresses are unaffected by the pressure reaching the tensile cutoff, and the pressure cutoff value p_{cut} remains unchanged throughout the analysis. The maximum principal stress spall model, $(ISPALL = 2)$, detects spall if the maximum (most tensile) principal stress σ_{max} exceeds the limiting value $-p_{cut}$. Note that the negative sign is required because p_{cut} is measured positive in compression, while σ_{max} is positive in tension. Once spall is detected with this model, the deviatoric stresses are set to zero, and no hydrostatic tension $(p < 0)$ is permitted. If tensile pressures are calculated, they are reset to 0 in the spalled material. Thus, the spalled material behaves as a rubble or incohesive material. The hydrostatic tension spall model, $(ISPALL = 3)$, detects spall if the pressure becomes more tensile than the specified limit, p_{cut}. Once spall is detected the deviatoric stresses are set to zero, and the pressure is required to be compressive. If hydrostatic tension $(p < 0)$ is subsequently calculated, the pressure is reset to 0 for that element.

An effective plastic strain failure criterion is provided in this model. When $\bar{\varepsilon}^p = \bar{\varepsilon}^p_f$, the element no longer can supports any deviatoric stresses.

The element may be removed from the calculation when either the plastic strain or spall criterion ($ISPALL$ 2 or 3 only) are satisfied by specifying the appropriate deletion flag. If both flags are set, element removal will be governed by which ever failure mechanisms is satisfied first.

This model is applicable to a wide range of materials, including those with pressure-dependent yield behavior. The use of 16 points in the yield stress vs. effective plastic strain curve allows com-

plex post-yield hardening behavior to be accurately represented. In addition, the incorporation of an equation of state permits accurate modeling of diverse volumetric behavior. The spall model options permit incorporation of material failure, fracture, and disintegration effects under tensile loads.

Material Type 11 (Steinberg-Guinan High Rate Elastic-Plastic)

An equation of state must be used with this model.

Columns		Quantity	Format
1-10	Card 3	Shear modulus constant, G_0	E10.0
11-20		Yield stress constant, σ_0	E10.0
21-30		Strain hardening law constant, β	E10.0
31-40		Strain hardening exponent, n	E10.0
41-50		Initial plastic strain, γ_i	E10.0
51-60		Element deletion flag for plastic strain EQ.0.0: No element removal upon failure EQ.1.0: Element deleted when $\bar{\varepsilon}^p = \bar{\varepsilon}_f^p$	E10.0
61-70		Element deletion flag for spall ($ISPALL = 2, 3$ only) EQ.0.0: No element removal upon spall EQ.1.0: Element deleted by spall criterion	E10.0
71-80		Element deletion flag for volumetric strain EQ.0.0: No element removal upon failure EQ.1.0: Element deleted when $\varepsilon_v = \varepsilon_v^f$	E10.0
1-10	Card 4	Yield stress work hardening limit, σ_m	E10.0
11-20		Shear modulus pressure constant, b	E10.0
21-30		Yield stress pressure constant, b'	E10.0
31-40		Energy coefficient, h	E10.0
41-50		Energy exponential coefficient, f	E10.0
1-10	Card 5	Atomic weight, A (if $A = 0$, R' must be defined)	E10.0
11-20		Melting temperature constant, T_{mo}	E10.0
21-30		Thermodynamic gamma, γ_0	E10.0
31-40		Thermodynamic constant, a	E10.0
41-50		Pressure cutoff, p_{cut}	E10.0
51-60		Room temperature, T_{room} EQ.0.0: default set to 300.0	E10.0
61-70		Debye coefficient, θ EQ.0.0: Debye correction ignored.	E10.0

Columns		Quantity	Format
71-80		Volumetric strain at failure, ε_v^f EQ.0.0: no failure	E10.0
1-10	Card 6	Spall model, *ISPALL* EQ.0.0: default set to 2.0 EQ.1.0: Pressure limit model EQ.2.0: Maximum principal stress spall criterion EQ.3.0: Hydrostatic tension spall criterion	E10.0
11-20		R' (if $R' \neq 0$, the atomic weight A is not used)	E10.0
21-30		Effective plastic strain at failure, $\bar{\varepsilon}_f^p$ EQ.0.0: no failure	E10.0
31-40		Polynomial order for fit, $NFIT$ $(1 \leq NFIT \leq 9)$	E10.0
41-50		Cold compression energy polynomial flag, *IVAR* EQ.0.0: Polynomial coefficients given or fit in terms of η EQ.1.0: Polynomial coefficients given or fit in terms of μ	E10.0
51-60		Optional minimum limit for energy fit Input η_{min} if $IVAR = 0$ Input μ_{min} if $IVAR = 1$	E10.0
61-70		Optional maximum limit for energy fit Input η_{max} if $IVAR = 0$ Input μ_{max} if $IVAR = 1$	E10.0
1-16	Card 7	First cold compression polynomial coefficient, EC_0	E16.0
17-32		EC_1	E16.0
33-48		EC_2	E16.0
49-64		EC_3	E16.0
65-80		EC_4	E16.0
1-16	Card 8	EC_5	E16.0
17-32		EC_6	E16.0
33-48		EC_7	E16.0
49-64		EC_8	E16.0
65-80		EC_9	E16.0

The formulation of this model is described by Steinberg and Guinan (1978), and some notes on the implementation are given in (Woodruff, 1973).

In terms of the foregoing input parameters, we define the shear modulus, G, before the material melts as:

$$G = G_0\left[1 + bpV^{\frac{1}{3}} - h\left(\frac{E_i - E_c}{3R'} - 300\right)\right]e^{-\frac{fE_i}{E_m - E_i}} \tag{50}$$

where p is the pressure, V is the relative volume, E_i is the current energy, E_c is the cold compression energy, and E_m is the melting energy. The cold compression energy is calculated using

$$E_c(x) = \int_0^x p\,dx\,, \tag{51}$$

where $x = 1 - V$. The equation is integrated using initial energy E_o and pressure P_o conditions that correspond to zero K and are given by

$$E_o = -3R'T_{room} \tag{52}$$

and

$$P_o = \gamma_o E_o \mathrm{Debye}\left(\frac{\theta}{T_{room}}\right). \tag{53}$$

Here Debye is the Debye correction factor, and has a default value of 1 when $\theta = 0$. (For values of θ, see Zemansky, 1951.) The melting energy is found from the cold compression energy and the melting temperature using

$$E_m(x) = E_c(x) + 3R'T_m(x)\,, \tag{54}$$

where the melting temperature T_m is given by

$$T_m(x) = \frac{T_{mo}\exp(2ax)}{V^{2\left(\gamma_0 - a - \frac{1}{3}\right)}} \tag{55}$$

and T_{mo} is the melting temperature at the initial density, ρ_0.

In the above equations, R' is defined by

$$R' = \frac{R\rho}{A}, \tag{56}$$

where R is the universal gas constant and A is the atomic weight. **Note that if R' is not defined, DYNA3D computes it with R in the cm-gram-microsecond system of units.** Thus, this option should not be used unless the entire model is defined in the cm-gram-microsecond second system of units.

If E_m exceeds E_i (i.e., the material has not melted), then the yield strength σ_y is given by:

$$\sigma_y = \sigma'_0 \left[1 + b' p V^{\frac{1}{3}} - h \left(\frac{E_i - E_c}{3R'} - 300 \right) \right] e^{-\frac{f E_i}{E_m - E_i}} \quad . \tag{57}$$

The work-hardened yield stress σ'_0 is found from the initial yield stress σ_0 and the accumulated effective plastic strain $\bar{\varepsilon}^p$ using the hardening law

$$\sigma'_0 = \sigma_0 \left[1 + \beta (\gamma_i + \bar{\varepsilon}^p) \right]^n , \tag{58}$$

where γ_i is the initial plastic strain. If the work-hardened yield stress σ_0 exceeds the limiting value σ_m, then σ'_0 is reset to σ_m. After the materials melts ($E_i > E_m$), the yield stress σ_y and shear modulus G are reset to one half their initial value.

The evaluation of the cold compression energy $E_c(x)$ using (51) is too expensive to perform at each step of a calculation. As an approximation, many codes (including DYNA3D) use a polynomial to interpolate cold compression energy data during execution. If $IVAR = 0$, then the independent variable is chosen as η, and the polynomial takes the form

$$E_c = \sum_{i=0}^{9} EC_i \eta^i , \tag{59}$$

and if $IVAR = 1$, then the independent variable is μ and the polynomial takes the form

$$E_c = \sum_{i=0}^{9} EC_i \mu^i . \tag{60}$$

Note that the density and compression variables are related by

$$x = 1 - V = \frac{\mu}{\mu + 1} = 1 - \frac{1}{\eta} . \tag{61}$$

The coefficients EC_0 through EC_9 may be defined in the input if they are known. If they are not specified in the input, DYNA3D will fit the cold compression energy with up to a ten term polynomial expansion using a least squares method. If the order of the polynomial is not specified, DYNA3D will automatically pick the best polynomial order that fits the EOS generated data. Otherwise, DYNA3D will attempt to fit the data to the polynomial order desired. When DYNA3D performs any fit, the exact cold compression energy is compared with the cold compression energy found using the fitted polynomial at selected values of x, and the results printed in the "`hsp`" output file. These results should be examined closely to verify that a reasonably accurate polynomial fit has been obtained.

A Debye correction can be applied to the cold compression energy to improve the model's temperature response. This option is activated by specifying non-zero values of the Debye room temperature and coefficient θ. The cold compress energy is then calculated at zero Kelvin, instead of using (51) which starts at 300 K.

A choice of three spall models is offered to represent material splitting, cracking, and failure under tensile loads. The pressure limit model, $(ISPALL = 1)$, limits the hydrostatic tension to the specified value, p_{cut}. If pressures more tensile than this limit are calculated, the pressure is reset to p_{cut}. This option is not strictly a spall model, since the deviatoric stresses are unaffected by the pressure reaching the tensile cutoff, and the pressure cutoff value p_{cut} remains unchanged throughout the analysis. The maximum principal stress spall model, $(ISPALL = 2)$, detects spall if the maximum (most tensile) principal stress σ_{max} exceeds the limiting value $-p_{cut}$. Note that the negative sign is required because p_{cut} is measured positive in compression, while σ_{max} is positive in tension. Once spall is detected with this model, the deviatoric stresses are set to zero, and no hydrostatic tension $(p < 0)$ is permitted. If tensile pressures are calculated, they are reset to 0 in the spalled material. Thus, the spalled material behaves as a rubble or incohesive material. The hydrostatic tension spall model, $(ISPALL = 3)$, detects spall if the pressure becomes more tensile than the specified limit, p_{cut}. Once spall is detected the deviatoric stresses are set to zero, and the pressure is required to be compressive. If hydrostatic tension $(p < 0)$ is subsequently calculated, the pressure is reset to 0 for that element.

A failure criterion based on either effective plastic strain or volumetric strain is provided in this model. When the effective plastic strain or the volumetric strain exceeds the prescribed value $\bar{\varepsilon}_f^p$ and ε_v^f respectively, the deviatoric stresses are zeroed, and the element can only support hydrostatic stresses consistent with the particular spall model.

The element maybe removed from the calculation when either the plastic strain or spall criterion ($ISPALL$ 2 or 3 only) are satisfied by specifying the appropriate deletion flag. If both flags are set, element removal will be governed by which ever failure mechanisms is satisfied first.

The Steinberg-Guinan model is applicable to metals at high strain rates (near $10^5 s^{-1}$), where the enhancement of the yield stress due to strain rate effects has reached a limiting value and compression heating effects are becoming important. Model predictions may become substantially less accurate at low strain rates (below $10^3 s^{-1}$). Examples of problems in this high strain rate regime include some explosive forming operations, metal penetration problems, and the simulation of high velocity ballistic impact.

Material Type 12 (Isotropic-Elastic-Plastic)

Columns		Quantity	Format
1-10	Card 3	Shear modulus, G	E10.0
11-20		Yield stress, σ_0 (see Figure 4)	E10.0
21-30		Tangent modulus, E_T	E10.0
1-10	Card 4	Bulk modulus, K	E10.0
	Card 5	Blank	
		.	
		.	
		.	
	Card 8	Blank	

This model produces bilinear elastoplastic behavior which is identical to Material Type 3 with $\beta = 1.0$, but is slightly faster and requires less storage. Note also that the input quantities vary slightly from those of Material Type 3.

The theoretical foundations of this model are similar to those described for Material Type 3. The numerical algorithms are based on those described in (Krieg and Key, 1976).

Material Type 13 (Elastic-Plastic with Failure)

Columns		Quantity	Format
1-10	Card 3	Shear modulus, G	E10.0
11-20		Yield stress, σ_0 (see Figure 4)	E10.0
21-30		Tangent modulus, E_T	E10.0
31-40		Effective plastic strain at failure, $\bar{\varepsilon}_f^p$	E10.0
41-50		Failure pressure, p_f (positive in compression)	E10.0
1-10	Card 4	Bulk modulus, K	E10.0
1-10	Card 5	Effective plastic strain based element deletion, $EFLAG$ EQ.0.0: Element remains active EQ.1.0: Element is removed when $\bar{\varepsilon}^p = \bar{\varepsilon}_f^p$	E10.0
11-20		Pressure-based element deletion, $PFLAG$ EQ.0.0: Element remains active EQ.1.0: Element is removed when $p < p_f$	E10.0
	Card 6	Blank	
	Card 7	Blank	
	Card 8	Blank	

This model produces bilinear elastoplastic behavior identical to Material Type 12, except that two failure criteria have been incorporated. Before failure occurs, this model will give exactly the same behavior as Material Type 12, or Material Type 3 with $\beta = 1.0$. The theoretical formulation for the elastoplastic models is described in detail for Material Type 3.

Two failure criteria have been implemented in this model: an effective plastic strain based criterion, and a hydrostatic tension based criterion. If the effective plastic strain reaches the failure value $\bar{\varepsilon}_f^p$, then all deviatoric stresses are set to zero, and the stress state becomes hydrostatic and remains hydrostatic for the duration of the analysis. This hydrostatic stress state may include tensile values which are admissible to the pressure criterion. The pressure criterion is checked even after the element fails due to the strain criterion, and if the failure pressure is subsequently exceeded due to hydrostatic tension, then the element fails completely and can support only hydrostatic compressive stresses. If the pressure in the element becomes more tensile (negative) than the failure pressure p_f, then all stresses are set to zero and the element can never again support any hydrostatic tension at all, and can never again support any deviatoric stresses. The only possible stress state in such an element is pure hydrostatic compression.

Elements may be optionally removed from the calculation based upon either or both failure criteria. When an element deletion option is activated, the element is removed from the calculation when the associated failure criterion is reached. If both $EFLAG = 1$ and $PFLAG = 1$, the element will be deleted when either criterion is satisfied. Note, deleted element behave differently than completely failed elements in that they support **no** stresses -- not even hydrostatic compression.

This model is useful as an approximate representation of ductile (strain-based) or brittle (stress-based) failure in elastic or elastoplastic materials. After a material fails completely, its behavior is similar to that of a fluid in that it can only support purely hydrostatic compressive stresses.

Material Type 14 (Soil and Crushable Foam with Failure)

Columns		Quantity	Format
1-10	Card 3	Shear modulus, G	E10.0
11-20		Bulk unloading modulus, K_u	E10.0
21-30		First yield function constant, a_0	E10.0
31-40		Second yield function constant, a_1	E10.0
41-50		Third yield function constant, a_2	E10.0
51-60		Failure pressure for hydrostatic tension criterion, p_f (used only if $IFLAG = 0$)	E10.0
61-70		Failure criterion flag, $IFLAG$ EQ.0.0: Hydrostatic tension criterion EQ.1.0: Maximum principal stress criterion	E10.0
71-80		Maximum principal stress for failure criterion, σ_f, (used only if $IFLAG = 1$)	E10.0
1-10	Card 4	First (most tensile) tabulated volumetric strain, ε_{v1} (see Figure 10)	E10.0
11-20		First tabulated pressure, p_1	E10.0
21-30		Second tabulated volumetric strain, ε_{v2}	E10.0
31-40		Second tabulated pressure, p_2	E10.0
1-10	Card 5	Third tabulated volumetric strain, ε_{v3}	E10.0
11-20		Third tabulated pressure, p_3	E10.0
21-30		Fourth tabulated volumetric strain, ε_{v4}	E10.0
31-40		Fourth tabulated pressure, p_4	E10.0
1-10	Card 6	Fifth tabulated volumetric strain, ε_{v5}	E10.0
11-20		Fifth tabulated pressure, p_5	E10.0
21-30		Sixth tabulated volumetric strain, ε_{v6}	E10.0
31-40		Sixth tabulated pressure, p_6	E10.0
1-10	Card 7	Seventh tabulated volumetric strain, ε_{v7}	E10.0
11-20		Seventh tabulated pressure, p_7	E10.0
21-30		Eighth tabulated volumetric strain, ε_{v8}	E10.0
31-40		Eighth tabulated pressure, p_8	E10.0

Columns		Quantity	Format
1-10	Card 8	Ninth tabulated volumetric strain, ε_{v9}	E10.0
11-20		Ninth tabulated pressure, p_9	E10.0
21-30		Modified elliptical surface flag, *AMOD*	E10.0
31-40		Unloading factor, α (UOPT=2 only)	E10.0
41-50		Initial relative volume EQ.0.0: no initial relative volume specified (default) GT.0.0: default initial relative volume	E10.0
51-60		Unloading option, UOPT EQ.0.0: volumetric crushing upon unloading EQ.1.0: no volumetric crushing upon unloading EQ.2.0: limited volumetric crushing - variable slope EQ.3.0: limited volumetric crushing - fixed slope	E10.0
61-70		Load curve number for time-dependent relative volume EQ.0.0: no load curve included (default) GT.0.0: load curve number describing relative volume	E10.0
71-80		Hysteresis factor, γ (UOPT=2,3 only)	E10.0

Before failure, the behavior of this model is identical to Material Type 5.

Pressure is positive in compression, and volumetric strain is negative in compression. Volumetric strain is given by the natural log of the relative volume. The tabulated pressure-volumetric strain data may contain up to nine pairs of points, and must be given in order of *increasing* compression.

The deviatoric perfectly plastic yield function ϕ is defined as

$$\phi = J_2 - [a_0 + a_1 p + a_2 p^2], \tag{62}$$

where a_0, a_1, and a_2 are constants, p is pressure, and J_2 is the second invariant of the deviatoric stress tensor $\boldsymbol{s}$ given by

$$J_2 = \frac{1}{2} s_{ij} s_{ij}. \tag{63}$$

Plastic flow is nonassociative if a_1 or a_2 is nonzero.

On the yield surface $J_2 = \frac{1}{3}\sigma_y^2$, where σ_y is the uniaxial yield stress. Thus, the yield stress at any pressure p is given by

$$\sigma_y = [3(a_0 + a_1 p + a_2 p^2)]^{\frac{1}{2}} . \quad (64)$$

There is no strain hardening in this model, so the yield stress is completely determined by the pressure.

To eliminate the pressure dependence of the yield strength, set $a_1 = a_2 = 0$ and $a_0 = \frac{1}{3}\sigma_y^2$. This approach is useful when a pressure-independent, elastic perfectly-plastic model with failure is desired for use with tabulated volumetric data.

This model allows one of two failure criteria to be used: a hydrostatic tension criterion $(IFLAG = 0)$ or a maximum principal stress criterion $(IFLAG = 1)$. The hydrostatic tension criterion detects failure if the pressure in the element is less than the specified failure pressure, p_f (recall that pressure is positive in compression). Once failure is detected by this criterion, all stresses in the element are set to zero, and the element can never again sustain any hydrostatic tension or shear stresses. The element can only support purely compressive hydrostatic stresses, and therefore behaves like a fluid. The maximum principal stress criterion detects failure if the largest (most tensile) principal stress exceeds the specified failure stress, σ_f. Once failure is detected by the maximum principal stress criterion, the deviatoric stresses are gradually reduced to zero over a few time steps, and the hydrostatic pressure is left unchanged. This gradual reduction of the deviatoric stresses has been found to introduce less noise into some problems than an abrupt reduction of the deviatoric stresses to zero.

This material model is useful as a simple representation of pressure hardening, where the deviatoric yield strength of a material increases as the hydrostatic pressure increases. At any constant pressure, the deviatoric behavior is elastic perfectly-plastic. A failure criterion based on either hydrostatic tension or maximum principal stress may be used to approximately represent the degradation of material strength under extreme loads. This model permits a general representation of the volumetric behavior of the material via a tabulated pressure-volumetric strain curve. This flexibility makes Material Type 14 useful for representing materials with a stiffening pressure-volume curve. Such stiffening behavior is frequently found in porous materials such as wood or foam. This model is also often used as a simplified model for concrete or soil.

If the material is pre-stressed, an initial relative volume can be input on the 8th card. This value may be overwritten or prescribed on an element by element basis by specifying an initial relative volume on the element definition card (see SOLID ELEMENTS on page 308). When an initial relative volume is present, a corresponding pressure is internally calculated from the pressure-

volumetric strain curve. The element's effective relative volume is the sum of the deformation induced relative volume, any prescribed initial relative volume, and an optionally included user-imposed complementary relative volume. The user-imposed complementary relative volume is defined as a function of time and specified with a load curve. It is useful for phasing in an initial volumetric deformation or cushioning the instantaneous high stresses that arise from some pre-stressing conditions.

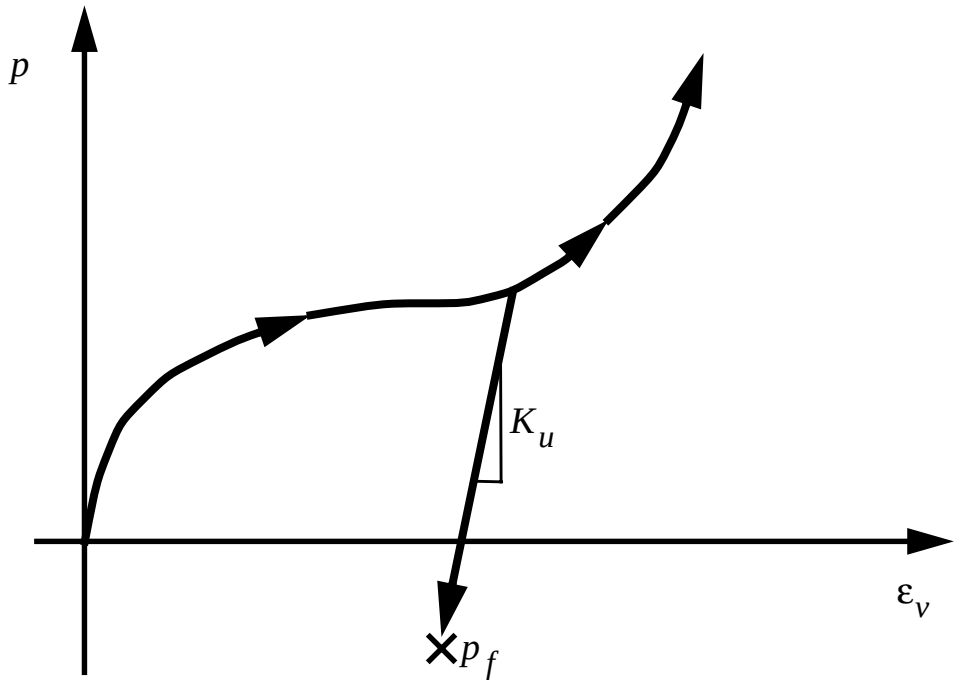

Figure 10
Pressure vs. volumetric strain curve for soil and crushable foam model.

A hysteresis effect, as shown in Figure 8, may be introduced into the volumetric response by using *UOPT*=2 or 3. Here the saturation portions of the unload pressure versus volumetric strain curve is given by $\gamma P(\varepsilon_v)$. The slope of the transition between the loading and unloading curves, K_{unload}, can be set proportional to the $P(\varepsilon_v)$ curve as

$$K_{unload} = \alpha \frac{dP(\varepsilon_v)}{d\varepsilon_v} \tag{65}$$

with *UOPT*=2, or be fixed as

$$K_{unload} = K_u \tag{66}$$

with *UOPT*=3.

Material Type 15 (Johnson/Cook Elastic-Plastic)

An equation of state must be used with this model for solid elements.

Columns		Quantity	Format
1-10	Card 3	Shear modulus, G (solid elements only, blank for shells)	E10.0
11-20		Yield stress constant, A	E10.0
21-30		Strain hardening coefficient, B	E10.0
31-40		Strain hardening exponent, n	E10.0
41-50		Strain rate dependence coefficient, C	E10.0
51-60		Temperature dependence exponent, m	E10.0
61-70		Melt temperature, T_m, in degrees Kelvin	E10.0
71-80		Room temperature, T_r, in degrees Kelvin	E10.0
1-10	Card 4	Reference strain rate, $\dot{\varepsilon}_0$	E10.0
11-20		Specific heat, c_v	E10.0
21-30		Pressure cutoff, p_{cut}, or failure stress, σ_m	E10.0
31-40		Spall model, *ISPALL* EQ.1.0: Pressure limit model (default - solids) EQ.1.0: No spall model (default - shells) EQ.2.0: Maximum principal stress spall criterion EQ.3.0: Hydrostatic tension spall criterion	
41-50		Plastic strain iteration flag, *ITER* EQ.0.0: fast approx. solution for plastic strain (default) EQ.1.0: accurate iterative solution for plastic strain (More expensive than default.)	E10.0
51-60		Element deletion flag based upon spall (solids only) EQ.0.0: No element removal EQ.1.0: Element deleted upon spall (*ISPALL* 2 & 3 only)	E10.0
1-10	Card 5	First failure parameter, D_1	E10.0
11-20		D_2	E10.0
21-30		D_3	E10.0
31-40		D_4	E10.0
41-50		D_5	E10.0

Columns		Quantity	Format
51-60		Element deletion flag for damage EQ.0.0: No element removal upon fracture EQ.1.0: Element deleted when $D = 1$	E10.0
.	Card 6	Blank	
.	Card 7	Blank	
1-10	Card 8	Young's modulus, E (shells only, blank for solid elements)	E10.0
11-20		Poisson's ratio, ν (shells only, blank for solid elements)	E10.0
21-30		Time step size for element deletion, Δt_{crit}	E10.0

The formulation of this model is described and constants for many materials are given in Johnson and Cook (1983).

The yield stress is written as

$$\sigma_y = [A + B(\bar{\varepsilon}^p)^n][1 + C ln(\dot{\varepsilon}^*)][1 - (T^*)^m] \quad , \tag{67}$$

where A, B, C, n and m are input constants, $\bar{\varepsilon}^p$ is the effective plastic strain, $\dot{\varepsilon}^*$ is the nondimensional strain rate, and T^* is the homologous temperature. The effective plastic strain $\bar{\varepsilon}^p$ is given by

$$\bar{\varepsilon}^p = \int_0^t d\bar{\varepsilon}^p, \tag{68}$$

where the incremental effective plastic strain $d\bar{\varepsilon}^p$ is found from the incremental plastic strain tensor $d\varepsilon_{ij}$ as

$$d\bar{\varepsilon}^p = \left\{\frac{2}{3} d\bar{\varepsilon}^p_{ij} d\bar{\varepsilon}^p_{ij}\right\}^{\frac{1}{2}}. \tag{69}$$

The nondimensional strain rate $\dot{\varepsilon}^*$ is calculated from

$$\dot{\varepsilon}^* = \frac{\dot{\bar{\varepsilon}}^p}{\dot{\varepsilon}_0} \tag{70}$$

where $\dot{\bar{\varepsilon}}^p$ is the effective plastic strain rate and $\dot{\varepsilon}_0$ is the reference strain rate defined in the input. The homologous temperature T^* is the ratio of the current temperature to the melting temperature when both are expressed in degrees Kelvin. Temperature change in this model is computed assuming adiabatic conditions, i.e., no heat transfer between elements. This is usually a good

assumption since transient dynamic problems typically occur over such a short time interval that the actual heat transfer is negligible. Heat is generated in an element by plastic work, and the resulting temperature rise is computed using the specific heat for the material.

Due to the nonlinearity in the dependence of the yield stress on plastic strain, an accurate value of the yield stress requires expensive iteration for calculation of the increment in plastic strain. However, by using a Taylor series expansion with linearization about the current state, σ_y can be approximated with sufficient accuracy to avoid iteration and achieve optimum execution speed.

This implementation of the Johnson-Cook model also contains a damage model. The strain at fracture ε_f is given by

$$\varepsilon_f = [D_1 + D_2 exp(D_3 \sigma^*)][1 + D_4 ln(\dot{\varepsilon}^*)][1 + D_5 T^*] \tag{71}$$

where σ^* is the ratio of pressure divided by effective stress

$$\sigma^* = \frac{p}{\bar{\sigma}}, \tag{72}$$

and effective stress $\bar{\sigma}$ is found from

$$\bar{\sigma} = \left\{ \frac{3}{2} s_{ij} s_{ij} \right\}^{\frac{1}{2}}. \tag{73}$$

Note that this definition of σ^* may be reversed in sign from convention in the original publications of Johnson and Cook; the sign of D_3 should be chosen carefully.

Fracture occurs when the damage parameter D exceeds the value of 1. The evolution of the damage parameter is given by

$$D = \sum \frac{\Delta \bar{\varepsilon}^p}{\varepsilon_f}, \tag{74}$$

where the summation is performed over all time steps in the analysis. When fracture occurs, all stresses are set to zero and remain zero for the rest of the calculation.

A choice of three spall models is offered to represent material splitting, cracking, and failure under tensile loads for solids. The pressure limit model, $(ISPALL = 1)$, limits the hydrostatic tension to the specified value, p_{cut}. If pressures more tensile than this limit are calculated, the pressure is reset to p_{cut}. This option is not strictly a spall model, since the deviatoric stresses are unaffected by the pressure reaching the tensile cutoff, and the pressure cutoff value p_{cut} remains unchanged throughout the analysis. The pressure cutoff, p_{cut}, is defined to be negative in tension. The maximum principal stress spall model, $(ISPALL = 2)$, detects spall if the maximum (most

tensile) principal stress σ_{max} exceeds the limiting value σ_m. Once spall is detected with this model, the deviatoric stresses are set to zero, and no hydrostatic tension $(p < 0)$ is permitted. If tensile pressures are calculated, they are reset to 0 in the spalled material. Thus, the spalled material behaves as a rubble or incohesive material. The hydrostatic tension spall model, $(ISPALL = 3)$, detects spall if the pressure becomes more tensile than the specified limit, p_{cut}. Once spall is detected, the deviatoric stresses are set to zero and the pressure is required to be compressive. If hydrostatic tension $(p < 0)$ is calculated, then the pressure is reset to 0 for that element. For shell elements, the option $(ISPALL = 1)$ deactivates the spall feature; however, the other two spall models are available.

In addition to the above failure criterion, this model also supports two element deletion criterion. When the element fails due to accumulated damage, it may be optionally removed from the calculation. Also, an optional maximum stable time step size, Δt_{crit} may be prescribed. It supersedes other material or globally specified values. Generally, Δt_{max} goes down as the element becomes more distorted. To assure stability of time integration, the global DYNA3D time step is the *minimum* of the Δt_{max} values calculated for all elements in the model. Using this option allows the selective deletion of elements whose time step Δt_{max} has fallen below the specified minimum time step, Δt_{crit}. Elements which are severely distorted often indicate that material has failed and supports little load, but these same elements may have very small time steps and therefore control the cost of the analysis. This option allows these highly distorted elements to be deleted from the calculation. Therefore the analysis can proceed at a larger time step and thus at a reduced cost. Deleted elements do not carry any load. Deleted shell elements are removed from all applicable slide surface definitions, while solid elements are only removed from applicable SAND slide surfaces. Clearly, this option must be judiciously used to obtain accurate results at a minimum cost.

Material Type 15 is applicable to the high rate deformation of many materials, including most metals. Unlike the Steinberg-Guinan model (Material Type 11), the Johnson-Cook model remains valid down to lower strain rates, and even into the quasistatic regime. Typical applications include explosive metal forming, ballistic penetration, and impact.

Material Type 16 (Concrete/Geological Material)

This model must be used with equation of state type 8, 9, or 11.

Columns		Quantity	Format
1-10	Card 3	First elastic constant Poisson's ratio, ν, for constant ν model Negative of shear modulus, $-G$, for constant G model	E10.0
11-20		Maximum principal stress at failure, σ_{cut}	E10.0
21-30		Cohesion, a_0	E10.0
31-40		Pressure hardening coefficient, a_1	E10.0
41-50		Pressure hardening coefficient, a_2	E10.0
51-60		Damage scaling factor, b_1	E10.0
61-70		Cohesion for failed material, a_{0f}	E10.0
71-80		Pressure hardening coefficient for failed material, a_{1f}	E10.0
1-10	Card 4	Percent reinforcement, $\hat{f}_r$ $(0 \le \hat{f}_r \le 100\%)$	E10.0
11-20		Elastic modulus for reinforcement, E_r	E10.0
21-30		Poisson's ratio for reinforcement, ν_r	E10.0
31-40		Initial yield stress, σ_0	E10.0
41-50		Tangent modulus, E_T	E10.0
51-60		Load curve giving rate sensitivity for principal material, N_1	E10.0
61-70		Load curve giving rate sensitivity for reinforcement, N_2	E10.0
1-10	Card 5	First tabulated effective plastic strain, $\bar{\varepsilon}_1^p$, or pressure, p_1	E10.0
.		.	.
.		.	.
.		.	.
71-80		$\bar{\varepsilon}_8^p$ or p_8	E10.0
1-10	Card 6	$\bar{\varepsilon}_9^p$ or p_9	E10.0
.		.	.
.		.	.
.		.	.
71-80		$\bar{\varepsilon}_{16}^p$ or p_{16}	E10.0

Columns		Quantity	Format
1-10	Card 7	First tabulated yield stress, σ_{y1}	E10.0
.		.	.
.		.	.
.		.	.
71-80		σ_{y8}	E10.0
1-10	Card 8	σ_{y9}	E10.0
.		.	.
.		.	.
.		.	.
71-80		σ_{y16}	E10.0

Material Type 16 was developed to give concrete and geological material modeling capabilities to DYNA3D. It can be used in two major modes - a fairly simple tabular pressure-dependent yield surface, and a potentially complex model featuring two yield versus pressure functions with various means of migrating from one curve to the other. For both modes, load curve N_1 is taken to be a strain rate multiplier for the yield strength.

Note that this model must be used with Equation-of-State type 8, 9 or 11.

Response Mode I. Tabulated Yield Stress Versus Pressure

This mode is well suited for implementing standard geologic models like the Mohr-Coulomb yield surface with a Tresca limit, as shown in Figure 11. Examples of converting conventional triaxial compression data to this type of model are found in (Desai and Siriwardane, 1984). Note that under conventional triaxial compression conditions, the DYNA3D input corresponds to an ordinate of $\sigma_1 - \sigma_3$ rather than the more widely used $\frac{\sigma_1 - \sigma_3}{2}$, where σ_1 is the maximum principal stress and σ_3 is the minimum principal stress.

Using Material Type 16 combined with Equation-of-State Type 9 (saturated) or Type 11 (air filled porosity), has been successfully used to model ground shocks and soil/structure interactions at pressures up to 100 kbar (approximately 1.5×10^6 psi).

To invoke Mode I of this model, set a_0, a_1, a_2, b_1, a_{0f}, and a_{1f} to zero. The tabulated values of pressure should then be specified on cards 5 and 6, and the corresponding values of yield stress should be specified on cards 7 and 8. The parameters relating to reinforcement properties, initial yield stress, and tangent modulus are not used in this response mode, and should be set to zero.

Simple tensile failure

Note that a_{1f} is reset internally to 1/3 even though it is input as zero; this defines a failed material curve of slope $3p$, where p denotes pressure (positive in compression). In this case the yield strength is taken from the tabulated yield vs. pressure curve until the maximum principal stress (σ_1) in the element exceeds the tensile cut-off (σ_{cut}). For every time step that $\sigma_1 > \sigma_{cut}$ the yield strength is scaled back by a fraction of the distance between the two curves until after 20 time steps the yield strength is defined by the failed curve. The only way to inhibit this feature is to set σ_{cut} arbitrarily large.

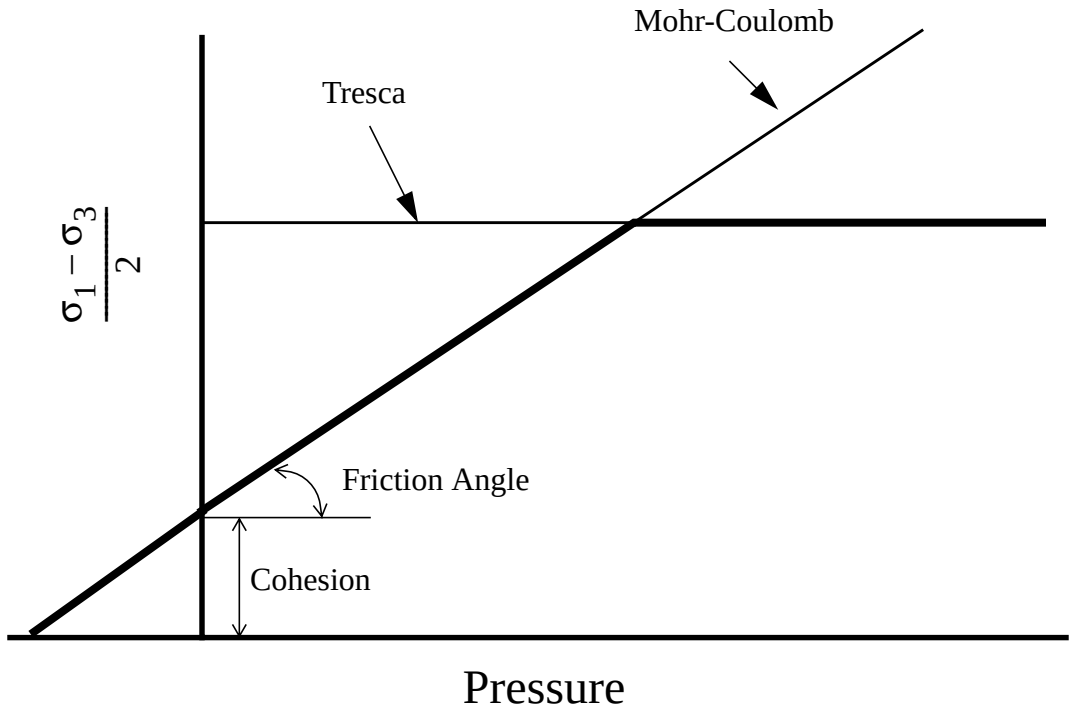

Figure 11
Mohr-Coulomb surface with a Tresca limit.

Response Mode II. Two Curve Model with Damage and Failure

This approach uses two yield versus pressure curves of the form

$$\sigma_y = a_0 + \frac{p}{a_1 + a_2 p}. \tag{75}$$

The upper curve is best described as the maximum yield strength curve and the lower curve is the failed material curve. There are a variety of ways of moving between the two curves, and each is discussed below.

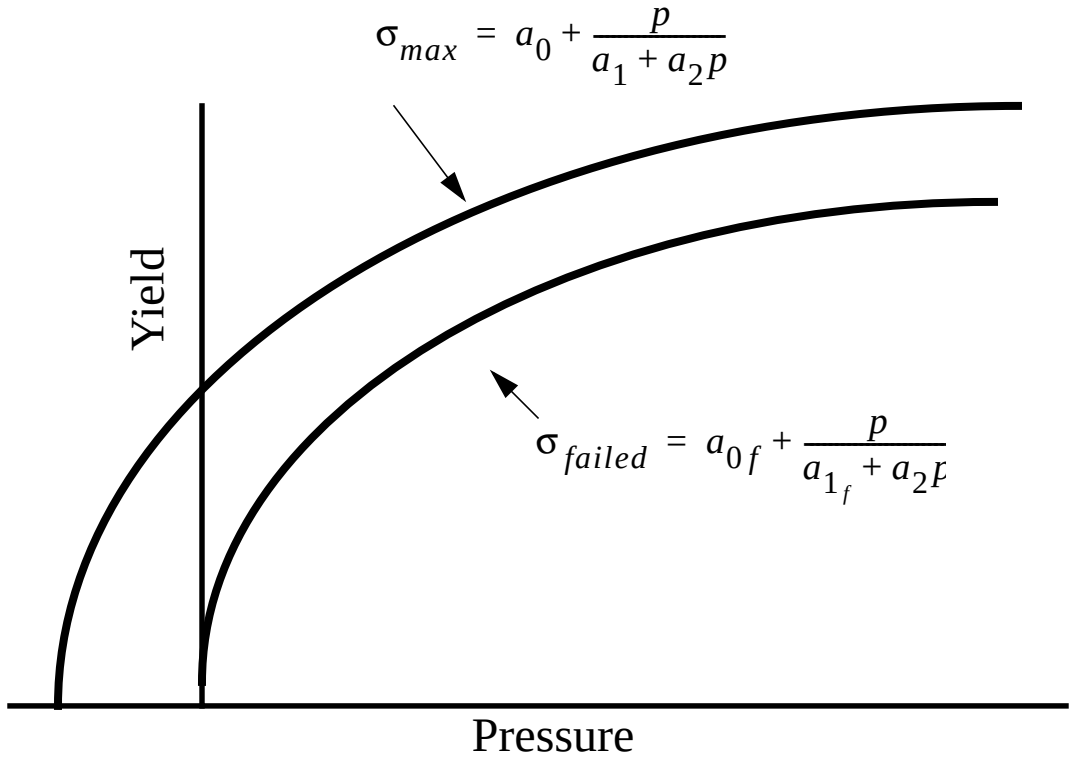

Figure 12
Two-curve concrete model with damage and failure.

Mode II.A: Simple tensile failure

Define a_0, a_1, a_2, a_{0f} and a_{1f}, set b_1 to zero, and leave cards 5 through 8 blank. In this case the yield strength is taken from the maximum yield curve until the maximum principal stress (σ_1) in the element exceeds the tensile cut-off (σ_{cut}). For every time step that $\sigma_1 > \sigma_{cut}$ the yield strength is scaled back by a fraction of the distance between the two curves until after 20 time steps the yield strength is defined by the failed curve.

Mode II.B: Tensile failure plus plastic strain scaling

Define a_0, a_1, a_2, a_{0f} and a_{1f}, set b_1 to zero, and use cards 5 through 8 to define a scale factor, η, versus effective plastic strain. DYNA3D evaluates η at the current effective plastic strain and then calculates the yield stress as

$$\sigma_{yield} = \sigma_{failed} + \eta\,(\sigma_{max} - \sigma_{failed}) \,, \tag{76}$$

where σ_{max} and σ_{failed} are found as shown in Figure 12. The yield strength is then subject to scaling for tensile failure as described above. This type of model allows the description of a strain hardening and/or softening material such as concrete.

Mode II.C: Tensile failure plus damage scaling

The change in yield stress as a function of plastic strain arises from physical mechanisms such as internal cracking, and the extent of this cracking is affected by the hydrostatic pressure when the cracking occurs. This mechanism gives rise to the “confinement” effect on concrete behavior. To account for this phenomenon a “damage” function was defined and incorporated into Material Type 16. The damage function is given by

$$\lambda = \int_0^{\bar{\varepsilon}^p} \frac{d\bar{\varepsilon}^p}{\left(1 + \dfrac{p}{\sigma_{cut}}\right)^{b_1}} \tag{77}$$

Define a_0, a_1, a_2, a_{0f}, a_{1f}, and b_1. Cards 5 through 8 now give η as a function of λ and scale the yield stress as

$$\sigma_{yield} = \sigma_{failed} + \eta\,(\sigma_{max} - \sigma_{failed}) \tag{78}$$

and then apply any tensile failure criteria.

Mode II Concrete Model Options

Material Type 16 in Mode II provides for the automatic internal generation of a simple "generic" model for concrete. If a_0 is negative, then σ_{cut} is assumed to be the unconfined concrete compressive strength (f_c') and $-a_0$ is assumed to be a conversion factor from DYNA pressure units to psi. In this case the parameter values generated internally are:

$$\sigma_{cut} = 1.7\left[\frac{(f_c')^2}{-a_0}\right]^{1/3} \tag{79}$$

$$a_0 = \frac{f_c'}{4} \tag{80}$$

$$a_1 = \frac{1}{3} \tag{81}$$

$$a_2 = \frac{1}{3f_c'} \tag{82}$$

$$a_{0f} = 0 \tag{83}$$

$$a_{1f} = 0.385 \tag{84}$$

Note that these a_{0f} and a_{1f} defaults will be overridden by nonzero entries on Card 3. If plastic strain or damage scaling is desired, Cards 5 through 8 and b_1 should be specified in the input. When a_0 is input as a negative quantity, the Equation-of-State can be given as 0 and a trilinear EOS Type 8 model will be automatically generated from the unconfined compressive strength and Poisson's ratio. The EOS 8 model is a simple pressure versus volumetric strain model with no internal energy terms, and should give reasonable results for pressures up to 5 kbar (approximately 75,000 psi).

Mixture model

A reinforcement fraction, $\hat{f}_r$, can be defined along with properties of the reinforcement material. The bulk modulus, shear modulus, and yield strength are then calculated from a simple mixture rule. This feature is *experimental* and should be used with caution. It gives an isotropic effect in the material instead of the true anisotropic material behavior. A reasonable approach would be to use mixture elements only where the reinforcing exists and plain elements elsewhere. When the mixture model is being used, the strain rate multiplier for the principal material is taken from load curve N_1 and the multiplier for the reinforcement is taken from load curve N_2.

A Suggestion

Moor (1991) suggests using the damage function (Mode II.C.) in Material Type 16 with the following set of parameters:

$$a_0 = \frac{f'_c}{4} \tag{85}$$

$$a_1 = \frac{1}{3} \tag{86}$$

$$a_2 = \frac{1}{3 f'_c} \tag{87}$$

$$a_{0f} = \frac{f'_c}{10} \tag{88}$$

$$a_{1f} = 1.5 \tag{89}$$

$$b_1 = 1.25 \tag{90}$$

and a damage table of:

Card 5	0.0	8.62e-06	2.15e-05	3.14e-05	3.95e-05	5.17e-04	6.38e-04	7.98e-04
Card 6	9.67e-04	1.41e-03	1.97e-03	2.59e-03	3.27e-03	4.00e-03	4.79e-03	0.909
Card 7	0.309	0.543	0.840	0.975	1.00	0.790	0.630	0.469
Card 8	0.383	0.247	0.173	0.136	0.114	0.086	0.056	0.0

This set of parameters should give results consistent with (Dilger, Koch, and Kowalczyk, 1984) for plain concrete. It has been successfully used for reinforced structures where the reinforcing bars were modeled explicitly with embedded beam and shell elements. The model does not incorporate the major failure mechanism - separation of the concrete and reinforcement leading to catastrophic loss of confinement pressure. However, experience indicates that this physical behavior will occur when this model shows about 4% strain.

Material Type 17 (Isotropic Elastic-Plastic with Oriented Cracks)

An equation of state must be used with this model.

Columns		Quantity	Format
1-10	Card 3	Young's modulus, E	E10.0
1-10	Card 4	Poisson's ratio, ν	E10.0
1-10	Card 5	Yield stress, σ_0	E10.0
1-10	Card 6	Tangent modulus, E_T	E10.0
1-10	Card 7	Fracture strength, σ_f	E10.0
1-10	Card 8	Pressure cutoff, p_{cut} (positive in compression)	E10.0

Material Type 17 is experimental, and should be used with caution.

This model provides isotropic elastic-plastic material response identical to Material Type 12, and additionally incorporates a fracture and failure model. In contrast to the fracture and failure models available in other elastic-plastic material models, this fracture model incorporates the effects of crack orientation.

The yield condition can be written

$$\phi = \bar{\sigma} - \sigma_y(\bar{\varepsilon}^p), \tag{91}$$

where $\bar{\sigma}$ is the effective stress and σ_y is the current yield stress, which may be a function of the effective plastic strain $\bar{\varepsilon}^p$ if strain hardening is included. The effective stress $\bar{\sigma}$ is given by

$$\bar{\sigma} = \left\{\frac{3}{2} s_{ij} s_{ij}\right\}^{\frac{1}{2}}, \tag{92}$$

where s_{ij} is the deviatoric stress tensor.

The linear isotropic strain hardening law has the form

$$\sigma_y = \sigma_0 + E_p \bar{\varepsilon}^p, \tag{93}$$

where σ_0 is the initial yield stress and E_p is the plastic modulus. The effective plastic strain $\bar{\varepsilon}^p$ is given by

$$\bar{\varepsilon}^p = \int_0^t d\bar{\varepsilon}^p, \tag{94}$$

where the incremental effective plastic strain $d\bar{\varepsilon}^p$ is found from the incremental plastic strain tensor $d\varepsilon_{ij}$ as

$$d\bar{\varepsilon}^p = \left\{ \frac{2}{3} d\bar{\varepsilon}^p_{ij} d\bar{\varepsilon}^p_{ij} \right\}^{\frac{1}{2}}. \tag{95}$$

The plastic modulus is found from Young's modulus E and the tangent modulus E_T using

$$E_p = \frac{E E_T}{E - E_T}. \tag{96}$$

The plastic hardening modulus E_p is the slope of the effective stress $\bar{\sigma}$ vs. effective plastic strain $\bar{\varepsilon}^p$ curve, and the tangent modulus E_T is the slope of the inelastic part of a uniaxial stress vs. strain curve (or equivalently, the effective stress vs. effective strain curve).

A pressure cutoff limits the hydrostatic tension to the specified value, p_{cut}. If pressures more tensile than this limit are calculated, the pressure is reset to p_{cut}.

The oriented crack fracture model is based on a maximum principal stress criterion. When the maximum principal stress exceeds the fracture stress, σ_f, the element fails on a plane perpendicular to the direction of the maximum principal stress. The normal stress and two shear stresses on that plane are then reduced to zero. This stress reduction is done according to a delay function that reduces the stresses gradually to zero over a small number of time steps. This delay function procedure is used to reduce the ''ringing,'' or high frequency noise, introduced into the system caused by the sudden fracture.

After a tensile fracture, the element will not support any tensile stresses on the fracture plane, but in compression will support both normal and shear stresses. The orientation of this fracture surface is tracked throughout the deformation, and is updated to properly model finite deformation effects. If the maximum principal stress subsequently exceeds the fracture stress in another direction, the element failure is isotropic. In this case the element completely loses its ability to support any shear stresses or hydrostatic tension, and only compressive hydrostatic stress states are possible. Thus, once isotropic failure has occurred, the material behaves like a fluid.

This model is applicable to elastic or elastoplastic materials under significant tensile or shear loadings when fracture is expected. Potential applications include brittle materials such as ceramics (with $\sigma_0 = \sigma_f$ in the yield function), as well as porous materials such as concrete in cases where pressure hardening effects are not significant.

Material Type 18 (Power Law Isotropic Elastic-Plastic)

Columns		Quantity	Format
1-10	Card 3	Young's modulus, E	E10.0
11-20		Poisson's ratio, ν	E10.0
21-30		Yield stress coefficient, k	E10.0
31-40		Strain hardening exponent, n n can not be 1.0.	E10.0
41-50		Optional: ε_o	E10.0
	Card 4	Blank	
	Card 5	Blank	
	.		
	.		
	.		
	Card 8	Blank	

The material behavior is elastoplastic with nonlinear isotropic strain hardening given by a power law expression. The yield condition can be written

$$\phi = \bar{\sigma} - \sigma_y(\bar{\varepsilon}^p), \tag{97}$$

where $\bar{\sigma}$ is the effective stress and σ_y is the current yield stress. The hardening law has the form

$$\sigma_y = k(\varepsilon_0 + \bar{\varepsilon}^p)^n, \tag{98}$$

where ε_0 is the initial yield strain and, if undefined, is given by

$$\varepsilon_0 = \left(\frac{E}{k}\right)^{\frac{1}{n-1}}. \tag{99}$$

This model is generally applicable to ductile materials such as metals. Although similar to Material Types 3 and 12, this model provides additional flexibility in specifying the post-yield behavior with a nonlinear isotropic hardening law.

Material Type 19 (Strain Rate Dependent Isotropic Elastic-Plastic)

Columns		Quantity	Format
1-10	Card 3	Young's modulus, E	E10.0
11-20		Poisson's ratio, ν	E10.0
21-30		Load curve number for yield stress σ_0 as a function of strain rate $\dot{\bar{\varepsilon}}$	E10.0
31-40		Tangent modulus, E_T	E10.0
41-50		Optional load curve number defining Young's modulus as a function of strain rate	E10.0
51-60		Optional load curve number defining the tangent modulus as a function of strain rate	E10.0
61-70		Optional load curve number defining the effective stress at failure $\bar{\sigma}_f$ as a function of strain rate	E10.0
71-80		Time step size for automatic element deletion, Δt_{crit}	E10.0
	Card 4	Blank	
	Card 5	Blank	
	.		
	.		
	.		
	Card 8	Blank	

The material behavior is elastoplastic with strain rate dependent isotropic hardening. The yield condition can be written

$$\phi = \bar{\sigma} - \sigma_y(\bar{\varepsilon}^p, \dot{\bar{\varepsilon}}) , \tag{100}$$

where $\bar{\sigma}$ is the effective stress and σ_y is the current yield stress, which may depend on the effective plastic strain $\bar{\varepsilon}^p$ and the current effective strain rate, $\dot{\bar{\varepsilon}}$. The effective stress is found from the deviatoric stress tensor s_{ij} as

$$\bar{\sigma} = \left\{ \frac{3}{2} s_{ij} s_{ij} \right\}^{\frac{1}{2}} . \tag{101}$$

The isotropic strain hardening law has the form

$$\sigma_y = \sigma_0(\dot{\bar{\varepsilon}}) + E_p \bar{\varepsilon}^p , \tag{102}$$

where σ_0 is the initial yield stress, determined by the load curve specification of σ_0 vs. $\dot{\bar{\varepsilon}}$, and E_p is the plastic hardening modulus. The effective strain rate $\dot{\bar{\varepsilon}}$ is defined as

$$\dot{\bar{\varepsilon}} = \left(\frac{2}{3}\dot{e}_{ij}\dot{e}_{ij}\right)^{\frac{1}{2}}, \tag{103}$$

where $\dot{e}_{ij}$ is the deviatoric strain rate tensor. The plastic modulus E_p represents the slope of the effective stress vs. effective plastic strain curve, and the tangent modulus E_T represents the slope of the inelastic portion of the uniaxial stress vs. uniaxial strain curve. The plastic modulus can be written in terms of the Young's modulus E and the tangent modulus E_T as

$$E_p = \frac{EE_T}{E - E_T}. \tag{104}$$

Both Young's modulus and the tangent modulus may optionally be made functions of strain rate by specifying a load curve number giving their values as a function of strain rate. If these load curve numbers are input as 0, then the constant values specified in the input are used.

Note: *All load curves used to define quantities as a function of strain rate must have the same number of points and the same strain rate values.* This requirement is used to allow vectorized interpolation to enhance the execution speed of this model.

This model also contains a mechanism for modeling material failure. This option is activated by specifying a load curve defining the effective stress at failure $\bar{\sigma}_f$ as a function of strain rate. For solid elements, once the effective stress exceeds $\bar{\sigma}_f$, the element is deemed to have failed. For shell elements, all integration point through the thickness must have an effective stress greater than σ_f. Once failure is detected in an element, all stresses are set to zero, and the element is removed from the problem.

In addition to the above failure criterion, this material model also supports a element deletion criterion based on the maximum stable time step size for this element, Δt_{max}. Generally, Δt_{max} goes down as the element becomes more distorted. To assure stability of time integration, the global DYNA3D time step is the *minimum* of the Δt_{max} values calculated for all elements in the model. Using this option allows the selective deletion of elements whose time step Δt_{max} has fallen below the specified minimum time step, Δt_{crit}. Elements which are severely distorted often indicate that material has failed and supports little load, but these same elements may have very small time steps and therefore control the cost of the analysis. This option allows these highly distorted elements to be deleted from the calculation, and therefore the analysis can proceed at a larger time step, and

thus at a reduced cost. Deleted elements do not carry any load. Shell elements are deleted from all applicable slide surface definitions. Solid elements are only deleted from SAND type slide surfaces. Clearly, this option must be judiciously used to obtain accurate results at a minimum cost.

Material Type 20 (Rigid)

Columns		Quantity	Format
1-10	Card 3	Young's modulus, E	E10.0
1-10	Card 4	Poisson's ratio, ν	E10.0
1-10	Card 5	Rigid body constraint option, $ICOPT$ EQ.0.0: Rigid body constraints found from nodal BC's EQ.1.0: Rigid body constraints input below	E10.0
1-10	Card 6	Rigid body translational constraint flag EQ.0: no constraints EQ.1: constrained x displacement EQ.2: constrained y displacement EQ.3: constrained z displacement EQ.4: constrained x and y displacements EQ.5: constrained y and z displacements EQ.6: constrained z and x displacements EQ.7: constrained x, y, and z displacements	E10.0
1-10	Card 7	Rigid body rotational constraint flag EQ.0: no constraints EQ.1: constrained x rotation EQ.2: constrained y rotation EQ.3: constrained z rotation EQ.4: constrained x and y rotations EQ.5: constrained y and z rotations EQ.6: constrained z and x rotations EQ.7: constrained x, y, and z rotations	E10.0
	Card 8	Blank	

This material model is used for modeling a rigid body, and may be used with all element classes (beams, shells, and solids). The rigid material provides an inexpensive method for modeling portions of a structure that are much stiffer than the regions of interest or which experience negligible deformations. For example, this approach may be used in many sheet metal forming problems, where the punch and die are often effectively rigid. In addition, the rigid material is very useful for debugging large models by making all materials rigid except the one of interest. This procedure can quickly isolate an incorrect material definition, even in a large model with many materials. The rigid material is considerably less expensive than any other material model, and may be used in parts of a mesh to minimize costs in the early stages of model development.

By default, rigid body constraints are automatically derived from the nodal boundary conditions specified for nodes of a rigid body. If desired, constraints on the rigid body center-of-mass degrees of freedom may be directly specified by setting $ICOPT = 1.0$ on Card 5 and then giving the appropriate translational and rotational constraint flags on Cards 6 and 7. These constraints override constraints computed from nodal boundary condition data.

This material model was updated in 1997 and now employs the momentum and energy conserving algorithm developed by Simo and Wong (1991). The finite deformation algorithm resolves arbitrary amounts of displacements and rotations within a single time step while it conserves the basic field quantities (energy, linear momentum, and angular momentum). When rotational constraints are imposed, rotations about the constrained directions are prohibited, but small, finite-deformation induced, instantaneous rotational velocities may arise. These non-zero rotational velocities do not alter the imposed constraint and decrease in magnitude as the time-step size is reduce. Furthermore, the development of large velocities in the constrained direction is an indicator that the time-step size should be reduced.

Two unique rigid materials may not be adjacent in the mesh unless a slide surface is defined between them (i.e., no one node may be used in the definition of two elements each of which use a different material if both materials are defined as rigid). Separate rigid material definitions should seldom be required for a single rigid body unless the mass density varies with position in the body. Adjacent rigid materials must be merged to form one rigid body using the Rigid Body Merge feature described in section 4.31 on page 384.

All elements which reference a given material number corresponding to the Rigid material must be contiguous. Thus, if two disjoint groups of elements on opposite sides of a model are modeled as rigid, separate material numbers should be created for each of the contiguous element groups. This requirement arises from the fact that DYNA3D internally computes the six degrees-of-freedom for each rigid body (rigid material or set of merged materials), and if disjoint groups of rigid elements use the same material number, the resulting rigid body properties internally calculated by DYNA3D may be inaccurate. This restriction should not pose an inconvenience is most models.

Inertial properties for rigid materials may be defined in either of two ways. By default, the inertial properties are calculated from the geometry of the elements of the rigid material and the density specified on the material control card. Alternatively, the inertial properties and initial velocity for a rigid body may be directly specified, and this overrides data calculated from the material property definition and nodal initial velocity definitions.

The material constants E and ν are used for determining sliding interface parameters if the rigid body interacts along sliding interfaces. Realistic values for these constants should be defined.

Material Type 21 (Thermal Orthotropic Elastic)

Columns		Quantity	Format
1-10	Card 3	Elastic modulus, E_a (see Figure 1 and Figure 2)	E10.0
11-20		Elastic modulus, E_b	E10.0
21-30		Elastic modulus, E_c	E10.0
1-10	Card 4	Poisson's ratio, ν_{ba}	E10.0
11-20		Poisson's ratio, ν_{ca}	E10.0
21-30		Poisson's ratio, ν_{cb}	E10.0
31-40		Coefficient of thermal expansion, α_a	E10.0
41-50		Coefficient of thermal expansion, α_b	E10.0
51-60		Coefficient of thermal expansion, α_c	E10.0
1-10	Card 5	Shear modulus, G_{ab}	E10.0
11-20		Shear modulus, G_{bc}	E10.0
21-30		Shear modulus, G_{ca}	E10.0
1-10	Card 6	Material axes definition option, AOPT	E10.0

EQ.0.0: locally orthotropic with material axes determined by element nodes n_1, n_2, and n_4 as shown in Figure 1. Cards 7 and 8 must be blank with this option.

EQ.1.0: locally orthotropic with material axes determined by a point in space P and the global location of the element center, as shown in Figure 1. Card 8 below is blank.

EQ.2.0: globally orthotropic with material axes determined by vectors defined on Cards 7 and 8. (See Figure 2).

EQ.3.0: applicable to shell elements only. This option determines locally orthotropic material axes by offsetting the material axis $\boldsymbol{a}$ by an angle β from a line in the plane of the shell determined by taking the cross product of the vector $\boldsymbol{v}$ defined on Card 7 with the shell normal vector (See Figure 2). The angle β is defined on Card 8, and may be overridden by specifying a value on the element card.

Columns		Quantity	Format
1-10	Card 7	x_p, define only if AOPT = 1.0	E10.0
11-20		y_p, define only if AOPT = 1.0	E10.0
21-30		z_p, define only if AOPT = 1.0	E10.0
1-10	Card 7	a_x, define only if AOPT = 2.0	E10.0
11-20		a_y, define only if AOPT = 2.0	E10.0
21-30		a_z, define only if AOPT = 2.0	E10.0
1-10	Card 7	v_x, define only if AOPT = 3.0	E10.0
11-20		v_y, define only if AOPT = 3.0	E10.0
21-30		v_z, define only if AOPT = 3.0	E10.0
1-10	Card 8	d_x, define only if AOPT = 2.0	E10.0
11-20		d_y, define only if AOPT = 2.0	E10.0
21-30		d_z, define only if AOPT = 2.0	E10.0
1-10	Card 8	Material angle β, define only if AOPT=3.0 (may be overridden on the element card)	E10.0

The constitutive matrix $\boldsymbol{C}$ that relates increments in stress to increments in strain (in the global coordinate system) is defined as:

$$\mathbf{C} = \mathbf{T}^T \mathbf{C}_L \mathbf{T}, \tag{105}$$

where $\mathbf{T}$ is the transformation matrix between the local material coordinate system and the global coordinate system, and $\mathbf{C}_L$ is the constitutive matrix defined in terms of the material constants of the local orthogonal material axes $\boldsymbol{a}$, $\boldsymbol{b}$, and $\boldsymbol{c}$.

Note that symmetry of the elastic compliance $\mathbf{C}_L^{-1}$ implies

$$\frac{\nu_{ab}}{E_a} = \frac{\nu_{ba}}{E_b}, \quad \frac{\nu_{ca}}{E_c} = \frac{\nu_{ac}}{E_a}, \text{ and } \frac{\nu_{cb}}{E_c} = \frac{\nu_{bc}}{E_b}. \tag{106}$$

Further, positive definiteness of $\mathbf{C}_L$ yields the following restrictions on the elastic constants:

$$\nu_{ba} < \left(\frac{E_b}{E_a}\right)^{\frac{1}{2}}, \quad \nu_{ca} < \left(\frac{E_c}{E_a}\right)^{\frac{1}{2}}, \text{ and } \nu_{cb} < \left(\frac{E_c}{E_b}\right)^{\frac{1}{2}}. \tag{107}$$

Nonphysical energy growth may occur in the solution if these restrictions on the elastic constants are not observed.

In the chosen local coordinate system, the components of the elastic compliance matrix are given by

$$C_L^{-1} = \begin{bmatrix} \frac{1}{E_a} & -\frac{\nu_{ba}}{E_b} & -\frac{\nu_{ca}}{E_c} & 0 & 0 & 0 \\ -\frac{\nu_{ab}}{E_a} & \frac{1}{E_b} & -\frac{\nu_{cb}}{E_c} & 0 & 0 & 0 \\ -\frac{\nu_{ac}}{E_a} & -\frac{\nu_{bc}}{E_b} & \frac{1}{E_c} & 0 & 0 & 0 \\ 0 & 0 & 0 & \frac{1}{G_{ab}} & 0 & 0 \\ 0 & 0 & 0 & 0 & \frac{1}{G_{bc}} & 0 \\ 0 & 0 & 0 & 0 & 0 & \frac{1}{G_{ca}} \end{bmatrix}. \quad (108)$$

Note that the values of Poisson's ratio are defined as

$$\nu_{ij} = \frac{-\varepsilon_j}{\varepsilon_i} \quad (109)$$

where ε_j is the strain in the j^{th} direction and ε_i is the strain in the i^{th} direction in a uniaxial stress test in the i^{th} direction.

This model is similar to Material Type 2, but includes thermal strains. It is applicable to a variety of orthotropic elastic materials such as fiber composites or textured materials.

Note that since temperatures are required to compute the thermal strains, the thermal effects option on Control Card 6 must be nonzero.

Material Type 22 (Fiber Composite with Damage)

Columns		Quantity	Format
1-10	Card 3	Elastic modulus in longitudinal direction, E_a	E10.0
11-20		Elastic modulus in transverse direction, E_b	E10.0
21-30		Elastic modulus in normal direction, E_c	E10.0
31-40		Bulk modulus of failed material, K_f (solid elements only)	E10.0
41-50		Normal tensile strength, S_n (solid elements only)	E10.0
51-60		Transverse shear strength, S_{bc} (solid elements only)	E10.0
61-70		Transverse shear strength, S_{ca} (solid elements only)	E10.0
71-80		Time step size for automatic element deletion, Δt_{crit} (shell elements only)	E10.0
1-10	Card 4	Poisson's ratio, ν_{ba}	E10.0
11-20		Poisson's ratio, ν_{ca}	E10.0
21-30		Poisson's ratio, ν_{cb}	E10.0
1-10	Card 5	Shear modulus, G_{ab}	E10.0
11-20		Shear modulus, G_{bc}	E10.0
21-30		Shear modulus, G_{ca}	E10.0
1-10	Card 6	Material axes definition option, AOPT	E10.0

EQ.0.0: locally orthotropic with material axes determined by element nodes n_1, n_2, and n_4 as shown in Figure 1. Cards 7 and 8 are blank with this option.

EQ.1.0: locally orthotropic with material axes determined by a point in space P and the global location of the element center, as shown in Figure 1. Card 8 below is blank.

EQ.2.0: globally orthotropic with material axes determined by vectors defined on Cards 7 and 8. (See Figure 2).

Columns		Quantity	Format
	EQ.3.0:	applicable to shell elements only. This option determines locally orthotropic material axes by offsetting the material axis ***a*** by an angle β from a line in the plane of the shell determined by taking the cross product of the vector ***v*** defined on Card 7 with the shell normal vector (See Figure 2). The angle β is defined as described below for each through-thickness integration point. In addition, a material angle may be specified on each element card, and these values are added	
11-20	Material axes change flag *for brick elements only* EQ.1.0: default EQ.2.0: switch material axes a and b EQ.3.0: switch material axes a and c		E10.0
1-10	Card 7	x_p, define only if AOPT = 1.0	E10.0
11-20		y_p, define only if AOPT = 1.0	E10.0
21-30		z_p, define only if AOPT = 1.0	E10.0
1-10	Card 7	a_x, define only if AOPT = 2.0	E10.0
11-20		a_y, define only if AOPT = 2.0	E10.0
21-30		a_z, define only if AOPT = 2.0	E10.0
1-10	Card 7	v_x, define only if AOPT = 3.0	E10.0
11-20		v_y, define only if AOPT = 3.0	E10.0
21-30		v_z, define only if AOPT = 3.0	E10.0
1-10	Card 8	d_x, define only if AOPT = 2.0	E10.0
11-20		d_y, define only if AOPT = 2.0	E10.0
21-30		d_z, define only if AOPT = 2.0	E10.0
31-40		Shear strength on ***a***-***b*** plane, S_c	E10.0
41-50		Longitudinal tensile strength along ***a*** axis, X_t	E10.0
51-60		Longitudinal tensile strength along ***b*** axis, Y_t	E10.0
61-70		Transverse compressive strength, Y_c	E10.0
71-80		Nonlinear shear stress parameter, α	E10.0

This material model allows a different fiber orientation to be specified at each through-thickness integration point for shell elements. This capability may be combined with the User-Defined Integration Rules option to accurately represent a general composite laminate.

Additional Material Type 22 Input For Shell Elements Only:

Define the material angle β for each of the through-the-thickness integration points for 4-node shell elements. This data must follow the Cross Section Properties data on Card 11.

Columns	Quantity	Format
1-10	Material angle at first integration point, β_1	E10.0
11-20	Material angle at second integration point, β_2	E10.0
21-30	Material angle at third integration point, β_3	E10.0
.	.	.
.	.	.
.	.	.
71-80	Material angle at eighth integration point, β_8	E10.0

Continue on additional cards until NIP points have been defined, where NIP is the number of thickness integration points specified on Card 10 for shell elements. Material angle values may also be specified on the element cards. The material angle used in the calculation is the sum of the value specified above for each integration point and the value specified on the element card.

The formulation of this model is described by Chang and Chang (1987a, 1987b).

The material behavior produced by this model is approximately orthotropic elastic, with the addition of a nonlinear shear stress term. A stress-based failure model is included to incorporate the effects of fiber breakage, matrix cracking, matrix crushing, and delamination. The failure criterion for fiber breakage is

$$e_f = \frac{max(0, \sigma_{aa}^2)}{X_t^2} + \frac{\sigma_{ab}^2 + \frac{3}{4}\alpha\sigma_{ab}^4}{\frac{S_c^2}{2G_{ab}} + \frac{3}{4}\alpha S_c^4} \leq 1.0 \quad . \tag{110}$$

Analogously, the criterion for matrix cracking is

$$e_m = \frac{max(0, \sigma_{bb}^2)}{Y_t^2} + \frac{\sigma_{ab}^2 + \frac{3}{4}\alpha\sigma_{ab}^4}{\frac{S_c^2}{2G_{ab}} + \frac{3}{4}\alpha S_c^4} \le 1.0 \quad . \tag{111}$$

The criterion to detect matrix crushing is

$$e_d = \frac{min(0, \sigma_{bb}^2)}{4S_c^2} + \left[\frac{Y_c^2}{4S_c^2} - 1\right]\frac{\sigma_{bb}}{Y_c} + \frac{\sigma_{ab}^2 + \frac{3}{4}\alpha\sigma_{ab}^4}{\frac{S_c^2}{2G_{ab}} + \frac{3}{4}\alpha S_c^4} \le 1.0 \quad , \tag{112}$$

and, for solid elements only, the criterion to detect delamination is

$$e_l = \frac{max(0, \sigma_{cc}^2)}{S_n^2} + \frac{\sigma_{bc}^2}{S_{bc}^2} + \frac{\sigma_{ca}^2}{S_{ca}^2} \le 1.0 \quad . \tag{113}$$

When failure is detected, the appropriate stress components are reduced to zero linearly over the next 100 time steps. This stress reduction function has been found useful to minimize spurious oscillations, or ringing, caused by the abrupt release of energy at failure.

This model is applicable to laminated fiber composites. It includes the effects of directionality in the material stress-strain response, and includes criteria to detect the major failure mechanisms in laminated fiber composites.

Shell elements are rendered incapable of carrying load and eliminated from the calculation after fiber breakage commences. Elements can also be eliminated after matrix cracking and/or matrix crushing occurs by specifying negative values for either or both Y_t and Y_c, respectively. When the SAND database is activated (see Control Card 3 in section 4.1 on page 62), failed elements will “disappear” during post-processing.

In addition to the above failure criteria, this model also supports a shell element deletion criterion based on the maximum stable time step size for this element, Δt_{max}. Generally, Δt_{max} goes down as the element becomes more distorted. To assure stability of the global time integration, the DYNA3D time step is the *minimum* of the Δt_{max} values calculated for all elements in the model. Using this option allows the selective deletion of elements whose time step Δt_{max} has fallen below the specified minimum time step, Δt_{crit}. If left unspecified, no elements are deleted based upon their time step size.

Material Type 23 (Thermal Orthotropic Elastic with Variable Properties)

Columns		Quantity	Format
1-10	Card 3	Number of points in material constant vs. temperature curves, N_{pts}, $(2 \le N_{pts} \le 48)$	E10.0
11-20		Load curve number defining thermal radius vs. time - define only for laser option.	E10.0
21-30		Load curve number defining normalized thermal profile vs. radius from spot center - define only for laser option.	E10.0
1-10	Card 4	x_s, spot center - define only for laser option:	E10.0
11-20		y_s, spot center - define only for laser option:	E10.0
21-30		z_s, spot center - define only for laser option:	E10.0
1-10	Card 5	Blank	E10.0
1-10	Card 6	Material axes definition option, $AOPT$	E10.0
	EQ.0.0:	locally orthotropic with material axes determined by element nodes n_1, n_2, and n_4 as shown in Figure 1. Cards 7 and 8 are blank with this option.	
	EQ.1.0:	locally orthotropic with material axes determined by a point in space P and the global location of the element center, as shown in Figure 1. Card 8 below is blank.	
	EQ.2.0:	globally orthotropic with material axes determined by vectors defined on Cards 7 and 8. (See Figure 2).	
	EQ.3.0:	applicable to shell elements only. This option determines locally orthotropic material axes by offsetting the material axis $\boldsymbol{a}$ by an angle β from a line in the plane of the shell determined by taking the cross product of the vector $\boldsymbol{v}$ defined on Card 7 with the shell normal vector (See Figure 2). The angle β is defined for each through-thickness integration point as described below. In addition, a material angle may be specified on the element cards, and the sum of these angles is used for computation.	
1-10	Card 7	x_p, define only if AOPT = 1.0	E10.0
11-20		y_p, define only if AOPT = 1.0	E10.0
21-30		z_p, define only if AOPT = 1.0	E10.0
1-10	Card 7	a_x, define only if AOPT = 2.0	E10.0

Columns		Quantity	Format
11-20		a_y, define only if AOPT = 2.0	E10.0
21-30		a_z, define only if AOPT = 2.0	E10.0
1-10	Card 7	v_x, define only if AOPT = 3.0	E10.0
11-20		v_y, define only if AOPT = 3.0	E10.0
21-30		v_z, define only if AOPT = 3.0	E10.0
1-10	Card 8	d_x, define only if AOPT = 2.0	E10.0
11-20		d_y, define only if AOPT = 2.0	E10.0
21-30		d_z, define only if AOPT = 2.0	E10.0

Define the following input card set for each of the 12 orthotropic material constants and the list of corresponding temperatures using the format (8E10.0). For shell elements, this data must follow the Cross Section Properties specified on cards 10 and 11. For solid elements, this data follows the eight Material Cards described above.

Columns	Quantity	Format
1-10	Elastic modulus E_a at temperature T_1	E10.0
11-20	Elastic modulus E_a at temperature T_2	E10.0
.	.	.
.	.	.
.	.	.
71-80	Elastic modulus E_a at temperature T_8	E10.0

Continue with additional cards in this format until N_{pts} points have been defined for E_a. Then, input definitions for the elastic moduli E_b and E_c, the Poisson's ratios ν_{ba}, ν_{ca}, and ν_{cb}, the coefficients of thermal expansion $\bar{\alpha}_a$, $\bar{\alpha}_b$, and $\bar{\alpha}_c$, the shear moduli G_{ab}, G_{bc}, and G_{ca}, and the list of temperatures T following the same format. In the above, subscripts a, b, and c denote the local material axes.

This model allows a different orientation to be specified at each through-thickness integration point for shell elements. This capability may be combined with the User-Defined Integration Rules option to accurately represent a general orthotropic elastic laminate.

Localized heating effects from point sources, such as lasers, can be modelled. The user must specify the spot center and two load curves. The first load curve defines the radius of the thermal zone verses time, while the second load curve gives the thermal variation within the zone verses normalized radial distance from the spot center. The normalized radial distance is defined to be the distance from the integration point to the spot center divided by the current radius of the thermal zone.

The additional input required to specify fiber orientation for each integration point of a shell element is described on the following page.

Additional Material Type 23 Input For Shell Elements Only:

For shell elements only, define the material angle for each through-thickness integration point.

Columns	Quantity	Format
1-10	Material angle at first integration point, β_1	E10.0
11-20	Material angle at second integration point, β_2	E10.0
21-30	Material angle at third integration point, β_3	E10.0
.	.	.
.	.	.
.	.	.
71-80	Material angle at eighth integration point, β_8	E10.0

For shell elements, continue on additional cards as necessary until NIP points have been defined, where NIP is the number of thickness integration points specified on Card 10. Material angles may also be specified on the element cards. The value used for computation is the sum of the material angle specified by integration point above and the value specified on the element card.

For shell elements, plane stress conditions are assumed on each laminae, but transverse shear stresses are included.

Since temperature dependent material properties are used, the thermal effects option on Control Card 6 must be nonzero.

This material model is useful for studying the thermoelastic behavior of orthotropic materials, including both homogeneous compositions and laminated materials such as fiber composites. It allows the material orientation angle to be specified by integration point and by element for shell elements, and by element for solid elements. This approach allows an accurate representation of laminates where the orientation of the fibers varies between laminae. This capability is frequently combined with user-defined integration rules for shell elements to define one integration point in each lamina or set of lamina in a multi-layer composite structure.

Material Type 24 (Rate-Dependent Tabular Isotropic Elastic-Plastic)

Columns		Quantity	Format
1-10	Card 3	Young's modulus, E	E10.0
1-10	Card 4	Poisson's ratio, ν	E10.0
1-10	Card 5	Yield stress, σ_0	E10.0
1-10	Card 6	Tangent modulus, E_T (not used if the stress-strain curve is defined below)	E10.0
11-20		Effective plastic strain at failure, $\bar{\varepsilon}_f^p$	E10.0
21-30		Time step size for automatic element deletion, Δt_{crit}	E10.0
31-40		Load curve number to scale yield stress for strain rate effects	E10.0
41-50		Element deletion flag for plastic strain EQ.0.0: No element removal upon failure EQ.1.0: Element deleted when $\bar{\varepsilon}^p = \bar{\varepsilon}_f^p$	E10.0
1-80	Card 7	Tabulated effective plastic strain values, $\bar{\varepsilon}^p$ (define up to 8 values)	E10.0
1-80	Card 8	Corresponding tabulated yield stress values, $\bar{\sigma}$	E10.0

This model yields rate-dependent elastoplastic material behavior. It is similar to Material Types 3, 12, and 19, but allows a general strain hardening law to be specified via tabulated data. In addition, arbitrary rate dependence of the yield stress is incorporated via a load curve.

The yield condition can be written

$$\phi = \bar{\sigma} - \sigma_y(\bar{\varepsilon}^p, \dot{\bar{\varepsilon}}) , \tag{114}$$

where $\bar{\sigma}$ is the effective stress and σ_y is the current yield stress, which may depend on the effective plastic strain $\bar{\varepsilon}^p$ and the current effective strain rate, $\dot{\bar{\varepsilon}}$. The effective stress is found from the deviatoric stress tensor s_{ij} as

$$\bar{\sigma} = \left\{ \frac{3}{2} s_{ij} s_{ij} \right\}^{\frac{1}{2}} . \tag{115}$$

If a tabulated yield stress vs. effective plastic strain curve is not defined, then a linear hardening law is used,

$$\sigma_y = \sigma_0 + E_p \bar{\varepsilon}^p , \tag{116}$$

where σ_0 is the initial yield stress. The hardening modulus E_p represents the slope of the effective stress vs. effective plastic strain curve, and the tangent modulus E_T represents the slope of the inelastic portion of the uniaxial stress vs. uniaxial strain curve. The hardening modulus can be written in terms of the Young's modulus E and the tangent modulus E_T as

$$E_p = \frac{EE_T}{E - E_T} \tag{117}$$

If a tabulated yield stress vs. effective plastic strain curve is defined, then the input value of the tangent modulus E_T is ignored and the current value of the effective plastic strain determines the yield stress from the tabulated function.

If a nonzero load curve number is specified, this yield stress is multiplied by a scale factor from the load curve based on the current effective strain rate, $\dot{\bar{\varepsilon}}$. The load curve should define a strain rate scale factor f as a function of strain rate $\dot{\bar{\varepsilon}}$. Thus, load curve points should be input as pairs of effective strain rate and the corresponding yield scale factor, $(\dot{\bar{\varepsilon}}, f(\dot{\bar{\varepsilon}}))$. A strain rate scale factor of 1.0 would give no strain rate effect, and values greater than one give material strengthening effects. The effective strain rate is defined as

$$\dot{\bar{\varepsilon}} = \left(\frac{2}{3} \dot{e}_{ij} \dot{e}_{ij} \right)^{\frac{1}{2}}, \tag{118}$$

where $\dot{e}_{ij}$ is the deviatoric strain rate tensor. If the load curve number is input as 0, then the constant value specified in the input is used with no modification for strain rate effects.

This model also contains a failure criterion based on the total accumulated effective plastic strain, $\bar{\varepsilon}^p$. When the effective plastic strain exceeds the specified value for the effective plastic strain at failure, $\bar{\varepsilon}_f^p$, failure is detected. (Failure is only active when $\bar{\varepsilon}_f^p > 0$.) For shell elements, element failure is assumed to occur when the effective plastic strain at *all* through-thickness integration point reaches $\bar{\varepsilon}_f^p$. Once an integration point in a shell element fails, the effective plastic strain is set to the failure value $\bar{\varepsilon}_f^p$ and the stresses are set to zero. The integration point remains failed throughout the rest of the calculation. For solid elements failure is detected when the effective plastic strain at the center of the element exceeds the critical value. When a solid element fails, the yield stress σ_0 and the hardening modulus E_p are cut by a factor of 1000. Thus, the solid element retains its hydrostatic strength even after failure has occurred. The effective plastic strain may reach large values using this formulation. Both element types can be removed from the calculation upon failure by prescribing a non-zero deletion flag.

In addition to the above failure criterion, this model also supports a element deletion criterion based on the maximum stable time step size for this element, Δt_{max}. Generally, Δt_{max} goes down as the element becomes more distorted. To assure stability of the global time integration, the DYNA3D time step is the *minimum* of the Δt_{max} values calculated for all elements in the model. Using this option allows the selective deletion of elements whose time step Δt_{max} has fallen below the specified minimum time step, Δt_{crit}. Non-zero values override any global or material specified time-step size element deletion criteria.

Elements which are severely distorted often indicate that material has failed and supports little load, but these same elements may have very small time steps and therefore control the cost of the analysis. This option allows these highly distorted elements to be deleted from the calculation, and therefore the analysis can proceed at a larger time step, and thus at a reduced cost. Deleted elements do not carry any load, and are deleted from all applicable slide surface definitions. Clearly, this option must be judiciously used to obtain accurate results at a minimum cost.

Material Type 25 (Extended Two Invariant Geologic Cap)

Columns		Quantity	Format
1-10	Card 3	Initial bulk modulus, K	E10.0
11-20		Initial shear modulus, G	E10.0
1-10	Card 4	Failure envelope parameter, α	E10.0
11-20		Failure envelope linear coefficient, θ	E10.0
21-30		Failure envelope exponential coefficient, γ	E10.0
31-40		Failure envelope exponent, β	E10.0
41-50		Cap surface axis ratio, R	E10.0
1-10	Card 5	Hardening law exponent, D	E10.0
11-20		Hardening law coefficient, W	E10.0
21-30		Hardening law parameter, X_0	E10.0
31-40		Kinematic hardening coefficient, $\bar{c}$	E10.0
41-50		Kinematic hardening parameter, N	E10.0
1-10	Card 6	Plot database flag, $IPLOT$ EQ.1.0: Hardening variable, κ EQ.2.0: Cap - J_1 axis intercept, $X(\kappa)$ EQ.3.0: Volumetric plastic strain, ε_v^p EQ.4.0: First stress invariant, J_1 EQ.5.0: Second stress invariant, $\sqrt{J_{2D}}$ EQ.6.0: Not used EQ.7.0: Not used EQ.8.0: Response mode number EQ.9.0: Number of iterations	E10.0
1-10	Card 7	Soil type, $ltype$ EQ.1.0: Soil EQ.1.0: Rock	E10.0
11-20		Vectorization flag, $IVEC$ EQ.0.0: Vectorized (fixed number of iterations) EQ.1.0: Fully iterative	E10.0
1-10	Card 8	Tension cutoff, $T < 0$ (positive in compression)	E10.0

This implementation of an extended two invariant cap model was developed by Whirley and Engelmann (1992) based on the formulations of Simo, Ju, Pister, and Taylor (1988), Simo, Ju, and Taylor (1990), and Sandler and Rubin, (1979). In this model, the two invariant cap theory is extended to include nonlinear kinematic hardening as suggested in (Isenberg, Vaughn, and Sandler, 1978). A brief discussion of the extended cap model and its parameters is given below.

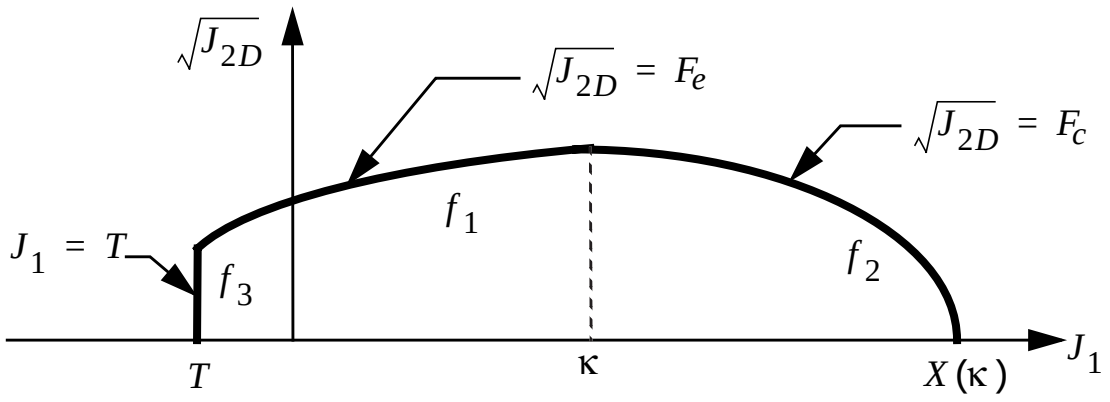

Figure 13
The yield surfaces of the two invariant cap model in $\sqrt{J_{2D}}$ - J_1 space. Surface f_1 is the failure envelope, f_2 is the cap surface, and f_3 is the tension cutoff.

The cap model is formulated in terms of the invariants of the stress tensor. The square root of the second invariant of the deviatoric stress tensor, $\sqrt{J_{2D}}$, is found from the deviatoric stresses $\boldsymbol{s}$ as

$$\sqrt{J_{2D}} \equiv \sqrt{\frac{1}{2} s_{ij} s_{ij}} \tag{119}$$

and is an objective scalar measure of the distortional or shearing stress. The first invariant of the stress, J_1, is simply the sum of the normal stresses, or equivalently, three times the pressure.

The cap model consists of three surfaces in $\sqrt{J_{2D}}$ - J_1 space, as shown in Figure 13. First, there is a failure envelope surface, denoted f_1 in the figure. The functional form of f_1 is

$$f_1 = \sqrt{J_{2D}} - min\left(F_e(J_1), T_{mises}\right), \tag{120}$$

where F_e is given by

$$F_e(J_1) \equiv \alpha - \gamma exp(-\beta J_1) + \theta J_1 \tag{121}$$

and $T_{mises} \equiv |X(\kappa_n) - L(\kappa_n)|$. This failure envelope surface is fixed in $\sqrt{J_{2D}}$ - J_1 space, and therefore does not harden, unless kinematic hardening is present. Next, there is a cap surface, denoted f_2 in the figure, with f_2 given by

$$f_2 = \sqrt{J_{2D}} - F_c(J_1, \kappa), \tag{122}$$

where F_c is defined by

$$F_c(J_1, \kappa) \equiv \frac{1}{R}\sqrt{[X(\kappa) - L(\kappa)]^2 - [J_1 - L(\kappa)]^2} \quad , \tag{123}$$

$X(\kappa)$ is the intersection of the cap surface with the J_1 axis,

$$X(\kappa) = \kappa + RF_e(\kappa) \ , \tag{124}$$

and $L(\kappa)$ is defined by

$$L(\kappa) \equiv \begin{array}{l} \kappa \ \text{ if } \ \kappa > 0 \\ 0 \ \text{ if } \ \kappa \le 0 \end{array} \ . \tag{125}$$

The hardening parameter κ is related to the plastic volume change ε_v^p through the hardening law

$$\varepsilon_v^p = W\{1 - exp[-D(X(\kappa) - X_0)]\} \ . \tag{126}$$

Geometrically, κ is seen in the figure as the J_1 coordinate of the intersection of the cap surface and the failure surface. Finally, there is the tension cutoff surface, denoted f_3 in the figure. The function f_3 is given by

$$f_3 \equiv T - J_1 \, , \tag{127}$$

where T is an input material parameter which specifies the maximum hydrostatic tension sustainable by the material. The elastic domain in $\sqrt{J_{2D}}$ - J_1 space is then bounded by the failure envelope surface above, the tension cutoff surface on the left, and the cap surface on the right.

An additive decomposition of the strain into elastic and plastic parts is assumed:

$$\mathsf{e} = \mathsf{e}^e + \mathsf{e}^p \, , \tag{128}$$

where e^e is the elastic strain and e^p is the plastic strain. Stress is found from the elastic strain using Hooke's law,

$$\mathsf{s} = \boldsymbol{C}(\boldsymbol{e} - \boldsymbol{e}^p), \tag{129}$$

where s is the stress and $\boldsymbol{C}$ is the elastic constitutive tensor.

The yield condition may be written

$$\begin{array}{c} f_1(\mathsf{s}) \le 0 \\ f_2(\mathsf{s}, \kappa) \le 0 \\ f_3(\mathsf{s}) \le 0 \end{array} \tag{130}$$

and the plastic consistency condition requires that

$$\begin{array}{l} \dot{\lambda}_k f_k = 0 \\ \dot{\lambda}_k \ge 0 \end{array} \quad k = 1, 2, 3 \, , \tag{131}$$

where λ_k is the plastic consistency parameter for surface k. If $f_k < 0$, then $\dot{\lambda}_k = 0$ and the response is elastic. If $f_k > 0$, then surface k is active and $\dot{\lambda}_k$ is found from the requirement that $\dot{f}_k = 0$.

Associated plastic flow is assumed, so using Koiter's flow rule the plastic strain rate is given as the sum of contributions from all of the active surfaces,

$$\dot{\boldsymbol{e}}^p = \sum_{k=1}^{3} \dot{\lambda}_k \frac{\partial f_k}{\partial \boldsymbol{s}}. \tag{132}$$

One of the major advantages of the cap model over other classical pressure-dependent plasticity models is the ability to control the amount of dilatency produced under shear loading. Dilatency is produced under shear loading as a result of the yield surface having a positive slope in $\sqrt{J_{2D}}$ - J_1 space, so the assumption of plastic flow in the direction normal to the yield surface produces a plastic strain rate vector that has a component in the volumetric (hydrostatic) direction (see Figure 13). In models such as the Drucker-Prager and Mohr-Coulomb, this dilatency continues as long as shear loads are applied, and in many cases produces far more dilatency than is experimentally observed in material tests. In the cap model, when the failure surface is active, dilatency is produced just as with the Drucker-Prager and Mohr-Coulomb models. However, the hardening law permits the cap surface to contract until the cap intersects the failure envelope at the stress point, and the cap remains at that point. The local normal to the yield surface is now vertical, and therefore the normality rule assures that no further plastic volumetric strain (dilatency) is created. Adjustment of the parameters that control the rate of cap contraction permits experimentally observed amounts of dilatency to be incorporated into the cap model, thus producing a constitutive law which better represents the physics to be modeled.

Another advantage of the cap model over other models such as the Drucker-Prager and Mohr-Coulomb is the ability to model plastic compaction. In these models all purely volumetric response is elastic. In the cap model, volumetric response is elastic until the stress point hits the cap surface. Thereafter, plastic volumetric strain (compaction) is generated at a rate controlled by the hardening law. Thus, in addition to controlling the amount of dilatency, the introduction of the cap surface adds another experimentally observed response characteristic of geological materials into the model.

The inclusion of kinematic hardening will result in hysteretic energy dissipation under cyclic loading conditions. Following the approach of (Isenberg, Vaughn, and Sandler, 1978), a nonlinear kinematic hardening law is used for the failure envelope surface when nonzero values of $\bar{c}$ and N

are specified. In this case, the failure envelope surface is replaced by a family of yield surfaces bounded by an initial yield surface and a limiting failure envelope surface. Thus, the shape of the yield surfaces described above remains unchanged, but they may translate in a plane orthogonal to the J_1 axis.

Translation of the yield surfaces is permitted through the introduction of a "back stress" tensor, α. The formulation including kinematic hardening is obtained by replacing the stress σ with the translated stress tensor $\boldsymbol{\eta} \equiv \sigma - \alpha$ in all of the above equations. The history tensor α is assumed deviatoric, and therefore has only 5 unique components. The evolution of the back stress tensor is governed by the nonlinear hardening law

$$\dot{\alpha} = \bar{c}\bar{F}(\sigma, \alpha)\dot{\boldsymbol{\varepsilon}}^p, \tag{133}$$

where $\bar{c}$ is a constant, $\bar{F}$ is a scalar function of σ and α, and $\dot{\boldsymbol{\varepsilon}}^p$ is the rate of deviatoric plastic strain. The constant $\bar{c}$ may be estimated from the slope of the shear stress - plastic shear strain curve at low levels of shear stress.

The function $\bar{F}$ is defined as

$$\bar{F} \equiv max\left\{0, 1 - \frac{(\sigma - \alpha)\bullet\alpha}{2NF_e(J_1)}\right\}, \tag{134}$$

where N is a constant defining the size of the yield surface. The value of N may be interpreted as the radial distance between the outside of the initial yield surface and the inside of the limit surface. In order for the limit surface of the kinematic hardening cap model to correspond with the failure envelope surface of the standard cap model, the scalar parameter α must be replaced with $\alpha - N$ in the definition of F_e.

The cap model contains a number of parameters which must be chosen to represent a particular material, and are generally based on experimental data. The parameters α, β, θ, and γ are usually evaluated by fitting a curve through failure data taken from a set of triaxial compression tests. The parameters W, D, and X_0 define the cap hardening law. The value of W represents the void fraction of the uncompressed sample and D governs the slope of the initial loading curve in hydrostatic compression. The value of R is the ratio of major to minor axes of the quarter ellipse defining the cap surface. Additional details and guidelines for fitting the cap model to experimental data are found in (Chen and Baladi, 1985).

This model represents a new implementation of the two-invariant cap model into DYNA3D. This version is highly vectorized and more reliable than the experimental implementation available in previous releases. In addition, this new implementation incorporates nonlinear kinematic hardening to model cyclic energy dissipation due to shear hysteresis.

Material Type 26 (Metallic Honeycomb)

Columns		Quantity	Format
1-10	Card 3	Young's modulus for fully compacted material, E	E10.0
11-20		Poisson's ratio for fully compacted material, ν	E10.0
21-30		Yield stress for fully compacted material, σ_0	E10.0
31-40		Load curve number for $\sigma_{aa,\max}$ vs. relative volume V	E10.0
41-50		Load curve number for $\sigma_{bb,\max}$ vs. relative volume V	E10.0
51-60		Load curve number for $\sigma_{cc,\max}$ vs. relative volume V	E10.0
61-70		Load curve number for $\sigma_{ab,\max}$, $\sigma_{bc,\max}$, and $\sigma_{ca,\max}$ vs. relative volume V	E10.0
71-80		Relative volume at full compaction, V_{min}	E10.0
1-10	Card 4	Initial elastic modulus, E_a	E10.0
11-20		Initial elastic modulus, E_b	E10.0
21-30		Initial elastic modulus, E_c	E10.0
31-40		Initial shear modulus, G_{ab}	E10.0
41-50		Initial shear modulus, G_{bc}	E10.0
51-60		Initial shear modulus, G_{ca}	E10.0
	Card 5	Blank	
	Card 6	Blank	
	Card 7	Blank	
	Card 8	Blank	

This model is an empirically based formulation for the representation of crushable metallic honeycomb materials, but it may be applicable to other materials as well. The initial behavior is orthotropic elastic with the Poisson's ratios equal to zero. Thus, the components of stress are uncoupled (i.e., an a-direction component of strain generates only an a-direction component of stress, and the other stress components are unaffected). As volumetric compaction occurs, the directional elastic moduli vary linearly from their initial values to the fully compacted value, E. In the partially compacted states, the stress components are limited by the maximum values at the

current relative volume V as specified on load curves. When full compaction is reached, the material behavior becomes isotropically elastic-plastic with no strain hardening. Additional details on the implementation of this model are given below.

The metallic honeycomb model is predicated on the observation that honeycomb materials markedly change their behavior as a function of volumetric crushing (compaction). Compaction is measured analytically by the relative volume V defined by

$$V \equiv \frac{V_{current}}{V_{initial}} = det(\boldsymbol{F}), \tag{135}$$

where $\boldsymbol{F}$ is the deformation gradient. Note that for an expanded material $V > 1$ and for a compacted material $V < 1$. The relative volume at which full compaction is achieved, V_{min}, is specified as an input parameter. In this model, compaction is measured as the minimum relative volume ever achieved by a given element over the history of the deformation. Thus, once an element begins compacting, it never loses its compaction. This is in accordance with physical observations.

For partially compacted states, a maximum stress magnitude may be specified for each component ($\sigma_{aa,\max}$, $\sigma_{bb,\max}$, $\sigma_{cc,\max}$, and $\sigma_{ab,\max}$) as a function of relative volume, using a load curve. In order to allow a vectorized interpolation scheme for good performance, *it is required that each load curve used for this model must have the same number of points and exactly the same abscissa (relative volume) points.* The first point in each load curve should correspond to a relative volume slightly less than the minimum relative volume for fully compacted material, V_{min}. The load curves define the maximum stress magnitude that each component is permitted to bear at a specific relative volume and *not the stress-strain relationship*. In general, $\sigma_{\max}(V = 1) > 0$. If load curves for $\sigma_{bb,\max}$, $\sigma_{cc,\max}$, and $\sigma_{ab,\max}$ are not specified, then the load curve defining $\sigma_{aa,\max}$ vs. relative volume is used automatically.

The constitutive equation used for materials in the initial or expanded configurations is directionally elastic with the components of stress uncoupled. The local $\boldsymbol{a}$, $\boldsymbol{b}$, and $\boldsymbol{c}$ axes are found from the local node numbers defining the solid element, as shown in Figure 14. First, the local $\boldsymbol{c}$ axis is found from the cross product of the two diagonals of the lower surface of the solid element (i.e., the surface bounded by nodes n_1, n_2, n_3, and n_4). Next, a temporary local $\hat{\boldsymbol{a}}$ axis is constructed as a vector from node n_1 to node n_2, and the local $\boldsymbol{b}$ axis is found by crossing the $\boldsymbol{c}$ axis with the $\hat{\boldsymbol{a}}$ axis. Finally, the local $\boldsymbol{a}$ axis is constructed by modifying the $\hat{\boldsymbol{a}}$ axis to be mutually perpendicular to the other two local axes. The resulting local coordinate system is also shown in Figure 14.

For partially compacted states ($V_{min} < V < 1$), a trial elastic stress is first computed using directionally elastic moduli. These moduli are linearly interpolated based on the current relative volume between the input initial directional values and the isotropic values of Young's modulus E and Poisson's ratio ν at $V = V_{min}$. Next, the limiting stress magnitudes are found for each component at the current relative volume by interpolation from the specified load curves. If the trial stress component is smaller in magnitude than this limiting value, then the trial stress component becomes the final stress component. If the magnitude of the trial stress component exceeds the limiting value, then the stress component is scaled back to this limiting value.

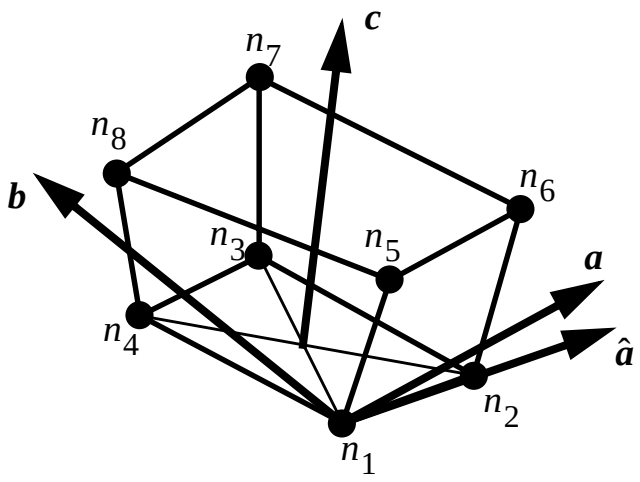

Figure 14
Material axes definition for metallic honeycomb model.

Once the material becomes fully compacted ($V = V_{min}$), it is modeled as isotropically elastic perfectly-plastic with a yield stress of σ_0. The behavior remains elastic-plastic for the remainder of the calculation, even if the element subsequently goes into tension.

When large volumetric changes occur, the bulk viscosity can corrupt the calculation by artificially increasing the "internal element pressure" and dissipating excessive amounts of energy, i.e. many times more than is dissipated by the constitutive relationships. Consequently, it is recommended that when a material is going to be substantially compacted that both hourglass viscosities be decreased or set essentially to zero, e.g. $1x10^{-10}$, for that material.

Material Type 27 (Compressible Mooney-Rivlin Hyperelastic Rubber)

Columns		Quantity	Format
1-10	Card 3	First invariant coefficient, A	E10.0
11-20		Second invariant coefficient, B	E10.0
21-30		Poisson's ratio, ν $(0.48 \le \nu < 0.50)$	E10.0
	Card 4	Blank	
	.	.	
	.	.	
	.	.	
	Card 8	Blank	

The strain energy density function is defined as:

$$W = A(I_1 - 3) + B(I_2 - 3) + C(I_3^{-2} - 1) + D(I_3 - 1)^2 \quad , \tag{136}$$

where

$$C = \frac{1}{2}A + B, \tag{137}$$

$$D = \frac{A(5\nu - 2) + B(11\nu - 5)}{2(1 - 2\nu)} \quad , \tag{138}$$

ν is Poisson's ratio, and I_1, I_2, and I_3 are the invariants of the right Cauchy-Green tensor, $\boldsymbol{C}$. The right Cauchy-Green tensor is found from the deformation gradient $\boldsymbol{F}$ using

$$\boldsymbol{C} = \boldsymbol{F}^T\boldsymbol{F}, \tag{139}$$

or from the Green-Lagrange strain $\boldsymbol{E}$ using

$$\boldsymbol{C} = 2\boldsymbol{E} + \boldsymbol{I}, \tag{140}$$

where $\boldsymbol{I}$ is the identity two-tensor. For small deformations, the shear modulus of linear elasticity G is given by

$$G = 2(A + B). \tag{141}$$

Poisson's ratio should be chosen such that $0.48 \le \nu < 0.50$, yielding a slightly compressible hyperelastic material.

This is a hyperelastic model and is often used to represent the behavior of rubber-like materials at moderate to large strains. Other rubber models include Material Type 7, the Blatz-Ko model, and Material Type 31, the Frazer-Nash rubber model.

The DYNA3D implementation of this model was developed by Brad Maker.

Material Type 28 (Resultant Plasticity)

Columns		Quantity	Format
1-10	Card 3	Young's modulus, E	E10.0
1-10	Card 4	Poisson's ratio, ν	E10.0
1-10	Card 5	Yield stress, σ_0	E10.0
1-10	Card 6	Hardening modulus, E_T (shells only)	E10.0
1-10	Card 7	Blank	
1-10	Card 8	Blank	

This model is formulated in terms of resultant quantities for structural elements, and is a*vailable for the Belytschko-Schwer beam and the Belytschko-Tsay shell elements only.* All other DYNA3D material models for structural elements relate stresses directly to strains, and numerical integration is performed over the beam or shell element cross section to calculate the resultant forces and moments. Formulating the material model directly in terms of resultants yields some improvements in speed, but sacrifices accuracy when the material behavior becomes plastic (Whirley, 1990). Therefore, this model is primarily useful for scoping calculations where precise results are not required. For more accurate results, the use of Material Type 3 or 12 is recommended.

The Illyushin yield criterion is used as described in (Kennedy, Belytschko, and Lin, 1986). For beams, the behavior is elastic-perfectly plastic. For shell elements, an approximation to isotropic hardening has been incorporated.

Material Type 29 (Mechanical-Threshold-Stress Model)

Columns		Quantity	Format
1-10	Card 3	Dislocation interaction - long-range barriers, $\hat{\sigma}_a$ (*SIGA*)	E10.0
11-20		Dislocation interaction - interstitial atoms, $\hat{\sigma}_i$ (*SIGI*)	E10.0
21-30		Dislocation interaction - solute atoms, $\hat{\sigma}_s$ (*SIGS)*	E10.0
31-40		Initial flow stress, $\hat{\sigma}$ (*SIGO*)	E10.0
41-50		First dislocation generation constant, a_o (*HF0*)	E10.0
51-60		Second dislocation generation constant, a_1 (*HF1*)	E10.0
61-70		Third dislocation generation constant, a_2 (*HF2*)	E10.0
71-80		Saturation threshold stress at 0K, $\hat{\sigma}_{so}$ (*SIGS0*)	E10.0
1-10	Card 4	Reference strain rate, $\dot{\varepsilon}_{so}$ (*EDOTS0R)*	E10.0
11-20		Magnitude of Burger's vector, b (*BURG*)	E10.0
21-30		Material constant, A (*CAPA*)	E10.0
31-40		Boltzmann's constant, k (*BOLTZ*)	E10.0
41-50		Shear modulus at 0K, b_0 (*SM0*)	E10.0
51-60		First shear modulus constant, b_1 (*SM1*)	E10.0
61-70		Second shear modulus constant, b_2 (*SM2*)	E10.0
71-80		Reference strain rate, $\dot{\varepsilon}_o$ (*LNED0*)	E10.0
1-10	Card 5	Normalized activation energy for a dislocation/dislocation interaction, G_o (*G0R*)	E10.0
11-20		Material constant, $1/p$ (*PINV*)	E10.0
21-30		Material constant, $1/q$ (*QINV*)	E10.0
31-40		Reference strain rate, $\dot{\varepsilon}_{o,i}$ (*LNEDI*)	E10.0
41-50		Normalized activation energy for a dislocation/interstitial interaction, $G_{o,i}$ (*G0IR*)	E10.0
51-60		Material constant, $1/p_i$ (*PINVI*)	E10.0
61-70		Material constant, $1/q_i$ (*QINVI*)	E10.0
71-80		Reference strain rate, $\dot{\varepsilon}_{o,s}$ (*LNEDS*)	E10.0

1-10	Card 6	Normalized activation energy for a dislocation/solute interaction, $G_{o,s}$ (*G0SR*)	E10.0
11-20		Material constant, $1/p_s$ (*PINVS*)	E10.0
21-30		Material constant, $1/q_s$ (*QINVS*)	E10.0
31-40		Density-heat capacity product, ρC_p (*RHOCPR*)	E10.0
41-50		Reference or room temperature, T_r (*TEMPRF*)	E10.0
	Card 7	Blank	E10.0
	Card 8	Blank	E10.0

The general form of the MTS model is given here and is discussed in detail in Maudlin, Davidson, and Henninger (1990). Forms for most other material can be obtained through simplification of the following equations. The flow stress σ is given by

$$\sigma = \frac{G}{G_o}\left(\hat{\sigma}_a + s_{th}\hat{\sigma} + s_{thi}\hat{\sigma}_i + s_{ths}\hat{\sigma}_s\right) \tag{142}$$

The first product in the equation for σ contains a micro-structure evolution variable, $\hat{\sigma}$, called the mechanical threshold stress, that is multiplied by a constant-structure deformation variable s_{th}. Here s_{th} is a function of absolute temperature T and plastic strain-rate $\dot{\varepsilon}^P$. The evolution equation for $\hat{\sigma}$ is a differential hardening law representing dislocation-dislocation interaction given by

$$\frac{\partial\hat{\sigma}}{\partial\varepsilon^p} = \Theta_o\left[1 - \frac{\hat{\sigma}}{\hat{\sigma}_s}\right]. \tag{143}$$

Here Θ_o represents hardening due to dislocation generation and the stress ratio represents softening due to dislocation recovery. The threshold stress at zero strain-hardening, $\hat{\sigma}_s$, is called the saturation threshold stress. Relationships for Θ_o and $\hat{\sigma}_s$ are expressed as

$$\Theta_o = a_o + a_1\ln\left(\dot{\varepsilon}^P\right) + a_2\sqrt{\dot{\varepsilon}^p} \tag{144}$$

and

$$\hat{\sigma}_s = \hat{\sigma}_{so}\left(\frac{\dot{\varepsilon}^p}{\dot{\varepsilon}_{so}}\right)^{\frac{kT}{GAb^3}}. \tag{145}$$

The shear modulus G explicitly depends upon temperature, and is assumed to have the form

$$G = b_o - \frac{b_1}{e^{b_2/T} - 1}. \tag{146}$$

For thermal-activation controlled deformation, s_{th}, s_{thi}, and s_{ths} have Arrhenius rate equations given by

$$s_{th} = \left[1 - \left\{\frac{kT\ln(\dot{\varepsilon}_o/\dot{\varepsilon}^P)}{Gb^3 g_o}\right\}^{1/q}\right]^{1/p}, \tag{147}$$

$$s_{thi} = \left[1 - \left\{\frac{kT\ln(\dot{\varepsilon}_{oi}/\dot{\varepsilon}^P)}{Gb^3 g_{oi}}\right\}^{1/(qi)}\right]^{1/(pi)} \tag{148}$$

and

$$s_{ths} = \left[1 - \left\{\frac{kT\ln(\dot{\varepsilon}_o/\dot{\varepsilon}^P)}{Gb^3 g_{os}}\right\}^{1/(qs)}\right]^{1/(ps)}. \tag{149}$$

The material temperature, *T*, is integrated in time assuming adiabatic conditions and is given by

$$T = T_r + \frac{1}{\rho C_p}\int_0^{\varepsilon_f} \sigma d\varepsilon. \tag{150}$$

Based upon the particular material, only a subset of the above mechanisms may be present. Maudlin, Davidson, and Henninger (1990) summarize the appropriate equations for copper, Ti-6Al-4V, and depleted α-uranium.

This material model was implemented and contributed to LLNL by John R. Baumgardner of the Los Alamos National Laboratory.

Material Type 30 (Closed-Form Update Elastic-Plastic for Shells)

Columns		Quantity	Format
1-10	Card 3	Young's modulus, E	E10.0
1-10	Card 4	Poisson's ratio, ν	E10.0
1-10	Card 5	Yield stress, σ_0	E10.0
1-10	Card 6	Tangent modulus, E_T	E10.0
	Card 7	Blank	
	Card 8	Blank	

This model implements a closed form solution for the plane stress constitutive update under conditions of perfect plasticity or kinematic hardening for a bilinear von Mises model. Thus, this model yields exactly the same behavior as Material Type 3 with $\beta = 0.0$ (i.e., purely kinematic hardening). The only difference between Material Type 3 and Material Type 30 lies in the numerical algorithms used to integrate the rate equations of plasticity under conditions of plane stress, as found in shell elements. The numerical implementation of Material Type 30 is described in (Whirley, Hallquist, and Goudreau, 1988).

The details of the constitutive equations and the resulting stress-strain behavior are discussed in the definition of Material Type 3.

Material Type 31 (Frazer-Nash Hyperelastic Rubber)

Columns		Quantity	Format
1-10	Card 3	First strain energy density coefficient, C_{001}	E10.0
11-20		Second strain energy density coefficient, C_{010}	E10.0
21-30		Third strain energy density coefficient, C_{020}	E10.0
31-40		Fourth strain energy density coefficient, C_{100}	E10.0
41-50		Fifth strain energy density coefficient, C_{101}	E10.0
1-10	Card 4	Sixth strain energy density coefficient, C_{110}	E10.0
11-20		Seventh strain energy density coefficient, C_{200}	E10.0
21-30		Eighth strain energy density coefficient, C_{210}	E10.0
31-40		Ninth strain energy density coefficient, C_{300}	E10.0
41-50		Tenth strain energy density coefficient, C_{400}	E10.0
1-10	Card 5	Strain limit option, *ILIMIT* EQ.0.0: stop if strain limits are exceeded EQ.1.0: continue if strain limits are exceeded	E10.0
1-10	Card 6	Maximum strain limit, E_{max}	E10.0
11-20		Minimum strain limit, E_{min}	E10.0
	Card 7	Blank	
	Card 8	Blank	

This model implements a hyperelastic constitutive law described in (Kenchington, 1988). It is useful for representing the behavior of rubber-like materials at moderate to large strains. Other hyperelastic models include Material Type 7 (Blatz-Ko) and Material Type 27 (Compressible Mooney Rivlin).

The strain energy density function is of the form

$$\begin{aligned} W \;=\; & C_{100}I_1 + C_{200}I_1^2 + C_{300}I_1^3 + C_{400}I_1^4 \\ & + C_{010}I_2 + C_{020}I_2^2 + C_{110}I_1I_2 + C_{210}I_1^2I_2 \\ & + C_{001}I_3 + C_{101}I_1I_3 \end{aligned} \tag{151}$$

where I_1, I_2, and I_3 are the strain invariants defined in terms of engineering components of the Green-Lagrange strain tensor $\boldsymbol{E}$ by

$$I_1 = E_{11} + E_{22} + E_{33}, \tag{152}$$

$$I_2 = (E_{11}E_{22} + E_{11}E_{33} + E_{22}E_{33}) - \frac{1}{4}(E_{12}^2 + E_{23}^2 + E_{31}^2), \tag{153}$$

and

$$I_3 = \left(E_{11}E_{22}E_{33} + \frac{1}{4}E_{12}E_{23}E_{31}\right) - \frac{1}{4}(E_{11}E_{23}^2 + E_{22}E_{31}^2 + E_{33}E_{12}^2). \tag{154}$$

The second Piola-Kirchhoff stress $\boldsymbol{T}$ is found by differentiating the strain energy density function W with respect to the Green-Lagrange strain,

$$\boldsymbol{T} = \frac{\partial W}{\partial \boldsymbol{E}}. \tag{155}$$

The Cauchy stress s is then found from the second Piola-Kirchhoff stress using

$$\mathsf{s} = \frac{1}{J}\boldsymbol{F}\boldsymbol{T}\boldsymbol{F}^T, \tag{156}$$

where $\boldsymbol{F}$ is the deformation gradient and J is its determinant.

The values of the ten C coefficients in the strain energy density function must be determined from experimental data on the material. A procedure is described in (Kenchington, 1988) to determine these parameters using data from a uniaxial stress test, a biaxial stress or strain test, and a shear test.

The model input includes a maximum strain limit E_{max}, a minimum strain limit E_{min}, and a strain limit option flag, $ILIMIT$. This feature is particularly useful if the model has been fitted to data only over a limited range, and therefore caution should be exercised if strains outside this range are encountered. At each step, the maximum and minimum normal strains are tested against the limit criteria. If the maximum normal strain is greater than E_{max} or the minimum normal strain is less than E_{min}, then a message is written to the screen and `hsp` printout file, and execution terminates if $ILIMIT = 0$ or continues if $ILIMIT = 1$.

Material Type 32 (Ramberg-Osgood Elastic-Plastic)

Columns		Quantity	Format
1-10	Card 3	Reference shear strain, γ_y	E10.0
1-10	Card 4	Reference shear stress, τ_y	E10.0
1-10	Card 5	Stress coefficient, α	E10.0
1-10	Card 6	Stress exponent, r	E10.0
1-10	Card 7	Bulk modulus, K	
	Card 8	Blank	

The Ramberg-Osgood equation is an empirical constitutive relation to represent the one-dimensional elastic-plastic behavior of many materials. This implementation of the model was developed by Whirley and Engelmann, and allows a simple rate-independent representation of the hysteretic energy dissipation observed in materials subjected to cyclic shear deformation. For monotonic loading, the stress-strain relationship is given by

$$\frac{\gamma}{\gamma_y} = \frac{\tau}{\tau_y} + \alpha\left|\frac{\tau}{\tau_y}\right|^r \quad \text{if} \quad \gamma \geq 0 \quad , \tag{157}$$

$$\frac{\gamma}{\gamma_y} = \frac{\tau}{\tau_y} - \alpha\left|\frac{\tau}{\tau_y}\right|^r \quad \text{if} \quad \gamma < 0 \quad , \tag{158}$$

where γ is the shear strain and τ is the stress. The model approaches perfect plasticity as the stress exponent $r \to \infty$. These equations must be augmented to correctly model unloading and reloading material behavior. The first load reversal is detected by $\gamma\dot{\gamma} < 0$. After the first reversal, the stress-strain relationship is modified to

$$\frac{\gamma - \gamma_0}{2\gamma_y} = \frac{\tau - \tau_0}{2\tau_y} + \alpha\left(\frac{\tau - \tau_0}{2\tau_y}\right)^r \quad \text{if} \quad \gamma > 0 \quad , \tag{159}$$

$$\frac{\gamma - \gamma_0}{2\gamma_y} = \frac{\tau - \tau_0}{2\tau_y} - \alpha\left(\frac{\tau_0 - \tau}{2\tau_y}\right)^r \quad \text{if} \quad \gamma < 0 \quad , \tag{160}$$

where γ_0 and τ_0 represent the values of strain and stress at the point of load reversal. Subsequent load reversals are detected by $(\gamma - \gamma_0)\dot{\gamma} < 0$.

The Ramberg-Osgood equations are inherently one-dimensional, and are assumed to apply to shear components. To generalize this theory to the multidimensional case, it is assumed that each component of the deviatoric stress and deviatoric tensorial strain is independently related by the one-dimensional stress-strain equations. A projection is used to map the result back into deviatoric stress space, if required. The volumetric behavior is elastic, and therefore the pressure p is found by

$$p = -K\varepsilon_V, \tag{161}$$

where ε_V is the volumetric strain.

This model is primarily intended as a simple model for shear behavior, as is often used in seismic analysis.

Material Type 33 (General Anisotropic Elastic-Plastic)

Columns		Quantity	Format
1-10	Card 3	Elastic modulus, E_a	E10.0
11-20		Elastic modulus, E_b	E10.0
21-30		Elastic modulus, E_c	E10.0
31-40		Anisotropy coefficient, R (1948 Hill theory)	E10.0
41-50		Anisotropy coefficient, P	E10.0
51-60		Anisotropy coefficient, Q_{bc}	E10.0
61-70		Anisotropy coefficient, Q_{ab}	E10.0
71-80		Anisotropy coefficient, Q_{ac}	E10.0
1-10	Card 4	Poisson's ratio, ν_{ba}	E10.0
11-20		Poisson's ratio, ν_{ca}	E10.0
21-30		Poisson's ratio, ν_{cb}	E10.0
31-40		Material axes option, $AOPT$	E10.0
1-10	Card 5	Yield stress in a-direction, σ_{ya}	E10.0
11-20		Material angle, β	E10.0
21-30		x_p for $AOPT = 1$ or a_x for $AOPT = 2$	E10.0
31-40		y_p for $AOPT = 1$ or a_y for $AOPT = 2$	E10.0
41-50		z_p for $AOPT = 1$ or a_z for $AOPT = 2$	E10.0
51-60		d_x for $AOPT = 2$ or v_x for $AOPT = 3$	E10.0
61-70		d_y for $AOPT = 2$ or v_y for $AOPT = 3$	E10.0
71-80		d_z for $AOPT = 2$ or v_z for $AOPT = 3$	E10.0
1-10	Card 6	Hardening modulus in a-direction, E_p^a	E10.0
11-20		Shear modulus, G_{bc}	E10.0
21-30		Shear modulus, G_{ab}	E10.0
31-40		Shear modulus, G_{ac}	E10.0
1-10	Card 7	Blank	
1-10	Card 8	Blank	

This model combines the orthotropic elasticity of Material Type 2 with the 1948 Hill orthotropic plasticity model described in (Hill, 1950). The numerical implementation at present is described in (Logan, 1988). This approach is based on a straightforward substepping method described in (Bathe, 1982) and elsewhere. It is most convenient to chose a reference direction when using the 1948 Hill theory, and in this model the a-direction is chosen.

The elastic parameters and material axes definition option $AOPT$ are specified as described for the Orthotropic Elastic model, Material Type 2**.**

This model include linear strain hardening. The linear strain hardening law has the form

$$\sigma_y = \sigma_0 + E_p \bar{\varepsilon}^p, \tag{162}$$

where the effective plastic strain $\bar{\varepsilon}^p$ is given by

$$\bar{\varepsilon}^p = \int_0^t d\bar{\varepsilon}^p, \tag{163}$$

and the increment in effective plastic strain $d\bar{\varepsilon}^p$ is found from the incremental plastic strain tensor $d\varepsilon_{ij}^p$ as

$$(d\bar{\varepsilon}^p)^2 = \frac{R+1}{(1+R+P)^2 R}[A+B+C] + \frac{R+1}{2}\left[\frac{(d\gamma_{bc}^p)^2}{L} + \frac{(d\gamma_{ab}^p)^2}{M} + \frac{(d\gamma_{ac}^p)^2}{N}\right] \tag{164}$$

where

$$\begin{aligned} A &= P((1+R)d\varepsilon_c^p + Rd\varepsilon_a^p)^2 \\ B &= R((1+P)d\varepsilon_a^p + Pd\varepsilon_c^p)^2. \\ C &= (Rd\varepsilon^p{}_a - Pd\varepsilon_c^p)^2 \end{aligned} \tag{165}$$

This expression evolves directly from the use of the effective stress in the 1948 Hill theory. Using the conventional variables F, G, H, L, M, and N for clarity, the effective stress may be written as

$$\bar{\sigma}^2 = \frac{F(\sigma_c - \sigma_b)^2 + G(\sigma_b - \sigma_a)^2 + H(\sigma_a - \sigma_c)^2 + D}{R+1}, \tag{166}$$

where

$$D = 2L\sigma_{ac}^2 + 2M\sigma_{ab}^2 + 2N\sigma_{bc}^2. \tag{167}$$

In the above equations, F, G, and H are found in terms of the anisotropy parameters R and P as

$$F = \frac{R}{P}, \tag{168}$$

$$G = 1, \tag{169}$$

and

$$H = R. \tag{170}$$

The shear terms L, M, and N are found using

$$L = \frac{1}{2}(R + Z) \tag{171}$$

$$M = \frac{1}{2}(R + Z), \tag{172}$$

$$N = \frac{1}{2}(Z + 1). \tag{173}$$

The anisotropy parameters R, P, Q_{bc}, Q_{ba}, and Q_{ca} can be determined from simple uniaxial material tension tests in orthogonal directions. Using the local coordinate system defined above,

$$R = \frac{\varepsilon_c}{\varepsilon_b}, \tag{174}$$

where ε_b and ε_c are the transverse strains measured in a uniaxial tension test in the a-direction. Similarly,

$$P = \frac{\varepsilon_a}{\varepsilon_b} \tag{175}$$

in a uniaxial tension test in the c-direction. In the b-c plane, the shear term Q_{bc} is found from

$$Q_{bc} = \frac{\varepsilon_{b'''}}{\varepsilon_a} \tag{176}$$

in a uniaxial tension test in the c''' direction. The b''' and c''' axes are defined by rotating the b and c axes by 45 degrees counterclockwise in the b-c plane. Similarly, in the a-b plane,

$$Q_{ba} = \frac{\varepsilon_{b''}}{\varepsilon_c} \tag{177}$$

for a uniaxial test in the a'' direction, where the a'' and b'' axes are rotated 45 degrees counter-clockwise in the a-b plane. In the a-c plane, the shear term Q_{ca} is found from

$$Q_{ca} = \frac{\varepsilon_{c'}}{\varepsilon_b} \tag{178}$$

in a uniaxial tension test in the a' direction, where the a' and c' axes are defined by rotating the a and c axes counterclockwise by 45 degrees in the a-c plane.

In the present model, only isotropic strain hardening is included. The a-direction hardening modulus E_p^a can be written in terms of the a-direction tangent modulus E_T^a as

$$E_p^a = \frac{E_a E_T^a}{E_a - E_T^a}, \tag{179}$$

where E_a is the elastic modulus in the a-direction. The plastic hardening modulus E_p^a is the slope of the stress vs. *plastic* strain curve in a uniaxial stress test, and the tangent modulus E_T^a is the slope of the inelastic portion of a uniaxial stress vs. strain curve.

Material Type 34 (Normal Anisotropic Elastic-Plastic for Shells)

Columns		Quantity	Format
1-10	Card 3	Young's modulus, E	E10.0
1-10	Card 4	Poisson's ratio, ν	E10.0
1-10	Card 5	Yield stress, σ_0	E10.0
1-10	Card 6	Tangent modulus, E_T	E10.0
1-10	Card 7	Anisotropy parameter, R	
	Card 8	Blank	

This model incorporates a version of Hill's model of anisotropic plasticity adapted for shell elements. The numerical algorithms used in this implementation are described in Whirley and Engelmann (1991). The yield criterion used in this model is specialized to normal anisotropy, where the properties do not vary with direction in the plane of the shell, but the transverse direction may have different properties. The anisotropy parameter R is the ratio of the in-plane plastic strain rate to the out-of-plane plastic strain rate. It can also be shown that

$$R = \frac{2}{K^2} - 1, \tag{180}$$

where $K = \frac{\sigma_0}{\sigma_{03}}$ is the ratio of the in-plane initial yield stress to the initial yield stress in the transverse (through-thickness) direction. Note that the model reverts to isotropically elastic-plastic when $R = 1$.

Using the assumption of plane stress on each lamina of the shell, the yield function may be written

$$F(\sigma_{ij}) = \left[\sigma_{11}^2 + \sigma_{22}^2 - \frac{2R}{R+1}\sigma_{11}\sigma_{22} + 2\frac{2R+1}{R+1}\sigma_{12}^2\right]^{\frac{1}{2}}, \tag{181}$$

where σ_{ij} denotes Cauchy stress in the local coordinates of the shell. Isotropic strain hardening is included, with the in-plane yield stress σ_y found from

$$\sigma_y = \sigma_0 + E_p\bar{\varepsilon}^p, \tag{182}$$

where E_p is the plastic hardening modulus and $\bar{\varepsilon}^p$ is the effective plastic strain. The plastic hardening modulus is found from the input values of Young's modulus E and the tangent modulus E_T using

$$E_p = \frac{EE_T}{E - E_T}. \tag{183}$$

The plastic hardening modulus E_p is the slope of the inelastic portion of the effective stress $\bar{\sigma}$ vs. effective plastic strain $\bar{\varepsilon}^p$ curve, and the tangent modulus E_T is the slope of the inelastic part of a uniaxial stress vs. strain curve (or equivalently, the effective stress vs. effective strain curve).

Normal anisotropic plasticity behavior arises in many metals used in sheet-forming operations.

Material Type 35 (Elastic-Plastic with Forming Limit Diagram)

Columns		Quantity	Format
1-10	Card 3	Young's modulus, E	E10.0
11-20		Forming Limit Failure Criterion Option, $IFLD$	E10.0
1-10	Card 4	Poisson's ratio, ν	E10.0
11-20		Load curve for left side of diagram, $LCLH$	E10.0
21-30		Load curve for right side of diagram, $LCRH$	E10.0
31-40		Load curve giving pressure dependence, $LCPX$	E10.0
41-50		Load curve giving rate dependence of FLD, $LCEDF$	E10.0
51-60		Load curve for rate dependent yield stress, $LCEDM$	E10.0
1-10	Card 5	Yield stress, σ_0	E10.0
11-20		Failure scale factor for deviatoric stresses, $SCLDEV$	E10.0
1-10	Card 6	Tangent modulus, E_T	E10.0
11-20		Hardening parameter, β	E10.0
1-10	Card 7	First tabulated effective plastic strain, $\bar{\varepsilon}_1^p$	E10.0
11-20		Second tabulated effective plastic strain, $\bar{\varepsilon}_2^p$	E10.0
.		.	.
.		.	.
.		.	.
71-80		Eighth tabulated effective plastic strain, $\bar{\varepsilon}_8^p$	E10.0
1-10	Card 8	First tabulated yield stress, σ_{y1}	E10.0
.		.	.
.		.	.
.		.	.
71-80		Eighth tabulated yield stress, σ_{y8}	E10.0

This model combines the elastic-plastic Material Type 3 with a Forming Limit Diagram (FLD) failure model developed by Logan and described in (Logan, 1991). The constitutive behavior of the material is exactly as in Material Type 3, with one exception (rate-dependent yield) which is

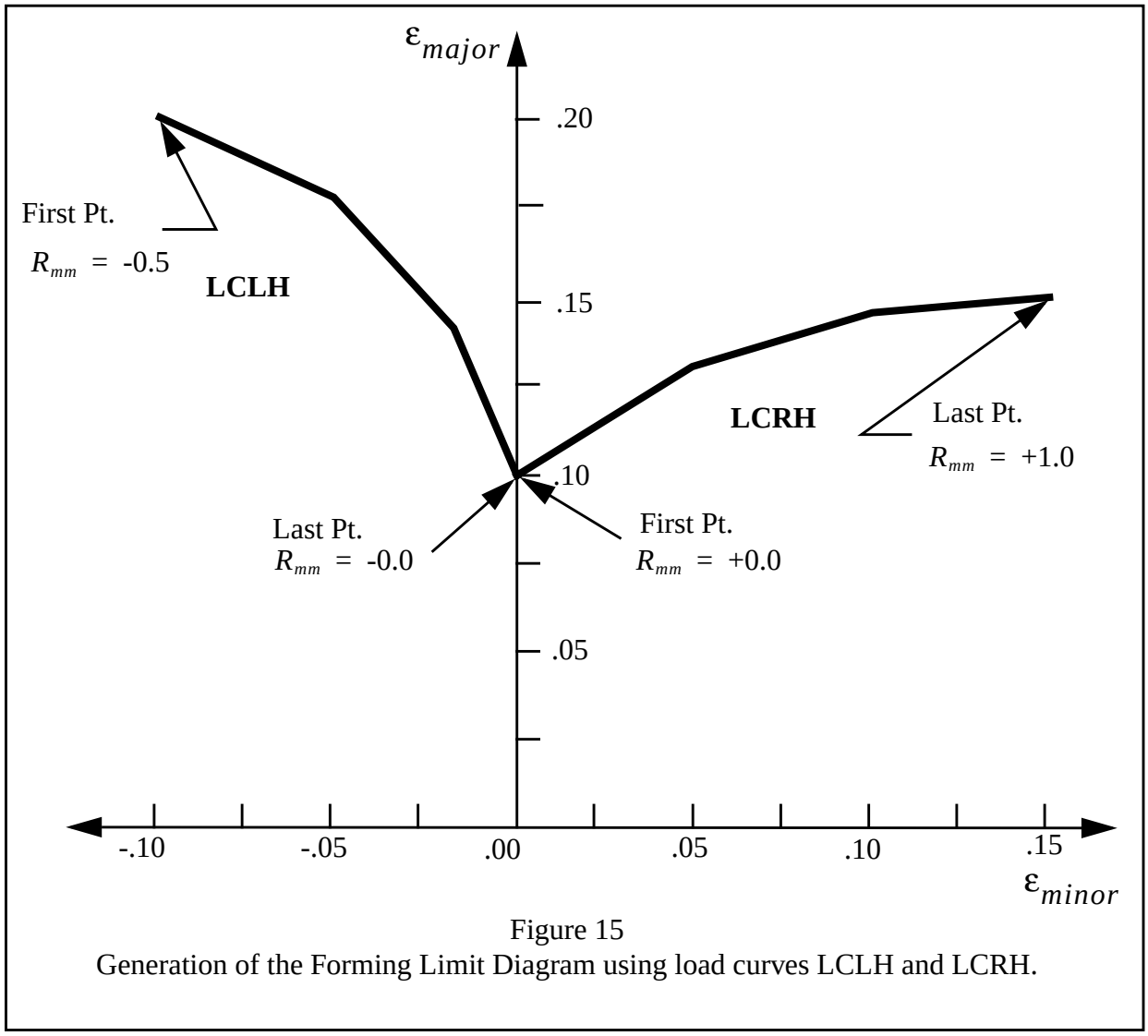

Figure 15
Generation of the Forming Limit Diagram using load curves LCLH and LCRH.

described below. The FLD method (Keeler, 1968) involves plotting the major (largest principal) strain versus the minor (next largest) principal strain. When the major strain reaches the FLD limiting value, which is a function of the minor strain, material failure is predicted. Once failure is detected in this model, the yield stress σ_y and the tangent modulus E_T are reduced by the factor $SCLDEV$. In addition, a failure-fraction parameter F is set to one to indicate that failure has occurred at a material point.

The shape of the forming limit diagram is determined by the left-hand and right-hand load curves, $LCLH$ and $LCRH$. The abscissa (first column) of each these load curves gives the ratio of minor true strain to major true strain, R_{mm}, and the ordinate (second column) gives the major true strain, ε_{maj}. The left-hand load curve should cover the minor/major strain ratio range of -0.5 to 0.0, and the right-hand curve should cover the strain ratio range from 0.0 to 1.0, as shown in Figure 15.

The pressure dependence of the forming limit diagram is determined by the pressure load curve, $LCPX$. Strictly speaking, the forming limit diagram is a plane-stress sheet forming concept. Thus, for any monotonic path on the forming limit diagram, there is an associated value of normalized pressure $\hat{p}$, where $\hat{p}$ is given by

$$\hat{p} = \frac{p}{\sigma_y}, \tag{184}$$

where p is the pressure and σ_y is the current yield stress. For uniaxial tension, $\hat{p} = -\frac{1}{3}$, and for biaxial tension $\hat{p} = -\frac{2}{3}$. Any additional normalized pressure, $\hat{p}$, beyond these standard values for plane stress conditions may cause the forming limit diagram to grow or shrink by an increment $d\varepsilon^{\hat{p}}_{maj}$ on each strain path R_{mm}. Load curve $LCPX$ should contain the additional normalized pressure on the abscissa and the corresponding increment $d\varepsilon^{\hat{p}}_{maj}$ on ordinate axis. Figure 16 illustrates the operation of the pressure-dependence load curve.

The size of the forming limit diagram (i.e., the limiting major strain for any given minor-to-major strain ratio) may be dependent on the total strain rate. The load curve $LCEDF$ specifies this strain rate dependence of the forming limit diagram. The load curve should contain strain rates on the abscissa, and corresponding $d\varepsilon^{\dot{\varepsilon}}_{maj}$ values on the ordinate. These $d\varepsilon^{\dot{\varepsilon}}_{maj}$ are applied along all R_{mm} paths given in the left-hand and right-hand FLD load curves to derive the curves actually used in the calculation. The operation of the rate-dependence load curves is illustrated in Figure 17.

The material constitutive behavior differs from the elastic-plastic model, Material Type 3, in that the yield stress may be multiplied by a strain rate dependent factor found from load curve $LCEDM$. The abscissa of this load curve should contain total strain rate values, and the ordinate should give the scale factor to be multiplied times the current yield stress, σ_y. Note that this strain rate scaling is applied after strain hardening is taken into account.

The load curves for pressure ($LCPX$), strain rate dependence of the FLD ($LCEDF$), and strain rate dependence of the yield stress ($LCEDM$), are optional; if these are input as zero, the option is ignored and the appropriate scale factor becomes unity. Load curves for the left-hand FLD ($LCLH$) and the right-hand FLD ($LCRH$) are required and must contain at least two points each.

The determination of failure or proximity to failure is made in one of three ways, depending on the value of the forming limit failure criterion option, $IFLD$. For the TOTAL FLD approach ($IFLD = 1$; see Figure 18), the total major and minor strains are compared to the limiting value given by the forming limit diagram, and the failure fraction parameter F is determined. The

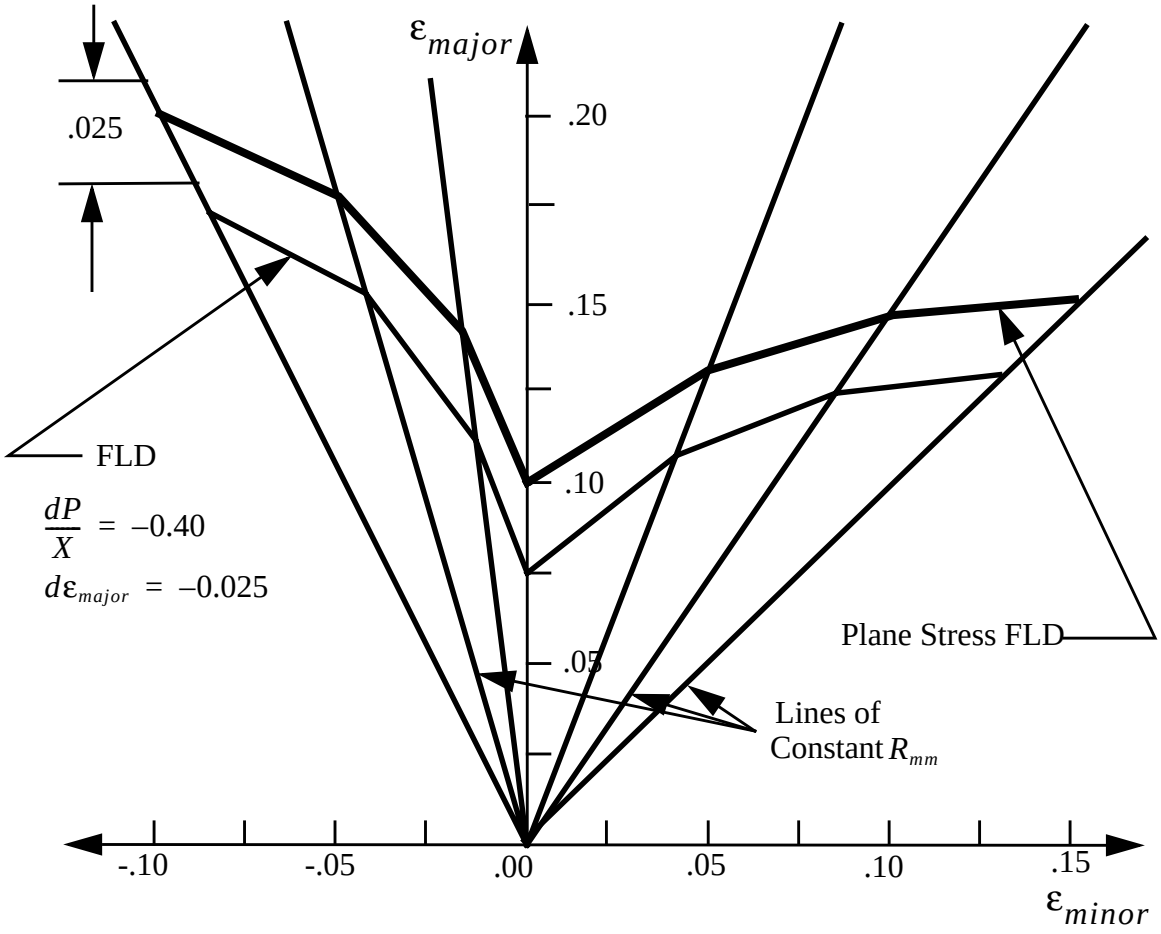

Figure 16
Effect of added hydrostatic pressure on the shape of the Forming Limit Diagram.

pressure used in pressure dependence option with this criterion is a “damped” pressure, which is a running average of the instantaneous pressures. The strain rate is similarly damped. This procedure approximates the “total” forming limit diagram method used in press shop practice. In the INCREMENTAL FLD approach ($IFLD = 2$; see Figure 19), the total value of the major strain is used to get the vertical position on the FLD. The current incremental value of minor-to-major strain ratio, dR_{mm}, is used to establish the R_{mm} line used. This R_{mm} line is traversed from the origin up to the current ε_{maj} value to establish the position on the FLD. The current pressure and strain rate are used for the pressure dependence and rate dependence options with this criterion, and this may lead to sudden failure when the loading path changes, as is sometimes observed in practice. For the DAMAGE FLD approach ($IFLD = 3$; see Figure 20), the increment in major strain is considered along with the current pressure and strain-rate. An increment in failure fraction ΔF is found from

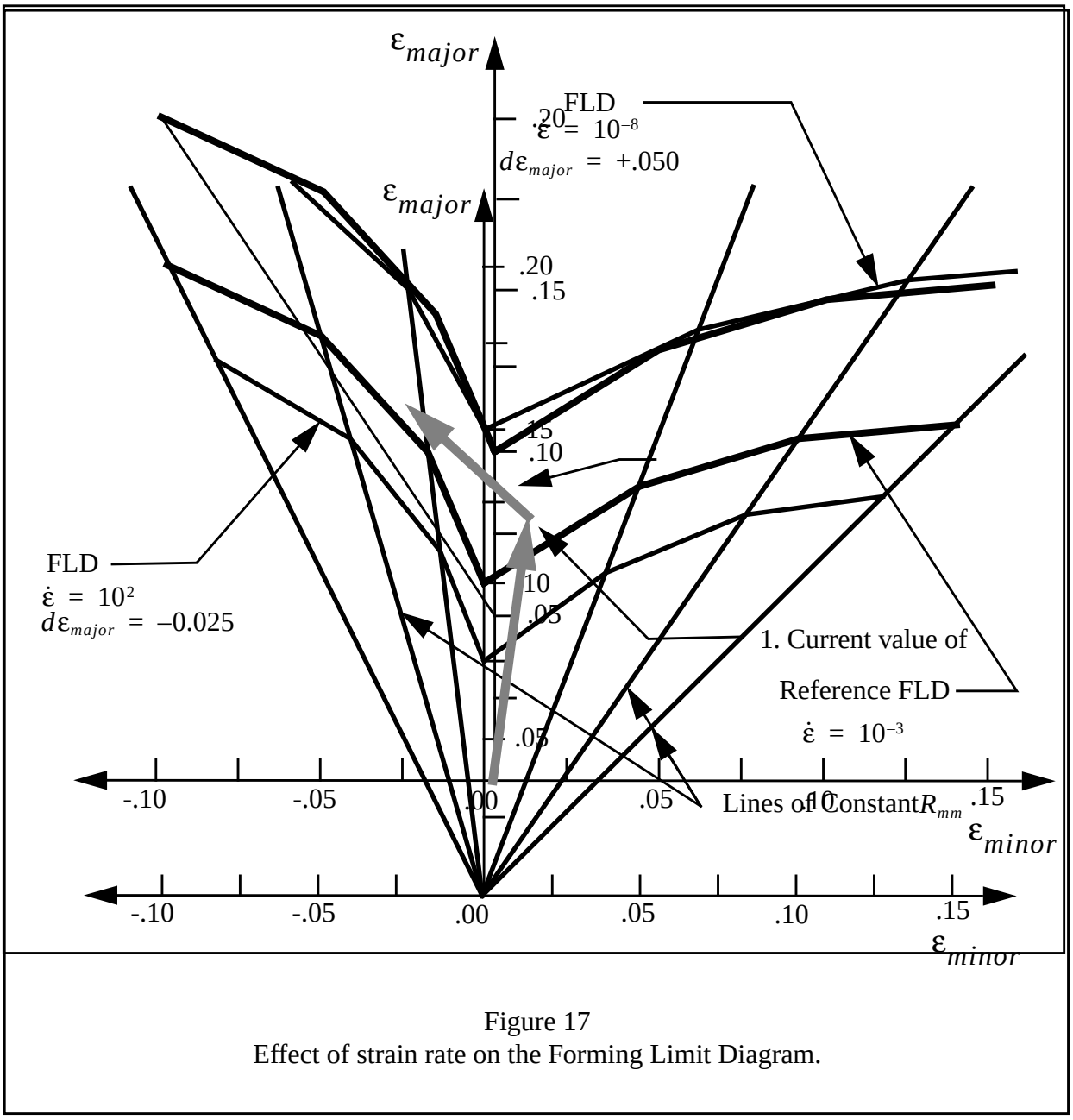

Figure 17
Effect of strain rate on the Forming Limit Diagram.

$$\Delta F = \frac{\Delta\varepsilon_{major}}{\Delta\varepsilon_{major}^{path}}, \tag{185}$$

where $\varepsilon_{major}^{path}$ is the major strain to failure in the direction of $\Delta\varepsilon_{major}$ on the current forming limit diagram (after pressure and strain rate effects are incorporated). The failure fraction then accumulates according to

$$F_{n+1} = F_n + \Delta F, \tag{186}$$

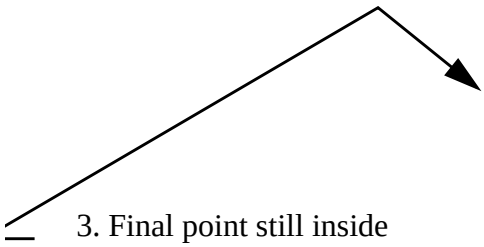

2. Increments
$d\varepsilon_{major}$ and $d\varepsilon_{minor}$
are added.

3. Final point still inside
FLD, so no failure
predicted.

ε_{major} and ε_{minor}

Figure 18
The TOTAL FLD approach predicts “no failure” in this example.

where the subscripts denote time step number. Failure occurs when $F \geq 1.0$. This failure criterion option accounts for strain path changes in a way that is less prone to spurious failures due to numerical noise than is the INCREMENTAL FLD criterion.

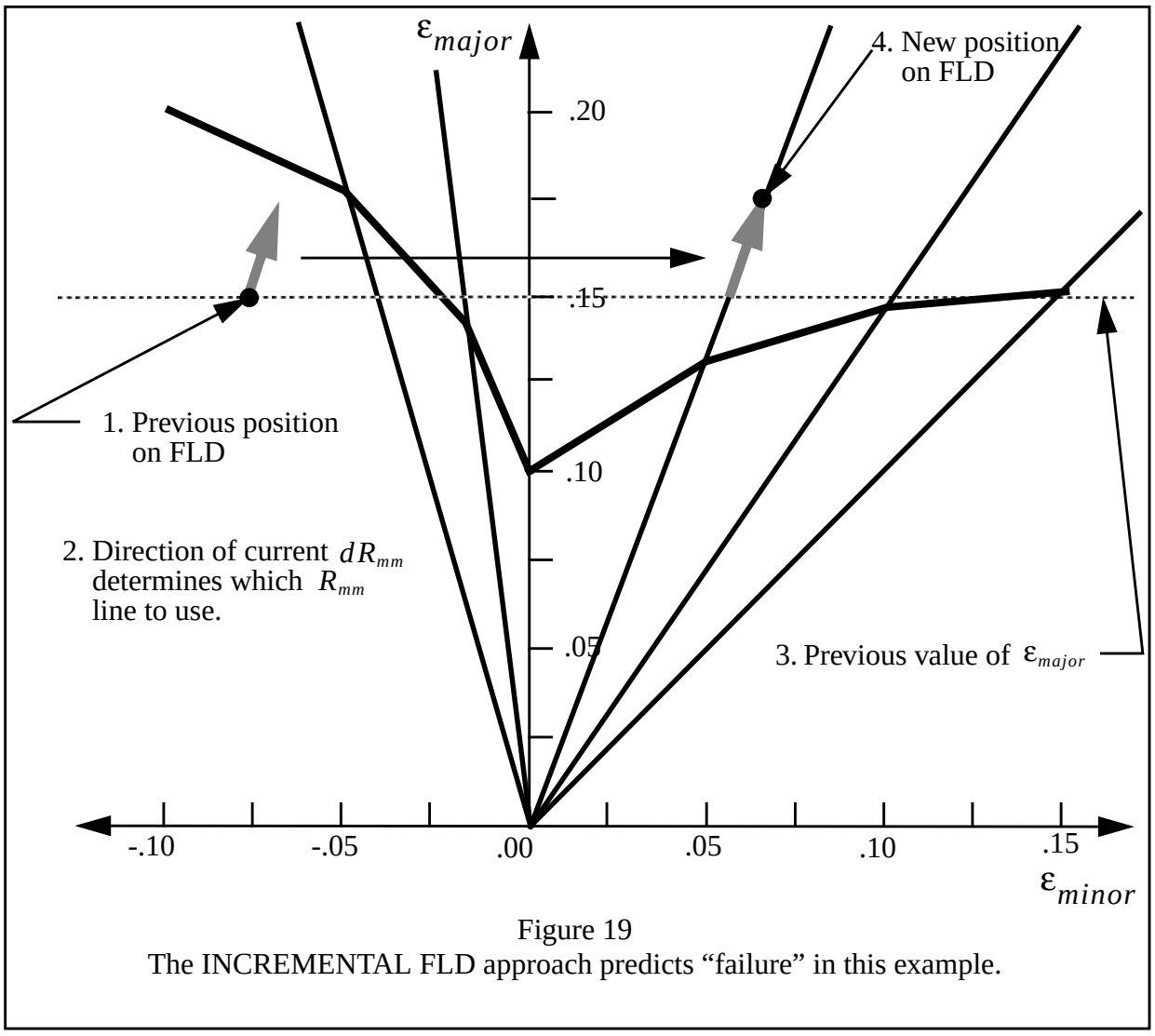

Figure 19
The INCREMENTAL FLD approach predicts “failure” in this example.

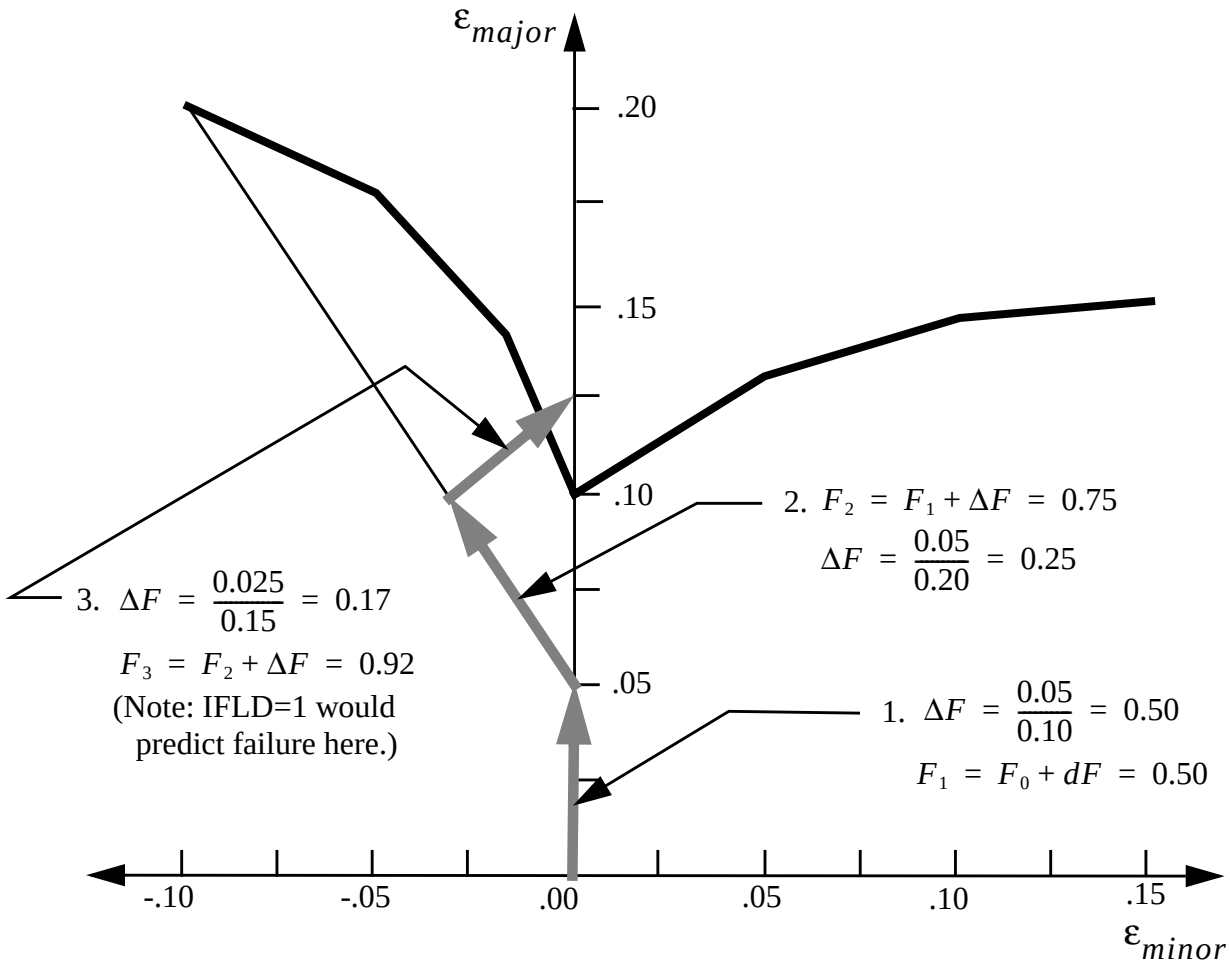

Figure 20
The DAMAGE FLD approach predicts “no failure,” but the TOTAL FLD approach predicts “failure” with this strain path.

Material Type 36 (Brittle Damage Model)

Columns		Quantity	Format
1-10	Card 3	Young's modulus, E	E10.0
1-10	Card 4	Poisson's ratio, ν	E10.0
1-10	Card 5	Tensile strength, f_{t0}	E10.0
11-20		Shear limit, f_{s0}	E10.0
21-30		Compressive yield, σ_y	E10.0
1-10	Card 6	Fracture toughness expressed as energy per unit area of crack advancement, g_c	E10.0
11-20		Optional damage level for element removal, D_r (default: 0.0 - no element removal)	E10.0
1-10	Card 7	Shear retention factor, β	E10.0
1-10	Card 8	Viscosity, η	E10.0

This model describes the anisotropic damage of brittle materials and is designed primarily for concrete. This model admits progressive degradation of tensile and shear strengths across smeared cracks that are initiated under tensile loadings. Damage, the evolution of cracks, is handled by treating the rank four elastic stiffness tensor as an evolving internal variable for the material. Softening induced mesh dependencies are addressed by a characteristic length method (Oliver, 1989). Under compressive conditions, the material behavior is governed by an elastic/perfectly-plastic response using J2 flow theory. (Various internal variables such as crack orientations and degraded stiffness tensors are internally calculated but are not currently outputted.)

The elastic properties E and ν define the undamaged or "virgin" material response. When the first principal stress reaches the initial tensile strength (stress), f_{t0}, a smeared crack is initiated in a plane normal to the first (or maximum) principal stress direction. Once damage initiates, the crack orientation is fixed at that location, though the orientation will convect with the motion of the body. As the loading advances the allowed tensile traction normal to the crack plane is progressively degraded to a small machine-dependent constant. The degradation is implemented by reducing the materials modulus normal to the smeared crack plane according to a "maximum dissipation" law that incorporates exponential softening. The restriction on the normal traction, t_n, defined as $t_n = (\boldsymbol{n} \otimes \boldsymbol{n}) \bullet \mathsf{s}$, is given by

$$t_n \leq f_{to} - (1 - \varepsilon) f_{to} (1 - exp(-H\alpha)) \tag{187}$$

where $\boldsymbol{n}$ is the smeared crack normal, ε is a small constant, s is the stress, H is the softening modulus, and α is an internal variable. H is calculated automatically based upon the fracture toughness g_c and the element geometry. The internal variable α, normalized and outputted in the "equivalent plastic strain field," measures the crack field's intensity. When the normalized value of α reaches unity, the material's strength has been reduced to two percent of its original value in the normal and parallel directions of the smeared crack. For plotting purposes $\alpha \le 5$. Similarly, the shear traction, t_s, that can be transmitted across a smeared crack plane is limited such that

$$t_s \le f_{so}(1-\beta)(1-exp(-H\alpha)) \tag{188}$$

where f_{so} is the initial shear traction that may be transmitted and β is the shear retention factor. Shear degradation uses two orthogonal shear damage surfaces and is coupled to the tensile degradation through α. Shear degradation is achieved by reducing the material's shear stiffness parallel to the smeared crack plane. As the damage progresses t_s asymptotes to βf_{so}.

The fracture toughness, g_c, of the material should be entered as the fracture energy *per unit area of crack advancement*.

To obtain mesh independent results, the characteristic element length, l^c, should be less than the material's characteristic dimension, i.e. $l^c \le \frac{2Eg_c}{f_{to}^2}$. Meshes with larger elements may dissipate too much energy during tensile damage.

Rate dependent or "viscous" behavior is implemented as a simple Perzyna regularization method and is controlled by the viscosity of the material η. Using $\eta = 0$ results in a rate-independent response.

Under compressive conditions, this model uses an elastic/perfectly-plastic response to limit excessive or runaway (compressive) stresses. A check is made on the compressive stress state using the J2 yield function $\sqrt{\frac{3}{2}\boldsymbol{S}\bullet\boldsymbol{S}} - \sigma_y \le 0$, where $\boldsymbol{S}$ is the stress deviator. If the yield function is violated, a J2 return mapping correction is executed and plastic strains are generated. If $\sigma_y = 0$, compressive plasticity is ignored. During simultaneous plasticity and cracking at a single point, the compressive plasticity is only approximate.

An optional element removal flag, D_r, may be set to remove elements after sufficient tensile damage accumulates. Elements are removed when α exceeds D_r. This feature should be used with caution since element removal may alter the results. Since $\alpha \le 5$, $D_r < 5$. When $D_r = 0$, elements are not removed.

Remark: A variety of experimental data, from quasi-static to explosive situations, has been replicated using this model. An example of typical properties for a standard grade concrete, without rate effects, are $E = 3.15 \times 10^6$ psi, $\nu = 0.2$, $f_{to} = 450$ psi, $f_{so} = 2100$ psi, $g_c = 0.872$ lbs/in, $\beta = 0.03$, and $\eta = 0.0$ psi-sec.

A full description of this material model is given in Govindjee, Kay, and Simo (1993).

Material Type 37 (Three-Invariant Viscoplastic Cap Model)

Columns		Quantity	Format
1-10	Card 3	Shear modulus, G	E10.0
11-20		Bulk modulus, K	E10.0
21-30		Gruneisen ratio (optional), Γ	E10.0
31-40		Shock parameter (optional), S_l	E10.0
41-50		Pore compression flag, $IPRES$ EQ.0.0: Explicit pore compression EQ.1.0: Constant bulk modulus	E10.0
1-10	Card 4	Shear failure surface constant, α	E10.0
11-20		Shear failure surface linear coefficient, θ	E10.0
21-30		Shear failure surface exponential coefficient, γ	E10.0
31-40		Shear failure surface exponent, β	E10.0
41-50		Tensile pressure cutoff (negative in tension)	E10.0
51-60		Tensile return mapping mode	E10.0
61-70		Kinematic hardening parameter, N^{α}	E10.0
71-80		Kinematic hardening coefficient, c^{α}	E10.0
1-10	Card 5	Initial ellipticity, R_0	E10.0
11-20		Initial J_1-axis intercept, X_0	E10.0
21-30		Cap contraction option, $IROCK$ EQ.0.0: Contraction allowed (soils) EQ.1.0: Contraction omitted (rocks) EQ.2.0: Contraction w/ hardening (rocks)	E10.0
31-40		Shear-enhanced compaction parameter	E10.0
1-10	Card 6	Maximum plastic volume strain, W	E10.0
11-20		Exponent D_1	E10.0
21-30		Exponent D_2	E10.0
31-40		Plot variable output option (see Table 1)	E10.0
41-50		Maximum strain increment	E10.0
1-10	Card 7	Three-invariant parameter Q_1	E10.0

Columns		Quantity	Format
11-20		Three-invariant parameter Q_2 GE.0.0: Formulation parameter LE.0.0: Friction angle, φ (degrees)	E10.0
21-30		Rounded vertices parameter, $\Delta\beta_0$ (degrees)	E10.0
31-40		Rounded vertices parameter, δ	E10.0
41-50		Viscoplasticity fluidity parameter	E10.0
51-60		Viscoplastic flow function form, *NFORM* LT.0.0: $\phi(f) = (f/f_0)^N$, where $N = \|NFORM\|$ GT.0.0: $\phi(f) = exp(f/f_0)^N - 1$	E10.0
	Card 8	Blank	

This model was developed by Len Schwer and Yvonne Murray and is described in (Schwer and Murray, 1994). For additional information on the viscoplastic aspects of this model see (Schwer, 1994).

Table 1: Output variables for NPLOT plotting option.

NPLOT	Function	Description
1	$L(\kappa)$	J_1 value at cap-shear surface intersection
2	$X(\kappa)$	J_1 intercept of cap surface
3	$R(\kappa)$	Cap surface ellipticity
4	$\bar{\varepsilon}_v^p$	Plastic volume strain
5	J_1	First stress invariant
6	J_2'	Second invariant of deviatoric stress
7	J_3'	Third invariant of deviatoric stress
8	$\hat{J}_3'$	$(3\sqrt{1.5}J_3')/(J_2')^{3/2} = -\sin(3\beta)$
9	β	Lode angle (degrees)
10	R	Octahedral plane radius
11	J	Relative volume
12	ϕ	Porosity

Table 1: Output variables for NPLOT plotting option.

NPLOT	Function	Description
13	ϕ_{cs}	Relative change in volume of solid phase
14	P_{hs}	Pressure in the solid phase
15	E_{hs}	Energy in the solid phase
16	nsubs	Number of strain subincrements
17	$1-(R^2F_f^2F_c)/J_2'$	Deviation from failure surface
18	G^{α}	Kinematic hardening limiting function
19*	J_2^{α}	Kinematic hardening backstress

Material Type 38 (Bammann Plasticity Model)

Columns		Quantity	Format
1-10	Card 3	Young's modulus, E	E10.0
11-20		Poisson's ratio, ν	E10.0
21-30		Initial temperature, T_0	E10.0
31-40		Heat generation coefficient, HC	E10.0
1-10	Card 4	C_1	E10.0
11-20		C_2	E10.0
21-30		C_3	E10.0
31-40		C_4	E10.0
1-10	Card 5	C_5	E10.0
11-20		C_6	E10.0
21-30		C_7	E10.0
31-40		C_8	E10.0
41-50		C_{13}	E10.0
51-60		C_{14}	E10.0
1-10	Card 6	C_9	E10.0
11-20		C_{10}	E10.0
21-30		C_{15}	E10.0
31-40		C_{16}	E10.0
41-50		C_{11}	E10.0
51-60		C_{12}	E10.0
61-70		C_{17}	E10.0
71-80		C_{18}	E10.0
1-10	Card 7	Initial tensor internal variable, α_{xx}	E10.0
11-20		Initial α_{yy}	E10.0
21-30		Initial α_{xy}	E10.0
31-40		Initial α_{yz}	E10.0
41-50		Initial α_{zx}	E10.0

Columns		Quantity	Format
51-60		Initial scalar internal variable, κ_0	E10.0
	Card 8	Blank	

This model is described in (Bammann, 1990) and (Bammann, Johnson, and Chiesa, 1990). It is a phenomenological plasticity model using a set of internal state variables whose evolution is based on micromechanics. The model includes rate and temperature dependence, and heat generation due to plastic work. Since internal state variables are used to track the deformation, the history effects of strain rate and temperature are correctly captured.

The number of material parameters may seem prohibitive, but rarely are all of the constants used. The model reduces to linear strain hardening with only two required parameters. For rate insensitive materials the number of parameters is reduced by four. If temperature dependence is not required (i.e. when heat generation is not important), then the number of parameters is reduced by a factor of two. All of the parameters can be determined using simple tension and compression data.

The evolution of the Cauchy stress $\mathbf{s}$ is governed by an equation of the form

$$\dot{\mathbf{s}} = \lambda Tr(\boldsymbol{d}^e)\mathbf{1} + 2G\boldsymbol{d}^e, \tag{189}$$

where $\boldsymbol{d}^e$ is the elastic part of the rate of deformation, λ is the elastic Lame parameter given by

$$\lambda = \frac{E\nu}{(1+\nu)(1-2\nu)}, \tag{190}$$

and G is the elastic shear modulus. The rate of deformation $\boldsymbol{d}$ (symmetric part of the velocity gradient) is decomposed as

$$\boldsymbol{d} = \boldsymbol{d}^e + \boldsymbol{d}^p + \boldsymbol{d}^{th}, \tag{191}$$

where $\boldsymbol{d}^p$ is the deviatoric plastic part, and $\boldsymbol{d}^{th}$ is the thermal expansion part. The deviatoric plastic part of the rate of deformation is given by

$$\boldsymbol{d}^p = f(T)\sinh\left[\frac{|\mathbf{x}| - \kappa - Y(T)}{V(T)}\right]\frac{\mathbf{x}}{|\mathbf{x}|} \quad \text{for } |\mathbf{x}| - \kappa - Y(T) \geq 0 \tag{192}$$

and

$$\boldsymbol{d}^p = 0 \text{ for } (|\mathbf{x}| - \kappa - Y(T)) < 0, \tag{193}$$

where T is temperature, κ is a scalar hardening variable, $\mathbf{x}$ is the translated stress found from the deviatoric Cauchy stress $\mathbf{s}$ and the tensor hardening variable $\mathbf{a}$ as

$$\boldsymbol{\chi} \equiv \boldsymbol{s} - \frac{2}{3}\boldsymbol{\alpha}, \tag{194}$$

and $f(T)$, $Y(T)$, and $V(T)$ are scalar functions. Assuming isotropic thermal expansion with coefficient $\hat{a}$, the thermal part of the rate of deformation can be written

$$\boldsymbol{d}^{th} = \hat{a}\dot{T}\mathbf{1}. \tag{195}$$

The evolution of the internal plasticity variables $\boldsymbol{\alpha}$ and κ is found from

$$\dot{\boldsymbol{\alpha}} = h(T)\boldsymbol{d}^{p} - [r_d(T)\bar{d} + r_s(T)]\bar{\alpha}\boldsymbol{\alpha} \tag{196}$$

$$\dot{\kappa} = H(T)|\boldsymbol{d}^{p}| - [R_d(T)\bar{d} + R_s(T)]\kappa^2 \quad , \tag{197}$$

where $h(T)$ and $H(T)$ are hardening moduli (which may be functions of temperature),

$$\bar{d} = \sqrt{\frac{2}{3}}|\boldsymbol{d}^{p}|, \tag{198}$$

$$\bar{\alpha} = \sqrt{\frac{2}{3}}|\boldsymbol{\alpha}|, \tag{199}$$

and $r_s(T)$, $R_s(T)$, $r_d(T)$, and $R_d(T)$ are scalar functions.

To compute temperature change, it is assumed that no heat is conducted out of an element and 90% of the plastic work is dissipated as heat, so it follows that

$$\dot{T} = \frac{0.9}{\rho c_v}(\boldsymbol{s} \bullet \boldsymbol{d}^{p}), \tag{200}$$

where ρ is the material density and c_v is the specific heat. To include this effect the heat generation coefficient, HC, should be defined in the input:

$$HC = \frac{0.9}{\rho c_v}. \tag{201}$$

Nine functions are used to describe the inelastic response. They can be grouped into three classes: those associated with the initial yield stress, the hardening functions, and the recovery functions. The temperature dependence of the yield functions are given by

$$V(T) = C_1 exp(-C_2/T) \tag{202}$$

$$Y(T) = C_3 exp(C_4/T) \tag{203}$$

$$F(T) = C_5 exp(-C_6/T). \tag{204}$$

The function $Y(T)$ describes the rate independent yield strength as a function of temperature. The function $F(T)$ determines the rate at which the material transitions from rate-insensitive to rate-dependent, and $V(T)$ describes the amount of rate dependence.

Two internal state variables are used to model hardening. The tensor variable α is used to describe the translation of the yield surface and the scalar variable κ is used to track growth of the yield surface. These two history variables evolve independently, and their evolution is characterized by a hardening contribution minus a recovery contribution. The hardening functions $h(T)$ and $H(T)$ are given by

$$h(T) = C_9 exp(C_{10}/T) \tag{205}$$

$$H(T) = C_{15} exp(C_{16}/T) . \tag{206}$$

Without recovery terms the model reduces to linear hardening with a tangent modulus of

$$E_T = (E(h + H))/(E + h + H) . \tag{207}$$

There are two recovery functions associated with each of the state variables α and κ. Larger values of recovery result in faster deviation from linear hardening and lower saturation stresses. The dynamic recovery function results in rate-independent hardening while the static (or thermal) recovery results in rate-dependent hardening.

The recovery functions are strongly temperature-dependent, and their form is given by

$$r_d(T) = C_7 exp(-C_8/T) \tag{208}$$

$$r_s(T) = C_{11} exp(-C_{12}/T) \tag{209}$$

$$R_d(T) = C_{13} exp(-C_{14}/T) \tag{210}$$

$$R_s(T) = C_{17} exp(-C_{18}/T) . \tag{211}$$

At higher strain rates and lower temperatures the dynamic recovery is dominant while at lower strain rates and higher temperatures the static recovery is dominant.

For high rate problems there can be a significant temperature increase due to plastic work. This allows the model to calculate thermal softening and thermal instabilities. Note that the heat generation coefficient HC will have no effect unless the functions are temperature-dependent. Typically, for strain rates less than 1.0 $\frac{1}{\text{sec}}$ the problem is not adiabatic and therefore the heat generation coefficient should *not* be included.

The parameters that give initial values to the components of the internal variable α may often be defined as zero. Nonzero values may be used to describe a material that is not initially isotropic, such as material deformed by a rolling process.

Material Type 39 (Sandia Damage Model)

Columns		Quantity	Format
1-10	Card 3	Young's modulus, E	E10.0
11-20		Poisson's ratio, ν	E10.0
21-30		Initial temperature, T_0	E10.0
31-40		Heat generation coefficient, HC	E10.0
1-10	Card 4	C_1	E10.0
11-20		C_2	E10.0
21-30		C_3	E10.0
31-40		C_4	E10.0
1-10	Card 5	C_5	E10.0
11-20		C_6	E10.0
21-30		C_7	E10.0
31-40		C_8	E10.0
41-50		C_{13}	E10.0
51-60		C_{14}	E10.0
1-10	Card 6	C_9	E10.0
11-20		C_{10}	E10.0
21-30		C_{15}	E10.0
31-40		C_{16}	E10.0
41-50		C_{11}	E10.0
51-60		C_{12}	E10.0
61-70		C_{17}	E10.0
71-80		C_{18}	E10.0
1-10	Card 7	Initial tensor internal variable, α_{xx}	E10.0
11-20		Initial α_{yy}	E10.0
21-30		Initial α_{xy}	E10.0
31-40		Initial α_{yz}	E10.0
41-50		Initial α_{zx}	E10.0

Columns		Quantity	Format
51-60		Initial scalar internal variable, κ_0	E10.0
61-70		Damage exponent, $\bar{m}$	E10.0
71-80		Initial void volume fraction (porosity), D_0	E10.0
	Card 8	Blank	

The constitutive equations of this model are described in (Bammann, 1990) and (Bammann, Johnson, and Chiesa, 1990). The damage model is described in (Bammann, Chiesa, McDonald, Kawahara, Dike, and Revelli, 1990) and Bammann, Chiesa, Horstemeyer, and Weingarten, 1993). This is a phenomenological plasticity model using a set of internal state variables whose evolutions based on micromechanics. The model includes rate and temperature dependence, and heat generation due to plastic work. Since internal state variables are used to track the deformation, the history effects of strain rate and temperature are correctly captured. Ductile failure in materials is predicted by the model using a void growth evolution law.

The number of material parameters may seem prohibitive, but rarely are all of the constants used. The model reduces to a linear strain hardening with only two required parameters. For rate insensitive materials the number of parameters is reduced by four. If temperature dependence is not required (i.e. when heat generation is not important), then the number of parameters is reduced by a factor of two. All of the parameters (except for the two associated with damage) can be determined using simple tension and compression data.

The evolution of the Cauchy stress $\boldsymbol{\sigma}$ is governed by an equation of the form

$$\dot{\boldsymbol{\sigma}} = \lambda(1-D)Tr(\boldsymbol{d}^e)\boldsymbol{1} + 2G(1-D)\boldsymbol{d}^e - \frac{\dot{D}}{1-D}\boldsymbol{\sigma} \quad , \tag{212}$$

where $\boldsymbol{d}^e$ is the elastic part of the rate of deformation, D is a scalar damage variable, λ is the elastic Lame parameter given by

$$\lambda = \frac{E\nu}{(1+\nu)(1-2\nu)} \quad , \tag{213}$$

and G is the elastic shear modulus. The rate of deformation $\boldsymbol{d}$ (symmetric part of the velocity gradient) is decomposed as

$$\boldsymbol{d} = \boldsymbol{d}^e + \boldsymbol{d}^p + \boldsymbol{d}^v + \boldsymbol{d}^{th}, \tag{214}$$

where $\boldsymbol{d}^p$ is the deviatoric plastic part, $\boldsymbol{d}^v$ is the dilatational plastic part, and $\boldsymbol{d}^{th}$ is the thermal expansion part. The deviatoric plastic part of the rate of deformation is given by

$$\boldsymbol{d}^p = f(T)\sinh\left[\frac{|\mathsf{x}| - \kappa - Y(T)(1-D)}{V(T)(1-D)}\right]\frac{\mathsf{x}}{|\mathsf{x}|} \quad \text{for} \quad |\mathsf{x}| - \kappa - Y(T)(1-D) \geq 0 \tag{215}$$

and

$$\boldsymbol{d}^p = 0 \text{ for } \quad (|\mathsf{x}| - \kappa - Y(T)(1-D)) < 0 \quad , \tag{216}$$

where T is temperature, κ is a scalar hardening variable, x is the translated stress found from the deviatoric Cauchy stress s and the tensor hardening variable a as

$$\mathsf{x} \equiv \mathsf{s} - \frac{2}{3}\mathsf{a}, \tag{217}$$

and $f(T)$, $Y(T)$, and $V(T)$ are scalar functions. The dilatational plastic part of the rate of deformation depends only on the damage variable and is given by

$$\boldsymbol{d}^v = \frac{D}{1-D}\mathbf{1}. \tag{218}$$

Assuming isotropic thermal expansion with coefficient $\hat{a}$, the thermal part of the rate of deformation can be written

$$\boldsymbol{d}^{th} = \hat{a}\dot{T}\mathbf{1}. \tag{219}$$

The evolution of the internal plasticity variables a and κ is found from

$$\dot{\mathsf{a}} = h(T)\boldsymbol{d}^p - [r_d(T)\bar{d} + r_s(T)]\bar{\alpha}\mathsf{a} \tag{220}$$

$$\dot{\kappa} = H(T)|\boldsymbol{d}^p| - [R_d(T)\bar{d} + R_s(T)]\kappa^2 \quad , \tag{221}$$

where $h(T)$ and $H(T)$ are hardening moduli (which may be functions of temperature),

$$\bar{d} = \sqrt{\frac{2}{3}}|\boldsymbol{d}^p|, \tag{222}$$

$$\bar{\alpha} = \sqrt{\frac{2}{3}}|\mathsf{a}|, \tag{223}$$

and $r_s(T)$, $R_s(T)$, $r_d(T)$, and $R_d(T)$ are scalar functions.

The evolution of the damage parameter D is given by

$$\dot{D} = \chi\left[\frac{1}{(1-D)^{\bar{m}}} - (1-D)\right]|\boldsymbol{d}^p| \quad , \tag{224}$$

where χ is a stress triaxiality factor given by

$$\chi = \sinh\left[\frac{2(2\bar{m}-1)p}{(2\bar{m}+1)\bar{\sigma}}\right], \tag{225}$$

$\bar{m}$ is a void growth constant, p is pressure, and $\bar{\sigma}$ is effective stress.

To compute temperature change, it is assumed that no heat is conducted out of an element and 90% of the plastic work is dissipated as heat, so it follows that

$$\dot{T} = \frac{0.9}{\rho c_v}(\mathbf{s} \bullet \mathbf{d}^p), \tag{226}$$

where ρ is the material density and c_v is the specific heat. To include this effect the heat generation coefficient, HC, should be defined in the input:

$$HC = \frac{0.9}{\rho c_v}. \tag{227}$$

Nine functions are used to describe the inelastic response. They can be grouped into three classes: those associated with the initial yield stress, the hardening functions, and the recovery functions. The temperature dependence of the yield functions are given by

$$V(T) = C_1 exp(-C_2/T) \tag{228}$$

$$Y(T) = C_3 exp(C_4/T) \tag{229}$$

$$F(T) = C_5 exp(-C_6/T). \tag{230}$$

The function $Y(T)$ describes the rate independent yield strength as a function of temperature. The function $F(T)$ determines the rate at which the material transitions from rate-insensitive to rate-dependent, and $V(T)$ describes the amount of rate dependence.

Two internal state variables are used to model hardening. A tensor variable $\boldsymbol{\alpha}$ is used to describe the translation of the yield surface and a scalar variable κ is used to track growth of the yield surface. These two history variables evolve independently, and their evolution is characterized by a hardening contribution minus a recovery contribution. The hardening functions $h(T)$ and $H(T)$ are given by

$$h(T) = C_9 exp(C_{10}/T) \tag{231}$$

$$H(T) = C_{15} exp(C_{16}/T). \tag{232}$$

Without recovery terms the model reduces to linear hardening with a tangent modulus of

$$E_T = (E(h+H))/(E+h+H). \tag{233}$$

There are two recovery functions associated with each of the state variables α and κ. Larger values of recovery result in faster deviation from linear hardening and lower saturation stresses. The dynamic recovery function results in rate-independent hardening while the static (or thermal) recovery results in rate-dependent hardening.

The recovery functions are strongly temperature-dependent, and their form is given by

$$r_d(T) = C_7 exp(-C_8/T) \tag{234}$$

$$r_s(T) = C_{11} exp(-C_{12}/T) \tag{235}$$

$$R_d(T) = C_{13} exp(-C_{14}/T) \tag{236}$$

$$R_s(T) = C_{17} exp(-C_{18}/T)\,. \tag{237}$$

At higher strain rates and lower temperatures the dynamic recovery is dominant while at lower strain rates and higher temperatures the static recovery is dominant.

For high rate problems there can be a significant temperature increase due to plastic work. This allows the model to calculate thermal softening and thermal instabilities. Note that the heat generation coefficient HC will have no effect unless the functions are temperature-dependent. Typically, for strain rates less than 1.0 $\frac{1}{\text{sec}}$ the problem is not adiabatic and therefore the heat generation coefficient should *not* be included.

The parameters that give initial values to the components of the internal variable α may often be defined as zero. Nonzero values may be used to describe a material that is not initially isotropic, such as material deformed by a rolling process.

The evolution of the damage internal state variable D is motivated by the Cocks-Ashby solution for the growth of a spherical void in a rate-dependent plastic material. Note that there is strong dependence on the ratio of mean stress to effective stress. Based on microscopic measurements of initial void volume fractions for metals, a value of 0.0001 is typically used for D_0. The value for $\bar{m}$ must be determined from test data, but unfortunately a simple procedure has not been found. Typically a notch tensile test is modeled and $\bar{m}$ is varied through a trial-and-error process until the correct strain to failure is produced. Other notch tests can then be used as validation. If no notch data exists, then a standard tensile test may be modeled and the strain at failure can be used (although this is less accurate). Most metals will fail at void fractions of several percent. However, at five percent damage, the growth rate is usually so large that a damage fraction of one (total material failure) is usually reached in a few time steps. For this reason the damage is limited to

0.99, at which point failure is assumed. The element stress and stiffness are inversely proportional to the damage, and at a damage level of 0.99 the element is essentially removed from the calculation.

Material Type 40 (Fahrenthold Brittle Damage)

Columns		Quantity	Format
1-10	Card 3	Elastic modulus, E (see Figure 1 and Figure 2)	E10.0
11-20		Damage evolution coefficient, A	E10.0
21-30		Damage evolution exponent, k	E10.0
1-10	Card 4	Poisson's ratio, ν	E10.0
	Card 5	Blank	
1-10	Card 6	Material axes definition option, AOPT	E10.0
		EQ.0.0: locally orthotropic with material axes determined by element nodes n_1, n_2, and n_4 as shown in Figure 1. Cards 7 and 8 must be blank with this option.	
		EQ.1.0: locally orthotropic with material axes determined by a point in space P and the global location of the element center, as shown in Figure 1. Note that $\boldsymbol{d}$ is parallel to the global z-axis. Card 8 below is blank.	
		EQ.2.0: globally orthotropic with material axes determined by vectors defined on Cards 7 and 8. (See Figure 2).	
		EQ.3.0: applicable to shell elements only. This option determines locally orthotropic material axes by offsetting the material axis $\boldsymbol{a}$ by an angle β from a line in the plane of the shell determined by taking the cross product of the vector $\boldsymbol{v}$ defined on Card 7 with the shell normal vector (See Figure 2). The angle β is defined on Card 8, and may be overridden by specifying a value on the element card.	
1-10	Card 7	x_p, define only if AOPT = 1.0	E10.0
11-20		y_p, define only if AOPT = 1.0	E10.0
21-30		z_p, define only if AOPT = 1.0	E10.0
1-10	Card 7	a_x, define only if AOPT = 2.0	E10.0
11-20		a_y, define only if AOPT = 2.0	E10.0
21-30		a_z, define only if AOPT = 2.0	E10.0
1-10	Card 7	v_x, define only if AOPT = 3.0	E10.0

Columns		Quantity	Format
11-20		v_y, define only if AOPT = 3.0	E10.0
21-30		v_z, define only if AOPT = 3.0	E10.0
1-10	Card 8	d_x, define only if AOPT = 2.0	E10.0
11-20		d_y, define only if AOPT = 2.0	E10.0
21-30		d_z, define only if AOPT = 2.0	E10.0
1-10	Card 8	Material angle β, define only if AOPT=3.0 (may be overridden on the element card)	E10.0

This is an experimental model for damage of brittle materials, such as ceramics. The theory and initial implementation was developed by Fahrenthold (1991), and the details of the formulation are described therein. This model is currently experimental in DYNA3D, and care should be exercised in its use.

Material Type 41 (Fabric with Damage)

Columns		Quantity	Format
1-10	Card 3	Elastic modulus in longitudinal direction, E_a	E10.0
11-20		Elastic modulus in transverse direction, E_b	E10.0
21-30		Elastic modulus in normal direction, E_c	E10.0
31-40		Bulk modulus of failed material, K_f (solid elements only)	E10.0
41-50		Normal tensile strength, S_n (solid elements only)	E10.0
51-60		Transverse shear strength, S_{bc} (solid elements only)	E10.0
61-70		Transverse shear strength, S_{ca} (solid elements only)	E10.0
1-10	Card 4	Poisson's ratio, ν_{ba}	E10.0
11-20		Poisson's ratio, ν_{ca}	E10.0
21-30		Poisson's ratio, ν_{cb}	E10.0
31-40		Ratio of soft E to stiff E in any direction, δ	E10.0
41-50		Stress value at transition, σ_{sl}	E10.0
51-60		Fillet radius for transition, R_{fil}	E10.0
61-70		Minimum time step for element deletion, Δt_f	E10.0
71-80		Stress/strain formulation (shell elements only)	E10.0
	EQ.0.0:	Hypo-elastic formulation using the Cauchy stress and the logarithmic strain. (default)	
	EQ.1.0:	Hyper-elastic formulation using the 2nd Piola-Kirchhoff stress and the right stretch tensor. (This option can only be used with one-point Belytschko-Tsay, YASE, or membrane shell formulations.)	
1-10	Card 5	Shear modulus, G_{ab}	E10.0
11-20		Shear modulus, G_{bc}	E10.0
21-30		Shear modulus, G_{ca}	E10.0
1-10	Card 6	Material axes definition option, AOPT	E10.0
	EQ.0.0:	locally orthotropic with material axes determined by element nodes n_1, n_2, and n_4 as shown in Figure 1. Cards 7 and 8 are blank with this option.	

Columns		Quantity	Format
	EQ.1.0:	locally orthotropic with material axes determined by a point in space P and the global location of the element center, as shown in Figure 1. Card 8 below is blank.	
	EQ.2.0:	globally orthotropic with material axes determined by vectors defined on Cards 7 and 8. (See Figure 2).	
	EQ.3.0:	applicable to shell elements only. This option determines locally orthotropic material axes by offsetting the material axis $\boldsymbol{a}$ by an angle β from a line in the plane of the shell determined by taking the cross product of the vector $\boldsymbol{v}$ defined on Card 7 with the shell normal vector (See Figure 2). The angle β is defined as described below for each through-thickness integration point. In addition, a material angle may be specified on each element card, and these values are added.	
1-10	Card 7	x_p, define only if AOPT = 1.0	E10.0
11-20		y_p, define only if AOPT = 1.0	E10.0
21-30		z_p, define only if AOPT = 1.0	E10.0
1-10	Card 7	a_x, define only if AOPT = 2.0	E10.0
11-20		a_y, define only if AOPT = 2.0	E10.0
21-30		a_z, define only if AOPT = 2.0	E10.0
1-10	Card 7	v_x, define only if AOPT = 3.0	E10.0
11-20		v_y, define only if AOPT = 3.0	E10.0
21-30		v_z, define only if AOPT = 3.0	E10.0
1-10	Card 8	d_x, define only if AOPT = 2.0	E10.0
11-20		d_y, define only if AOPT = 2.0	E10.0
21-30		d_z, define only if AOPT = 2.0	E10.0
31-40		Shear strength on $\boldsymbol{a}$-$\boldsymbol{b}$ plane, S_c	E10.0
41-50		Longitudinal tensile strength along $\boldsymbol{a}$ axis, X_t	E10.0
51-60		Longitudinal tensile strength along $\boldsymbol{b}$ axis, Y_t	E10.0
61-70		Transverse compressive strength, Y_c	E10.0
71-80		Nonlinear shear stress parameter, α	E10.0

This experimental material model allows for the initial slack effect on stiffness in a woven fabric material under tension. It is experimental, and further refinement is expected to improve its general utility. A different fiber orientation may be specified at each through-thickness integration point for shell elements to represent complex weaves. This capability may be combined with the User-Defined Integration Rules option.

The hyper-elastic stress formulation is based upon the 2nd Piola-Kirchhoff stress measure and assumes that the stress is the product of the current elasticity tensor operating on the strain, where the strain is defined as the right stretch tensor minus the identity tensor. This formulation removes artificial stiffening caused by excessive tensile deformation and damage as well as ensures that the global time-step size is correctly calculated. Note, material properties and strengths should be specified in terms of force per unit undeformed area.

Additional Material Type 41 Input:

Define the material angle β for each of the through-the-thickness integration points for 4-node shell elements. This data must follow the Cross Section Properties data on Card 11.

Columns	Quantity	Format
1-10	Material angle at first integration point, β_1	E10.0
11-20	Material angle at second integration point, β_2	E10.0
21-30	Material angle at third integration point, β_3	E10.0
.	.	.
.	.	.
.	.	.
71-80	Material angle at eighth integration point, β_8	E10.0

Continue on additional cards until NIP points have been defined, where NIP is the number of thickness integration points specified on Card 10 for shell elements. Material angle values may also be specified on the element cards. The material angle used in the calculation is the sum of the value specified above for each integration point and the value specified on the element card.

This model is based on an extension of the Composite Damage model, (material type 22) which accounts for the effects of loose weave in fabrics. The elastic portion of this model is bilinear in each direction, with the soft branch of the curve ($\sigma < \sigma_{sl}$) having elastic modulus $E_{sl} = \delta E$. A smooth transition with radius of curvature R_{fil} is used between the two moduli. The moduli are evaluated independently in each direction based on the normal stress in that direction.

The material behavior produced by this model is approximately orthotropic elastic, with the addition of a nonlinear shear stress term. A stress-based failure model is included to incorporate the effects of fiber breakage, matrix cracking, matrix crushing, and delamination. The failure criterion for fiber breakage is

$$e_f = \frac{max(0, \sigma_{aa}^2)}{X_t^2} + \frac{\sigma_{ab}^2 + \frac{3}{4}\alpha\sigma_{ab}^4}{\frac{S_c^2}{2G_{ab}} + \frac{3}{4}\alpha S_c^4} \leq 1.0 \quad . \tag{238}$$

Analogously, the criterion for matrix cracking is

$$e_m = \frac{max(0, \sigma_{bb}^2)}{Y_t^2} + \frac{\sigma_{ab}^2 + \frac{3}{4}\alpha\sigma_{ab}^4}{\frac{S_c^2}{2G_{ab}} + \frac{3}{4}\alpha S_c^4} \le 1.0 \quad . \tag{239}$$

The criterion to detect matrix crushing is

$$e_d = \frac{min(0, \sigma_{bb}^2)}{4S_c^2} + \left(\frac{Y_c^2}{4S_c^2} - 1\right)\frac{\sigma_{bb}}{Y_c} + \frac{\sigma_{ab}^2 + \frac{3}{4}\alpha\sigma_{ab}^4}{\frac{S_c^2}{2G_{ab}} + \frac{3}{4}\alpha S_c^4} \le 1.0 \quad , \tag{240}$$

and, for solid elements only, the criterion to detect delamination is

$$e_l = \frac{max(0, \sigma_{cc}^2)}{S_n^2} + \frac{\sigma_{bc}^2}{S_{bc}^2} + \frac{\sigma_{ca}^2}{S_{ca}^2} \le 1.0 \quad . \tag{241}$$

When either fiber breakage or matrix cracking is detected, the appropriate stress components are reduced to zero linearly over the next 100 time steps. This stress reduction function has been found useful to minimize spurious oscillations, or ringing, caused by the abrupt release of energy at failure. Nonetheless, the element remains active and continues to carry load perpendicular to the damage direction until both fiber breakage and matrix cracking occur. Only at this time is the element deactivated and rendered incapable of carrying any load. When the SAND database is active, the element remains visually present until both fiber breakage and matrix cracking occurs.

When matrix crushing is detected σ_{bb} and σ_{ab} are fixed at their current level. In its normal mode, matrix crushing does not render an element incapable of carrying load even if fiber breakage or matrix cracking also occur. However, by specifying $Y_c < 0$, where $|Y_c|$ is the transverse compressive strength, the appropriate stress components are zeroed when matrix crushing occurs and the element is deactivated when both matrix crushing and fiber breakage are detected.

Material Type 42 (Multi-Material Shell Element Model)

Columns		Quantity	Format
1-10	Card 3	Material number of 1-st integration point	E10.0
11-20		Material number of 2-nd integration point	E10.0
21-30		Material number of 3-rd integration point	E10.0
.		.	.
.		.	.
.		.	.
71-80		Material number of 8-th integration point	E10.0
1-10	Card 4	Material number of 9-th integration point	E10.0
.		.	.
.		.	.
71-80		Material number of 16-th integration point	E10.0
1-10	Card 5	Material number of 17-th integration point	E10.0
.		.	.
.		.	.
71-80		Material number of 24-th integration point	E10.0
.		.	.
.		.	.
.		.	.
1-10	Card 8	Material number of 41-th integration point	E10.0
.		.	.
.		.	.
61-70		Material number of 47-th integration point	E10.0

This new (and experimental) material model permits shell elements to be defined with completely different material models and data sets at each integration point in the through-the-thickness direction. By careful selection of the integration rule or by use of User Defined Integration Rules, many laminated structures can be modelled efficiently and accurately. The model is currently limited to 47 or less through-the-thickness integration points.

The user specifies a material identification number for each integration point. With Gauss quadrature integration, the isoparametric coordinate ζ $(-1.0 \le \zeta \le 1.0)$ of the k-th integration point is:

Table 2

Integration Point Number (k)	Gauss Quadrature Order				
	1	2	3	4	5
1	0.0	-0.58	0.0	-0.86	0.0
2		0.58	-0.77	-0.33	-0.91
3			0.77	0.33	-0.54
4				0.86	0.54
5					0.91

The lower and upper surfaces are located at $\zeta = -1.0$ and $\zeta = 1.0$, respectively. When trapezoidal integration is used, the first and last integration points are located on the lower and upper surfaces, respectively. The intermediate points are distributed consecutively between the lower and upper points. When user defined integration rules are employed, the integration points are arranged in the same order as the integration rule.

All element attributes must be fully specified for this material model. The hourglass stabilization method and coefficient, bulk viscosity types and coefficients, gravity loading flags, Rayleigh damping coefficients, and integration rule data specified for this material definition supersede any defined in the individual integration-point material model data sets. Although an effective mass density is required on input, the mass density is internally recalculating to ensure consistency. The user must specify the correct “lamina” density of each material model defined. These densities, along with each lamina’s elastic properties, are used to determine the maximum sound speed of the entire element. Although shell integration rules are still required for each integration-point material model, they are ignored during execution.

Note, it is more efficient computationally to use the User Defined Integration Rules if one material type is used for the entire element, but different data sets are desired at each integration point.

Material Type 43 (Transversely Isotropic Visco-Hyperelasticity)

Columns		Quantity	Format
1-10	Card 3	Mooney-Rivlin Coefficient, C_1	E10.0
11-20		Mooney-Rivlin Coefficient, C_2	E10.0
21-30		Exponential Stress Coefficient, C_3	E10.0
31-40		Fiber Uncrimping Coefficient, C_4	E10.0
41-50		Modulus of Straightened Fibers, C_5	E10.0
51-60		Viscoelastic Coefficient γ_1	E10.0
61-70		Viscoelastic Coefficient γ_2	E10.0
71-80		Viscoelastic Coefficient γ_3	E10.0
1-10	Card 4	Bulk Modulus, $\boldsymbol{K}$	E10.0
11-20		Fiber stretch for straightened fibers, λ^*	E10.0
51-60		Relaxation time, τ_1	E10.0
61-70		Relaxation time, τ_2	E10.0
71-80		Relaxation time, τ_3	E10.0
1-10	Card 5	Initial Stretch Flag .EQ. 1.0: activate initial stretch option	E10.0
11 -20		Load Curve, *n*, for applying initial stretch	E10.0
51-60		Viscoelastic Coefficient γ_4	E10.0
61-70		Viscoelastic Coefficient γ_5	E10.0
71-80		Viscoelastic Coefficient γ_6	E10.0
1-10	Card 6	Material axes option, AOPT Note: Fiber direction is always aligned with local axis **a**. EQ.0.0: local material axes given by local element nodes specified on Card 7 below. Fig. 4-1 indicates local axes resulting from default node choices. Card 8 is blank. EQ.0.0: local material axes determined by a point in space and global location of each element integration point (see Fig. 4-1). Card 8 below is blank. EQ.2.0: local material axes determined using normalized vectors **a** and **d** defined below, where **c** = **a** x **d** ; **b** = **c** x **a**	E10.0
51-60		Relaxation time, τ_4	E10.0

61-70		Relaxation time, τ_5	E10.0
71-80		Relaxation time, τ_6	E10.0
1-30	Card 7	AOPT.EQ.0.0: local element nodes (default = 1,2,4)	3E10.0
1-30		AOPT.EQ.1.0: x_p, y_p, z_p	3E10.0
1-30		AOPT.EQ.2.0: a_1,a_2, a_3	3E10.0
1-30	Card 8	d_1,d_2, d_3	3E10.0

This material provides a capability for modeling fiber reinforced visco-hyperelastic materials. Large strain hyperelastic response is determined by the strain energy formulation described as follows. Rate dependence can be added to the model by prescribing relaxation times in the input. Leaving columns 51-60 on Card 3 blank defaults the material with the non-rate dependent hyperelastic behavior. The input format and implementation follows that of NIKE3D Material Type 18, with the exception that fully incompressible material behavior via augmented Lagrangian method is not supported in the DYNA3D implementation.

Hyperelastic Response

The isotropic behavior of an "uncoupled" version of the Mooney-Rivlin model (Material Type 27) is modified by the addition of a strain energy term $F(\lambda)$ resulting from stretch λ along a fiber direction:

$$W = C_1(\tilde{I}1 - 3) + C_2(\tilde{I}_2 - 3) + \tfrac{1}{2}K[ln(J)]^2 + F(\lambda) \tag{242}$$

Here the invariants used are the deviatoric invariants, J represents the volume ratio, and K is the effective bulk modulus. Thus the strain energy has uncoupled terms to represent deviatoric and dilational contributions. The fiber stretch λ along the current fiber direction **a** is given by $\lambda \mathbf{a} = \mathbf{F}\mathbf{a}_0$, where **F** is the deformation gradient, and $\mathbf{a}_0$ is the fiber direction in the undeformed configuration. The fiber strain term $F(\lambda)$ includes an exponential "toe region," followed by a linear region, to represent the uncrimping behavior of fibers in biological soft tissues. The transition from exponential to linear behavior is governed by specifying a fiber stretch λ^*. The material model was designed to represent the behavior of ligaments and tendons, however the exponential behavior of skeletal and cardiac muscle may be represented by setting λ^* to a large value.

The additional contribution to Cauchy stress due to the fiber stretch is given by the term:

$$\frac{\partial F}{\partial \lambda} = \begin{cases} \dfrac{c_3}{\lambda}(\exp(C_4(\lambda - 1)) - 1) & , \quad \lambda < \lambda^* \\ \dfrac{1}{\lambda}(C_5\lambda + C_6) & , \quad \lambda \geq \lambda^* \end{cases} \tag{243}$$

Here, C_3 scales the exponential stresses, C_4 controls the rate of uncrimping of the collagen fibers, C_5 is the modulus of the straightened fibers, and C_6 is chosen by DYNA3D to ensure C^0 continuity between the two functional regions.

The model also supports the application of initial tension to the material through specification of an initial fiber stretch, λ_0. The initial stretch is applied using load curve *n*, specified above.

Viscoelastic Response

Viscoelasticity is provided by adding additional time dependent stress terms to the elastic stress calculated above. The following formula is used to calculate the 2nd Piola Kirchhoff stress at time *t*.

$$\boldsymbol{S}(\boldsymbol{E}, t) = \frac{\partial W}{\partial \boldsymbol{E}}(\boldsymbol{E}(t)) + \int_o^t G(t-\tau)\frac{\partial W}{\partial \boldsymbol{E}}(\boldsymbol{E}(\tau))d\tau \tag{244}$$

where *W* is the strain energy as given above and $\boldsymbol{E}$ is the Green strain. The equilibrium elastic response is given by the first term on the right hand side of the above formula. A six-term Prony series is used for the kernel *G* (*t*) such that

$$G(t) = \sum_{i=1}^{6} \gamma_i \exp(t/\tau_i) \tag{245}$$

Up to six viscoelastic coefficients γ_i and relaxation times τ_i can be prescribed as shown in the table for the material model. Different methods can be used to fit the viscoelastic parameters to experimental data. A method to fit the coefficients to the form of Fung's quasilinear viscoelastic model for biological soft tissues [Fung, 1981] is given in [Puso and Weiss, 1997]. Details of the elastic constitutive model and its implementation can be found in [Weiss et. al., 1996]. Dr. Weiss is responsible for the DYNA3D implementation of this model.

Material Type 44(Rigid Foam)

Columns		Quantity	Format
1-10	Card 3	Young's modulus, E^c	E10.0
11-20		Young's modulus, E^d	E10.0
1-10	Card 4	Poisson's ratio, υ^c	E10.0
11-20		Poisson's ratio, υ^d	E10.0
1-10	Card 5	Yield stress, k^c	E10.0
1-10	Card 6	Yield parameter, a	E10.0
1-10	Card 7	Hydrostatic yield stress, p^c	E10.0
1-10	Card 8	Rate of densification, c	E10.0
11-20		Lock up strain, J^{vd}	E10.0
21-30		blank	E10.0
31-40		Viscosity, η	E10.0
41-50		Power law coefficient, n	E10.0

The uniaxial compression stress versus strain curve for rigid foam has three regions: elastic, plateau, and densification (Figure 21). Elastic deformation is due to elastic bending and stretching of the cell walls. The plateau or yield occurs when this bending and stretching causes plastic hinges and buckling of the cell walls. Densification occurs due to contact of the cell walls and compression of pore fluid as the cells collapse and rupture. To model these regions the stress is split into two parts such that $\mathbf{s} = \mathbf{s}^c + \mathbf{s}^d$. The stress $\mathbf{s}^c$ represents stress due to bending and stretching of cell walls and $\mathbf{s}^d$ represents the stress due to densification of the cells.

The stiffness of the foam in the elastic region is given by;

$$\dot{\mathbf{s}}^c = E^c \dot{\mathbf{e}} \tag{246}$$

Typically Poisson's effects are neglected for the foam. The yield surface is given by the envelope of the surfaces f_1 and f_2 where:

$$f_1(\sigma^c) = 1/k^c\sqrt{J^c} + a(I^c/k^c)^2 - 1 = 0 \tag{247}$$

$$f_2(\sigma^c) = J^c + \frac{1}{9}[(I^c)^2 - 9(p^c)^2] = 0 \tag{248}$$

J^c is the second invariant of the cell wall deviatoric stress S_{ij}^c and I^c is the trace of σ_{ij}^c such that:

$$J^c = \sqrt{\frac{3}{2} S^c{}_{ij} S^c{}_{ij}} \quad \text{and} \quad I^c = \sigma^c{}_{ii} \tag{249}$$

. The surface f_1 is the cell wall plastic hinge surface where $a = 0.09\rho_{rel}$, ρ_{rel} is the relative density of the foam and k^c is the yield parameter. Usually f_1 controls the uniaxial yield response. Typically $0.02 < \rho_{rel} < 0.4$, such that a can be neglected and k^c becomes the uniaxial yield stress. The surface f_2 controls the hydrostatic behavior of the foam such that p^c becomes the yield pressure for purely volumetric loading ($J^c = 0$). Where hydrostatic compression data is not available $p^c = k^c$ is a good approximation. The usual additive split of the strain is used such that the plastic response ($\nu^c = 0$) is governed by:

$$\dot{s}^c = E^c(\dot{e} - \dot{e}^p) \tag{250}$$

where the following flow law

$$\dot{e}^p = \dot{\gamma}\, s \tag{251}$$

is used so that the foam does not expand transversely in uniaxial compression.

The hardening in this model comes from the densification stress s^d

$$\dot{s}^d = f(\varepsilon^v) E^d \dot{e} \tag{252}$$

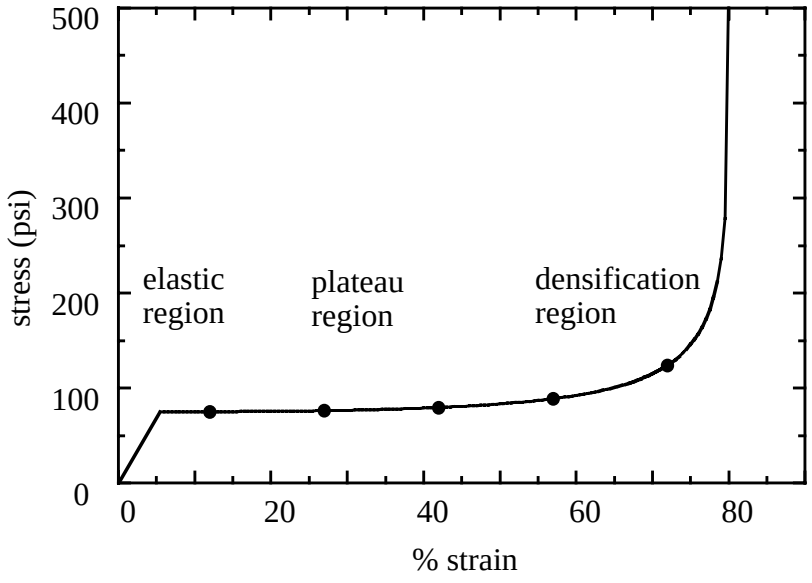

Figure 21 Regions in uniaxial compression curve

where E^d is the stiffness of the solid parent material composing the foam (Poisson's effects are small due to voids), ε^v is the logarithmic volumetric strain i.e. $\varepsilon^v = ln(J)$, and J is the relative volume (V/V_o for homogenous deformation). The function $f(\varepsilon^v)$ is 0 for tensile volumetric strain. In the compressive region $f(\varepsilon^v)$ is given by:

$$f(\varepsilon^v) = \frac{\tan^{-1}(c\ \varepsilon^{vd}) + \tan^{-1}[c(\varepsilon^v - \varepsilon^{vd})]}{\tan^{-1}(c\ \varepsilon^{vd}) - \pi/2} \tag{253}$$

This function varies from 0 at $\varepsilon^v = 0$ to 1 at $\varepsilon^v \approx \varepsilon^{vd}$ where $\varepsilon^{vd} = ln(J^{vd})$ and J^{vd} is the lockup strain. During uniaxial compression the foam does not strain transversely; therefore, the relative volume J equals the stretch such that $J = (L/L_o)$ where L is the current length of the specimen and L_o is the initial length. Furthermore, $J^{vd} = (L^{vd}/L_o)$ where L^{vd} is the length of the specimen at lockup: e.g. $J^{vd} = 0.2$ in Figure 21. The parameter c determines the transition to lockup as seen from Figure 22. Higher density foams transition more smoothly whereas lower density foams transition more abruptly. Therefore, by adjusting the parameters E^d, ε^{vd}, and c most uniaxial compression data for foam can be fit with this model.

..

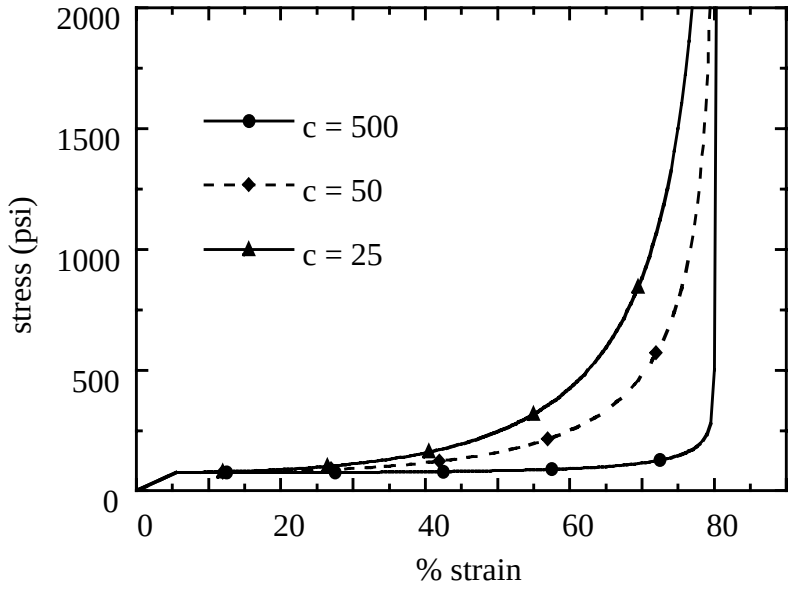

Figure 22 Different rates of densification

In order to capture rate dependent effects, the following flow law is substituted for (250):

$$\dot{e}^p = \frac{\|s^c - s^c_\infty\|^n}{J\ \eta\ E^d}(s^c - s^c_\infty) \tag{254}$$

where σ^c_∞ is the equilibrium stress given by the rate independent formulation in (246)-(251), J is the relative volume, n is the power law coefficient and η is some viscosity. For example, by substituting (254) into (250) gives the following equation for uniaxial compression in the 11 direction:

$$\dot{\sigma}^c_{11} + \frac{1}{J\eta}\left(\sigma^c_{11} - k^c\right)^{n+1} = E^c\,\dot{\varepsilon}_{11} \tag{255}$$

Details of this constitutive model and its implementation can be found in Puso (1995).

When large volumetric changes occur, the bulk viscosity can corrupt the calculation by artificially increasing the “internal element pressure” and dissipating excessive amounts of energy, i.e. many times more than is dissipated by the constitutive relationships. Consequently, it is recommended that when a material is going to be substantially compacted that both hourglass viscosities be decreased or set essentially to zero, e.g. $1x10^{-10}$, for that material.

Material Type 45 (DTRA Concrete/Geological Material)

Columns		Quantity	Format
1-10	Card 3	Poisson's ratio ν	E10.0
11-20		Unconfined tensile strength, f_t	E10.0
21-30		Cohesion for max. failure surface, a_0	E10.0
31-40		Max. failure surface coefficient, a_1	E10.0
41-50		Max. failure surface coefficient, a_2	E10.0
51-60		Compressive damage scaling exponent, b_1	E10.0
61-70		Fractional dilatency, ω	E10.0
71-80		Residual failure surface coefficient, a_{1f}	E10.0
1-10	Card 4	"Lambda stretch" factor, s: 0 for no stretch, 100 for stretching inversely with rate enhancement.	E10.0
11-20		Output selector for epx1 (Taurus comp. 7), integer from 1 to 4, see text.	E10.0
21-30		Exponent *edrop* on η for post peak dilatency decay (1 for linear drop, big for rapid drop)	E10.0
31-40		Critical value for plastic volumetric strain failure. An elemet fails and carries no stresses if its plastic volumetric strain exceeds this value.	E10.0
41-50		Not used	E10.0
51-60		Load curve giving rate sensitivity	E10.0
61-70		Not used	E10.0
71-80		Number of points in $\lambda - \eta$ relation (must be 13)	E10.0
1-10	Card 5	First tabulated value of damage function, λ_1 (=0)	E10.0
11-20		2nd tabulated value of damage function, λ_2	E10.0
21-30		3rd tabulated value of damage function, λ_3	E10.0
31-40		4th tabulated value of damage function, λ_4	E10.0
41-50		5th tabulated value of damage function, λ_5	E10.0
51-60		6th tabulated value of damage function, λ_6	E10.0
61-70		7th tabulated value of damage function, λ_7	E10.0
71-80		8th tabulated value of damage function, λ_8	E10.0

1-10	Card 6	9th tabulated value of damage function, λ_9	E10.0
11-20		10th tabulated value of damage function, λ_{10}	E10.0
21-30		11th tabulated value of damage function, λ_{11}	E10.0
31-40		12th tabulated value of damage function, λ_{12}	E10.0
41-50		13th tabulated value of damage function, λ_{13}	E10.0
51-60		Damage scaling coefficient for triaxial tension, b_3	E10.0
61-70		Cohesion for initial yield surface, a_{o_y}	E10.0
71-80		Initial yield surface coefficient, a_{1_y}	E10.0
1-10	Card 7	First tabulated value of scale factor, η_1	E10.0
11-20		2nd tabulated value of scale factor, η_2	E10.0
21-30		3rd tabulated value of scale factor, η_3	E10.0
31-40		4th tabulated value of scale factor, η_4	E10.0
41-50		5th tabulated value of scale factor, η_5	E10.0
51-60		6th tabulated value of scale factor, η_6	E10.0
61-70		7th tabulated value of scale factor, η_7	E10.0
71-80		8th tabulated value of scale factor, η_8	E10.0
1-10	Card 8	9th tabulated value of scale factor, η_9	E10.0
11-20		10th tabulated value of scale factor, η_{10}	E10.0
21-30		11th tabulated value of scale factor, η_{11}	E10.0
31-40		12th tabulated value of scale factor, η_{12}	E10.0
41-50		13th tabulated value of scale factor, η_{13}	E10.0
51-60		Tensile damage scaling exponent, b_2	E10.0
61-70		Residual failure surface coefficient, a_{2_f}	E10.0
71-80		Initial yield surface coefficient, a_{2_y}	E10.0

This material model was developed by Javier Malvar, Jim Wesevich, and John Crawford of Karagozian & Case, and Don Simon of Logicon RDA (Malvar, et. al., 1996) in support of the Defense Threat Reduction Agency's (DTRA, formerly Defense Nuclear Agency) programs.

Plastic flow is governed by a failure surface whose compressive meridian is determined in part by two of the three functions

$$\Delta\sigma_y = a_{0y} + \frac{p}{a_{1y} + a_{2y}p} \qquad \text{(initial yield surface)} \tag{256}$$

$$\Delta\sigma_m = a_0 + \frac{p}{a_1 + a_2 p} \quad \text{(maximum failure surface)} \tag{257}$$

$$\Delta\sigma_r = \frac{p}{a_{1f} + a_{2f}p} \qquad \text{(residual failure surface)} \tag{258}$$

After the stress point reaches the initial yield surface but before the maximum failure surface, the current surface is obtained as a linear interpolation between the two:

$$\Delta\sigma = \eta(\Delta\sigma_m - \Delta\sigma_y) + \Delta\sigma_y \tag{259}$$

where η varies from 0 to 1 depending on the non-decreasing damage parameter λ. After reaching the maximum surface, the current failure surface is similarly interpolated between the maximum and the residual:

$$\Delta\sigma = \eta(\Delta\sigma_m - \Delta\sigma_r) + \Delta\sigma_r . \tag{260}$$

The function $\eta(\lambda)$ is input as a series of exactly 13 ($\eta\lambda$) pairs. The values of λ must start at 0 and increase in sequence. The values of η would normally begin at 0 when λ=0, increase to 1 at some intermediate value $\lambda = \lambda_m$, and then decrease to 0 at some larger value of λ. (This would permit $\Delta\sigma$ sequentially to take on the values $\Delta\sigma_y$, $\Delta\sigma_m$, and $\Delta\sigma_r$.)

Damage scaling exponents b_1 and b_2 and "lambda-stretch" factor s affect plastic straining by modifying the relation between increments of effective plastic strain

$$d\bar{\varepsilon}^p = \sqrt{(2/3)\dot{\varepsilon}_{ij}^p \dot{\varepsilon}_{ij}^p} \tag{261}$$

and damage parameter λ. The incremental increase is

$$d\lambda = \begin{cases} \dfrac{d\bar{\varepsilon}^p}{[1 + (s/100)(r_f - 1)](1 + p/r_f f_t)^{b_1}}, & p > 0 \\ \dfrac{d\bar{\varepsilon}^p}{[1 + (s/100)(r_f - 1)](1 + p/r_f f_t)^{b_2}}, & p < 0 \end{cases} \tag{262}$$

where r_f is the rate-enhancement factor and f_t is the static unconfined tensile strength. Note that at p=0, the denominator is a continuous function. In this way, the damage evolution can be different in tension and compression, if needed. Note also that the factor in square brackets is unity if s=0 and r_f if s=100. Thus setting s=100 eliminates "lambda stretching." Note also that s is expressed as a percentage, due to the way it was processed in its previous life.

With damage accumulation as just described, if an isotropic tension test were modeled, wherein the pressure decreases from 0 to $-f_t$ with no deviators, then no damage accumulation would occur. The parameter λ would remain 0 and so would η. The equation of state would decrease the pressure to $-f_t$ but keep it at that level thereafter. To implement a pressure decay after isotropic tensile failure (which we believe to be physically more realistic), a volumetric damage increment can be added to the deviatoric damage whenever the stress path is "close" to the triaxial tensile test path, i.e., the negative hydrostatic axis. The closeness to this path is measured by the ratio $\left|(3J_2)^{\frac{1}{2}}/p\right|$, which, for example, is 1.5 for the biaxial tensile test. To limit the effects of this change to the paths close to the triaxial tensile path, the incremental damage is multiplied by a factor f_d given by

$$f_d = \begin{cases} 1 - \dfrac{\left|\sqrt{3J_2}/p\right|}{0.1}, & 0 \le \left|\sqrt{3J_2}/p\right| < 0.1 \\ 0, & \left|\sqrt{3J_2}/p\right| \ge 0.1 \end{cases} \tag{263}$$

This modified effective plastic strain is incremented by

$$\Delta\lambda = b_3 f_d k_d (\varepsilon_v - \varepsilon_{v,yield}) \quad (264)$$

where b_3 = input scalar multiplier, k_d = internal scalar multiplier, ε_v = volumetric strain, and $\varepsilon_{v,yield}$ = volumetric strain at yield. We have been using a value for b_3 between 1.1 and 1.6; in fact there are no direct data to select this parameter and the occurrence of stress states close enough to the negative pressure axis for it to matter is extremely unlikely.

The fractional dilatancy parameter ω is the initial ratio of the plastic volume strain increment to that which would occur if the plastic flow were fully associated in the hydrostatic plane. We have been using values between 0.3 and 0.5. There are some test data to help calibrate this parameter but we haven't finalized a best value for it yet. This value obtains until the stress point reaches the maximum failure surface. As damage progresses further, the current value of ω must decay to zero since dilatancy cannot proceed forever. Thus in this range the current, effective fractional dilatancy is the initial value ω multiplied by η**edrop. If edrop=1, the post-peak dilatancy rate decays linearly with η; if edrop is large, the decay is rapid; and if edrop=0, decay is deferred until the residual failure surface is reached.

Other Important Matters

This version of model 45 is intended for use only with EOS 8. We have not made any attempt to maintain compatibility with other EOS's; nor have we considered the effects of our modifications to EOS 8 on its use with other material models.

There is an element output variable epx1 available through TAURUS as component 7, referred to as effective plastic strain. We have provided four options for its contents, controlled by input variable emr on Card 4. If emr=1, epx1 contains the current failure surface radius (at the current strain rate and Lode angle). If emr=2, it contains a scaled damage measure δ given by

$$\delta = \frac{2\lambda}{\lambda + \lambda_m} \quad (265)$$

This goes from 0 to 1 to 2 as the failure surface migrates from initial yield to maximum failure to residual failure respectively. We have found contour and fringe plots of this variable to be useful in tracking the evolution of damage. If emr=3 or 4, it contains $\dot{\sigma}_{ij}\dot{\varepsilon}_{ij}$ or $\dot{\sigma}_{ij}\dot{\varepsilon}^p_{ij}$ respectively. These may be useful in identifying whether softening is occurring.

Rate-enhancement of the strength is defined by a factor r_f, a strain-rate-dependent factor applied radially (in stress space) to all points on the static failure surface to get the current one. It is input as a single load curve; however rate-enhancement can be different in tension and compression. This

is accomplished by inputting, as abscissas of the load curve, negative values of effective strain rate for the tensile enhancement and positive values for compression. The abscissas must be entered in ascending order and there cannot be more than 16 in total. If only positive abscissas are entered, a single rate enhancement is used regardless of the stress state.

The sequence of events in fitting the model is up to the user and will depend on how much data are available. After getting elastic and EOS parameters in conventional ways, we have generally proceeded by next fitting the failure surface constants to best represent desired failure envelopes. Then $\lambda(\eta)$ and b_1 are found to best fit stress strain curves in triaxial compression at various confinements. Finally b_2 is set to give the desired failure energy in unconfined tension. If the computational model involves zones of different sizes, then different b_2-values are needed if the tensile failure energy per unit crack area is to be preserved.

The option for implicit reinforcement, which was in the LLNL version of the model, has been removed. Note that this frees up a number of input variables, which could come in handy if any user undertakes further revisions.

The LLNL version was coded with an eye toward vector processing: the subroutine processes up to 128 elements on each call, and all repetitive operations are consigned to multiple “do” loops with no internal logical branching. In the current version of the subroutine, we have not followed through on this; in fact, many do loops have been consolidated. Users anticipating large runs on vector-processing machines may want to reorganize the coding.

Material Type 46 (Anisotropic Elastic)

Columns		Quantity	Format
1-10	Card 3	Stiffness, C_{11} (see Figure 1, Figure 2, and Figure 2)	E10.0
11-20		Stiffness, C_{12}	E10.0
21-30		Stiffness, C_{13}	E10.0
31-40		Stiffness, C_{14}	E10.0
41-50		Stiffness, C_{15}	E10.0
51-60		Stiffness, C_{16}	E10.0
61-70		Stiffness, C_{22}	E10.0
71-80		Stiffness, C_{23}	E10.0
1-10	Card 4	Stiffness, C_{24}	E10.0
11-20		Stiffness, C_{25}	E10.0
21-30		Stiffness, C_{26}	E10.0
31-40		Stiffness, C_{33}	E10.0
41-50		Stiffness, C_{34}	E10.0
51-60		Stiffness, C_{35}	E10.0
61-70		Stiffness, C_{36}	E10.0
71-80		Stiffness, C_{44}	E10.0
1-10	Card 5	Stiffness, C_{45}	E10.0
11-20		Stiffness, C_{46}	E10.0
21-30		Stiffness, C_{55}	E10.0
31-40		Stiffness, C_{56}	E10.0
41-50		Stiffness, C_{66}	E10.0
1-10	Card 6	Material axes definition option, AOPT	E10.0

EQ.0.0: locally orthotropic with material axes determined by element nodes n_1, n_2, and n_4 as shown in Figure 1. Cards 7 and 8 must be blank with this option.

EQ.1.0: locally anisotropic with material axes determined by a point in space P and the global location of the element center, as shown in Figure 1. Note that $\boldsymbol{d}$ is parallel to the global z-axis. Card 8 below is blank.

EQ.2.0: globally anisotropic with material axes determined by vectors defined on Cards 7 and 8. (See Figure 2).

EQ.3.0: applicable to shell elements only. This option determines locally anisotropic material axes by offsetting the material axis $\boldsymbol{a}$ by an angle β from a line in the plane of the shell determined by taking the cross product of the vector $\boldsymbol{v}$ defined on Card 7 with the shell normal vector (See Figure 2). The angle β is defined on Card 8, and may be overridden by specifying a value on the element card.

EQ.4.0: locally anisotropic with cylindrical material axes determined by a point P, located on the axis of revolution, and the vector $\boldsymbol{d}$, which parallels axis of revolution. (See Figure 2.)

1-10	Card 7	x_p, define only if AOPT = 1.0 or 4.0	E10.0
11-20		y_p, define only if AOPT = 1.0 or 4.0	E10.0
21-30		z_p, define only if AOPT = 1.0 or 4.0	E10.0
1-10	Card 7	a_x, define only if AOPT = 2.0	E10.0
11-20		a_y, define only if AOPT = 2.0	E10.0
21-30		a_z, define only if AOPT = 2.0	E10.0
1-10	Card 7	v_x, define only if AOPT = 3.0	E10.0
11-20		v_y, define only if AOPT = 3.0	E10.0
21-30		v_z, define only if AOPT = 3.0	E10.0
1-10	Card 8	d_x, define only if AOPT = 2.0 or 4.0	E10.0
11-20		d_y, define only if AOPT = 2.0 or 4.0	E10.0
21-30		d_z, define only if AOPT = 2.0 or 4.0	E10.0
1-10	Card 8	Material angle β, define only if AOPT=3.0 (may be overridden on the element card)	E10.0

The constitutive matrix $\boldsymbol{C}$ that relates increments in global components of stress to increments in global components of strain is defined as:

$$\mathbf{C} = \mathbf{T}^T \mathbf{C}_L \mathbf{T}, \tag{266}$$

where $\mathbf{T}$ is the transformation matrix between the local material coordinate system and the global coordinate system. The inputted constitutive matrix $\mathbf{C}_L$, defined in terms of the local orthogonal material axes $\boldsymbol{a}$, $\boldsymbol{b}$, and $\boldsymbol{c}$, relates the local engineering strains (ε_{aa}, ε_{bb}, ε_{cc}, γ_{ab}, γ_{bc}, γ_{ac}) to the local stresses (σ_{aa}, σ_{bb}, σ_{cc}, σ_{ab}, σ_{bc}, σ_{ac}), and is given by

$$C_L = \begin{bmatrix} C_{11} & C_{12} & C_{13} & C_{14} & C_{15} & C_{16} \\ C_{12} & C_{22} & C_{23} & C_{24} & C_{25} & C_{26} \\ C_{13} & C_{23} & C_{33} & C_{34} & C_{35} & C_{36} \\ C_{14} & C_{24} & C_{34} & C_{44} & C_{45} & C_{46} \\ C_{15} & C_{25} & C_{35} & C_{45} & C_{55} & C_{56} \\ C_{16} & C_{26} & C_{36} & C_{46} & C_{56} & C_{66} \end{bmatrix}. \tag{267}$$

For shell elements, only a sub-set of the complete stiffness matrix is utilized, due to the plane stress assumptions, and therefore $\mathbf{C}_L$ is defined as,

$$C_L = \begin{bmatrix} C_{11} & C_{12} & C_{13} & C_{14} & 0 & 0 \\ C_{12} & C_{22} & C_{23} & C_{24} & 0 & 0 \\ C_{13} & C_{23} & C_{33} & C_{34} & 0 & 0 \\ C_{14} & C_{24} & C_{34} & C_{44} & 0 & 0 \\ 0 & 0 & 0 & 0 & C_{55} & C_{56} \\ 0 & 0 & 0 & 0 & C_{56} & C_{66} \end{bmatrix}, \tag{268}$$

independent of the input.

A hyperelastic formulation is implemented for solid elements while a hypo-elastic formulation is utilized for shell elements. Thus, differences in results may be exists between solid and shell element models due solely to the constitutive implementation.

The stiffness matrix must be positive definite, or nonphysical energy growth may appear in the solution.

Finally, when orthotropic symmetry exists, the stiffness matrix, expressed in terms of the material constants of the local orthogonal material system, is given by

$$C_L^{-1} = \begin{bmatrix} \frac{1}{E_a} & -\frac{\nu_{ba}}{E_b} & -\frac{\nu_{ca}}{E_c} & 0 & 0 & 0 \\ -\frac{\nu_{ab}}{E_a} & \frac{1}{E_b} & -\frac{\nu_{cb}}{E_c} & 0 & 0 & 0 \\ -\frac{\nu_{ac}}{E_a} & -\frac{\nu_{bc}}{E_b} & \frac{1}{E_c} & 0 & 0 & 0 \\ 0 & 0 & 0 & \frac{1}{G_{ab}} & 0 & 0 \\ 0 & 0 & 0 & 0 & \frac{1}{G_{bc}} & 0 \\ 0 & 0 & 0 & 0 & 0 & \frac{1}{G_{ca}} \end{bmatrix}. \quad (269)$$

Material Type 47 (MIG–Material Interface Guide)

Free format beginning at Card 3

MIG_Keywords
  model input
MIG_Keywords
  *
  *
MIG DONE

List of Basic MIG Keywords and Model Input

Commands	Comment
DYROTE	Default rotation options, takes input from iorder of Control Card
DYELAS *E* *v*	Hooke's Law isotropic elasticity *E* is Young's modulus and *v* is Poisson ratio
DYIELD *A B C D n m*	Norton-Hoff flow strength law, $\sigma_f = [A + B(\bar{\varepsilon}^{p^n})][C(\dot{\varepsilon}')^m][\exp(-D/T)]$. (270)
DPLAS	Radial return plasticity algorithm
DYVISC	Default DYNA3D hourglass viscosity
DYENER	Default DYNA3D internal energy calculations
MIG DONE	Terminate MIG model input

The DYNA3D MIG model implementation adapts the MIG Version 0.0 standard, as defined in the Sandia Report SAND96-2000, into a material model which users are encouraged to employ for defining their own material behaviors. In its current form, the MIG model has a set of predefined basic capabilities: rotation options, elasticity, nonlinear flow strength, radial-return plasticity, artificial viscosity with minimum time step and internal energy. These capabilities allow users to study and test the DYNA3D/MIG implementation so that they may better understand how to create and modify the material behavior they need to model. By adhering to the MIG standard, code developers can more easily incorporate new material models into DYNA3D which are also then more portable to other numerical simulation codes. MIG ASCII text files are not used as input by DYNA3D. Instead they are used as an aid to the MIG model installer.

Material 47 is actually a model which organizes and executes the collection of MIG models for DYNA3D. MIG material models are subdivided into ten categories (Table 3) to allow for flexible and modular code development and usage. Six of the ten categories have predefined MIG models which users can test and use as is. The current categories correspond to the execution order within Material 47. Four of the ten categories are essential routines which are executed automatically unless there is a user override. The DYNA3D source contains subroutines for the six example categories indicated in the table. All MIG source subroutines are prefixed with mig_. Code developers should only have to modify mig_* subroutines to implement new models.

Table 3: DYNA3D MIG Model Categories

Category	Essential	Example
1) Rotation	*	*
2) Elasticity	*	*
3) Yield Stress		*
4) Plasticity		*
5) Fracture and Failure		
6) Temperature		
7) EOS1		
8) Artificial viscosity and time step	*	*
9) Internal energy	*	*
10) EOS2		

The MIG model uses free formatting for entering input parameters. MIG_Keywords identify each of the MIG models in use. Input parameters specific to the MIG model are entered beginning on the next line after the MIG_Keyword. The “MIG DONE” keyword is used to terminate the input. The simplest example of Material 47 is:

Card 1 (standard)
Card 2 (standard)
DYELAS
30.0e6 0.3
MIG DONE

Report UCRL #### provides additional information on the use and development of MIG material models.

Material Type 48 (Visco-Elastic with Statistical Crack Mechanics)

Manual pages to be completed

Material Type 49 (LANL Hyperfoam material)

Manual pages to be completed

Material Type 50 (Braided Composite Model with Damage)

Columns		Quantity	Format
1-10	Card 3	Longitudinal modulus, E_1	E10.0
11-20		Transverse modulus, E_2	E10.0
21-30		Longitudinal-transverse Poisson's ratio, υ_{12}	E10.0
31-40		Longitudinal-transverse shear modulus, μ_{12}	E10.0
41-50		Transverse-transverse shear modulus, μ_{23}	E10.0
51-60		Longitudinal-transverse shear modulus, μ_{13}	E10.0
61-70		Material orientation option, *AOPT*	E10.0
	EQ.0.0:	locally orthotropic with material axes determined by element nodes n_1, n_2, and n_4 as shown in Figure 1. Cards 7 and 8 must be blank with this option.	
	EQ.3.0:	applicable to shell elements only. This option determines locally anisotropic material axes by offsetting the material axis ***a*** by an angle β from a line in the plane of the shell determined by taking the cross product of the vector ***v*** defined on Card 7 with the shell normal vector (See Figure 2). The angle β is defined on Card 8, and may be overridden by specifying a value on the element card.	
71-80		Plot variable option, *POPT*	E10.0
1-10	Card 4	Reference yield stress, σ_o	E10.0
11-20		Reference strain, ε_o	E10.0
21-30		Strain hardening exponent, *n*	E10.0
31-40		Transverse tensile strength, $\hat{\sigma}_{ften}$	E10.0
41-50		Transverse tensile damage energy, $\hat{\Omega}_{ten}$	E10.0
51-60		Transverse tensile saturation stress, $\hat{\sigma}_{SatTen}$	E10.0
61-70		First transverse damage shear factor, D_{44}	E10.0
71-80		Second transverse damage shear factor, D_{55}	E10.0
1-10	Card 5	Transverse compressive failure strain, $\hat{\varepsilon}_{fComp}$	E10.0
11-20		Transverse compressive damage energy, $\hat{\Omega}_{Comp}$	E10.0

21-30		Transverse compressive saturation stress, $\hat{\sigma}_{SatComp}$	E10.0
31-40		Transverse shear yield factor, ι	E10.0
41-50		Transverse shear failure factor, v_f	E10.0
51-60		Minimum time-step for element deletion, Δt_{min}	E10.0
1-10	Card 6	Fiber tensile failure strain, ε_{fTen}	E10.0
11-20		Fiber tensile damage energy, Ω_{Ten}	E10.0
21-30		Fiber tensile shear damage factor, z	E10.0
31-40		Fiber tensile saturation stress, σ_{SatTen}	E10.0
41-50		Fiber compressive failure strain, ε_{fComp}	E10.0
51-60		Fiber compressive damage energy, Ω_{Comp}	E10.0
61-70		Fiber compressive saturation stress, $\sigma_{SatComp}$	E10.0
1-10	Card 7	Fiber direction visualization flag, *Fvis* EQ.0.0:Default EQ.1.0: step debug run. Stress components *xx*, *yy*, and *zz*, and *xy*, *yz*, and *zx* hold the material direction vectors **a** and **b**, respectively.	E10.0
11-20		Fiber direction characteristic length, l_f EQ.0.0: regularized by element size (default) GT.0.0: fixed fiber-direction regularization length	E10.0
21-30		Transverse direction characteristic length, l_t EQ.0.0: regularized by element size (default) GT.0.0: fixed transverse-direction regularization length	E10.0
31-40		Kinematic formulation, *Ifdrm* EQ.0.0: hypoelastic formulation (default) EQ.1.0: hyperelastic formulation	E10.0
1-10	Card 8	v_x, define only if AOPT = 3.0	E10.0
11-20		v_y, define only if AOPT = 3.0	E10.0
21-30		v_z, define only if AOPT = 3.0	E10.0
31-60		Blank	E10.0
61-70		Material offset angle, β	E10.0

Material model 50 is a progressive damage model applicable to a wide variety of fiber-reinforced composite material (Zywicz, 1997). The model uses lamina properties to track both tensile and compressive damage. Note, transverse direction material properties are hatted.

Within the material framework, the fiber direction is aligned with the 1-axis and the transverse direction is aligned with the 2-axis. The lamina is idealized as transversely isotropic, but with independent shear properties. It plastic response is governed by the generalized Hill yield surface

$$\phi_p = \sqrt{s \bullet \boldsymbol{P} \bullet s} - G(\bar{\varepsilon}^p) \tag{271}$$

where

$$\boldsymbol{P} = \begin{bmatrix} \alpha & -\frac{\alpha}{2} & 0 & 0 & 0 \\ -\frac{\alpha}{2} & \delta & 0 & 0 & 0 \\ 0 & 0 & \iota & 0 & 0 \\ 0 & 0 & 0 & \rho & 0 \\ 0 & 0 & 0 & 0 & \iota \end{bmatrix} \tag{272}$$

$$G(\bar{\varepsilon}^p) = \sigma_o(1 + \bar{\varepsilon}^p/\varepsilon_o)^n \tag{273}$$

$$\rho = 4 + \alpha \tag{274}$$

$$\alpha = ((G(\bar{\varepsilon}^p))/\hat{\sigma}_y)^2 \tag{275}$$

Here $\bar{\varepsilon}^p$ represents the equivalent plastic strain, $\hat{\sigma}_y$ is the axial compressive yield strength (determined from ε_{fComp} and the plasticity parameters), and prior to the onset of compressive failure, plasticity does not occur in the fiber direction, i.e., $\alpha \ll 1$, $\delta = 1$, and $\rho \approx 4$. Curve fitting the compressive transverse response is the best way to obtain the plasticity variables σ_o, ε_o, and *n*. Subsequent curve fitting of the shear response allows determination of ι.

Tensile damage is tracked in two directions, the fiber and transverse directions, and is modeled as as increase in the elastic compliance. Under uniaxial loading in either the fiber or transverse directions, the stress-strain curve appears tri-linear as shown in Figure 23. The initial portion uses the inputted elastic constants until either the tensile failure strain (for fiber direction) or stress (for transverse direction) is reached. In the second region, the compliance is enhanced and the material softens. The slope is determined such that the dissipated energy by the element is a function of Ω and the element size. In the absence of a saturation stress, the softening curve intersects the abscissa at ε_{max}. To prevent numerical problems, a saturation region is included and the softening region is altered slightly to produce a continuous stress-strain response. (In general, the saturation stress should be set to a small value of the failure stress.) During elastic unloading and loading in either the softening or saturation regions, the secant modulus is used.

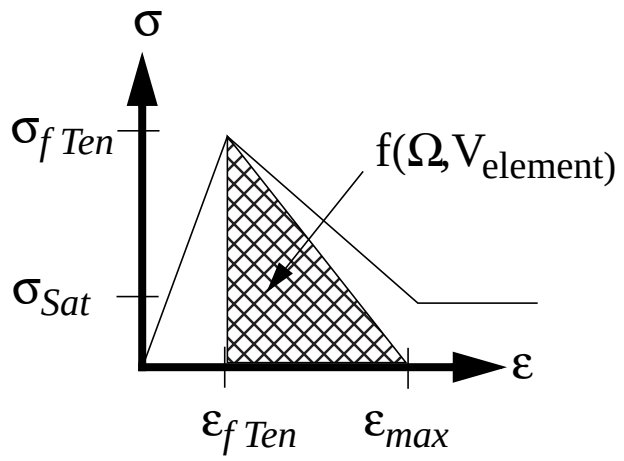

Figure 23
Schematic stress-strain response for model 50

Tensile damage in the fiber-direction initiates when the fiber-direction strain exceeds ε_{fTen} and increases both the fiber-direction and inplane shear compliances. Compliance enhancement of the the later term is z times the amount added to the formed term. Thus, $z < 1$ and can often be reasonably approximated as zero.

Tensile damage in the transverse direction is controlled by the damage surface

$$\phi_p = \sqrt{s \bullet \boldsymbol{M} \bullet s} - \hat{\sigma}_{fTen}\left[(1-\delta)Exp\left(-\frac{d}{d_o}\right) + \delta\right] \tag{276}$$

where

$$\boldsymbol{M} = \begin{bmatrix} 0 & 0 & 0 & 0 & 0 \\ 0 & 1 & 0 & 0 & 0 \\ 0 & 0 & D_{44} & 0 & 0 \\ 0 & 0 & 0 & D_{55} & 0 \\ 0 & 0 & 0 & 0 & 0 \end{bmatrix} \tag{277}$$

(278)

d is the internal damage variable, d_o is a normalization constant dependent upon element size and $\hat{\Omega}_{Ten}$, and $\delta = \frac{\hat{\sigma}_{SatTen}}{\hat{\sigma}_{fTen}}$. Transverse damage increases the normal (22) and shear (44 and 55) compliance components. The shear weights D_{44} and D_{55} are easily obtained from off axis tests, and D_{55} can be reasonably approximated equal to D_{44}.

Compressive damage is also tracked in two directions, but is modeled as plastic flow. Pure uniaxial compression in either the fiber or transverse directions would yield a stress-strain curve similar to that shown in Figure 23. In the fiber direction, compressive failure begins when $\varepsilon_{11} < \varepsilon_{fComp}$ and mathematically increases α in an irreversible manner with damage. The evolution of α is controlled by ε_{11}, the element size, and Ω_{Comp}. The saturation stress is influenced by many factors, but is typically between 0.2 and 0.8 of $\sigma_{fComp} = E_{11}\varepsilon_{fComp}$. In the transverse direction, compressive damage begins when $\hat{\varepsilon} > \hat{\varepsilon}_{fComp}$, where

$$\hat{\varepsilon} = \sqrt{\varepsilon_{ww}\frac{(\varepsilon_{22} - \|\varepsilon_{22}\|)}{2} + \nu_f \gamma_{12}^2} \tag{279}$$

and increases δ in an irreversible manner dependent upon $\hat{\varepsilon}$, $\hat{\Omega}_{Comp}$, and element size.

The model contains several other non-material related options. By default, $\bar{\varepsilon}^p$ is placed in the equivalent plastic strain slot. However, as described in Zywicz (1997), other internal variables can be placed in the equivalent plastic strain slot. To reduce computational costs, elements whose time-step size drops below Δt_{min} can automatically be deleted from the calculation by prescribing a non-zero value to Δt_{min}. To verify the correct material orientation, the fiber directions can be outputted in a debug run. Using GRIZ's vector plotting capability, the stress components σ_{xx}, σ_{yy}, and σ_{zz} can be used to construct the fiber-direction vector. The default constitutive framework is a hypoelastic formulation which updates the stresses based upon the symmetric part of the velocity gradient. However, a hyperelastic framework which derives the strains from the deformation gradient can also be used. Care should be used when curve-fitting unknown constants since their value depends upon which formulation is employed.

The present implementation internally regularizes the constitutive model during initialization to eliminate mesh dependency based upon the element size. For example, it assumes that a single fiber-direction crack forms in the middle of the element and adjusts the internal softening modulus such that the total energy dissipated in damage by the element equals the postulated ''crack area'' times Ω_{Ten}. When the element is too large, it is not possible to regularize the constitutive law. When this happens, a warning is printed to the screen and a detailed report is included in the `hsp` file. The user may chose to, in part, circumvent the regularization. This can be done by prescribing non-zero values to l_f and l_t, the fiber- and transverse-direction characteristic length, respectively. When this is done, l_f and l_t are used to regularize the constitutive model instead of the actual element dimensions. In this case, the results are not mesh independent.

Material Type 56 (Uni-Directional Elasto-Plastic Composite)

Columns		Quantity	Format
1-10	Card 3	Matrix Young's modulus, E_m	E10.0
11-20		Matrix Poisson's ratio, υ_m	E10.0
21-30		Matrix Yield stress coefficient, k	E10.0
31-40		Matrix strain hardening exponent, n n can not be 1.0.	E10.0
41-50		Optional: ε_o	E10.0
1-10	Card 4	Fiber longitudinal Young's modulus, E_l	E10.0
11-20		Fiber transverse Young's modulus, E_t	E10.0
21-30		Fiber longitudinal-transverse Poisson's ratio, υ_{lt}	E10.0
31-40		Fiber transverse-transverse Poisson's ratio, ν_{tt}	E10.0
41-50		Fiber longitudinal-transverse shear modulus, μ_{lt}	E10.0
51-60		Fiber volume fraction, v_f	E10.0
	Card 5	Blank	
1-10	Card 6	Material axes definition option, AOPT	E10.0

EQ.0.0: locally orthotropic with material axes determined by element nodes n_1, n_2, and n_4 as shown in Figure 1. Cards 7 and 8 must be blank with this option.

EQ.1.0: locally anisotropic with material axes determined by a point in space P and the global location of the element center, as shown in Figure 1. Note that $\boldsymbol{d}$ is parallel to the global z-axis. Card 8 below is blank.

EQ.2.0: globally anisotropic with material axes determined by vectors defined on Cards 7 and 8. (See Figure 2).

EQ.4.0: locally anisotropic with cylindrical material axes determined by a point P, located on the axis of revolution, and the vector $\boldsymbol{d}$, which parallels axis of revolution. (See Figure 2.)

11-20		Plot option, *POPT* EQ.0.0: default (*POPT*=2) EQ.1.0: Matrix stress in fiber direction EQ.2.0: Fiber direction strain EQ.3.0: Equivalent plastic strain	E10.0
21-30		Debug option, *DOPT* EQ.0.0: Default EQ.1.0: 1-step debug run. Stress components *xx, yy,* and *zz,* and *xy, yz,* and *zx* hold the material direction vectors **a** and **b**, respectively.	E10.0
1-10	Card 7	x_p, define only if AOPT = 1.0 or 4.0	E10.0
11-20		y_p, define only if AOPT = 1.0 or 4.0	E10.0
21-30		z_p, define only if AOPT = 1.0 or 4.0	E10.0
1-10	Card 7	a_x, define only if AOPT = 2.0	E10.0
11-20		a_y, define only if AOPT = 2.0	E10.0
21-30		a_z, define only if AOPT = 2.0	E10.0
1-10	Card 7	v_x, define only if AOPT = 3.0	E10.0
11-20		v_y, define only if AOPT = 3.0	E10.0
21-30		v_z, define only if AOPT = 3.0	E10.0
1-10	Card 8	d_x, define only if AOPT = 2.0 or 4.0	E10.0
11-20		d_y, define only if AOPT = 2.0 or 4.0	E10.0
21-30		d_z, define only if AOPT = 2.0 or 4.0	E10.0

This model depicts the behavior of a moderate to high fiber volume fraction uni-directional composite. The fiber is assumed transversely isotropic and the matrix's behavior is elasto-plastic with nonlinear isotropic matrix strain hardening given by a power law expression. The yield condition can be written

$$\phi = \bar{\sigma} - \sigma_y(\bar{\varepsilon}^p), \tag{280}$$

where $\bar{\sigma}$ is the effective matrix stress and σ_y is the current yield stress. The hardening law has the form

$$\sigma_y = k(\varepsilon_0 + \bar{\varepsilon}^p)^n, \tag{281}$$

where ε_0, if undefined, is the initial yield strain given by

$$\varepsilon_0 = \left(\frac{E}{k}\right)^{\frac{1}{n-1}} . \quad (282)$$

The fiber orientation is advected with deformation.

This model is generally applicable to uni-directional composites with a polymeric matrix. It employes a geometric independent idealization. Namely, it assumes that the fiber direction strain in constant in both the fiber and matrix. In the other directions, the stress is the same in both the fiber and matrix. This simple idealization reasonably predicts elasto-plastic results for many glass-, carbon-, or graphite-epoxy composites.

During initialization, the effective transversely isotropic elastic composite properties are printed in the `hsp` file. Thus, by selectively altering either the fiber or matrix properties, the composite properties can be tuned to specified values.

Material Type 57 (An upcoming material model from LANL)

Manual pages to be completed

EQUATION OF STATE DEFINITION

An equation-of-state defines the volumetric behavior of a material, and must be used *only* in combination with a hydrodynamic material model for solid elements.

Define equation-of-state cards only for Material Types 8, 9, 10, 11, 15, 16, and 17.

Card 9

Columns	Quantity	Format
1-72	Equation-of-state identification	12A6

This equation-of-state title will appear in the printed output. It is often helpful to use this heading to identify the physical material for which the DYNA3D equation of state model was constructed.

Cards 10, . . .

Equation-of-State Form 1 (Linear Polynomial)

Columns		Quantity	Format
1-10	Card 10	Pressure constant, C_0	E10.0
11-20		Linear compression coefficient, C_1	E10.0
21-30		Quadratic compression coefficient, C_2	E10.0
31-40		Cubic compression coefficient, C_3	E10.0
41-50		First energy coefficient, C_4	E10.0
51-60		Second energy coefficient, C_5	E10.0
61-70		Third energy coefficient, C_6	E10.0
71-80		Initial internal energy, E_0	E10.0
1-10	Card 11	Initial relative volume, V_0	E10.0

The linear polynomial equation-of-state is linear in internal energy. The pressure is given by:

$$p = C_0 + C_1\mu + C_2\bar{\mu}^2 + C_3\mu^3 + (C_4 + C_5\mu + C_6\bar{\mu}^2)E \tag{283}$$

where the excess compression μ is given by

$$\mu \equiv \frac{\rho}{\rho_0} - 1 , \tag{284}$$

E is the internal energy, ρ is the current density, and ρ_0 is the initial density. The tension-limited excess compression $\bar{\mu}$ is given by

$$\bar{\mu} = max(\mu, 0) . \tag{285}$$

Relative volume is related to excess compression and density by

$$V = \frac{1}{1+\mu} = \frac{\rho_0}{\rho} . \tag{286}$$

This equation-of-state is linear in internal energy, and may be used to fit experimental data for many materials. If $C_1 = K$ (the elastic bulk modulus) and all other $C_i = 0$, then linear elastic volumetric response is obtained.

This form of equation-of-state was adapted from that discussed in (Woodruff, 1973).

Equation-of-State Form 2 (JWL)

Columns		Quantity	Format
1-10	Card	A	E10.0
11-20		B	E10.0
21-30		R_1	E10.0
31-40		R_2	E10.0
41-50		ω	E10.0
51-60		Initial internal energy, E_0	E10.0
61-70		Initial relative volume, V_0	E10.0

The JWL equation-of-state defines the pressure as

$$p = A\left(1-\frac{\omega}{R_1 V}\right)e^{-R_1 V} + B\left(1-\frac{\omega}{R_2 V}\right)e^{-R_2 V} + \frac{\omega E}{V}\ , \tag{287}$$

where V is relative volume and E is internal energy.

The JWL equation of state is often used for detonation products of high explosives. Additional information in given in (Dobratz, 1981).

Equation-of-State Form 3 (Sack)

Columns		Quantity	Format
1-10	Card 10	A_1	E10.0
11-20		A_2	E10.0
21-30		A_3	E10.0
31-40		B_1	E10.0
41-50		B_2	E10.0
51-60		Initial internal energy, E_0	E10.0
61-70		Initial relative volume, V_0	E10.0

The Sack equation-of-state defines pressure p as

$$p = \frac{A_3}{V^{A_1}} e^{-A_2 V} \left(1 - \frac{B_1}{V}\right) + \frac{B_2}{V} E \,, \tag{288}$$

where V is relative volume and E is the internal energy.

This equation-of-state form is often used for detonation products of high explosives, and was adapted from (Woodruff, 1973).

Equation-of-State Form 4 (Gruneisen)

Columns		Quantity	Format
1-10	Card 10	Velocity curve intercept, C	E10.0
11-20		First slope coefficient, S_1	E10.0
21-30		Second slope coefficient, S_2	E10.0
31-40		Third slope coefficient, S_3	E10.0
41-50		Gruneisen coefficient, γ_0	E10.0
51-60		First order volume correction coefficient, a	E10.0
61-70		Initial internal energy, E_0	E10.0
71-80		Initial relative volume, V_0	E10.0

The Gruneisen equation-of-state with cubic shock velocity-particle velocity defines pressure for compressed materials ($\mu > 0$) as

$$p = \frac{\rho_0 C^2 \mu \left[1 + \left(1 - \frac{\gamma_0}{2} \right) \mu - \frac{a}{2} \mu^2 \right]}{\left[1 - (S_1 - 1)\mu - S_2 \frac{\mu^2}{\mu + 1} - S_3 \frac{\mu^3}{(\mu + 1)^2} \right]^2} + (\gamma_0 + a\mu)E \quad , \tag{289}$$

and for expanded materials ($\mu < 0$) as

$$p = \rho_0 C^2 \mu + (\gamma_0 + a\mu)E \, , \tag{290}$$

where C is the intercept of the shock velocity vs. particle velocity ($v_s - v_p$) curve, S_1, S_2, and S_3 are the coefficients of the slope of the $v_s - v_p$ curve, γ_0 is the Gruneisen gamma, and a is the first order volume correction to γ_0. The excess compression μ is defined by

$$\mu \equiv \frac{\rho}{\rho_0} - 1 \, , \tag{291}$$

where ρ is the current density and ρ_0 is the initial density.

The implementation of the Gruneisen equation-of-state is adapted from (Woodruff, 1973).

Equation-of-State Form 5 (Ratio of Polynomials)

Columns		Quantity	Format
1-16	Card 10	A_{10}	E16.0
17-32		A_{11}	E16.0
33-48		A_{12}	E16.0
49-64		A_{13}	E16.0
1-16	Card 11	A_{20}	E16.0
17-32		A_{21}	E16.0
33-48		A_{22}	E16.0
49-64		A_{23}	E16.0
1-16	Card 12	A_{30}	E16.0
17-32		A_{31}	E16.0
33-48		A_{32}	E16.0
49-64		A_{33}	E16.0
1-16	Card 13	A_{40}	E16.0
17-32		A_{41}	E16.0
33-48		A_{42}	E16.0
49-64		A_{43}	E16.0
1-16	Card 14	A_{50}	E16.0
17-32		A_{51}	E16.0
33-48		A_{52}	E16.0
49-64		A_{53}	E16.0
1-16	Card 15	A_{60}	E16.0
17-32		A_{61}	E16.0
33-48		A_{62}	E16.0
49-64		A_{63}	E16.0

Columns		Quantity	Format
1-16	Card 16	A_{70}	E16.0
17-32		A_{71}	E16.0
33-48		A_{72}	E16.0
49-64		A_{73}	E16.0
1-16	Card 17	α	E16.0
17-32		β	E16.0
33-48		A_{14}	E16.0
49-64		A_{24}	E16.0
1-16	Card 18	Initial internal energy, E_0	E16.0
17-32		Initial relative volume, V_0	E16.0

The ratio of polynomials equation-of-state defines the pressure as

$$p = \frac{F_1 + F_2 E + F_3 E^2 + F_4 E^3}{F_5 + F_6 E + F_7 E^2}(1 + \alpha\mu) \tag{292}$$

where the each of the F_i are polynomials in terms of the excess compression μ of the form

$$F_i = \sum_{k=0}^{n} A_{ik}\mu^k \tag{293}$$

with $n = 4$ for F_1 and F_2, and $n = 3$ for F_3 through F_7. The excess compression μ is defined by

$$\mu \equiv \frac{\rho}{\rho_0} - 1 , \tag{294}$$

where ρ is the current density and ρ_0 is the initial density.

In expanded elements ($\mu < 0$), F_1 in (292) is replaced by $\bar{F}_1$, where $\bar{F}_1$ is defined by

$$\bar{F}_1 = F_1 + \beta\mu^2 . \tag{295}$$

This equation-of-state was adapted from (Woodruff, 1973).

Equation-of-State Form 6 (Linear Polynomial with Energy Deposition)

Columns		Quantity	Format
1-10	Card 10	Pressure constant, C_0	E10.0
11-20		Linear compression coefficient, C_1	E10.0
21-30		Quadratic compression coefficient, C_2	E10.0
31-40		Cubic compression coefficient, C_3	E10.0
41-50		First energy coefficient, C_4	E10.0
51-60		Second energy coefficient, C_5	E10.0
61-70		Third energy coefficient, C_6	E10.0
71-80		Initial internal energy, E_0	E10.0
1-10	Card 11	Initial relative volume, V_0	E10.0
11-20		Load curve number giving energy deposition rate, LC	E10.0

This equation-of-state form is similar to equation-of-state form 1 except that this form allows internal energy to be deposited into the material at a specified rate. The pressure is given by:

$$p = C_0 + C_1\mu + C_2\bar{\mu}^2 + C_3\mu^3 + (C_4 + C_5\mu + C_6\bar{\mu}^2)E \tag{296}$$

where the excess compression μ is given by

$$\mu \equiv \frac{\rho}{\rho_0} - 1\,, \tag{297}$$

E is the internal energy, ρ is the current density, and ρ_0 is the initial density. The tension-limited excess compression $\bar{\mu}$ is given by

$$\bar{\mu} = max(\mu, 0)\,. \tag{298}$$

Relative volume is related to excess compression and density by

$$V = \frac{1}{1+\mu} = \frac{\rho_0}{\rho}\,. \tag{299}$$

Internal energy is added into the material at a rate specified by load curve LC. This feature allows energy transfer mechanisms to be included which are not considered in detail in the analysis model.

This equation-of-state is linear in internal energy, and may be used to fit experimental data for many materials.

Equation-of-State Form 7 (Ignition and Growth of Reaction in HE 2-Term)

Columns		Quantity	Format
1-10	Card 10	A_p	E10.0
11-20		B_p	E10.0
21-30		R_{1p}	E10.0
31-40		R_{2p}	E10.0
41-50		Second ignition coefficient, G	E10.0
1-10	Card 11	$\omega_p c_p$	E10.0
11-20		A_e	E10.0
21-30		B_e	E10.0
31-40		$\omega_e c_e$	E10.0
41-50		R_{1e}	E10.0
1-10	Card 12	R_{2e}	E10.0
11-20		Critical fraction reacted, F_{crit}, (usually = 1.0)	E10.0
21-30		First ignition coefficient, I	E10.0
31-40		Growth coefficient, H	E10.0
41-50		Pressure exponent, z	E10.0
1-10	Card 13	Unreacted fraction exponent, x	E10.0
11-20		Reacted fraction exponent, y	E10.0
21-30		Heat capacity of reaction products, c_p	E10.0
31-40		Heat capacity of unreacted HE, c_e	E10.0
1-10	Card 14	Product compression exponent, m (often $m = 0$)	E10.0
11-20		Initial energy of HE per unit volume, E_0	E10.0
21-30		Initial temperature, T_0 (in $^\circ K$)	E10.0
	Card 15	Blank	

The pressure in the unreacted HE is given by a JWL equation of state,

$$p_e = A_e\left(1 - \frac{\omega_e}{R_{1e}V_e}\right)e^{-R_{1e}V_e} + B_e\left(1 - \frac{\omega_e}{R_{2e}V_e}\right)e^{-R_{2e}V_e} + \frac{\omega_e E_e}{V_e}\ , \qquad (300)$$

and the pressure in the reaction products is defined by another JWL equation of state,

$$p_p = A_p\left(1 - \frac{\omega_p}{R_{1p}V_p}\right)e^{-R_{1p}V_p} + B_p\left(1 - \frac{\omega_p}{R_{2p}V_p}\right)e^{-R_{2p}V_p} + \frac{\omega_p E_p}{V_p}, \quad (301)$$

where p is the pressure, V is the relative volume, and E is the internal energy. Subscript e denotes quantities applicable to the unreacted HE, and subscript p indicates quantities applicable to reacted HE products.

The mixture of unreacted explosive and reaction products is defined by the fraction reacted, F ($F = 0$ indicates no reaction, while $F = 1$ indicates complete conversion from explosive to products). The pressures and temperature are assumed to be in equilibrium and the volumes are assumed to be additive,

$$V = (1 - F)V_e + FV_p. \quad (302)$$

The reaction rate is given by

$$\dot{F} = I(F_{crit} - F)^y (V_e^{-1} - 1)^3 [1 + G(V_e^{-1} - 1)] + H(1 - F)^y F^x P^z (V_p^{-1} - 1)^m \quad . \quad (303)$$

This equation-of-state is based in part on work reported in (Woodruff, 1973). The JWL equations of state and the reaction rates have been fitted to one- and two-dimensional shock initiation and detonation data for four explosives: PBX-9404, RX-03-BB, PETN, and cast TNT. The details of the calculational method are described in (Cochran and Chan, 1979). The detailed one-dimensional calculations and parameters for the four explosives are given in (Lee and Tarver, 1980).

Equation-of-State Form 8 (Tabulated with Compaction)

Columns		Quantity	Format
1-16	Card 10	ε_{v1}	E16.0
17-32		ε_{v2}	E16.0
33-48		ε_{v3}	E16.0
49-64		ε_{v4}	E16.0
65-80		ε_{v5}	E16.0
1-16	Card 11	ε_{v6}	E16.0
17-32		ε_{v7}	E16.0
33-48		ε_{v8}	E16.0
49-64		ε_{v9}	E16.0
65-80		ε_{v10}	E16.0
1-16	Card 12	C_1	E16.0
17-32		C_2	E16.0
33-48		C_3	E16.0
49-64		C_4	E16.0
65-80		C_5	E16.0
1-16	Card 13	C_6	E16.0
17-32		C_7	E16.0
33-48		C_8	E16.0
49-64		C_9	E16.0
65-80		C_{10}	E16.0
1-16	Card 14	First temperature, T_1	E16.0
17-32		Second temperature, T_2	E16.0
33-48		T_3	E16.0
49-64		T_4	E16.0
65-80		T_5	E16.0
1-16	Card 15	T_6	E16.0

Columns		Quantity	Format
17-32		T_7	E16.0
33-48		T_8	E16.0
49-64		T_9	E16.0
65-80		Tenth temperature, T_{10}	E16.0
1-16	Card 16	First unloading bulk modulus, K_1	E16.0
17-32		Second unloading bulk modulus, K_2	E16.0
33-48		K_3	E16.0
49-64		K_4	E16.0
65-80		K_5	E16.0
1-16	Card 17	K_6	E16.0
17-32		K_7	E16.0
33-48		K_8	E16.0
49-64		K_9	E16.0
65-80		Tenth unloading bulk modulus, K_{10}	E16.0
1-16	Card 18	γ	E16.0
17-32		Initial internal energy, E_0	E16.0
33-48		Initial relative volume, V_0	E16.0

Pressure is positive in compression, and volumetric strain ε_v is positive in tension. The tabulated compaction model is linear in internal energy. Pressure is defined by

$$p = C(\varepsilon_v) + \gamma T(\varepsilon_v) E \tag{304}$$

during loading (compression). Note that in (304) $C(\varepsilon_v)$ denotes a function evaluation, not a multiplication. Thus, the input coefficients C_i have the units of pressure. Unloading occurs at a slope corresponding to the bulk modulus at the peak (most compressive) volumetric strain, as shown in Figure 24. Reloading follows the unloading path to the point where unloading began, and then continues on the loading path described by (304).

The volumetric strain is found from the relative volume V as

$$\varepsilon_v = ln(V). \tag{305}$$

The tabulated functions may contain from 2 to 10 points, and the model will extrapolate (using the last two points) to find the pressure if required.

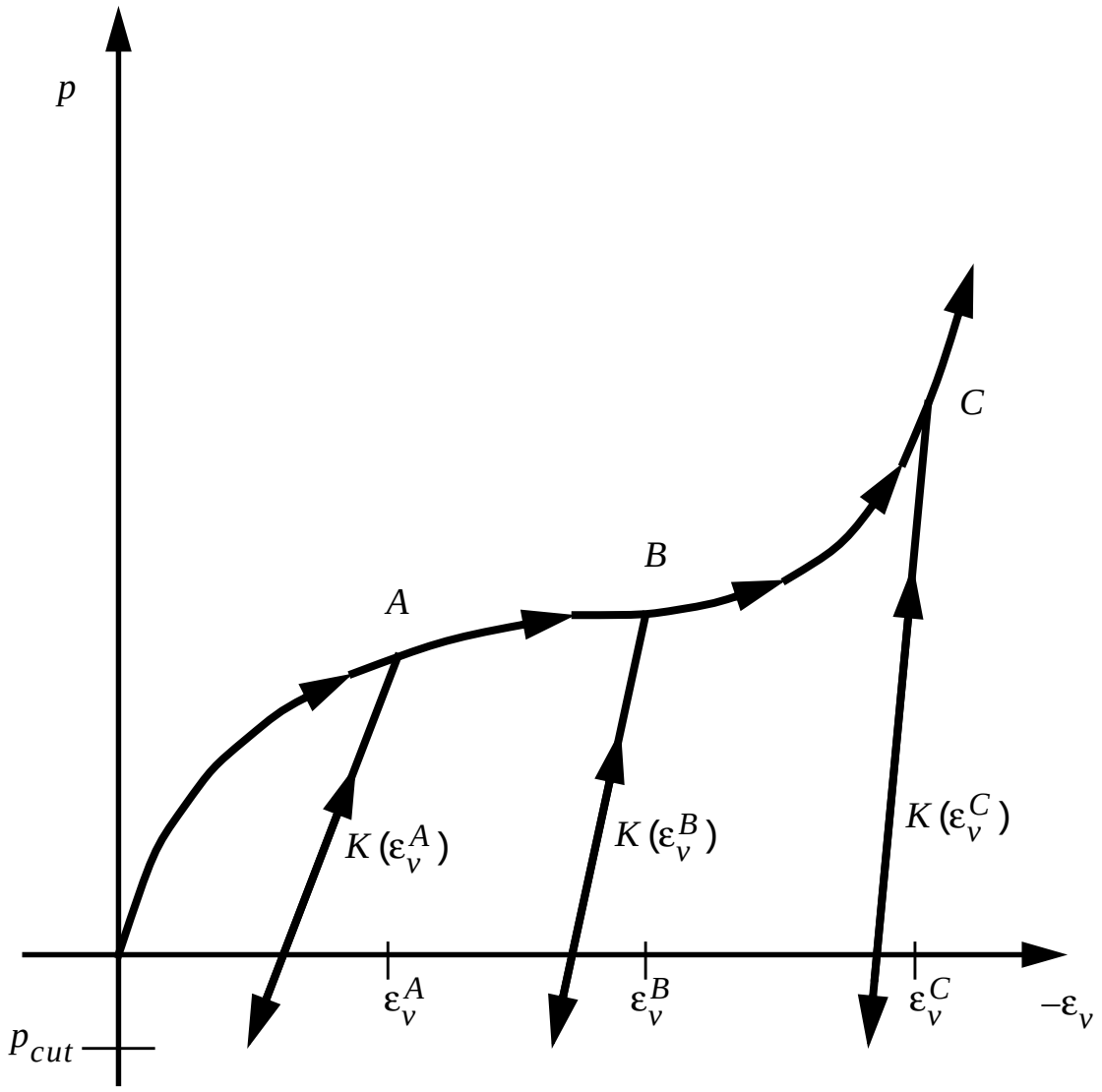

Figure 24

Pressure vs. volumetric strain curve for equation-of-state Form 8 with compaction. The unloading bulk modulus K depends on the peak volumetric strain. The tension limit p_{cut} is defined in the material model definition. Note p is positive in compression and ε_v is positive in tension.

Equation-of-State Form 9 (Tabulated)

Columns		Quantity	Format
1-16	Card 10	ε_{v1}	E16.0
17-32		ε_{v2}	E16.0
33-48		ε_{v3}	E16.0
49-64		ε_{v4}	E16.0
65-80		ε_{v5}	E16.0
1-16	Card 11	ε_{v6}	E16.0
17-32		ε_{v7}	E16.0
33-48		ε_{v8}	E16.0
49-64		ε_{v9}	E16.0
65-80		ε_{v10}	E16.0
1-16	Card 12	C_1	E16.0
17-32		C_2	E16.0
33-48		C_3	E16.0
49-64		C_4	E16.0
65-80		C_5	E16.0
1-16	Card 13	C_6	E16.0
17-32		C_7	E16.0
33-48		C_8	E16.0
49-64		C_9	E16.0
65-80		C_{10}	E16.0
1-16	Card 14	First temperature, T_1	E16.0
17-32		Second temperature, T_2	E16.0
33-48		T_3	E16.0
49-64		T_4	E16.0
65-80		T_5	E16.0

Columns		Quantity	Format
1-16	Card 15	T_6	E16.0
17-32		T_7	E16.0
33-48		T_8	E16.0
49-64		T_9	E16.0
65-80		Tenth temperature, T_{10}	E16.0
1-16	Card 16	γ	E16.0
17-32		Initial internal energy, E_0	E16.0
33-48		Initial relative volume, V_0	E16.0

Pressure p is positive in compression, and volumetric strain ε_v is positive in tension. The tabulated compaction model is linear in internal energy. Pressure is defined by

$$p = C(\varepsilon_v) + \gamma T(\varepsilon_v)E \ , \tag{306}$$

where E is internal energy. Note that in (304) $C(\varepsilon_v)$ denotes a function evaluation, not a multiplication. Thus, the input coefficients C_i have the units of pressure.

The volumetric strain is found from the relative volume V as

$$\varepsilon_v = ln(V) . \tag{307}$$

The tabulated functions may contain from 2 to 10 points, and the model will extrapolate to find the pressure if required.

Equation-of-State Form 10 (Not Available)

Columns	Quantity	Format

Equation-of-state form 10 is not used in this version.

Equation-of-State Form 11 (Pore Collapse)

Card 10

Columns	Quantity	Format
1-5	Number of Virgin Loading Curve points, NLD	15
6-10	Number of Completely Crushed Curve points, NCR	15
11-20	Excess Compression required before any pores can collapse, μ_1	E10.0
21-30	Excess Compression point where the Virgin Loading Curve and the Completely Crushed Curve intersect, μ_2	E10.0
31-40	Initial Internal Energy, E_0	E10.0
41-50	Initial Excess Compression, μ_0	E10.0

Virgin Loading Curve Definition

Cards 11 thru NLD+10

Columns	Quantity	Format
1-15	Excess Compression, μ	E15.0
16-30	Corresponding pressure, p	E15.0

Continue on additional Virgin Loading Curve Definition Cards until all NLD pairs have been defined.

Completely Crushed Curve Definition

Cards NLD+11 thru NLD+NCR+10

Columns	Quantity	Format
1-15	Excess Compression, μ	E15.0
16-30	Corresponding pressure, p	E15.0

Continue on additional Completely Crushed Curve Definition cards until all NCR points have been defined.

The Pore Collapse equation-of-state is based on (Burton, 1982) and uses two curves: the virgin loading curve and the completely crushed curve, as shown in Figure 25. Two critical points are defined: the excess compression point required for pore collapse to begin (μ_1), and the excess compression point required to completely crush the material (μ_2). From this data and the maximum compression the material has attained (μ_{max}), the pressure for any excess compression μ can be determined. Unloading occurs along the virgin loading curve until the excess compression surpasses μ_1. After that, the unloading follows a path between the completely crushed curve and the virgin loading curve. Reloading will follow this curve back up to the virgin loading curve. Once the excess compression exceeds μ_2, then all unloading will follow the completely crushed curve.

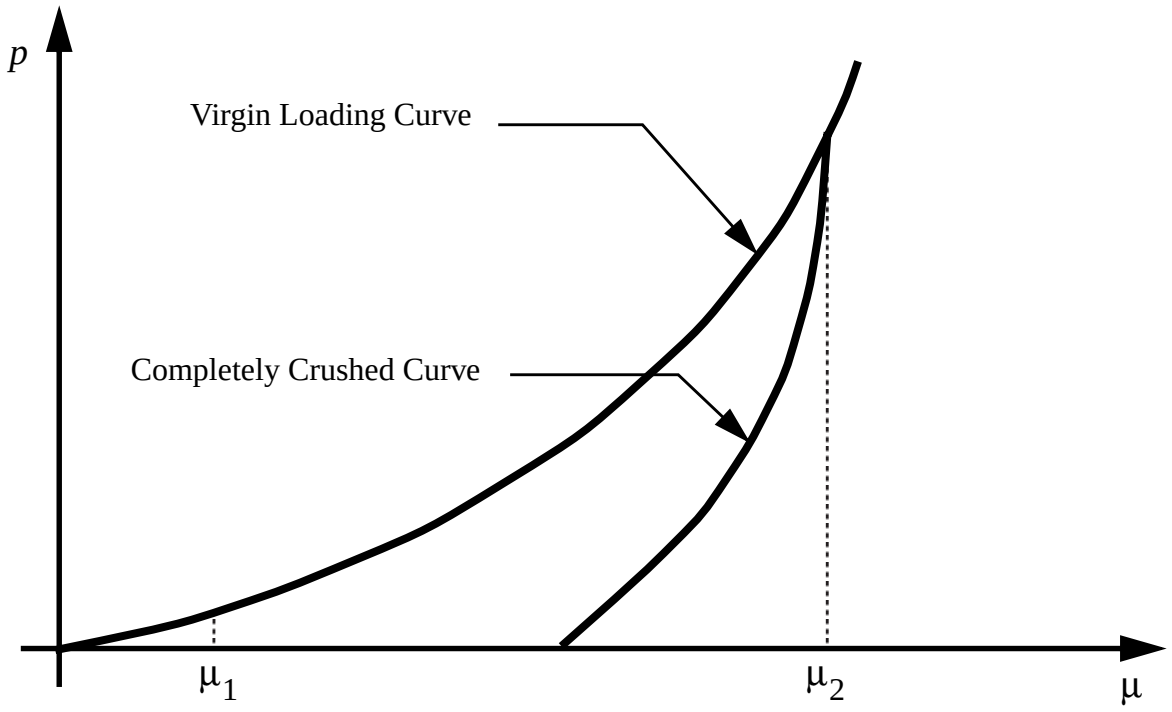

Figure 25
Pressure vs. excess compression for the Pore Collapse equation-of-state. The partially crushed curve lies between the Virgin Loading Curve and the Completely Crushed Curve.

For unloading between μ_1 and μ_2 a partially crushed curve is determined by the relationship:

$$p_{pc}(\mu) = p_{cc}\left[\frac{(1+\mu_B)(1+\mu)}{1+\mu_{max}} - 1\right], \tag{308}$$

where

$$\mu_B = p_{cc}^{-1}(p_{max}) \tag{309}$$

is the excess compression corresponding to a pressure of p_{max} on the completely crushed curve. In the above, subscript pc refers to the partially crushed state and subscript cc refers to the completely crushed state.

In terms of the relative volume V,

$$V = \frac{1}{1+\mu}, \tag{310}$$

$$p_{pc}(V) = p_{cc}\left(\frac{V_B}{V_{min}}V\right). \tag{311}$$

Thus, for a fixed $V_{min} = \frac{1}{\mu_{max}+1}$, the partially crushed curve will separate linearly from the completely crushed curve as V increases to account for pore recovery in the material.

The bulk modulus K is determined as one plus the excess compression times the slope of the current curve,

$$K = (1+\mu)\frac{\partial p}{\partial \mu}. \tag{312}$$

It then follows that the slope for the partially crushed curve is

$$\frac{\partial p}{\partial \mu} = \frac{(1+\mu_B)}{1+\mu_{max}}\frac{\partial p_{cc}}{\partial \mu}\left(\frac{(1+\mu_B)(1+\mu)}{(1+\mu_{max})}\right). \tag{313}$$

The bulk sound speed is determined from the slope of the completely crushed curve at the current pressure to avoid instabilities. The virgin loading and completely crushed curves are modeled with monotonic cubic splines. An optimal vectorized interpolation scheme is then used to evaluate the cubic splines as required during the solution. The bulk modulus and sound speed are derived from a linear interpolation on the derivatives of the cubic splines.

Equation-of-State Form 13 (Ignition and Growth of Reaction in HE 3-Term)

Columns		Quantity	Format
1-10	Card 10	R_{1p}	E10.0
11-20		R_{2p}	E10.0
21-30		R_{5p}	E10.0
31-40		R_{6p}	E10.0
41-50		Second ignition coefficient, F_r	E10.0
1-10	Card 11	R_{3p}	E10.0
11-20		R_{1e}	E10.0
21-30		R_{2e}	E10.0
31-40		R_{3e}	E10.0
41-50		R_{5e}	E10.0
1-10	Card 12	R_{6e}	E10.0
11-20		$F_{max,ig}$	E10.0
21-30		F_q	E10.0
31-40		G_1	E10.0
41-50		m	E10.0
1-10	Card 13	a_1	E10.0
11-20		s_1	E10.0
21-30		Heat capacity of reaction products, c_{vp}	E10.0
31-40		Heat capacity of unreacted HE, c_{ve}	E10.0
41-50		η	E10.0
1-10	Card 14	C_{crit}	E10.0
11-20		Q_r	E10.0
21-30		Initial temperature, T_0 (in $^\circ K$)	E10.0
31-40		Minimum fraction reacted, $fcut$	E10.0
41-50		Tolerance for pressure iteration, $ptol$	E10.0
51-60		Maximum reaction per cycle, chi	E10.0

Columns		Quantity	Format
1-10	Card 15	G_2	E10.0
11-20		a_2	E10.0
21-30		s_2	E10.0
31-40		n	E10.0
41-50		$F_{max,\,gr}$	E10.0
51-60		$F_{min,\,gr}$	E10.0

Equation of State Form 7 was developed by Tarver et. al. and is used to calculate the shock initiation and detonation wave propagation of solid high explosive materials. It should be used instead of the programmed burn (ideal burn) options whenever:

- there is a question whether the high explosive will react,
- there is a finite time required for a shock wave to build up to cause detonation,
- there is a finite thickness of the chemical reaction zone in a detonation wave.

At relatively low initial pressures (less than 2 or 3 GPa), this equation of state should be used with DYNA3D Material Type 10 (elastic-plastic hydrodynamic) for an accurate calculation of the stress state in the unreacted HE. At higher initial pressures, the deviatoric stress state in the HE is less important and Material Type 9 (fluid) may be used at lower cost.

In the following description, a subscript ‘‘e’’ denotes quantities for the unreacted explosive, a subscript ‘‘p’’ denotes quantities for the reaction products, p is the pressure, V is the relative volume, and T is the absolute temperature.

The pressure in the unreacted explosive is given by a JWL equation of state,

$$p_e = R_{1e}e^{-R_{5e}V_e} + R_{2e}e^{-R_{6e}V_e} + R_{3e}\frac{T_e}{V_e} \tag{314}$$

where R_{3e} is a given constant related to the specific heat c_{ve} and JWL parameter ω by

$$R_{3e} = \omega_e c_{ve}\,. \tag{315}$$

The pressure in the reaction products is defined by another JWL equation of state,

$$\mathfrak{I}_p = R_{1p}e^{-R_{5p}} + R_{2p}e^{-R_{6p}V_p} + R_{3p}\frac{T_p}{V_p}, \tag{316}$$

and R_{3p} is a given constant related to the specific heat and JWL parameter as above.

As the chemical reaction converts unreacted explosive to reaction products, these JWL equations of state are used to calculate the pressure in the mixture. This mixture is defined by the fraction reacted, F, where $F = 0$ represents no reaction (all explosive) and $F = 1.0$ represents complete reaction (all products). The temperatures and pressures of reactants and products are assumed to be in equilibrium (i.e., $T_e = T_p$ and $p_e = p_p$), and the relative volumes are additive,

$$V = (1 - F)V_e + V_p . \tag{317}$$

The assumed form of the chemical reaction rate for conversion of unreacted explosive to reaction products consists of three physically realistic terms: an ignition term $\dot{F}_1$ which models the reaction of a small amount of explosive soon after the shock wave compresses it, a slow growth of reaction term $\dot{F}_2$ which models the spread of this initial reaction, and a rapid completion of reaction term $\dot{F}_3$ which dominates at high pressure and temperature. The assumed forms for the reaction rate is then

$$\frac{\partial F}{\partial t} = \dot{F}_1 + \dot{F}_2 + \dot{F}_3 , \tag{318}$$

where the ignition term is given by

$$\dot{F}_1 = F_q (1 - F)^{F_r} \left[\frac{1}{V_e} - 1 - C_{crit} \right]^{\eta} , \tag{319}$$

the growth term is given by

$$\dot{F}_2 = G_1 (1 - F)^{s_1} F^{a_1} p^m , \tag{320}$$

and the completion term is given by

$$\dot{F}_3 = G_2 (1 - F)^{s_2} F^{a_2} p^n , \tag{321}$$

and F_q, F_r, C_{crit}, η, G_1, s_1, a_1, m, G_2, s_2, a_2, and n are given constants.

The ignition rate $\dot{F}_1$ is set to zero when $F \geq F_{max,ig}$, the growth term $\dot{F}_2$ is set to zero when $F \geq F_{max,gr}$, and the completion term $\dot{F}_3$ is set to zero when $F \leq F_{min,gr}$.

Details of the computational methods and many examples of one and two-dimensional shock initiation and detonation wave calculations can be found in (Cochran and Chan, 1979), (Lee and Tarver, 1980), (Tarver and Hallquist, 1981), (Tarver, Hallquist, and Erickson, 1985), and (Tarver, 1990).

Unfortunately, sufficient experimental data has been obtained for only two solid explosives to develop reliable shock initiation models: PBX-9404 (and the related HMX-based explosives LX-14, LX-10, LX-04, etc.), and LX-17 (the insensitive TATB-based explosive). Reactive flow models for other explosives (such as TNT, PETN, Composition B, propellants) have been developed but

are based on very limited experimental data. The standard models for PBX-9404 and LX-17 (in the centimeters, grams, and microseconds units system) are given in Table 4 and Table 5.

Table 4: Material Type 10 Constants for Two HE Materials

Material	density	shear modulus	yield strength
PBX-9404	1.842	0.0454	0.002
LX-17	1.900	0.0354	0.002

Table 5: Equation of State Form 7 Constants for Two HE Materials

Constant	PBX-9404	LX-17
R_{1p}	8.524	5.31396
R_{2p}	0.1802	0.0270309
R_{5p}	4.6	4.1
R_{6p}	1.3	1.1
F_r	0.667	0.667
R_{3p}	3.8E-6	4.60E-6
R_{1e}	9522.0	778.1
R_{2e}	-0.05944	-0.05031
R_{3e}	2.4656E-5	2.2229E-5
R_{5e}	14.1	11.3
R_{6e}	1.41	1.13
$F_{max,ig}$	0.3	0.5
F_q	7.43E+11	4.0E+6
G_1	3.1	0.6
m	1.0	1.0
a_1	0.111	0.111
s_1	0.667	0.667
c_{vp}	1.0E-5	1.0E-5

Table 5: Equation of State Form 7 Constants for Two HE Materials

Constant	PBX-9404	LX-17
c_{ve}	2.7813E-5	2.487E-5
η	20.0	7.0
C_{crit}	0.0	0.22
Q_r	0.102	0.069
T_0	298.0	298.0
G_2	400.0	400.0
a_2	1.0	1.0
s_2	0.333	.333
n	2.0	3.0
$F_{max,\,gr}$	0.5	0.5
$F_{min,\,gr}$	0.0	0.0

CROSS SECTION PROPERTY DEFINITION FOR STRUCTURAL ELEMENTS

Define structural element cross section parameters if this material applies to truss, beam, shell, or thick shell elements.

Card 9

Columns	Quantity	Format
1-10	Cross section identification	12A6

This title will be printed with the Cross Section Properties in the `hsp` printout file. It is useful for labeling the physical cross section for which this property set is applicable.

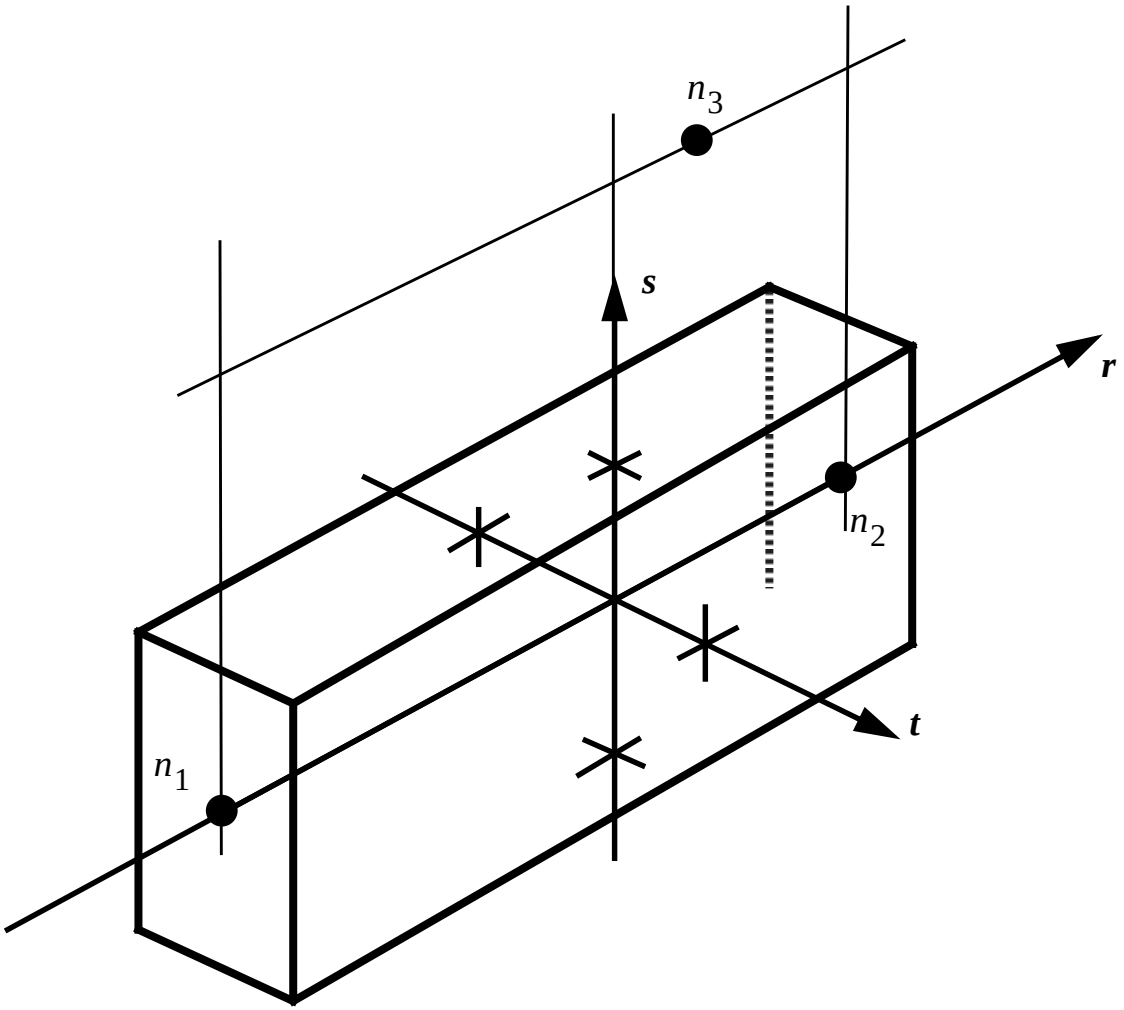

Figure 26
Element geometry for DYNA3D truss and beam elements. Node n_3 determines the initial orientation of the element local s and t axes.

Truss Element Cross Section Properties

Columns		Quantity	Format
	Card 10	Blank	
1-10	Card 11	Cross-sectional area, A	E10.0

The geometry of DYNA3D truss elements is shown in Figure 26. Note that the position of the orientation node, node n_3, is not significant for truss elements. Node n_3 must be defined in the input, however.

This is a simple truss element, which transmits only axial force.

Hughes-Liu Beam Element Cross Section Properties

Columns		Quantity	Format
1-10	Card 10	Shear factor, κ (default is $\kappa = 1.0$)	E10.0
11-20		Quadrature rule for beam element cross section LT.0: absolute value is User-Defined Integration Rule number EQ.1.0: degenerate beam (truss) EQ.2.0: 2×2 Gauss quadrature (default) EQ.3.0: 3×3 Gauss quadrature EQ.4.0: 3×3 Lobotto quadrature EQ.5.0: 4×4 Gauss quadrature	E10.0
21-30		Cross section type, *ICROSS* EQ.0.0: rectangular EQ.1.0: tubular EQ.2.0: arbitrary (User-Defined Integration Rule)	E10.0
1-10	Card 11	Geometric dimension *at node* n_1 *ICROSS*.EQ.0: beam thickness in s direction *ICROSS*.EQ.1: beam *outer* diameter *ICROSS*.EQ.2: beam thickness in s direction	E10.0
11-20		Geometric dimension a*t node* n_2 *ICROSS*.EQ.0: beam thickness in s direction *ICROSS*.EQ.1: beam *outer* diameter *ICROSS*.EQ.2: beam thickness in s direction	E10.0
21-30		Geometric dimension *at node* n_1 *ICROSS*.EQ.0: beam thickness in t direction *ICROSS*.EQ.1: beam *inner* diameter *ICROSS*.EQ.2: beam thickness in t direction	E10.0
31-40		Geometric dimension *at node* n_2 *ICROSS*.EQ.0: beam thickness in t direction *ICROSS*.EQ.1: beam *inner* diameter *ICROSS*.EQ.2: beam thickness in t direction	E10.0
41-50		Location of reference surface normal to s axis .EQ. 1.0: on beam outer surface at $s = 1$ .EQ. 0.0: at beam centerline (default) .EQ.-1.0: on beam outer surface at $s = -1$	E10.0
51-60		Location of reference surface normal to t axis .EQ. 1.0: on beam outer surface at $t = 1$ .EQ. 0.0: at beam centerline (default) .EQ.-1.0: on beam outer surface at $t = -1$	E10.0

The geometry of DYNA3D beam elements is shown in Figure 26. Note that the position of the orientation node, node n_3, determines the *initial* element coordinate system. The coordinate system remains fixed in the element, and thus rotates with the element during the deformation.

The Hughes-Liu beam element was adapted from the degenerated continuum shell element described in (Hughes and Liu, 1981a) and (Hughes and Liu, 1981b). All constitutive computations are performed at the stress-strain level, and numerical integration is performed over the cross section to evaluate forces and moments.

Two reference surfaces may be defined to include effects of loads applied to the beam on its outer surface rather than on its centerline. This situation typically occurs when beam elements are used as stiffeners for thin shell structures. In that case, the load is transferred to the beam along the beam surface which contacts the shell. These effects may be incorporated into the analysis model by defining the Hughes-Liu beam element reference surface as the surface in contact with another body. Note that if the either reference surface is displaced from the center of the beam, a purely axial deformation will induce moments into the beam.

Hughes-Liu Beam Cross Section Property Notes

card:field	Comments
10:2	Choose the desired numerical integration rule for the integration over the element cross section. For rectangular or tubular cross sections, either Gauss or Lobotto quadrature may be used. Gauss quadrature gives increased accuracy for a fixed number of points, but generally does not include an integration point on the outer element surface. Lobotto integration is somewhat less accurate than Gauss for the same number of points, but always has points located on the outermost fibers of the beam. For complex cross sections, User-Defined Integration rules must be used to accurately evaluate the element forces and moments.
10:3	Choose the appropriate cross section geometry. Solid cylindrical beams may be modeled by specifying tubular cross section and giving the inner diameter as 0.0. If the User-Defined Integration rule is selected, it must be defined as described in section 4.5 on page 303. Note that if a negative number is input for the Quadrature Rule option, then the cross-section type must be selected as 2.0 (User-Defined Integration Rule).
11:1-4	Beam dimensions may be defined independently at each of the two end nodes. Linear variation is assumed along the element length.
11:5-6	Choose the location of the reference surface to correspond with the point of application of the load. The reference surface should be the contact surface if beam elements are used as shell stiffeners. The default reference location is at the element center, which is appropriate for most applications.

Belytschko-Schwer Beam Element Cross Section Properties

Columns		Quantity	Format
1-10	Card 10	Shear factor, κ (default is $\kappa = 1.0$)	E10.0
1-10	Card 11	Cross-sectional area, A	E10.0
11-20		Area moment of inertia about s axis, I_{ss}	E10.0
21-30		Area moment of inertia about t axis, I_{tt}	E10.0
31-40		Polar moment of inertia about r axis, I_{rr}	E10.0
41-50		Shear area, A_s	E10.0

The Belytschko-Schwer beam element is based on a classical resultant beam formulation, and is described in (Belytschko, Schwer, and Klein, 1977). Constitutive evaluations are performed at the resultant level, where forces and moments are related to displacements and curvatures. This element is somewhat faster in computation since no numerical integration is performed over the cross section, but may be less accurate for elastoplastic analysis when partial section yield is important. Since the Belytschko-Schwer beam is a resultant-based formulation, any type of cross-section may be easily modeled by specifying its cross-sectional area and area moments of inertia. Experience has shown that this element performs well in a wide range of analysis situations.

Belytschko-Schwer Beam Cross Section Property Notes

card:field	Comments
11:1	The cross-sectional area A is used in computing axial forces and bending moments, and additionally to compute the element mass.
11:2-4	It is assumed that the r, s, and t axes are principal axes of the cross section, so that all cross-terms in the moment of inertia matrix vanish.
11:5	The shear area A_s is used in computing shear forces.

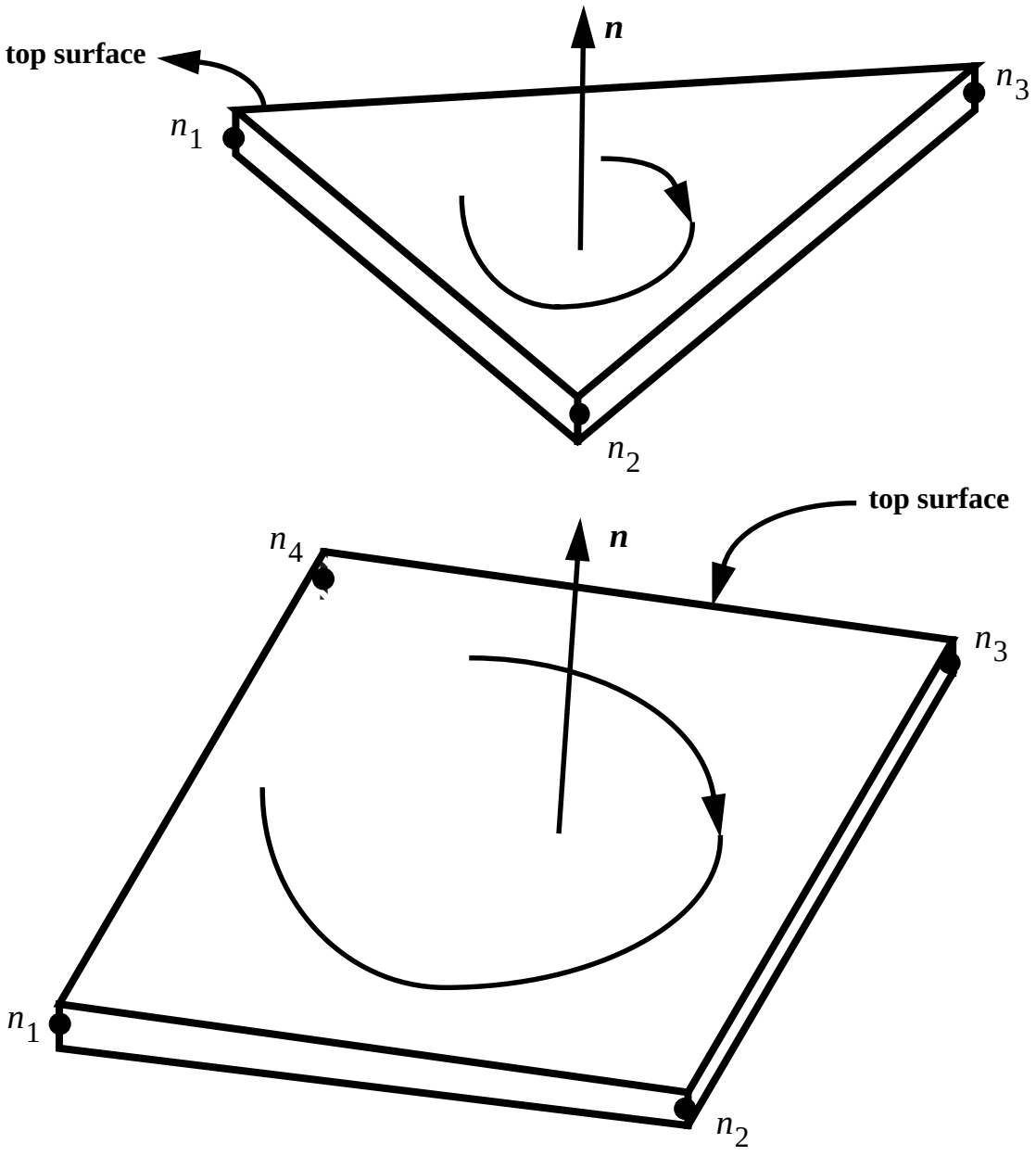

Figure 27

Shell element geometry in DYNA3D. Counterclockwise node numbering determines sense of shell outward normal vector ***n*** using the "right-hand rule." Top and bottom surfaces are determined from the sense of the normal vector.

Shell Element Cross Section Properties

Columns		Quantity	Format
1-10	Card 10	Shear factor, κ (default is $\kappa = 1.0$)	E10.0
11-20		Number of through-thickness integration points EQ.1: 1 point (membrane element) EQ.2: 2 points EQ.3: 3 points EQ.4: 4 points EQ.5: 5 points GT.5: trapezoidal rule or User-Defined Integration Rule	E10.0
21-30		Shell element printed output option EQ.1: average resultants and fiber lengths EQ.2: resultants at plan points and fiber lengths EQ.3: resultants, stresses at all points, fiber lengths (default)	E10.0
31-40		Integration rule LT.0: absolute value is User-Defined Integration Rule number EQ.0: Gauss quadrature (maximum of 5 points) EQ.1: trapezoidal rule (any number of pts may be used)	E10.0
1-10	Card 11	Shell thickness at node n_1	E10.0
11-20		Shell thickness at node n_2	E10.0
21-30		Shell thickness at node n_3	E10.0
31-40		Shell thickness at node n_4	E10.0
41-50		Reference surface location (Hughes-Liu formulation only) EQ. 1.0: top surface EQ. 0.0: midsurface (default) EQ.-1.0: bottom surface	E10.0

The above Cross Section Properties should be defined for all 4-node quadrilateral and 3-node triangular shell elements. These shell thickness values can be overridden on the element cards. The above values are used if the thickness values are zero on the element cards.

Shell Element Cross Section Property Notes

card:field	Comments
10:1	The elastic moduli are scaled by the shear correction factor κ for calculating the transverse shear stresses.
10:2	Numerical integration is used to compute element resultant forces and moments from stresses calculated at discrete points through the shell element thickness. Several different integration methods (rules) are supported, and each may be used with a selected number of points. Using more integration points through the shell thickness increases the cost, but also increases the accuracy of the element, particularly when partial section yielding is expected in predominantly bending deformations. Two integration points will exactly capture linearly elastic material behavior.
10:3	This option governs the amount of printout written to the "`hsp`" file when shell elements are specified in Element Time History Blocks, as described in section 4.17 on page 326.
10:4	Three numerical integration algorithms are available. Gauss quadrature gives the best accuracy for a fixed number of points, but may not have points exactly on the upper and lower shell surface. Up to five points are allowed with Gauss quadrature. The trapezoidal rule is slightly less accurate than Gauss quadrature for a fixed number of points, but always has points on the endpoints of the interval (i.e., on the upper and lower surface of the shell). User-Defined Integration Rules allow a general integration scheme to be defined with an arbitrary number of points through the thickness. This feature is often used to construct accurate integration algorithms for laminated composite shells by putting one integration point in each lamina or group of lamina. Shell results are output to the TAURUS database at three planes through the thickness: the bottom-most integration point, the midsurface, and the top-most integration point. The desired plane is selected in TAURUS using the **shell inner**, **shell middle**, and **shell outer** commands, respectively. Note that if Gauss integration is used, the bottom-most integration point may not be physically on the shell bottom surface, and similarly with the top-most integration point. If surface stresses are desired, trapezoidal rule integration should be used. See the TAURUS manual (Spelce and Hallquist, 1991) for further details.
11-5	The location of the reference surface can be important whenever beam elements, shell elements, and solid elements are interconnected. It is often desirable to have beam elements and shell elements share a common reference surface when beams are used as shell stiffeners. In these cases, the reference surface for the shell element and beam element should be on the interface surface.

Thick Shell Element Cross Section Properties

Columns		Quantity	Format
1-10	Card 10	Shear factor, κ (default is $\kappa = 1.0$)	E10.0
11-20		Number of through-thickness integration points EQ.1: 1 point (membrane element) EQ.2: 2 points EQ.3: 3 points EQ.4: 4 points EQ.5: 5 points GT.5: trapezoidal rule or User-Defined Integration Rule	E10.0
31-40		Integration rule LT.0: absolute value is User-Defined Integration Rule number EQ.0: Gauss quadrature (maximum of 5 points) EQ.1: trapezoidal rule (any number of pts may be used)	E10.0
	Card 11	Blank	

Thick Shell Element Cross Section Property Notes

card:field	Comments
10:1	The elastic moduli are scaled by the shear correction factor κ for calculating the transverse shear stresses.
10:2	Numerical integration is used to compute element resultant forces and moments from stresses calculated at discrete points through the shell element thickness. Several different integration methods (rules) are supported, and each may be used with a selected number of points. Using more integration points through the shell thickness increases the cost, but also increases the accuracy of the element, particularly when partial section yielding is expected in predominantly bending deformations. Two integration points will exactly capture linearly elastic material behavior.
10:4	Three numerical integration algorithms are available. Gauss quadrature gives the best accuracy for a fixed number of points, but may not have points exactly on the upper and lower shell surface. Up to five points are allowed with Gauss quadrature. The trapezoidal rule is slightly less accurate than Gauss quadrature for a fixed number of points, but always has points on the endpoints of the interval (i.e., on the upper and lower surface of the shell). User-Defined Integration Rules allow a general integration scheme to be defined with an arbitrary number of points through the thickness.

4.5 HUGHES-LIU BEAM USER DEFINED INTEGRATION RULES

Define *NUSBIR* Card sets in this section.

Card 1

Columns	Quantity	Format
1-5	Number of integration points, *NIP*	15
6-15	Relative area of cross section, A_{rel} . $$A_{rel} = \frac{A_{cs}}{t_s t_t},$$ where A_{cs} is the actual cross-sectional area, t_s is the specified thickness in the s direction, and t_t is the specified thickness in the t direction.	E10.0

Cards 2, 3, . . . , NIP+1

Columns	Quantity	Format
1-10	s coordinate of integration point, ξ_k $(-1.0 \le \xi_k \le 1.0)$	E10.0
11-20	t coordinate of integration point, η_k $(-1.0 \le \eta_k \le 1.0)$	E10.0
21-30	Weighing factor, W_k. This is typically the area associated with integration point divided by actual cross sectional area	E10.0

User-Defined Integration Rules are based on the general numerical integration formula

$$\int f(\xi, \eta)dx \approx \sum_{k=1}^{NIP} f(\xi_k, \eta_k)W_k \ , \tag{322}$$

where $f(\xi, \eta)$ is the function to be integrated, ξ_k, η_k, $k = 1,...,NIP$, are the integration point coordinates, and W_k is the integration weight for point k.

4.6 SHELL USER DEFINED INTEGRATION RULES

Define *NUSSIR* card sets in this section.

Card 1

Columns	Quantity	Format
1-5	Number of integration points, *NIP*	I5
6-10	Equal spacing of integration points option, *ISPACE* EQ.0: integration point locations are defined below EQ.1: integration points are equally spaced through the shell thickness such that the shell is subdivided into NIP layers of equal thickness.	I5

Cards 2, 3, . . . , NIP+1

Define these cards only if the equal-spacing option is *not* active, ($ISPACE = 0$).

Columns	Quantity	Format
1-10	Coordinate of integration point, ζ_k $(-1.0 \le \zeta_k \le 1.0)$	E10.0
11-20	Weight factor, W_k. This is typically the thickness associated with the integration point divided by actual shell thickness.	E10.0
21-25	Optional material number for this integration point if different than the number specified on the element card. The material type must be the same as for the material number given on the element card.	I5

User-Defined Integration Rules are based on the general numerical integration formula

$$\int f(\zeta)dx \approx \sum_{k=1}^{NIP} f(\zeta_k)W_k, \tag{323}$$

where $f(\zeta)$ is the function to be integrated, ζ_k, $k = 1,...,NIP$, are the integration point coordinates, and W_k is the integration weight for point k.

Shell User-Defined Integration Rule Notes

card:field	Comments
1:2	This option is most useful for quickly defining a large number of points for even-thickness layers in a shell.
2:3	This option allows a different set of material constants to be specified at each thickness integration point to model a shell element with properties which vary through the thickness. If only the orientation angle varies for an orthotropic elastic material, this may be more easily specified as described for Material Types 2, 21, 22, and 23. *NOTE: The density is always taken from the data for the material number specified on the element card.*

4.7 NODES

Define *NUMNP* nodes in this section. Column numbers in parenthesis apply for the "large" input option which allows more than 99,999 nodes.

Columns		Quantity	Format	
1-5	(1-8)	Node number	I5	(I8)
6-10	(9-13)	Displacement boundary condition code EQ.0:no constraints EQ.1:constrained x displacement EQ.2:constrained y displacement EQ.3:constrained z displacement EQ.4:constrained x and y displacements EQ.5:constrained y and z displacements EQ.6:constrained z and x displacements EQ.7:constrained x, y, and z displacement EQ.8:constrained in direction specified on the first Sliding Boundary Plane card. EQ.9:constrained in direction specified on the second Sliding Boundary Plane card. . . EQ.7 + n constrained in direction specified on the n^{th} Sliding Boundary Plane card.	I5	(I5)
11-30	(14-33)	x-coordinate	*E20.0	(E20.0)
31-50	(34-53)	y-coordinate	E20.0	(E20.0)
51-70	(54-73)	z-coordinate	E20.0	(E20.0)
71-75	(-)	Nodal increment for generation, k	I5	(omit)
76-80	(74-78)	Rotational boundary condition code EQ.0:no constraints EQ.1:constrained x rotation EQ.2:constrained y rotation EQ.3:constrained z rotation EQ.4:constrained x and y rotations EQ.5:constrained y and z rotations EQ.6:constrained z and x rotations EQ.7:constrained x, y, and z rotations	I5	(I5)

* or as defined on Control Card 3.

Node cards do not need to be in order, but the first node card must define node 1, and the last node card must define node $NUMNP$. Gaps are not permitted in node numbering, and nodes may be generated internally in DYNA3D. Whenever node definitions are missing, node numbers are automatically generated according to the sequence

$$n_i, n_i + k, n_i + 2k, \ldots, n_j \tag{324}$$

where n_i and n_j are the node numbers defined on two consecutive cards, and k is taken from the card defining n_i. Linear interpolation is used to obtain the coordinates of the generated nodes. The boundary condition code for generated nodes is set to zero if the boundary condition code of n_i differs from that of n_j, otherwise it is set to the boundary condition code of node n_i. Unconstrained nodes can be generated between constrained nodes that have the same boundary condition code by making the code negative on one of the two input node cards. After the nodal data is generated, all negative boundary condition codes are reset to positive values.

Boundary conditions which are not parallel to a global axis may be defined using Sliding Boundary Planes, as described in section 4.14 on page 321, or Nodal Single Point Constraints, as described in section 4.13 on page 319. Boundary conditions parallel to the global axes should be defined on the node cards as described above for fastest computation.

Rotational boundary conditions imposed on rigid-body nodes may generate small, finite-deformation induced, non-zero instantaneous rotational velocities. Nonetheless, the constraint is still fully enforced and rotations about the constrained directions are prohibited. These non-zero rotational velocities can be reduced by decreasing the timestep size.

4.8 SOLID ELEMENTS

Define the following card for each of the *NUMELH* solid elements. All solid elements are numbered sequentially starting from 1.

Columns		Quantity	Format	
1-5	(1-8)	Solid element number	I5	(I8)
6-10	(9-13)	Material number	I5	(I5)
11-15	(-)	Generation increment, k	I5	(omit)
16-20	(14-21)	Node n_1	I5	(I8)
21-25	(22-29)	Node n_2	I5	(I8)
26-30	(30-37)	Node n_3	I5	(I8)
.		.	.	
.		.	.	
51-55	(70-77)	Node n_8	I5	(I8)
	(78-87)	Initial relative volume		(E10.3)

Nodes n_1 - n_8 define the corner nodes of the 8-node solid elements. Elements having fewer than 8 nodes are defined by repeating one or more nodes to “collapse” the appropriate side of the brick element into the desired shape. Four, six, and eight node elements are shown in Figure 28. Input of nodes on the element cards for the two degenerate elements is:

4-node	$n_1\ n_2\ n_3\ n_4\ n_4\ n_4\ n_4\ n_4$
6-node	$n_1\ n_2\ n_3\ n_4\ n_5\ n_5\ n_6\ n_6$

Note: In all cases the first four node numbers must be unique.

Element cards must be in element number order. The first card must contain data for the first solid element, and the last card must contain data for the last solid element. Cards containing intermediate element data may be omitted and these element definitions will be generated internally. Connecting node numbers n_j are automatically generated with respect to the first card prior to the omitted data by

$$n_j^{i+1} = n_j^i + k, \qquad j = 1,..., 8 \tag{325}$$

where superscripts denote the element number to be defined and subscripts denote the local node number (in the connectivity list) which is to be incremented. The generation increment k and the element attributes, such as the material number, for the generated elements are taken from the last element card before the omitted data. The default value of the generation increment k is l. An initial relative volume is allowed for pre-stressed elements. This initial relative volume will overwrite relative volume imposed by the material entry or the equation of state entry.

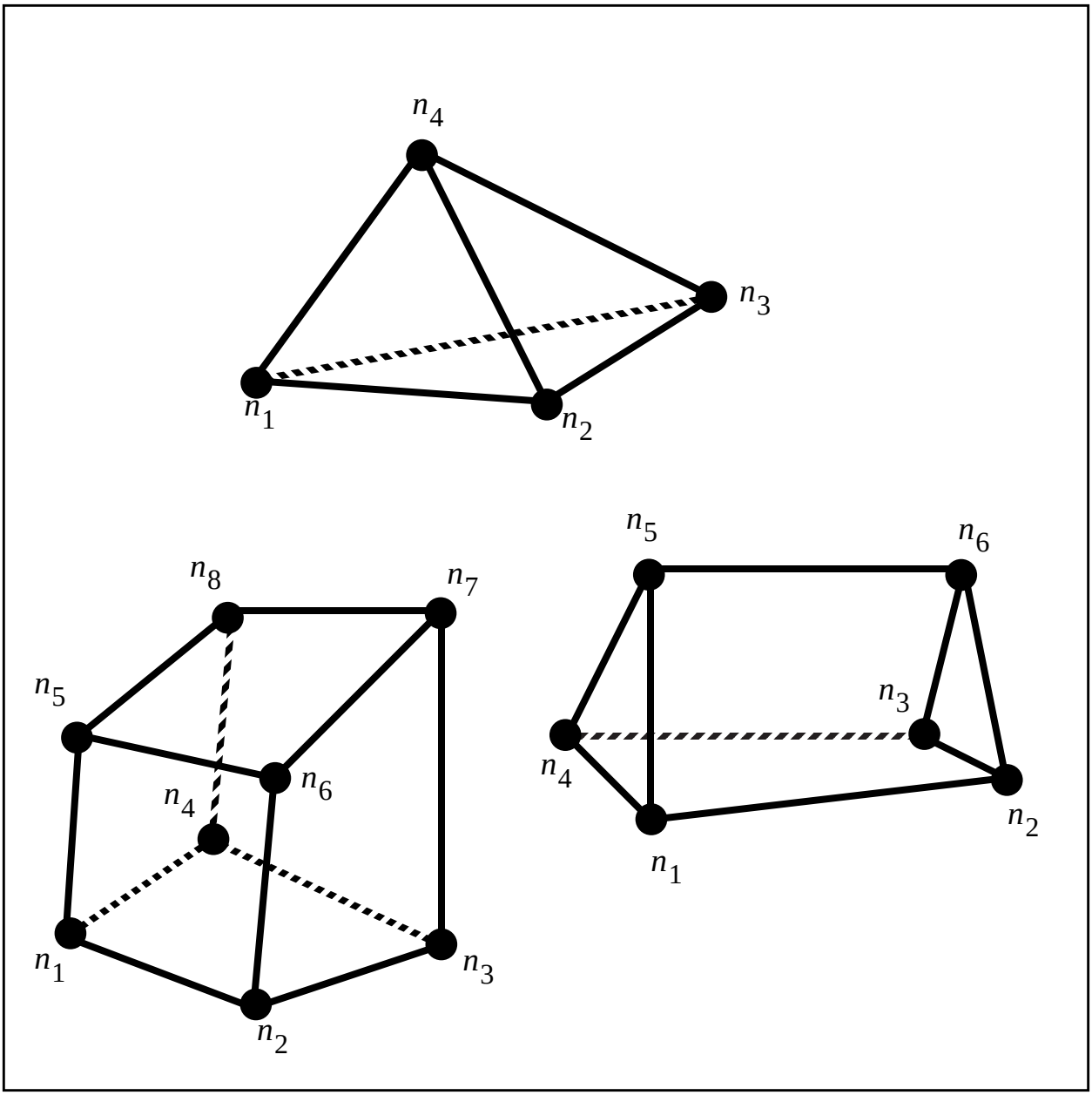

Figure 28
DYNA3D solid element geometry in four-node, six-node, and eight-node configurations.

4.9 BEAM AND TRUSS ELEMENTS

Define the one of the following cards for each of the *NUMELB* truss or beam elements. All truss and beam elements are numbered sequentially, starting from 1, regardless of the formulation used. The element formulation is specified on the Material Control Card as described in section 4.4 on page 92.

Hughes-Liu Beam Element

Columns		Quantity	Format	
1-5	(1-8)	Beam element number	I5	(I8)
6-10	(9-13)	Material number	I5	(I5)
11-15	(-)	Generation increment, k	I5	(omit)
16-20	(14-21)	Node n_1	I5	(I8)
21-25	(22-29)	Node n_2	I5	(I8)
26-30	(30-37)	Node n_3 (see Figure 26)	I5	(I8)
31-40	(38-45)	Beam thickness in s direction at node n_1	E10.0	(E8.0)
41-50	(46-53)	Beam thickness in s direction at node n_2	E10.0	(E8.0)
51-60	(54-61)	Beam thickness in t direction at node n_1	E10.0	(E8.0)
61-70	(62-69)	Beam thickness in t direction at node n_2	E10.0	(E8.0)

Belytschko-Schwer Beam Element

Columns		Quantity	Format	
1-5	(1-8)	Beam element number	I5	(I8)
6-10	(9-13)	Material number	I5	(I5)
11-15	(-)	Generation increment, k	I5	(omit)
16-20	(14-21)	Node n_1	I5	(I8)
21-25	(22-29)	Node n_2	I5	(I8)

Columns		Quantity	Format	
26-30	(30-37)	Node n_3 (see Figure 26)	I5	(I8)
31-40	(38-45)	Cross-sectional area, A	E10.0	(E8.0)
41-50	(46-53)	Moment of inertia about s axis, I_{ss}	E10.0	(E8.0)
51-60	(54-61)	Moment of inertia about t axis, I_{tt}	E10.0	(E8.0)
61-70	(62-69)	Polar moment of inertia about r axis, I_{rr}	E10.0	(E8.0)
71-78	(70-77)	Shear area, A_s	E10.0	(E8.0)

Truss Element

Columns		Quantity	Format	
1-5	(1-8)	Beam element number	15	(I8)
6-10	(9-13)	Material number	15	(I5)
11-15	(-)	Generation increment, k	I5	(omit)
16-20	(14-21)	Node n_1	I5	(I8)
21-25	(22-29)	Node n_2	I5	(I8)
26-30	(30-37)	Node n_3 (see Figure 26)	I5	(I8)
31-40	(38-45)	Cross-sectional Area, A	E10.0	(E8.0)

Element cards must be in element number order. The first card must contain data for the first beam or truss element, and the last card must contain data for the last beam or truss element. Cards containing intermediate element data may be omitted and these element definitions will be generated internally. Connecting node numbers n_j are automatically generated with respect to the first card prior to the omitted data by

$$n_j^{i+1} = n_j^i + k, \qquad j = 1, 2 \tag{326}$$

where superscripts denote the element number to be defined and subscripts denote the local node number (in the connectivity list) which is to be incremented. Note that the orientation node n_3 is not incremented. The generation increment k and the element attributes, such as the material number, cross section properties, and orientation node, for the generated elements are taken from the last element card before the omitted data. The default value of the generation increment k is l.

If any cross-sectional properties are undefined (or are defined as 0.0) on the element card, these values are taken from the data specified in the Material Cards. Thus, if many elements share the same properties with only a few elements differing, the common properties may be specified in the Material Cards, and only the unique element properties need be defined on the element cards.

4.10 SHELL AND MEMBRANE ELEMENTS

Define the following card set for each of the *NUMELS* shell or membrane elements. All shell and membrane elements are numbered sequentially, starting from 1, regardless of the formulation used. Note that *two cards per element* are required if the LARGE input option is active.

Columns		Quantity	Format	
1-5	(1-8)	Shell element number	15	(I8)
6-10	(9-13)	Material number	15	(I5)
11-15	(-)	Generation increment *k*	I5	(omit)
16-20	(14-21)	Node n_1 (see Figure 27)	I5	(I8)
21-25	(22-29)	Node n_2	I5	(I8)
26-30	(30-37)	Node n_3	I5	(I8)
31-35	(38-45)	Node n_4	I5	(I8)
		second card here if LARGE input option is active		
36-45	(1-10)	Shell thickness at node n_1 (optional)	E10.0	(E10.0)
46-55	(11-20)	Shell thickness at node n_2 (optional)	E10.0	(E10.0)
56-65	(21-30)	Shell thickness at node n_3 (optional)	E10.0	(E10.0)
66-75	(31-40)	Shell thickness at node n_4 (optional)	E10.0	(E10.0)
76-80	(41-50)	Orthotropic material angle, β, in degrees (optional)	E5.00	(E10.0)

Triangular elements are defined by repeating the third node (i.e., by setting $n_4 = n_3$). It should be noted that quadrilateral shell elements perform very poorly in bending when degenerated into triangles. In this case, the use of one of the triangular shell element formulations is recommended. Shell and membrane element formulations are discussed in section 2.6 on page 15.

Element cards must be in element number order. The first card must contain data for the first shell or membrane element, and the last card must contain data for the last shell or membrane element. Cards containing intermediate element data may be omitted and these element definitions will be generated internally. Connecting node numbers n_j are automatically generated with respect to the last element card prior to the omitted data by

$$n_j^{i+1} = n_j^i + k, \qquad j = 1, 2, 3, 4 \tag{327}$$

where superscripts denote the element number to be defined and subscripts denote the local node number (in the connectivity list) which is to be incremented. The generation increment k and the element attributes, such as the material number and cross section properties, for the generated elements are taken from the last element card before the omitted data. The default value of the generation increment k is l.

If any element thicknesses are undefined (or are defined as 0.0) on the element card, these values are taken from the data specified in the Material Cards. Thus, if many elements share the same properties with only a few elements differing, the common properties may be specified in the Material Cards, and only the unique element properties need be defined on the element cards.

4.11 THICK SHELL ELEMENTS

Define the following card for each of the $NUMELT$ 8-node thick shell elements. All thick shell elements are numbered sequentially starting from 1.

Columns		Quantity	Format	
1-5	(1-8)	Thick shell element number	I5	(I8)
6-10	(9-13)	Material number	I5	(I5)
11-15	(-)	Generation increment, k	I5	(omit)
15-20	(14-21)	Node n_1	I5	(I8)
21-25	(22-29)	Node n_2	I5	I8)
26-30	(30-37)	Node n_3	I5	(I8)
.		. .		.
.		. .		.
.		. .		.
.		. .		.
51-55	(70-77)	Node n_8	I5	(I8)

Element cards must be in element number order. The first card must contain data for the first thick shell element, and the last card must contain data for the last thick shell element. Cards containing intermediate element data may be omitted and these element definitions will be generated internally. Connecting node numbers n_j are automatically generated with respect to the first card prior to the omitted data by

$$n_j^{i+1} = n_j^i + k,\ j = 1,...,8 \tag{328}$$

where superscripts denote the element number to be defined and subscripts denote the local node number (in the connectivity list) which is to be incremented. The generation increment k and the element attributes, such as the material number, for the generated elements are taken from the last element card prior to the omitted data. The default value of the generation increment k is l.

Nodes n_1 - n_8 define the corner nodes of the 8-node thick shell elements. Nodes n_1 to n_4 define the lower surface, and nodes n_5 to n_8 define the upper surface. The integration points lie along the t axis as depicted in Figure 29. Care should be used in defining the connectivity to insure the proper element orientation.

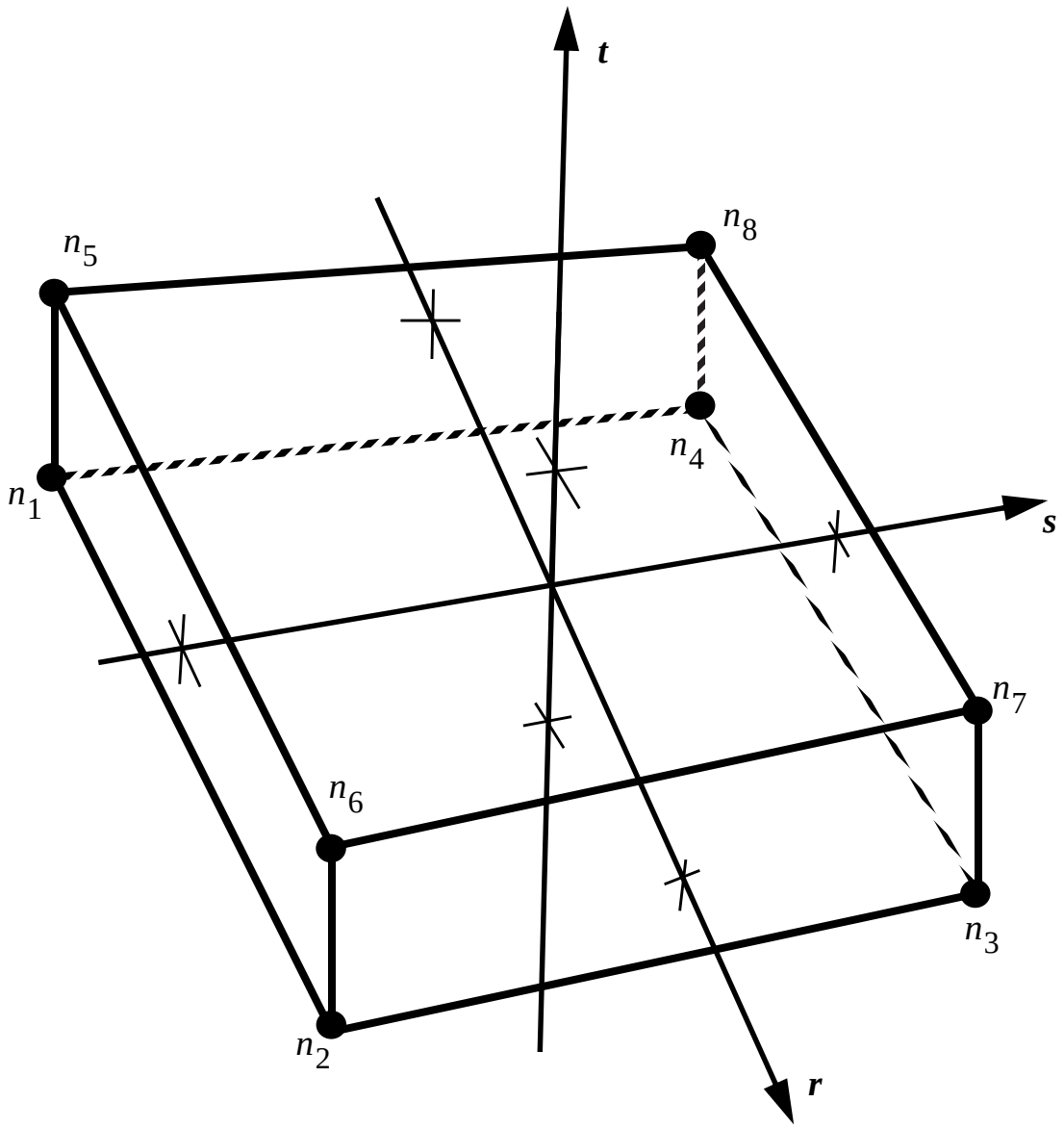

Figure 29
Geometric configuration for 8-node thick shell element.

4.12 INTERFACE SAVE SEGMENT DEFINITION

Define *NUMIFS* Interface Save Segments.

Columns		Quantity	Format	
1-5	(1-8)	Interface segment number	I5	(I8)
6-10	(-)	Generation increment, k	I5	(omit)
11-15	(9-16)	Node n_1	I5	(I8)
16-20	(17-24)	Node n_2	I5	(I8)
21-25	(25-32)	Node n_3	I5	(I8)
26-30	(33-40)	Node n_4	I5	(I8)

Omitted segment definitions are automatically generated with respect to the last card prior to the omitted data using the generation increment k to compute connecting nodes for the missing segment definitions. The generation parameter k is taken from the first card. Node numbering may be either clockwise or counterclockwise. Nodes n_1 - n_4 define the corner nodes of the segments as shown in Figure 35. Triangular segments are defined by repeating a node.

Interface save segments are used to define a surface for which the displacement and velocity time history will be saved during an analysis. This surface is then used as the master surface of a tied slide surface in a second analysis, where the discretization may be arbitrarily modified. This feature is especially useful for studying the detailed response of a small member in a large structure. For the first analysis, the member of interest need only be discretized sufficiently that the displacements and velocities on its boundaries are reasonable approximations to the actual solution. After the first analysis is completed, the member is finely discretized in another model, and the interface save segments are defined to correspond with the first analysis. Finally, the second analysis is performed to obtain highly detailed information in the local region of interest.

An analysis using interface save segments consists of two phases (DYNA3D runs). In the input file for the first analysis, specify the number of interface segments for linking (*NUMIFS*) and the output interval for the interface save segment file on Control Card 2 (as described in section 4.1 on page 62). Then define the interface save segments as described above. Next, execute the first phase analysis, and specify a name for the interface save segment file using the "**u**=*isf1*" parameter on the execution line (as described in section 3.2 on page 51). This will save the displacement and velocity at every interface save segment defined in the first model into the specified file. Now, construct the

finite element model for the second phase analysis, and in this input file the number of interface segments and the time interval for interface data output should be set to zero. The second phase model typically contains a more detailed model of the subregion of interest than was present in the first phase model. Define the slave surface of a type 2 (tied) sliding interface over the portion of the new model which corresponds to the interface save segments from the first phase model. It is *not* necessary that the node and element positions in this area be the same in the two models. Define the master surface as 0 in this type 2 slide surface definition. Finally, when starting the second phase analysis using this new model, specify the name of the interface save segment file (created by the first run) using the "**v**=*isf2*" parameter on the DYNA3D execution line. The displacements and velocities for the interface region will then be read from this file and applied as external boundary conditions onto the phase two model.

4.13 NODAL SINGLE POINT CONSTRAINTS

Define *NODSPC* cards to specify single point constraints on nodes.

Columns		Quantity	Format	
1-5	(1-8)	First node number, n_{first}	I5	(I8)
6-10	(9-13)	Local coordinate system number ($\leq NSPCOR$)	I5	(I5)
11-14	(14-17)	Blank		
15	(18)	Translation code in local x direction	I1	(I1)
16	(19)	Translation code in local y direction	I1	(I1)
17	(20)	Translation code in local z direction	I1	(I1)
18	(21)	Rotation code about local x axis	I1	(I1)
19	(22)	Rotation code about local y axis	I1	(I1)
20	(23)	Rotation code about local z axis	I1	(I1)
21-25	(24-31)	Last node number, n_{last} EQ.O: $n_{last} = n_{first}$ (no generation)	I5	(I8)
26-30	(32-39)	Increment for generation, k EQ.O: default set to 1	I5	(I8)

Single point constraints allow the definition of a completely arbitrary local coordinate system, and the specification of nodal boundary conditions (constraints) in this local system. One local system may be used for many nodes, or a different local system may be defined for each node. *A boundary code of 1 specifies a constrained degree-of-freedom, while a boundary condition code of 0 indicates an unconstrained degree-of-freedom.* This option was originally developed by Dr. C. S. Tsay.

A set of nodal single point constraints may be generated by specifying the first node number in the sequence, n_{first}, the last node number in the sequence, n_{last}, and the node number increment for generation, k. Nodal single point constraints will be generated for nodes between n_{first} and n_{last} using the set of boundary condition codes as specified for n_{first}.

Nodal single point constraints require the definition of a local coordinate system, as described on the following page.

Define $NSPCOR$ local coordinate systems for single point constraints.

Columns	Quantity	Format
1-5	Local coordinate system number ($\leq NSPCOR$)	I5
6-15	x-coordinate of point P	E10.0
16-25	y-coordinate of point P	E10.0
26-35	z-coordinate of point P	E10.0
36-45	x-coordinate of point Q	E10.0
46-55	y-coordinate of point Q	E10.0
56-65	z-coordinate of point Q	E10.0

The local coordinate system is constructed at the global origin by specifying two points, P and Q, as shown in Figure 30. First, the local x-axis is constructed by defining a vector $\boldsymbol{x}_L$ from the global origin through point P. Next, a temporary vector $\boldsymbol{t}$ is constructed from the global origin through point Q. The local z-axis is then found by computing a vector which is mutually perpendicular to $\boldsymbol{x}_L$ and $\boldsymbol{t}$,

$$\boldsymbol{z}_L = \boldsymbol{x}_L \times \boldsymbol{t}. \tag{329}$$

Finally, the local y-axis is found as the vector which is mutually perpendicular to $\boldsymbol{x}_L$ and $\boldsymbol{z}_L$,

$$\boldsymbol{y}_L = \boldsymbol{z}_L \times \boldsymbol{x}_L. \tag{330}$$

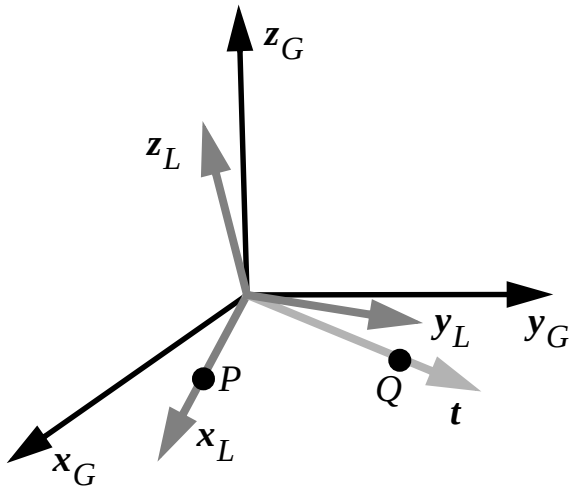

Figure 30
Local coordinate system for Single Point Constraints.

4.14 SLIDING BOUNDARY PLANES

Define the number of Sliding Boundary Plane Cards specified on Control Card 4 of section 4.1 on page 62.

Columns	Quantity	Format
1-10	x-coordinate of vector from global origin	E10.0
11-20	y-coordinate of vector from global origin	E10.0
21-30	z-coordinate of vector from global origin	E10.0
31-40	Constraint option, $IOPT$ EQ.0.0: node is constrained to move on normal plane EQ.1.0: node is constrained to translate in vector direction	E10.0

Sliding Boundary Planes allow any node to be constrained to move on an arbitrarily oriented plane or line. Each Sliding Boundary Plane card defines a vector originating at the global origin and terminating at the coordinates defined above. This vector can be of arbitrary length; DYNA3D internally converts it to a unit vector for computation.

If $IOPT = 0$, then the vector is interpreted as defining a plane which has the given vector as its normal, and nodes are constrained to move only on this plane. Nodes may not separate from this plane, but may move freely in any direction in the plane. An arbitrary oblique boundary condition may be defined using this option. One common application is the definition of a “pie-slice” three-dimensional model of an axisymmetric problem, where all nodes on the side faces of the model must be constrained from translating in the circumferential direction. The Sliding Boundary Plane vector is defined as the normal to the side face, and all nodes on that face are given appropriate boundary condition codes to reference the Sliding Boundary Plane.

If $IOPT = 1$, then the vector is interpreted as defining a line, and nodes are allowed to translate only along that line. Since nodes can move in either direction along this line, the orientation of the given vector along the desired line is not significant. This type of constraint can also be equivalently defined using Nodal Single Point Constraints, as described in section 4.13 on page 319.

To constrain a node to move on a Sliding Boundary Plane, set its displacement boundary condition code (described on the Node Card, section 4.7 on page 306) to $7 + n$, where n is the number of the Sliding Boundary Plane to be used. Any number of Sliding Boundary Planes may be defined.

4.15 SYMMETRY PLANES WITH FAILURE

Define the number of cards specified on Control Card 4 of section 4.1 on page 62.

Card 1

Columns	Quantity	Format
1-5	Number of segments in Symmetry Plane with Failure, *NSGNDS*	I5
6-15	x-coordinate of tail point P	E10.0
16-25	y-coordinate of tail point P	E10.0
26-35	z-coordinate of tail point P	E10.0
36-45	x-coordinate of head point Q	E10.0
46-55	y-coordinate of head point Q	E10.0
56-65	z-coordinate of head point Q	E10.0
66-75	Tensile failure stress, σ_f (positive in tension)	E10.0

As shown in Figure 31, the outward normal vector $\boldsymbol{n}$ is defined from point P and passes through point Q. This vector should originate on the symmetry plane and point toward the body.

Cards 2, 3, . . . , NSGNDS+1

Columns		Quantity	Format	
1-5	(1-8)	Segment number	I5	(I8)
6-10	(9-16)	Node n_1	I5	(I8)
11-15	(17-24)	Node n_2	I5	(I8)
16-20	(25-32)	Node n_3	I5	(I8)
21-25	(33-40)	Node n_4	I5	(I8)
26-35	(41-50)	Failure stress, σ_f, if different from default value	E10.0	(E10.0)

Symmetry Planes with Failure are specified by listing quadrilateral or triangular segments which initially lie on the symmetry plane. Segments are defined by their corner nodes, and normally each segment represents one element face. Triangular segments may be defined by repeating the last node ($n_4 = n_3$). The symmetry plane is defined by its normal vector, which is assumed to be drawn from point P to point Q, as shown in Figure 31.

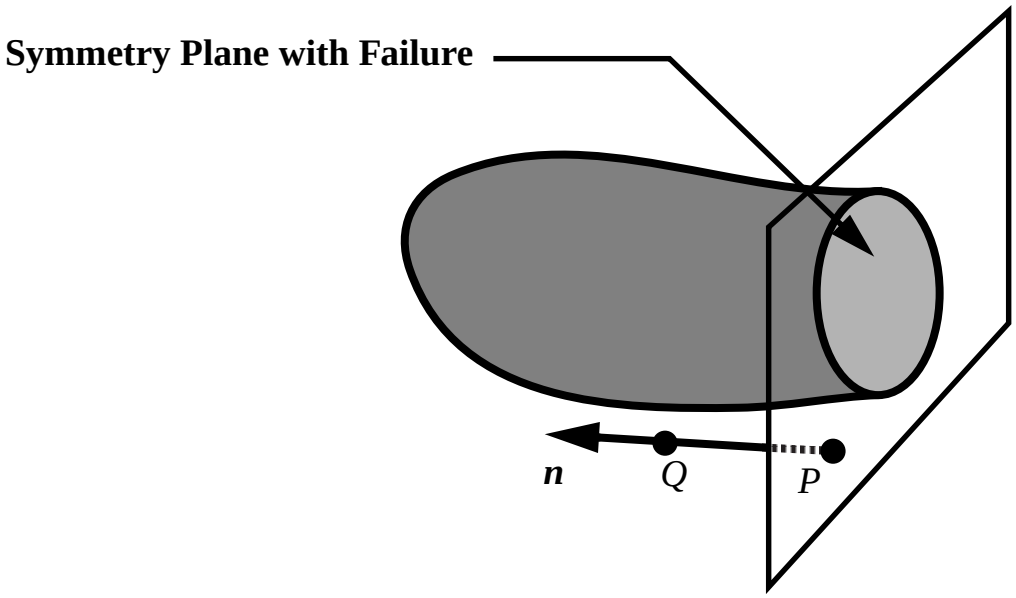

Figure 31
Symmetry Planes with failure.

As long as the normal stress (in the direction of $\boldsymbol{n}$) remains less than the failure stress σ_f, the Symmetry Plane with Failure acts just like a Sliding Boundary Plane. Nodes initially on the symmetry plane may move freely in any direction in the plane, but may not move normal to the plane. When the normal stress exceeds σ_f, the nodes are released and may move freely throughout the remainder of the calculation.

Symmetry Planes with Failure are frequently used to model oblique penetration. One half-space of the target material is modeled, and the vertical symmetry plane is defined as a Symmetry Plane with Failure. The projectile may be given an initial velocity into the target material at any angle, and nodes on the Symmetry Plane with Failure will separate when the tensile criterion is exceeded, thus simulating a penetration process. In this application, the segments on the symmetry plane must also be defined as one side of a sliding interface, with the other side defined as the external part of the penetrating object. This approach has proven effective in modeling 3-D penetration problems.

4.16 NODE TIME HISTORY BLOCKS

Skip this section if the number of node time history blocks is zero on Control Card 3 of section 4.1 on page 62. Otherwise, define up to 2000 history blocks that may contain a total of 2000 nodes. Use only the number of cards required to define all blocks.

Columns		Quantity	Format	
1-5	(1-8)	First node of first time history block	I5	(I8)
6-10	(9-16)	Last node of first time history block	I5	(I8)
11-15	(17-24)	First node of second time history block	I5	(I8)
16-20	(25-32)	Last node of second time history block	I5	(I8)
.	.	.	.	
.	.	.	.	
.	.	.	.	
.	.	.	.	

Node time history blocks are used to define sets of nodes for inclusion in the time history plot database. Typically, the time interval between writes to this time history plot database is much smaller than the time interval between writes to the state plot database, which contains information for the complete analysis model at each plot time point (state). Thus, for the nodes included in the time history plot database, much higher frequency resolution is possible in post-processing time history plots than is available in time history plots made from the state plot database. The plot databases are described in more detail in section 3.5 on page 58.

The time history plot database may be post-processed using TAURUS or other codes to generate time-history plots of nodal quantities such as displacement, velocity, or acceleration.

4.17 ELEMENT TIME HISTORY BLOCKS

(Solid Elements)

Skip this section if the number of solid element time history block is zero on Control Card 3 of section 4.1 on page 62. Otherwise, define up to 2000 time history blocks that may contain a total of 2000 solid elements. Use as many cards as required to define the specified number of blocks. All cards are given in the format shown below.

Columns		Quantity	Format	
1-5	(1-8)	First element of first time history block	I5	(I8)
6-10	(9-16)	Last element of first time history block	I5	(I8)
11-15	(17-24)	First element of second time history block	I5	(I8)
16-20	(25-32)	Last element of second time history block	I5	(I8)
.	.	.		
.	.	.		
.	.	.		

(Beam Elements)

Skip these cards if the number of beam element time history blocks is zero on Control Card 3 of section 4.1 on page 62. Up to 2000 time history blocks may be defined containing a total of 2000 beam and truss elements. The input format is as shown above.

(Shell Elements)

Skip these cards if the number of shell element time history blocks is zero on Control Card 3 of section 4.1 on page 62. Up to 2000 time history blocks may be defined containing a total of 2000 4-node shell elements. The input format is as shown above.

(Thick Shell Elements)

Skip these cards if the number of solid shell element time history blocks is zero on Control Card 3 of section 4.1 on page 62. Up to 2000 time history blocks may be defined containing a total of 2000 8-node thick shell elements. The input format is as shown above.

Element time history blocks are used to define sets of elements for inclusion in the time history plot database. The time history plot database is typically written at a much smaller time increment than the state database, and therefore contains more high frequency response information.

The time history plot database may be post-processed using TAURUS or other codes to generate time-history plots of element quantities such as stress or strain.

4.18 GRAVITY STRESS INITIALIZATION

Skip this section if the number of points in the density versus depth curve is zero on Control Card 4 of section 4.1 on page 62. Otherwise, supply $NUMDP + 1$ cards.

Card 1

Columns	Quantity	Format
1-10	Gravitational acceleration, g	E10.0
15	Direction of gravitational loading EQ.1: global x-direction EQ.2: global y-direction EQ.3: global z-direction	I1
16-20	Material number of materials to be initialized (maximum of 12) EQ.0: all EQ.n: define list of n materials below ($n \leq 12$)	I5
21-25	Material number of first material to be initialized	I5
26-30	Material number of second material to be initialized	I5
.	.	..
.	.	..
.	.	..
.	.	..

Define $NUMDP$ cards giving the mass density as a function of depth.

Cards 2, 3, . . . , NUMDP+1

Columns	Quantity	Format
1-10	Mass density, ρ	E10.0
11-20	Depth, d	E10.0

Density vs. depth curves are often used to initialize hydrostatic stresses arising in a material due to gravity acting on an overburden material. The hydrostatic pressure acting on a material point at a depth d_0 is given by

$$p = -\int_{d_0}^{d_{top}} \rho(z) g \, dz \,, \tag{331}$$

where p is pressure, d_{top} is depth at the top of the material to be initialized (usually $d_{top} = 0$), $\rho(z)$ is the mass density at depth z, and g is the acceleration of gravity. This integral is evaluated numerically for each material to be initialized.

Depth may be measured along any of the global coordinate axes, and the sign convention of the global coordinate system should be respected. The sign convention of gravity also follows that of the global coordinate system. For example, if the positive z axis points “up,” then gravitational acceleration should be input as a negative number.

4.19 BRODE FUNCTIONS

Skip this section if columns 21-25 are blank on Control Card 4 in section 4.1 on page 62. Otherwise, enter two cards for the pertinent Brode function data.

Card 1

Columns	Quantity	Format
1-10	Yield (Kt)	E10.0
11-20	Height of burst	E10.0
21-30	Model x coordinate of Brode origin, x_{BO}	E10.0
31-40	Model y coordinate of Brode origin, y_{BO}	E10.0
41-50	Model z coordinate of Brode origin, z_{BO}	E10.0
51-60	Model time at Brode time origin, t_{BO}	E10.0
61-65	*Load curve number giving time of arrival versus range relative to Brode origin	E10.0
66-70	Load curve giving yield scaling versus scaled time (time relative to Brode origin divided by [yield$^{(1/3)}$])	E10.0

Card 2

Columns	Quantity	Format
1-10	Conversion factor - kft to DYNA length units	E10.0
11-20	Conversion factor - milliseconds to DYNA time units	E10.0
21-30	Conversion factor - psi to DYNA pressure units	E10.0

*Both load curves must be specified for the variable yield option. If this option is used, the shock time of arrival is found from the time of arrival curve. The yield used in the Brode formulas is computed by taking the value from the yield scaling curve at the current time/[yield$^{(1/3)}$] and multiplying that value by yield.

The development and limitations of the equations underlying this option are given in (Speicher and Brode, 1987).

4.20 CROSS SECTION DEFINITIONS FOR FORCE OUTPUT

Define only if *NUMCSD* is nonzero on Control Card 4 in section 4.1 on page 62. For each cross section where force output is desired, define the following card sets.

Define *NUMCSD* Cross Section Definition Control Cards:

Cards 1,2, ..., NUMCSD

Columns	Quantity	Format
1-5	Number of nodes in this cross section definition	I5
6-10	Number of beam elements in this cross section definition	I5
11-15	Number of shell elements in this cross section definition	I5

Define *NUMCSD* Cross Section Definition data card sets (nodes, beam elements, and shell elements) as described below:

NODES

Repeat the following card until all nodes have been defined for this Cross Section Definition.

Cards NUMCSD+1, . . .

Columns	Quantity	Format
1-10	First cross section node	I10
11-20	Second cross section node	I10
.	.	.
.	.	.
.	.	.
71-80	Eighth cross section node	I10

BEAM ELEMENTS

Repeat the following card until all beam elements have been defined for this Cross Section Definition.

Columns	Quantity	Format
1-10	First beam element	I10
11-20	Second beam element	I10
.	.	.
.	.	.
.	.	.
71-80	Eighth beam element	I10

SHELL ELEMENTS

Repeat the following card until all shell elements have been defined for this Cross Section Definition.

Columns	Quantity	Format
1-10	First shell element	I10
11-20	Second shell element	I10
.	.	.
.	.	.
.	.	.
71-80	Eighth shell element	I10

Repeat the last 3 card groups for each Cross Section Definition until all *NUMCSD* cross sections have been defined.

DYNA3D allows a cross section to be defined through a structural model, and at selected intervals will output the total resultant force on this cross section. This feature is often used to quickly evaluate a global response quantity, such as the total force transmitted from one part of a model to another. The current implementation only computes forces arising from structural elements (truss, beam, and shell elements), but is fully supported for all element formulation options.

The first step in defining a cross section for force output is to select a group of nodes in the model to define the cross section cutting plane. These nodes need not all lie in the same plane, but should not overlap along the load path, or misleading results may be obtained. Typically, a group of nodes is chosen which defines a cut or slice through the analysis model. Once the group of nodes is selected, the next step is to define all elements which connect to this plane of nodes *on one side only*. Elements may be defined on either side of the cross section, but not both sides. The global components of the total resultant force on the cross sectional plane will be written to the “hsp” printout file at the time interval specified on Control Card 4 in section 4.1 on page 62.

4.21 LOAD CURVES

Define the number of load curves specified on Control Card 5 in section 4.1 on page 62. Repeat the following card set for each load curve.

Card 1

Columns	Quantity	Format
1-5	Load curve number	I5
6-10	Number of points in this load curve, *NPTS*	I5
11-15	Load curve option, *LCOPT* EQ.0: load curve used in transient dynamic analysis only EQ.1: load curve used in dynamic relaxation solution but not in transient dynamic analysis EQ.2: load curve used in both dynamic relaxation solution and transient analysis. Separate portions of the curve may be optionally specified for the dynamic relaxation solution and transient dynamic analysi	I5
16-20	Load curve input format: either blank or E20.0. If left blank, E10.0 format is used to read the following load curve values.	A5

Cards 2, . . . ,NPTS+1

Columns	Quantity	Format
1-10	Time, t, or independent variable, x	E10.0
11-20	Load value, $f(t)$, or function value, $f(x)$	E10.0

Various options in DYNA3D use load curves to define arbitrary functional relationships. Many loads and boundary conditions are functions of time, and for these options, the specified load curve should relate load (or boundary condition) value $f(t)$ to time t. Some material models require the specification of load curves defining the variation of material parameters $f(x)$ with temperature x. Other models require the specification of load curves defining effective stress $f(x)$ as a function of effective plastic strain or other material variable, x.

Load curve option 2 permits either: 1) a single load curve to be specified and used for both the dynamic relaxation solution and transient analysis, or 2) two distant load curve regimes, combined and referenced by a single load curve number, to be specified. In the later case, the first regime is used only during the dynamic relaxation solution while the second regime is used only during the transient analysis. This option is extremely useful when initializing loads that can be only specified with one load curve number.

Based upon the t and $f(t)$ or x and $f(x)$ pairs entered, DYNA3D automatically determines if one or two load curve regimes are being defined for load curve option 2. The single load curve is defined by entering all the t and $f(t)$ or x and $f(x)$ pairs in ascending t or x order. The dual load curve is defined by entering all the t and $f(t)$ or x and $f(x)$ pairs for the dynamic relaxation regime first followed by all the t and $f(t)$ or x and $f(x)$ pairs for the transient analysis regime. All t or x values must be listed in ascending order, and the last t or x value in the dynamic relaxation curve must be larger than the first t or x value in the transient analysis curve. The number of points in the load curve is the total number of points used in both regimes.

It is recommended to select the E20.0 format on Card 1 for load curve values input when higher accuracy is desired. When E20.0 format is chosen, both entries on a card must be input with E20.0 format.

There is no limit on the number of load curves, or on the number of points in a load curve definition.

DYNAMIC RELAXATION STATIC ANALYSIS

DYNA3D contains a limited capability for performing quasistatic analysis using a dynamic relaxation algorithm. This feature is primarily intended to be used to generate a static stress solution as an initial condition for a transient dynamic analysis, but it has been applied with some success to the solution of more general static problems.

During then DR static solution process, ‘‘time’’ is really just a parameter to describe the solution process, and does not correspond to physical time.The current implementation uses a DR time step equal to the standard dynamic time step. Thus, if it is desired to slowly apply the static loads to minimize overshoot in the solution, then a short trial dynamic run can be made to determine the

time step size. The static loads to be applied during the DR solution can then be applied over some number of time steps (typically 5000-10,000 but problem dependent), and this determines the time points to be used on the load curve controlling the static loads.

The current implementation of DR in DYNA3D is susceptible to dynamic overshoot if static loads are applied too quickly. If only history-independent material models (such as elasticity) are used, then the resulting solution will still be correct and this overshoot behavior is of little consequence. If history-dependent material models (such as plasticity) are used, however, this dynamic overshoot can cause yielding which is erroneous, and therefore an incorrect static solution is obtained. Thus, the DR static solution capability can be used with confidence for elastic initialization, but must be carefully used with slowly applied loads to prevent overshoot and inaccuracy in history-dependent static problems.

An “elastic only” option is included in DYNA3D for DR. The flag, $MATDRE$, set on Control Card 4 is discussed in section 4.1 on page 62. This feature increases the yield parameters of many material models during DR to avoid overshoot in history-dependent materials. The material parameters are then reset at the start of the transient analysis.

A DR static solution is activated by specifying the “load curve option” $LCOPT = 1$ for a load curve to control the application of the static loads, as discussed in section 4.21 on page 334. The dynamic relaxation factor, the DR time step, and the DR convergence tolerance can be modified from default values on Control Card 8 as described in section 4.1 on page 62.

DR analyses terminate when the DR convergence tolerance is satisfied or after the user enters a **sw5.** control switch (see section 3.3 on page 54). Upon termination, DYNA3D writes a stress initialization file for subsequent use and begins the transient analysis.

4.22 NODAL FORCES AND FOLLOWER FORCES

Define the number of concentrated nodal loads specified on Control Card 5 in section 4.1 on page 62.

Columns		Quantity	Format	
1-5	(1-8)	Node number, m_1, on which this load acts	I5	(I8)
6-10	(9-13)	Direction in which this load acts, *IDIR* EQ.1: x-direction EQ.2: y-direction EQ.3: z-direction EQ.4: follower force EQ.5: moment about the global x-axis EQ.6: moment about the global y-axis EQ.7: moment about the global z-axis	I5	(I5)
11-15	(14-18)	Load curve number giving time variation	I5	(I5)
16-25	(19-28)	Scale factor (default =1.0)	E10.0	(E10.0)
26-30	(29-36)	Node m_1 (define only for follower force, $IDIR = 4$)	I5	(I8)
31-35	(37-44)	Node m_2 (define only for follower force, $IDIR = 4$)	I5	(I8)
36-40	(45-52)	Node m_3 (define only for follower force, $IDIR = 4$)	I5	(I8)

Nodal loads and follower forces may be imposed as a prescribed function of time. The time variation is taken from a load curve, and may be arbitrarily scaled in the nodal load or follower force definition.

A follower force $\boldsymbol{F}$ acts normal to the plane defined by nodes m_1, m_2, and m_3 as shown in Figure 32. The positive direction is determined by a counterclockwise orientation (“right-hand-rule”) of the nodes. The follower force *remains normal* to the plane throughout the deformation.

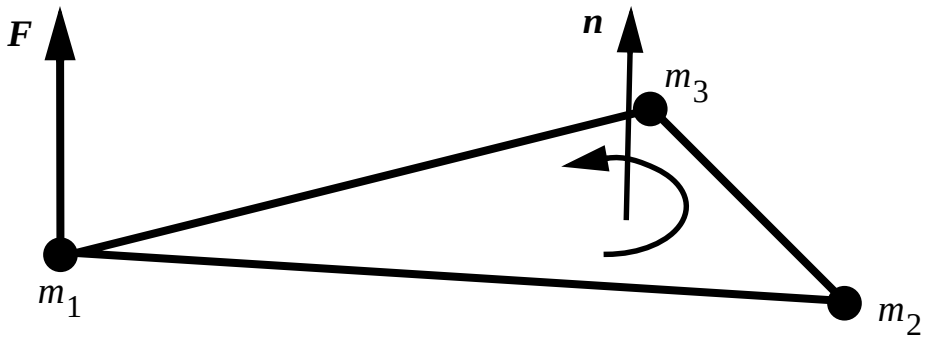

Figure 32
Follower force acts normal to a plane defined by m_1, m_2, m_3. The load is applied to node m_1, and is positive in the direction given by the normal vector to the plane, $\boldsymbol{n}$.

4.23 PRESSURE LOADS

Define the number of element face pressure cards specified on Control Card 5 in section 4.1 on page 62.

Columns		Quantity	Format	
1-5	(-)	Pressure card number	I5	(omit)
6-10	(1-5)	Load curve number, N_L, giving time variation EQ.-1: Brode function is used to determine pressure EQ.-2: HE function is used to determine pressure EQ.-3: Pressure is calculated by PENCRV3D module.	I5	(I5)
11-15	(6-13)	Node n_1 (see Figure 33)	I5	(I8)
16-20	(14-21)	Node n_2	I5	(I8)
21-25	(22-29)	Node n_3	I5	(I8)
26-30	(30-37)	Node n_4	I5	(I8)
31-40	(38-47)	Load curve multiplier at node n_1 EQ. 0.0: default set to 1.0	E10.0	(E10.0)
41-50	(48-57)	Load curve multiplier at node n_2 EQ. 0.0: default set to 1.0	E10.0	(E10.0)
51-60	(58-67)	Load curve multiplier at node n_3 EQ. 0.0: default set to 1.0	E10.0	(E10.0)
61-70	(68-77)	Load curve multiplier at node n_4 EQ. 0.0: default set to 1.0	E10.0	(E10.0)
71-80	(-)	Time pressure begins acting on surface, t_0 GT. 0.0: Load curve is offset by t_0 LT. 0.0: Pressure begin acting on surface at $-t_0$. Load cure is not offset.	E10.0	(omit)

Element face pressures always act normal to the element face in the current configuration, and positive pressure acts toward the element face, as shown in Figure 33. Pressure loads may be applied to solid elements, shell elements, or thick shell elements. The load curve multipliers may be used to increase or decrease the pressure given in the load curve definition. Triangular element faces may be defined by repeating the last node, ($n_4 = n_3$).

If the load curve number, N_L, is set to -1, then the pressure time history to be applied is computed from the Brode function data given in section 4.19 on page 330. The time-of-arrival of the pressure is then computed based on the distance from the Brode origin to the centroid of the element face receiving the pressure loading. In penetration analysis, setting N_L to -3 invokes the PENCRV3D pressure load modules for calculating the target resistance. The description of PENCRV3D is given in section 2.28 on page 48.

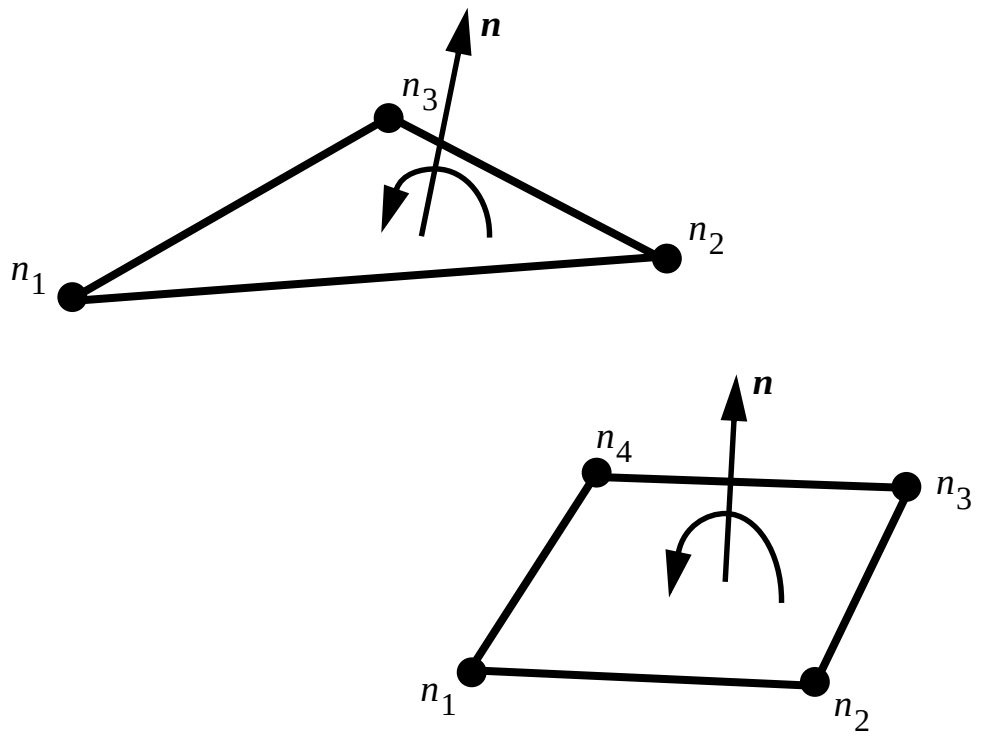

Figure 33
Node numbering for element face pressure loads for quadrilateral and triangular faces. Pressure always acts in the opposite direction to the segment normal vector $\boldsymbol{n}$.

The time that pressure starts acting on a surface can be altered by specifying non-zero values for t_0. Positive t_0 values offset, in time, the profile described by the specified load curve. Negative t_0 values artificially zero the load curve value until the analysis time exceeds the absolute value of t_0.

4.24 PRESCRIBED VELOCITIES AND ACCELERATIONS

Define the number of cards specified on Control Card 5 in section 4.1 on page 62.

Columns		Quantity	Format	
1-5	(1-8)	Node number or rigid body material number GT.0: node number LT.0: absolute value is material number of the rigid body	I5	(I8)
6-10	(9-13)	Load curve number giving time variation	I5	(I5)
11-15	(14-18)	Applicable degrees-of-freedom, *IDOF* EQ.1: x-translational degree-of-freedom EQ.2: y-translational degree-of-freedom EQ.3: z-translational degree-of-freedom EQ.4: translational velocity in direction of vector $\boldsymbol{v}$ defined below (see note) EQ.5: x-rotational degree-of-freedom EQ.6: y-rotational degree-of-freedom EQ.7: z-rotational degree-of-freedom EQ.8: rotational velocity about vector $\boldsymbol{v}$ defined below (see note) EQ.9: tangential component for rotation about an axis parallel to the global x axis and passes through point v EQ.10: tangential component for rotation about an axis parallel to the global y axis and passes through point v EQ.11: tangential component for rotation about an axis parallel to the global z axis and passes through point v	I5	(I5)
16-25	(19-28)	Scale factor	E10.0	(E10.0)
26-35	(29-38)	x-coordinate of the point, or the head of vector, $\boldsymbol{v}$	E10.0	(E10.0)
36-45	(39-48)	y-coordinate of the point, or the head of vector, $\boldsymbol{v}$	E10.0	(E10.0)
46-55	(49-58)	z-coordinate of the point, or the head of vector, $\boldsymbol{v}$	E10.0	(E10.0)
56-60	(59-63)	velocity/acceleration flag, *IACCEL* EQ.0: velocity (rigid bodies and nodes) EQ.1: acceleration (nodes only)	I5	(I5)

Nodal velocities or accelerations may be imposed as a prescribed function of time. The time variation is taken from a load curve, and may be arbitrarily scaled in the prescribed velocity/acceleration definition. This is convenient when many nodes have the same velocity or acceleration time history but different amplitudes, since only one load curve needs to be defined in that case. Nodal

velocities or accelerations may be specified with respect to the global axes or with respect to the user defined vector $\boldsymbol{v}$. The vector $\boldsymbol{v}$ originates at the origin and points toward the point specified in the input. Further, velocities and accelerations may be specified as either translational or rotational. Note that solid elements do not have rotational degrees-of-freedom, and therefore rotational velocities ($IDIR = 5 - 8$) should not be prescribed for nodes connected only to solid elements.

Caution should be used when using $IDIR = 4$ or $IDIR = 8$. These options specify the magnitude and sign of the nodal velocity or nodal acceleration **component** in the ν direction. This feature permits boundary conditions to be prescribed in the global direction ν without excessively constraining the kinematics in the other directions. These options **do not** impose an absolute nodal velocity or nodal acceleration of specified magnitude (scale factor times load curve value) in the ν direction. To achieve this, each nodal velocity or nodal acceleration DOF should be uniquely defined.

Option $IDIR = 9, 10, 11$ influence only the tangential component of the velocity. They have no effect on the other components.

It is not required that velocities be initially zero. However, if zero velocity initial conditions are specified in section 4.27 on page 350 and prescribed velocity load curves are not 0 at $t = 0$, then a discontinuity in initial conditions is created, and this may excite very high frequency response in the model.

Nodal velocities/accelerations may be prescribed *only* for nodes of deformable bodies. Prescribed translational and rotational velocities may be specified for an entire rigid body by giving the negative of its material number in the node number field of the input. The acceleration flag $IACCEL$ pertains to nodes of deformable bodies only; acceleration may not be directly prescribed for a rigid body.

Angular velocity may be specified for an entire rigid body by choosing $IDOF = 8$. Velocity is then specified in the units of radians per unit time. The rigid body is assumed to rotate about a vector $\boldsymbol{v}$ passing through its center of mass if constraints permit, otherwise it will rotate as permitted by the constraints to achieve the prescribed angular velocity at its center of mass. Rotation of a rigid body about an axis other than its natural center of mass may be achieved by prescribing Rigid Body Inertial Properties (section 4.41 on page 405) to relocate the center of mass to the desired axis of rotation.

For nodes of a deformable material, choosing $IDOF \geq 9$ interprets the prescribed quantity (velocity or acceleration) as a tangential nodal component for rotation about an axis that passes through the point v and parallels the global axis. This option is useful for prescribing a spin velocity about an axis, such as for the outer nodes of a cylinder spinning about the global z-axis ($v = 0, 0, 0$). Using this approach, only the magnitude of the tangential velocity of the node needs to be prescribed along with the center of rotation, and DYNA3D internally accounts for the change in velocity components due to the rotation. Since $IDOF \geq 9$ generates nodal velocity boundary conditions, it is applicable *only* to non-rigid materials.

4.25 RIGID WALLS

Define the number of rigid walls specified on Control Card 5 in section 4.1 on page 62. Repeat the following set of cards for each
definition.

Card 1

Columns		Quantity	Format	
1-5	(1-8)	Number of slave nodes Leave this entry blank for automatic sorting of slave nodes.	I5	(I8)
6-15	(9-18)	x-coordinate of point P (must be on rigid wall)	E10.0	(E10.0)
16-25	(19-28)	y-coordinate of point P	E10.0	(E10.0)
26-35	(29-38)	z-coordinate of point P	E10.0	(E10.0)
36-45	(39-48)	x-coordinate of point Q (must be in space)	E10.0	(E10.0)
46-55	(49-58)	y-coordinate of point Q	E10.0	(E10.0)
56-65	(59-68)	z-coordinate of point Q	E10.0	(E10.0)
66-70	(69-73)	Moving rigid wall option, *IMSWF* EQ.0: rigid wall is fixed in space EQ.1: rigid wall has mass m_{wall} and initial velocity v_0	I5	(I5)
71-75	(74-78)	Stick condition option, *ISTICK* EQ.0: frictionless sliding after contact EQ.1: no sliding after contact EQ.-1: finite friction; input the coefficient of friction in the following card.	I5	(I5)
76-80	(79-80)	Finite size rigid wall option, *LIMIT* EQ.0 rigid wall extends to infinity EQ.1: size and orientation is defined	I5	(I2)

The geometry of rigid wall definitions is shown in Figure 34. Point P is at the origin of the rigid wall local coordinate system, and therefore must lie on the rigid wall surface. Point Q is a point in space, and the rigid wall normal vector $\boldsymbol{n}$ is defined as a vector from P to Q. This normal vector must point towards the impacting body. If $LIMIT = 1$, the dimensions of the rigid wall plane l_x and l_y (as specified on the next card) are measured from the origin at point P.

Users can ask DYNA3D to sort out the rigid wall slave nodes automatically by not defining the number of the slave nodes in Card 1. DYNA3D would then include all nodes between the rigid wall and the imaginary plane that is parallel to the rigid wall and passes through point Q as the slave nodes.

After impact, three friction options are available for rigid walls. If $ISTICK = 0$, then the wall is frictionless, and no resistance is provided to transverse motion in the plane of the wall. If $ISTICK = 1$, then sufficient friction is provided to prevent any transverse motion of the contacting body in the plane of the wall. If $ISTICK = -1$, a coefficient of friction is read from the nex card and finite frictional forces proportional to the coefficient are applied to resist the transerse motion.

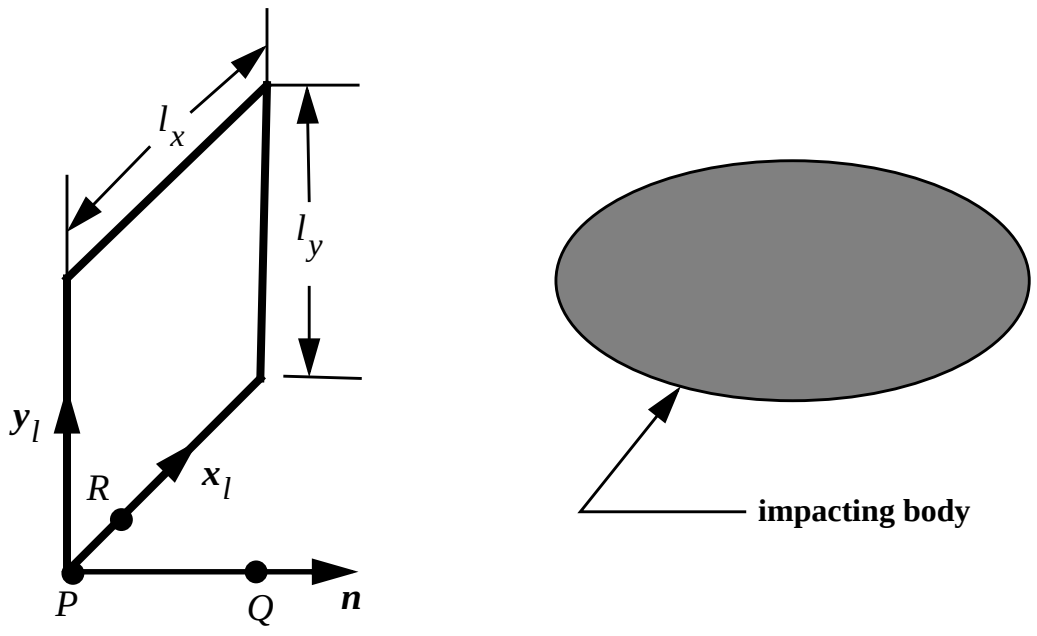

Figure 34
Rigid wall definition.

Card 1A

Define this card only if $STICK = -1$.

Columns	Quantity	Format
1-10	Coefficient of Friction	E10.0

Card 1 + LIMIT

Define this card only if $LIMIT = 1$.

Columns	Quantity	Format
1-10	x-coordinate of point R	E10.0
11-20	y-coordinate of point R	E10.0
21-30	z-coordinate of point R	E10.0
31-40	Length of $\boldsymbol{x}_l$ edge, l_x (see Figure 34) EQ.0.0: extends from negative to positive infinity	E10.0
41-50	Length of $\boldsymbol{y}_l$ edge, l_y EQ.0.0: extends from negative to positive infinity	E10.0

Note that l_x and l_y cannot both be zero if the finite rigid wall option is active ($LIMIT = 1$).

Card 1+LIMIT+IMSWF

Define this card only if $IMSWF = 1$.

Columns	Quantity	Format
1-10	Total mass of rigid wall, m_{wall}	E10.0
11-20	Initial velocity of rigid wall, v_0, in direction of normal vector, $\boldsymbol{n}$	E10.0

Card 2+LIMIT+IMSWF, . . .

Define these cards for all rigid walls only if a non-zero number of slave nodes is specified in Card 1. (Use parenthetical values for large format input.)

Columns		Quantity	Format	
1-10	(1-8)	Slave number	I5	(I8)
6-10	(9-16)	Node number	I5	(I8)

Omitted slave nodes are automatically generated using node numbers found from the formula

$$n_{i+1} = n_i + k \tag{332}$$

where the node number increment k is given by

$$\frac{n_i - n_j}{s_i - s_j}. \tag{333}$$

A rigid wall is a flat surface defined by a normal vector, $\boldsymbol{n}$. It may be of infinite extent in each direction ($LIMIT = 0$), or may be finite in either or both in-plane directions ($LIMIT = 1$). The rigid wall may be fixed in space ($IMSWF = 0$), or may have a defined mass and initial velocity in the direction of the normal vector $\boldsymbol{n}$ ($IMSWF = 1$). The surface of the wall may be frictionless ($ISTICK = 0$) or frictional ($ISTICK = 1$). The impacting body is defined by listing nodes which are not permitted to penetrate the rigid wall. Nodes which are *not* listed may penetrate the wall without resistance. Defining a rigid wall of finite extent allows the possibility that the impacting body may pass outside the area of the rigid wall, and in that case no impact will occur.

Rigid walls are an inexpensive method for modeling unilateral contact (i.e., contact between a deforming body and a rigid body) when the target surface is planar. Moving rigid walls can be useful in modeling pendulum impact tests.

The normal force componet of each Rrgid wall is contained in the time history files and may be optionally printed out to the `FORCES` file via the rigid_wall switch (see KEYWORD-BASED CONTROL FEATURES on page 73).

4.26 NODAL CONSTRAINTS

Define the number of nodal constraint sets specified on Control Card 5 in section 4.1 on page 62.

Card 1

Columns		Quantity	Format	
1-5	(1-8)	Number of nodes that share degrees-of-freedom, N_c	I5	(I8)
6-10	(9-13)	Degrees-of-freedom in common, *IDOF* EQ.0: special "spotwelded nodes" option EQ.1: x-translational degree-of-freedom EQ.2: y-translational degree-of-freedom EQ.3: z-translational degree-of-freedom EQ.4: x and y-translational degrees-of-freedom EQ.5: y and z-translational degrees-of-freedom EQ.6: z and x-translational degrees-of-freedom EQ.7: x, y, and z-translational degrees-of-freedom EQ.8: special ''rigid node set'' option	I5	(I5)
11-20	(14-23)	*SWMAX*, extension limit for *IDOF*=0. Must be 0.0 or a positive number.	E10.0	(E10.0)
21-30	(24-33)	*SWMIN*, compression limit for *IDOF*=0 Must be 0.0 or a negative number.	E10.0	(E10.0)

Card 2

Columns		Quantity	Format	
1-5	(1-8)	Node number of first node to be tied	I5	(I8)
6-10	(9-16)	Node number of second node to be tied	I5	(I8)
11-15	(17-24)	Node number of third node to be tied	I5	(I8)
.		.	.	
.		.	.	

Continue on additional cards in the same format until N_c nodes have been specified.

Nodal constraints allow sets of nodes to share a common degree-of-freedom. These degrees-of-freedom are in the global coordinate system if $IDOF \geq 1$. Any number of nodes may be included in a nodal constraint set.

The "spotwelded nodes option," ($IDOF = 0$), constraints two nodes to move only along the direction defined by these two nodes while rotating into arbitrary configurations during the deformation. The constraint only applies to the translation degrees-of-freedom (DOF). *Only two nodes may be specified if the spotwelded nodes option is used.* With this option, a vector is internally defined from node n_1 to node n_2. The distance between n_1 and n_2 could vary between $(1+SWMAX)l_0$ and $(1+SWMIN)l_0$ during the deformation, where l_0 is the original length between n_1 and n_2. When both *SWMAX* and *SWMIN* are zero, it is equivalent to using a rigid beam or truss element between nodes n_1 and n_2. However the present option is less expensive and simpler to define. The nodes cannot be coincidental. (Nodes which are found to be coincidental have their $IDOF$ internally switched to $IDOF = 7$.)

The ''rigid node set'' option ($IDOF = 8$) allows a set of nodes to translate and *rotate* through space as if the nodes formed a single rigid body. Unlike $IDOF = 0$ to 7, this option couples nodal rotational DOF. Although this response could equivalently be modeled using rigid beam or truss elements between the different nodes, this option is less expensive and simpler to use.

4.27 INITIAL CONDITIONS

Cards 1, . . .

Define these cards if the initial condition flag is nonzero on Control Card 5 in section 4.1 on page 62.

Columns		Quantity	Format	
1-5	(1-8)	Node number	I5	(I8)
6-15	(9-18)	Initial velocity in x-direction	E10.0	(E10.0)
16-25	(19-28)	Initial velocity in y-direction	E10.0	(E10.0)
26-35	(29-38)	Initial velocity in z-direction	E10.0	(E10.0)
36-40	(39-43)	Generation increment, k	I5	(I5)

Nodal velocity initial conditions are defined in this section. Initial velocities must be input for the first node, node 1, and the last node, $NUMNP$, if the initial condition flag on Control Card 5 is nonzero. Initial velocities for intermediate nodes may be input directly, or may be generated internally using a node number increment k. Linear interpolation between specified values is used to define initial velocities for omitted nodes.

Initial velocities for rotating bodies may be easily generated in DYNA3D using the Material Initialization for Rotational Motion option described in section 4.46 on page 413.

If prescribed nodal velocities (section 4.24 on page 341) are also present in the model, care should be taken to ensure that the given initial velocity agrees with the prescribed nodal velocity at $t = 0$.

4.28 SLIDING INTERFACE DEFINITIONS

Define *NUMSI* sliding interfaces as specified on Control Card 5 in section 4.1 on page 62. Define all *NUMSI* slide surface control card sets first, then define slave and master segment/node cards as needed. Note that the type 11 (SAND) slide surface requires several control cards, and that additional control data can be entered with keywords.

Card Sets1, . . ., NUMSI

Columns		Quantity	Format	
1-5	(1-8)	Number of slave segments (types 1-4, 9-11, & optionally 12 &13) or slave nodes (types 5-8), *NSS*	I5	(I8)
6-10	(9-16)	Number of master segments (types 1-3, 5-11, & optionally 12 & 13), *NMS*	I5	(I8)
11-15	(17-21)	Slide surface type, *ITYPE*: 1-sliding only 2-tied 3-sliding with separation and friction 4-single surface contact 5-discrete nodes impacting surface 6-discrete nodes tied to surface 7-shell edge tied to shell surface 8-nodes spotwelded to surface 9-tied with failure 10-one way algorithm for sliding with separation and friction 11-SAND (adaptive) contact for material failure 12-automatic contact: all materials 13-automatic contact: domain and material limited 14-automatic contact with SAND: domain and material limited	I5	(I5)
16-25	(22-31)	Static coefficient of friction, μ_s	E10.0	(E10.0)
26-35	(32-41)	Dynamic coefficient of friction, μ_k	E10.0	(E10.0)
36-45	(42-51)	Exponential friction decay coefficient, β	E10.0	(E10.0)
46-50	(52-56)	If *ITYPE*<12, small penetration search flag, *IPEN* EQ.0:default EQ.1:penetration > element thickness ignored	I5	(I5)

Columns		Quantity	Format	
		If $ITYPE$>12, initial penetration option, $IPEN$ EQ.0:default is set to 1 GT.0:exclude all nodes that generate contact on initialization from the set of active slave nodes. LT.0: exclude no nodes during initialization.		
51-55	(57-61)	Output slave side data in printed interface force file EQ.0:don't print (default) EQ.1:print total slave force only EQ.2:print individual node and total forces (very verbose)	I5	(I5)
56-60	(62-66)	Output master side data in printed interface force file EQ.0:don't print (default) EQ.1:print total master force only EQ.2:print individual node and total forces (very verbose)	I5	(I5)
61-70	(67-73)	Scale factor on default slave penalty stiffness, S_s GT.0.0:Scale factor on default slave penalty stiffness EQ.0.0:Default set to 1.0	E10.0	(E7.0)
71-80	(74-80)	Scale factor on default master penalty stiffness, S_m GT.0.0:Scale factor on default master penalty stiffness EQ.0.0:Default set to 1.0	E10.0	(E7.0)

ADDITIONAL CONTROL CARDS FOR SAND (TYPE 11) CONTACT SURFACES

Define the following additional Slide Surface Control Cards for SAND (type 11) contact:

Columns		Quantity	Format	
1-5	(1-5)	No. of materials in slave SAND volume, NSVM	I5	(I5)
6-10	(6-10)	No. of materials in master SAND volume, NMRM	I5	(I5)

Next, define NSVM cards listing the material numbers which comprise the slave side SAND volume. Each card should have the following format:

Columns		Quantity	Format	
1-5	(1-5)	Material number to be included in the slave SAND volume	I5	(I5)

Now, define NMRM cards listing the material numbers which comprise the master side SAND volume. Each card should have the following format:

Columns		Quantity	Format	
1-5	(1-5)	Material number to be included in the master SAND volume	I5	(I5)

Note that the same material number should never appear in both a slave SAND volume definition and a master SAND volume definition. It is acceptable to have no SAND volumes on either the slave or master sides, but in this case the slide surface will not be adaptively redefined, and slide surface type 3 may yield a more efficient solution to the problem. Other than the definition of SAND volumes as described above, type 11 (SAND) contact is defined in exactly the same way as type 3 slide surface (sliding with separation and friction).

Optional Keyword Prescribed Slidesurface Control Features

An assortment of optional slidesurface features are available via keyword input. The keyword definitions must immediately follow the last line of the required control card(s) data and be terminated with the **endfree** keyword. The keyword and associated parameters are prescribed follow the same convention used to define the analysis control cards (see section 4.2 on page 73) and override any values defined in the main slidesurface control card. Note, not all keywords are valid for all slidesurface types.

General Control Options

	Friction factors:
static μ_s	Static coefficient of friction
dynamic μ_k	Dynamic coefficient of friction
decay β	Exponential friction decay coefficient
endfree	End keyword input
exp_n *n*	Default normal failure criterion exponent *n* (type 8). This value is used when type 8 slave surfaces are self-generated or when *n* is zero on the slave segment cards. (Default: *exp_n*=0.0)
exp_s *m*	Default shear failure criterion exponent *m* (type 8). This value is used when type 8 slave surfaces are self-generated or when *m* is zero on the slave segment cards. (Default: *exp_s*=0.0)
failure_n F_{fn} or σ_{nf}	Default value for F_{fn} (type 8) or σ_{nf} (type 9). This value is used when type 8 or 9 surfaces are self-generated or when F_{fn} or σ_{nf} is zero on the slave segment cards. (Default: *failure_n*=0.0)
failure_s F_{fs} or σ_{ns}	Default value for F_{fs} (type 8) or σ_{sf} (type 9). This value is used when type 8 or 9 surfaces are self-generated or when F_{fs} or σ_{sf} is zero on the slave segment cards. (Default: *failure_s*=0.0)
icurve *icurve*	Load curve number used to scale the penetration distance with time. (Types 3, 5, and 9-14 only) EQ.0.0: penetration amounts are not scaled (default) GT.0.0: load curve number whose temporal value is used to

scale the penetration distance. During initialization of slidesurface type 3, 5, 9, and 10, initial penetration is ignored.

ipen *ipen* Small penetration search flag, $IPEN$ ($ITYPE \le 11$)
- EQ.0.0: default
- EQ.1.0: penetration > element thickness ignored

Initial penetration option,$IPEN$ ($12 \le ITYPE \le 14$)
- EQ.0.0: default is set to 1
- GT.0.0: exclude all nodes that generate contact on initialization from the set of active slave nodes.
- LT.0.0: exclude no nodes during initialization.

itype *itype* Slide surface type

lagop *lagop* Lagrange constraint option
- EQ.0.0: penalty method (default)
- EQ.2.0: direct Lagrange constraint enforcement method (slide surface type 10 only)
- EQ.3.0: iterative Lagrange constraint enforcement method (slide surface types 3, 5, 10, 12, 13, and 14 only)

master_smooth Activate spherical representation of the master surface. The slave nodes locally see a spherical surface defined by the current position of the master nodes (obtained via a least squares fit).

mfactor S_m Master surface scale factor
- GT.0.0: scale factor on default master penalty stiffness
- EQ.0.0: default set to 1.0

no_relocate Do not relocate nodes during initialization to eliminate initial interpenetration. Automatically activated when $icurve \ne 0$. (Slide surface types 1, 3, 5, 8, 9, 10, and 11 only)

prints *prints* Output slave side data in interface force file
- EQ.0.0: don't print (default)
- EQ.1.0: print total slave force only
- EQ.2.0: print individual node and total forces (very verbose)

printm *printm* Output master side data in interface force file
- EQ.0.0: don't print (default)
- EQ.1.0: print total master force only
- EQ.2.0: print individual node and total forces (very verbose)

radius *radius*	Default slave node *radius* (type 5). This value is used when type 5 slave surfaces are self-generated or when *radius* is zero on the slave segment cards. (Default: *radius*=0.0)
sfactor S_s	Slave surface scale factor GT.0.0: scale factor on default slave penalty stiffness EQ.0.0: default set to 1.0
slave_smooth	Activate spherical representation of the slave surface. The master nodes locally see a spherical surface defined by the current position of the slave nodes (obtained via a least squares fit).
thickness	Account for shell element thickness (type 3, 5, 8, 9, and 10 only). Note, types 4, 11, 12, 13, and 14 automatically account for shell element thickness in their formulations.

Self-Generation Options

(Valid for Types 1, 2, 3, 5, 6, 7, 8, 9, and 10)

flip_master After the master segments are internally generated, reverse the orientation for segments generated from shell elements.

flip_slave After the slave segments are internally generated, reverse the orientation for segments generated from shell elements.

master_in *mat#1 mat#2 mat#3 ... mat#n*
Consider only elements with these *n* material numbers when constructing the master segments for this surface.

master_ex *mat#1 mat#2 mat#3 ... mat#n*
Consider all elements *except* those with these *n* material numbers when constructing the master segments for this surface.

slave_in *mat#1 mat#2 mat#3 ... mat#n*
Consider only elements with these *n* material numbers when constructing the slave segments or nodes for this surface.

slave_ex *mat#1 mat#2 mat#3 ... mat#n*
Consider all elements *except* those with these *n* material numbers when constructing the slave segments or nodes for this surface.

sym_plane $n_x\ n_y\ n_z\ x_{o-x}\ x_{o-y}\ x_{o-z}\ Tol$
Contact symmetry plane defined by equation (337) (on page 374)
$\boldsymbol{n}$ - vector normal to surface
$\boldsymbol{x}_o$ - point on plane
Tol - tolerance

Components of the domain limiting box:

xmin *xmin* Minimum *x*-direction value. (default=-1.0e+25)
xmax *xmax* Maximum *x*-direction value. (default=1.0e+25)
ymin *ymin* Minimum y-direction value. (default=-1.0e+25)
ymax *ymax* Maximum *y*-direction value. (default=1.0e+25)
zmin *zmin* Minimum *z*-direction value. (default=-1.0e+25)
zmax *zmax* Maximum *z*-direction value. (default=1.0e+25)

Automatic Contact Options
(Types 12, 13, and 14)
General Features

gap_mult g_{mult} Non-linear penalty method option (default 0.0)
EQ.0: linear penalty method used
GT.0.0: multiplier used to scale non-linear penalty stiffness

gap_offset g_{offset} Non-linear penalty method offset (default 0.10)

ibkuac *ibkuac* Number of cycles between bucket sorts (default - variable)

ibkuacmin *ibkuacmin*
Minimum # of cycles between bucket sorts (default 10)

ibkuacmax *ibkuacmax*
Maximum # of cycles between bucket sorts (default 100)

ilocac *ilocac* Number of cycles between characteristic dimension updates (default 10)

iactkup *iactkupx* # of cycles between thickness update of segments associated with hex elements (default 500). [Decrease this value if hex elements are crushed more than 50% in *iactkupx* cycles.]

ipen *ipen* Initial penetration option
EQ.0: default is set to 1
GT.0.0: exclude all nodes that generate contact less than -*pen_thres* on initialization from the set of active slave nodes.
LT.0.0: exclude no nodes during initialization.

pen_thres *pen_thres*
Penetration threshold for initialization (default 0.0).

thicsl *thicsl* Shell thickness scale factor
EQ.0.0: default is set to 1.0
GT.0.0: Shell element thicknesses are scaled by *thicsl* in the contact idealization.

Manual Segment Definition
(Types 12 and 13)

segments *segments* User defined segment option:
- EQ.0: Segments internally generated (default)
- EQ.1.0: User defined slave and/or master segments specified. Segments associated with shell elements are treated as shell elements, with thickness, by the AC algorithm.
- GT.1.0: Users defined slave and/or master segments specified. Segments associated with shell elements are treated as brick elements, with out thickness, by the AC algorithm and have an effective depth of $segments \times thickness$. (This option generates behavior similar to type 3 contact, but is potentially more robust then $segments = 1$.)

Domain Limiting and Geometry Features
(Types 13 and 14)

Components of the domain limiting box:

xmin *xmin* Minimum *x*-direction value. (default=-1.0e+25)

xmax *xmax* Maximum *x*-direction value. (default=1.0e+25)

ymin *ymin* Minimum y-direction value. (default=-1.0e+25)

ymax *ymax* Maximum *y*-direction value. (default=1.0e+25)

zmin *zmin* Minimum *z*-direction value. (default=-1.0e+25)

zmax *zmax* Maximum *z*-direction value. (default=1.0e+25)

mat_in *mat#1 mat#2 mat#3 ... mat#n*
Include only these *n* material numbers in the contact domain

mat_ex *mat#1 mat#2 mat#3 ... mat#n*
Include all material numbers in the contact domain *except* these *n*

sym_plane n_x n_y n_z x_{o-x} x_{o-y} x_{o-z} Tol
Contact symmetry plane defined by equation (337) (on page 374)
- $\boldsymbol{n}$ - vector normal to surface
- $\boldsymbol{x}_o$ - point on plane
- Tol - tolerance

SAND Volume Limiters
(Type 14 only)

smat_in *mat#1 mat#2 mat#3 ... mat#n*

Consider only elements with these *n* material numbers as active SAND volumes. Only material numbers and elements already in the contact domain will be included.

smat_ex *mat#1 mat#2 mat#3 ... mat#n*

Consider all elements and material numbers already in the contact domain *except* these *n* material numbers as active SAND volumes.

Rigid-Body Sphere-to-Sphere Idealization

(For type 3 contact only)

piv μ_{pivot} Coefficient of pivoting resistance

rigid *rigid* Rigid spherical contact idealization configuration
- EQ.2: Slave and master spheres are external to each other
- EQ.3: Master sphere resides inside the slave sphere
- EQ.4: Slave sphere resides inside the master sphere

rigid_master *rigid_master*
ABS(*rigid_master*): Material number of master rigid-body
- GT.0: Master surface is a full sphere
- LT.0: Master surface is a hemi-sphere

rigid_slave *rigid_slave*
ABS(*rigid_slave*): Material number of slave rigid-body
- GT.0: Slave surface is a full sphere
- LT.0: Slave surface is a hemi-sphere

roll μ_{roll} Coefficient of rolling resistance

stiff *stiff* Penalty stiffness

No additional input is needed for type 12, 13, and 14 (automatic) contact or for self-generated slave and/or master surface definitions. In all other cases, define $NUMSI$ sets of slave segments or nodes and master segments as specified on the Slide Surface Control Cards described above. For each sliding interface, define first any needed slave segments or nodes, then the necessary master segments. Repeat this pattern until slave segments or nodes and master segments are defined for all $NUMSI$ sliding interfaces.

SLAVE SEGMENTS

Cards NUMSI+1, . . . , NUMSI+NSS

Define the slave surface using the following *slave segment* cards for sliding interface types 1-4, 9-11 and, optionally, for 12 and 13. For slide surface types 5-8, omit this slave surface definition and instead use the slave node definitions described later in this section.

Columns		Quantity	Format	
1-5	(1-8)	Slave segment number	I5	(I8)
6-10	(-)	Generation increment, k	I5	(omit)
11-15	(9-16)	Node n_1	I5	(I8)
16-20	(17-24)	Node n_2	I5	(I8)
21-25	(25-32)	Node n_3	I5	(I8)
26-30	(33-40)	Node n_4	I5	(I8)
31-40	(41-50)	Normal failure stress, σ_{nf} (Type 9 only)	E10.0	(E10.0)
41-50	(51-60)	Shear failure stress, σ_{sf} (Type 9 only)	E10.0	(E10.0)

Omitted slave segment definitions are automatically generated by incrementing the node numbers by the generation increment, k.

σ_{nf} and σ_{sf} should be assigned sufficiently high values if no failure mechanism is needed. It would be equivalent to type 2 slideline, but at a higher cost. Leaving σ_{nf} and σ_{sf} blank or assigning zero to them does not disable the failure mechanism.

Define the discrete *slave nodes* for sliding interface types 5-8. For sliding interface types 1-4, 9-11, and, optionally, 12 and 13, omit this slave node definition and instead use the slave surface definition described previously.

SLAVE NODES

Columns		Quantity	Format	
1-5	(1-8)	Slave number	I5	(I8)
6-10	(9-16)	Node number	I5	(I8)
11-20	(17-26)	Normal force at failure, F_{fn} (type 8 only) Slave node radius, Rad (type 5 only)	E10.0	(E10.0)
21-30	(27-36)	Shear force at failure, F_{fs} (type 8 only)	E10.0	(E10.0)
31-40	(37-46)	Failure criterion exponent for normal force, n (type 8 only)	E10.0	(E10.0)
41-50	(47-56)	Failure criterion exponent for shear force, m (type 8 only)	E10.0	(E10.0)

Define the master surface using the following master segment cards *for sliding interface types 1-3, 5-11 and, optionally, 12 and 13, only. A master surface is not defined for single surface contact* (sliding interface type 4).

MASTER SEGMENTS

Cards NUMSI+NSS+1, . . . , NUMSI+NSS+NMS

Columns		Quantity	Format	
1-5	(1-8)	Master segment number	I5	(I8)
6-10	(-)	Generation increment, k	I5	(omit)
11-15	(9-16)	Node n_1	I5	(I8)
16-20	(17-24)	Node n_2	I5	(I8)
21-25	(25-32)	Node n_3	I5	(I8)
26-30	(33-40)	Node n_4	I5	(I8)

Node numbers for omitted master segments are generated internally using a node number increment of k.

SEGMENT DEFINITION

Sliding interfaces are described by defining one slave surface and one master surface. Each surface is then described as a collection of quadrilateral or triangular segments. Master and slave segments are described by listing four corner nodes, n_1 - n_4; triangular segments may be defined by repeating the last node ($n_4 = n_3$). Sliding interface segments correspond to element faces on the contact surface. For faces of solid elements, the ordering of nodes defining the slide surface segment may be either clockwise or counterclockwise; DYNA3D internally computes the correct segment outward normal vector. *For faces of shell elements, the nodes defining the slide surface segment must be counterclockwise such that the resulting segment normal vector, computed using the "right-hand rule" as seen in Figure 35, points toward the potentially contacting surface.* That

is, normal vectors for slave segments should point toward the master surface, and normal vectors for master segments should point toward the slave surface (see Figure 36). Segments may be given in any order to define a master or slave surface.

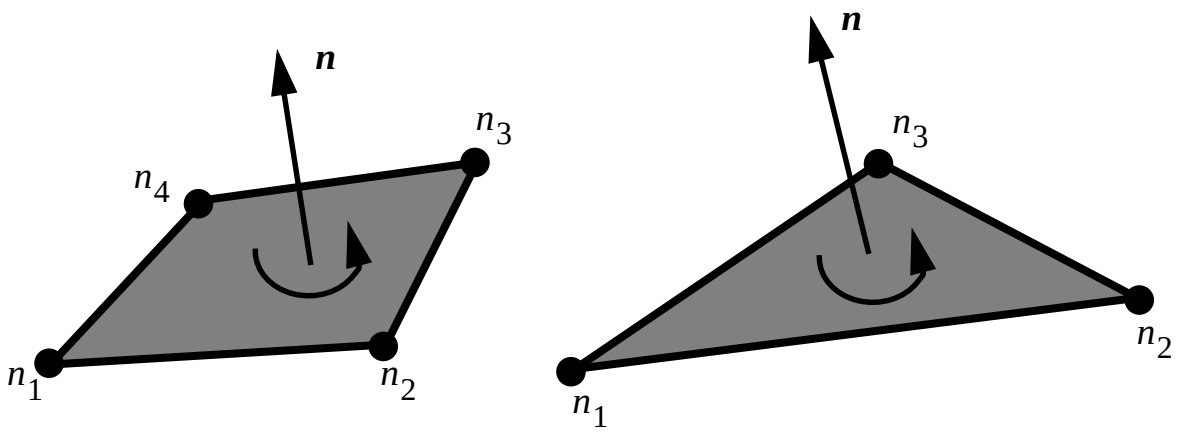

Figure 35:
Numbering and normals for slide surface segment definitions.

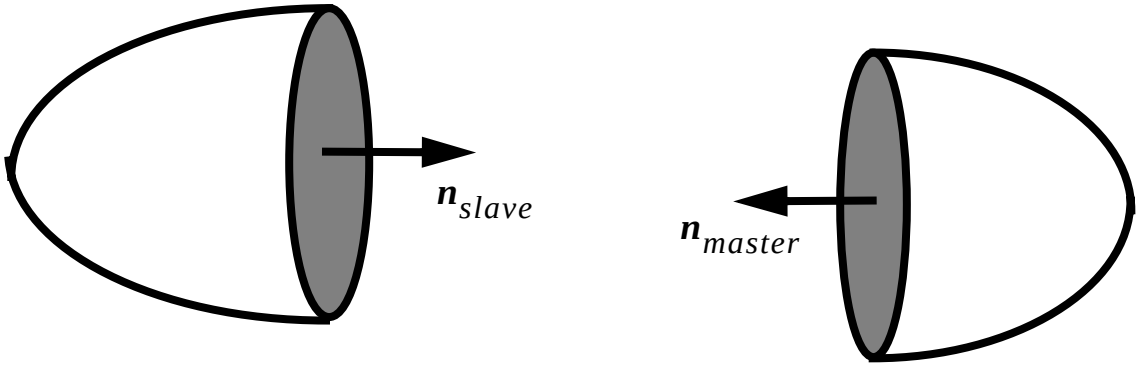

Figure 36
Sliding interface definition showing opposing orientation of normal vectors.

SELF-GENERATION OF SEGMENT DEFINITIONS

The slave segments, the slave nodes, and the master segments, as well as their corresponding numbers, may be automatically generated for slide surface types 1, 2, 3, 5, 6, 7, 8, 9, and 10 using the new self-generation features. The user specifies the material numbers associated with the slave and/or master sides and, optionally, a set of domain limiters. The exterior facets on the selected materials are assembled and used as the contact segments. Slave nodes for type 5, 6, 7, and 8 surfaces are generated from the nodes on exterior facets as well as from any beam elements whose material numbers have been specified. After the segments have been determined, their orientation is established.

The segment orientations for each surface is determined using brick and thick shell data, element connectivity, and the initial geometry. The orientation of all segments associated with brick or thick shell elements are established so that their outward normals point away from the element's interior. When present, brick-based and thick shell-based segments are used to determine the orientation of topologically connected shell-based segments. When this information is not available or the surface is disjoint, the node closest to the mating surface (or node set) is used to established the shell-based segment orientation. Again, using local element connectivity, the outward normal is propagated across the surface. The process is repeated until the outward normals for all the segments have been defined.

When shell-based segments are present, the segment orientation may be deficient. This typically arises because the relative location of the master and slave surface differ between initialization and at contact, the slide surface has initial penetration, or the shell element thickness has not been accounted for in the initial geometry. To over come this, the user can optionally "flip" the segment orientation of the shell elements. Unfortunately, some geometries are too complex for self-generation to correctly establish segment orientation, and the user must explicitly define the segments or break the surface into several more tractable surfaces.

SHELL THICKNESS

The contact formulations used in single surface (type 4), SAND (types 11 and 14), and Automatic Contact (types 12, 13, and 14) account for the thickness of a shell element in contact calculations. All other contact options operate using the midplane definition of shell elements for the surface definition. However, for slide surface types 3, 5, 8, 9, and 10, the user can optionally account for shell element thickness.

SLIDING INTERFACE TYPES

The **sliding only** (type 1) slide surface is a two-surface method based on a nodal constraint formulation. The two surfaces are allowed to slide arbitrarily large distances without friction, but are not permitted to separate or interpenetrate. This option performs well when extremely high interface pressures are present. The more coarsely meshed surface should be chosen as the master surface for best performance.

The **tied** (type 2) slide surface is not really a slide surface at all, but is a feature for joining two parts of a mesh with differing mesh refinement. This is also a nodal constraint formulation, so the more coarsely meshed surface should be chosen as the master surface. Tied interfaces may only be defined between surfaces of bodies discretized with solid elements.

The **sliding with separation and friction** (type 3) slide surface is the most generally applicable option. This implementation is a penalty formulation, and allows two bodies to be either initially separate or in contact. Large relative motions are permitted, and Coulomb friction is included. Surfaces may separate and come together in a completely arbitrary fashion. Contact between shell surfaces and solid body surfaces is supported. The choice of master and slave surfaces is not important in this formulation.

A rate-dependent Coulomb friction model is used in DYNA3D. The coefficient of friction is given by

$$\mu = \mu_k + (\mu_s - \mu_k)e^{-\beta v_{rel}}, \tag{334}$$

where μ_s and μ_k are the static and kinetic friction coefficients, β is a transition coefficient governing the rate of change from static friction to kinetic friction, and v_{rel} is the relative velocity between the two sliding surfaces. Note that if $\mu_k = 0$ and $\beta = 0$, then a rate-independent friction model is recovered with $\mu = \mu_s$.

The **single surface contact** (type 4) slide surface is a penalty formulation used for modeling two portions of the same body which may come into contact. This situation often arises in buckling problems, where one surface develops folds and comes into contact with itself. This option may be used with either solid or shell element surfaces. Frictional sliding is permitted between surfaces in contact. When used with shell element surfaces, it is only necessary to define one side of the surface in the slide surface definition; internal logic accounts for the possibility that contact may occur on either side. Due to the complexity of this algorithm, it is slightly more expensive than the other slide surface options, and therefore should only be used where necessary. Note that no master surface is defined for single surface contact.

The **discrete nodes impacting surface** (type 5) slide surface is a penalty formulation which allows separate definition of the slave *nodes* and master *surface*. This option is necessarily not symmetric, since no slave segments are defined. This feature can be used to model the impact of beams or shell edges onto a solid or shell surface, for example. The target surface is specified as the master surface, and the nodes of the beams or the shell edge nodes are defined as the slave nodes. Coulomb friction may be defined between the nodes and the master surface. An optional slave node radius, Rad, may be included to account for thickness effects. Contact then occurs when the distance between the node and surface is less than Rad.

The **discrete nodes tied to surface** (type 6) slide surface is analogous to the “discrete nodes impacting surface” option described above except that the slave nodes are required to remain rigidly attached to the master surface at their initial location. This feature is sometimes useful in joining two parts of a difficult mesh.

The **shell edge tied to shell surface** (type 7) slide surface is another specialization of the tied slide surface idea, although the implementation is somewhat different. This option allows the easy definition of intersections between a shell edge and a shell surface when the mesh spacing prevents merging nodes. Nodes should be merged in lieu of using this slide surface when possible, however, to obtain the least expensive solution.

The **node spotwelded to surface** (type 8) slide surface is a combination of the type 5 and type 6 slide surfaces. Slave nodes are constrained to remain on the master surface until a prescribed failure criterion is satisfied. Once the spotweld has "failed," the node is released and then the slide surface functions as a type 5 slide surface.

The failure criterion for spotwelds is

$$\left(\frac{F_n}{F_{fn}}\right)^n + \left(\frac{F_s}{F_{fs}}\right)^m \geq 1 \,, \tag{335}$$

where F_{fn} and F_{fs} are the specified normal and shear failure strengths, F_n and F_s are the current normal and shear forces in the spotweld, and n and m are the specified failure criterion exponents.

The **tied with failure** (type 9) slide surface is an *experimental* penalty method formulation. This option functions as a tied slide surface until a prescribed failure criterion is satisfied, thereafter the slide surface functions as a type 3 slide surface. This option may only be used between surfaces defined from solid elements, and the designation of the master and slave surfaces does not affect the results with this formulation.

The failure criterion for the type 9 "tie-break" interface is

$$\left(\frac{F_n}{F_{nf}}\right)^2 + \left(\frac{F_s}{F_{sf}}\right)^2 \geq 1 \,, \tag{336}$$

where F_n and F_s are the total normal and shear forces acting on a segment, and F_{nf} and F_{sf} are the normal and shear failure forces for the segment; these values are internally computed based on the segment area and the specified normal and shear failure stresses, σ_{nf} and σ_{sf}.

The **one-way algorithm for sliding with separation and friction** (type 10) slide surface is an unsymmetric implementation of the algorithm described for type 3 above. This option may effectively be used when one surface is defined as part of a rigid body, as often occurs in metal forming problems. This algorithm is somewhat less expensive than the symmetric type 3 algorithm, but may yield poor results if used between two deformable bodies. The master surface should correspond to the rigid surface, and the slave surface should correspond to the deformable surface.

This slide surface contains a modified Lagrange formulation designed for forming processes in which the slave surface is a deformable body and the master surface is a rigid material with prescribed kinematics. In this case the contact force can be determined "exactly". To activate this constraint enforcement option, the slave constraint factor should be set to $S_s = -2$.

The **SAND (Slidesurfaces with Adaptive New Definitions)** (type 11) slide surface is an algorithm for modeling material failure along contact surfaces. A failure criterion is defined for a volume of material adjacent to a SAND contact surface; these volumes of potentially failing material are called *SAND volumes* (see Figure 38). As material within an element on the contact surface fails, the failed element is removed from the calculation and the slidesurface definition adapts to the new exterior boundary of the unfailed material. SAND contact may include arbitrary mixtures of solid elements and shell elements, as shown in Figure 37. A SAND volume may be composed entirely of solid elements or shell elements for simple structures, or may include an external layer of shell elements followed by layers of solid elements and shell elements as needed to model a honeycomb or composite structure. Only the outside surface region of potential contact needs to be included in the initial sliding interface definition, so this definition is exactly the same as it would be for the usual (type 3) slide surface. SAND volumes are defined by listing the DYNA3D material numbers (not material types) for all materials which comprise the SAND volume. A SAND contact interface may have a SAND volume on only the master side, on only the slave side, or on both the master and slave sides. This capability allows efficient modeling of problems where failure is expected to occur only on one side and problems where failure may occur on both sides of a sliding interface. SAND contact interfaces allow improved modeling of many penetration and failure problems with DYNA3D.

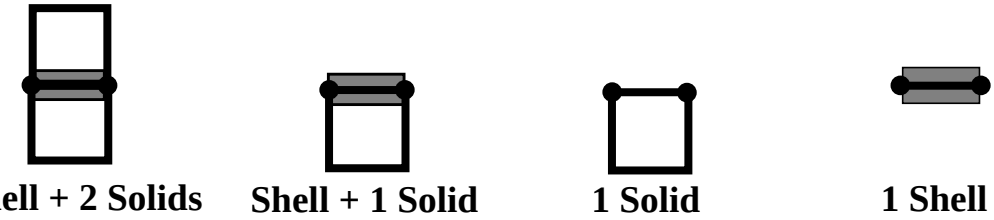

Figure 37:
Various combinations of shell and solid elements which can be used in a SAND contact definition to model composite and ‘‘built-up’’ structures.

Notes for Using SAND: *SAND requires that the results be processed using an appropriate postprocessor, as the plot database must contain new information. To signal DYNA3D to write this new format database, the SAND database flag must be set on Control Card 3 (section 4.1 on page 62). Also, the current SAND algorithms only adapt when elements are removed from the calculation. Thus, the user must now specify both a material or time-step failure criteria as well as an element deletion criteria to activate the SAND algorithm.*

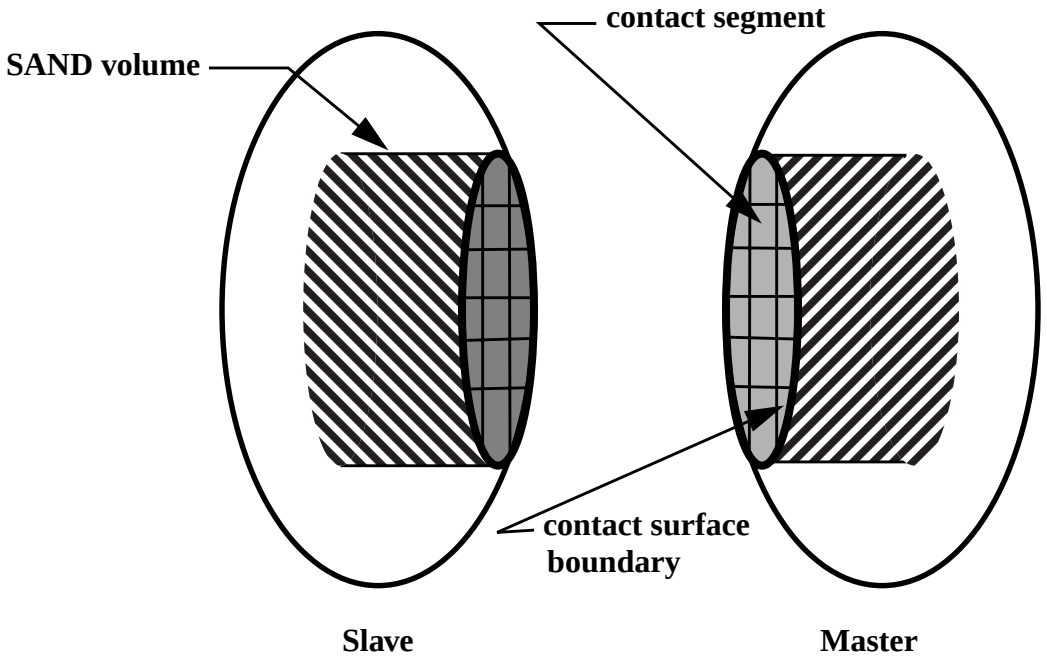

Figure 38:
Definition of SAND volumes containing material which can potentially fail. SAND volumes are adjacent to a SAND contact surface on one or more sides.

Automatic contact (types 12, 13, and 14) is a relatively new and continuously evolving slides-urface type in DYNA3D, e.g. in 1998, the basic algorithm was substantially updated. Although the underlying search and detection algorithms used jointly by all three automatic contact types differ greatly from the other DYNA3D contact options, from a user's perspective the main difference is that automatic contact does *not* require the specification of contact surfaces - they are "automatically" defined, but currently only for nodes and facets of solid and shell elements. This greatly simplifies the development of complex DYNA3D models, but may lead to a slight increase in computation time. Optionally, the user may specify either or both slave and master segments. In either case, all segments are internally treated as slave segments.

The current implementation assigns a "pin-ball" thickness to all shell element nodes. The nodal thickness is the smallest thickness or characteristic element dimension, defined as 2/5-th of the shortest element side or diagonal, of all shell elements attached to a node. Using the nodal thicknesses, a three-dimensional "pen" is created around each shell element. (The pen's thickness equals the nodal thickness at the element's corners.) Contact occurs whenever any "pen" or brick element interpenetrates another "pen" or brick element.

Because of the “pen” concept used, shell element nodes that are coincidental in space, even if constrained together, will generate penetration forces between each other. Thus, shell element geometries must be constructed accounting for the shell thickness. Furthermore, mesh refinement is not guaranteed to yield convergent results whenever the characteristic inplane shell element dimension becomes smaller than the element thickness. When this occurs, the pen size changes with mesh refinement.

Automatic contact detects contact only when the slave node resides within a shell’s ‘pen’ or the front half of a brick element. Thus, timestep sizes should be limited such that a slave node moves less than about 1/8 of an elements thickness in a single timestep. This can be easily achieved by using a load curve to limit the timestep size (see the *LCTM* option in CONTROL CARDS on page 62). Also, the Lagrange solver option reduces many automatic contact issues and is recommended especially for high-velocity impact problems.

In the current implementation, the initial mesh is evaluated for contact during the first time step the slidesurface is active. Slave nodes that generate contact forces during the first step are deactivated for the remainder of the calculation. A listing of the deactivated slave nodes and the master segments that produced the contact is provided in the `hsp` file. This nodal deactivation feature can be disabled by specifying the negative of *IPEN*, the robustness option.

The automatic contact debug option is useful when debugging models that employ automatic contact. (The debug option is enabled by setting the ninth-field on control card 3, the SAND database flag - keyword *isandb*, to “2”.) This option initializes the model and runs it a few cycles creating a plot state for each slide surface in the problem. Both the plot state number and analysis time correspond to the slidesurface number. For each automatic contact surface, the plot state contains only elements whose facets were master segments involved in contact during initialization. For convenience the last plot state shows the entire model. This feature also extends the output included in the `hsp` file about contact detected on initialization. A separate file, named `mover`, contains information about the initial contact detected. It gives the slave node number, penetration vector (approximately the “surface normal” times penetration depth), penetration depth, distance from the slave node to the master segment, and suggests two possible alternative initial coordinates for the slave node. This information is intended to assist the user in modifying the input deck to eliminate initial contact.

Automatic contact employs several competing sorting techniques to minimize computational cost. Using a bucket-sort algorithm and a course position- and velocity-based screening criterion, all potential contact segments are periodically identified for each active node - every *ibkuac* cycles. At ever cycle, the list of potential contact segments for each node is then used to determine if contact or interpenetration exists. The present algorithm permits nodes to be in contact with multiple segments. This greatly improves robustness especially in shell-to-shell-to-shell contact situations.

The default values of *ilocac* and *ibkuac* can be altered. In most problems, the default *ilocac* and *ibkuac* values provides excellent results, but in extreme cases a smaller interval may be desirable. Since *ilocac* controls how often the characteristic dimensions used to evaluate contact are updated, most problems are insensitive to a reduction in its value. On the other hand, the optimal *ibkuac* value varies during a problem and depends upon both problem type and computational platform. The number of cycles between bucket sorts, *ibkuac*, greatly influence the total compositional cost of contact and can be allowed to vary between *ibkuacmin* and *ibkuacmax* (the present default method) or fixed by externally specifying *ibkuac*. While increasing *ibkuac* decreases the number bucket-sorts performed, it increases both the bucket- and local-sort costs and, in high velocity impacts, decreases the bucket-sort accuracy. The variable method attempts to dynamically minimize the total contact cost by picking the best value of *ibkuac* based upon the geometry and dynamics present at the beginning of each bucket sort. In limited testing of high velocity impact events, the default approach has yielded near optimal results in terms of overall computational performance.

Types 12 and **13** automatic contacts are identical, but are maintained as separate types to provide downward compatibility during input. By default all brick and shell elements are included in the contact definition. However, several features exist in types 12 and 13 contact to reduce computational time in large or complex problems. The physical extent or domain of the automatic contact can be limited within a model. During initialization, automatic contact determines the exterior surfaces of all brick and shell element parts within the model and designates them as potential contact segments. The list of contact segments can be reduced by removing all segments that do not exist *completely* in a user-defined contact box during initialization. The segment list is further decreased by deleting any segments formed from elements whose material numbers are explicitly excluded from automatic contact. In many problems where contact occurs only in a region of the mesh, substantial computational savings can be achieved without scarifying any of the benefits of automatic contact.

When symmetry has been used to reduce a model, contact symmetry planes should be defined to correctly enforce contact conditions along the planes. An automatic-contact symmetry plane is defined by its normal vector $\boldsymbol{n}$ and passes through the point $\boldsymbol{x}_o$. A point $\boldsymbol{x}$ lies on the plane if

$$\left|\boldsymbol{n} \cdot (\boldsymbol{x} - \boldsymbol{x}_o)\right| < Tol \tag{337}$$

is satisfied, where Tol is a tolerance. Automatic-contact symmetry planes are used during initialization to remove interior surfaces which otherwise would be considered as exterior surfaces. The `hsp` file contains a summary of how many and, in verbose mode, which segments each symmetry plane removes. Note, these surfaces do not alter boundary conditions or prevent slave nodes from passing across the plane.

Automatic contact with SAND (Slidesurfaces with Adaptive New Definitions**)** (**type 14**) permits the modeling of progress material failure with contact in an automated fashion. The concepts of SAND volumes and surfaces from type 11 are combined with the benefits of arbitrary contact of automatic contact to better model penetration and failure problems in DYNA3D. As hex and shell elements are removed from the calculation due to material failure or time step size, their associated segments are removed from the slidesurface and the slidesurface definition adapts to the new boundary of the unfailed material. Unlike type 11 surfaces, contacts between any material boundaries, including internal voids and self contact, are captured.

During initialization, all brick and shell elements and their associated facets are identified as potential contact surfaces as well as SAND volumes and surfaces. Similar to type 13, the list of potential contact surfaces and SAND volumes and surfaces can be reduced by excluding materials from the contact domain as well as by a user-defined contact box. Segments that do not exist completely within the box during initialization are removed, and if all the segments associated with an element are removed, so is the element. In addition, SAND volumes and segments can be eliminated explicitly by material number during initialization with out excluding their “boundary” segments from the contact definition. This feature reduces computational and storage costs and should always be used to remove non-failable materials as well as materials not anticipated to fail from the list of active SAND volumes and segments. Note, the contact surface is continuously constructed from all the currently “exposed” boundary segments independent of whether the segment is an active SAND segment.

Notes for Using SAND: *SAND requires that the results be processed using an appropriate postprocessor, as the plot database must contain new information. To signal DYNA3D to write this new format database, the SAND database flag must be set on Control Card 3 (section 4.1 on page*

62). Also, the current SAND algorithms only adapt when elements are removed from the calculation. Thus, the user must now specify both a material or time-step failure criteria as well as an element deletion criteria to activate the SAND algorithm.

SMALL PENETRATION FLAG

If this option is activated, then DYNA3D ignores any apparent penetration found by the contact algorithm when the penetration depth is greater than one element thickness. Actual contact penetrations are usually much less than an element thickness, so it is likely that a large penetration is found due to a convex contact surface and a node getting “behind” the opposite surface. This behavior is usually indicated when a calculation is interrupted by nodes on a contact surface “shooting” off in random directions. The small penetration flag can almost always be used without harm, except in hypervelocity impact problems. Many analysts activate this option in all analysis models.

PRINTED INTERFACE FORCE FILE

If this option is activated on the slidesurface control card, a file called “FORCES” will be generated at run time containing the contact force at each node of the contact surface. This file is written at the interval prescribed as the time history plot interval on Control Card 6 in section 4.1 on page 62. For each node on the contact surface, the total interface force at that node
is printed in both global and local coordinates. The total force across the interface is also written to this file. Results from this file may be processed to yield a variety of interface force results.

Interface force data may also be written to a binary plot file as discussed in section 2.15 on page 32 and section 3.6 on page 59.

SPHERICAL REPRESENTATION

A new spherical representation option has been added for contact types 3, 5, 8, 9, and 10. These options reduce faceting problems associated with spherical or locally surfaces.

When the master surface is smoothed, it appears as an analytical sphere to the slave surface nodes. The center and radius of the sphere is constructed using nodes from the master surface. When the slave surface is smoothed, it appears as an analytical sphere to the master surface nodes. In this case, the sphere is constructed using the nodes from the slave surface. When either or both options are employed, the spherically represented surface(s) should contain only segments or nodes that form the spherical region. For example, in the case of an object inside a spherically capped cylinder, three separate slidesurfaces might be defined. One surface between the interior object and the cylindrical region, and one surface defined between the object and each spherical end.

RIGID-BODY SPHERE-TO-SPHERE CONTACT

For type 3 contact between two spherical rigid bodies, a special **rigid-body sphere-to-sphere** idealization exists. It uses analytical surfaces to detect contact between two locally spherical portions of disconnected rigid bodies. This contact method eliminates “faceting” induced problems, and is ideally suited to model the interactions between spherical or locally spherical rigid components. The two spherical components maybe adjacent to each other or inside one another. In the later case, the interior body may be spherical or hemi-spherical. To active this new and exper-imental contact feature, the rigid-body sphere-to-sphere keywords **stiff, rigid**, **rigid_master**, and **rigid_slave** must defined and the surface should be specified as a usual type 3 contact surface.

This implementation allows two bodies to be either initially separate or in contact and works with either the penalty or the Lagrange formulations. Large relative motions are permitted, and surfaces may separate and come together in a completely arbitrary fashion. Coulomb friction, as described for type 3 contact, as well as rate-independent rolling and pivoting friction are included.

A pivoting resistance torque is applied to the center of mass of the rigid-bodies when an non-zero pivoting component exists in the relative angular velocity vector. The pivoting torque vector, whose magnitude is given by

$$\tau_{pivot} = \mu_{pivot} F_n \tag{338}$$

where μ_{pivot} is the coefficient of pivoting resistance and F_n is the normal contact forces, parallels the ray connecting the centers of the spherical contact centers.

A rolling resistance torque is applied to the center of mass of the rigid bodies when the relative velocity at the contact point is essentially zero and the tangential component of the relative angular velocity is non-zero The rolling torque is given by

$$\tau_{roll} = \mu_{roll} F_n \tag{339}$$

where μ_{roll} is the coefficient of rolling resistance. The rolling resistance torque vector parallels the tangential component of the relative angular velocity vector.

The hemisphere option, used to model the contact of a hemisphere inside a sphere, limits the geometrical representation of one of the contact surfaces, and ensures that contact along the waist region is captured correctly. To active this feature, the negative of the material number should be defined for the appropriate rigid body.

CONTACT CONSTRAINT ENFORCEMENT OPTIONS

DYNA3D uses the penalty method by default to enforce the no-interpenetration contact constraint. A non-linear penalty method has been implemented for type 12, 13, and 14. As an alternative to the penalty method, a Lagrange multiplier formulation has also been implemented in this version of DYNA3D for slidesurface types 3, 5, 10, 12, 13, and 14.

The penalty formulation enforces the contact constraint by generating a restoring force that is applied to the penetrating node to return it to the surface. This force, F, is proportional to the penetration depth, g, the bulk modulus of the penetrated material, the dimensions of the penetrated element, and a scale factor specified by the user. (The later quantities are used to calculate the nominal stiffness K for each segment.) The amount of penetration observed is inversely proportional to the chosen scale factor. Using a larger penalty scale factor reduces the observed penetration, but may make the problem more difficult to solve. Using a smaller penalty scale factor makes the problem easier to solve, but may lead to unacceptably large interpenetrations. One global penalty scale factor is defined in the Control Section of the DYNA3D input file, and another penalty scale factor may be defined separately for each surface of a slide surface pair. The default value of the global penalty scale factor is 0.10, and the default for the local penalty scale factors is 1.0. These two factors are combined multiplicatively to arrive at the actual penalty scale factor used for computations.

The default penalty method generates the normal force F_n as

$$F_n = Kg. \tag{340}$$

The non-linear penalty method increases the penalty force F_n in a non-linear manner based upon penetration depth g of the contacting node and segment. While $g \le g_{offset}$ where g_{offset} is the gap offset, the penalty stiffness K is not scaled and Eq. (340) is used to calculate F_n. When $g > g_{offset}$, the effective penalty stiffness is increased in a parabolic manner such that

$$F_n = \left(1 + g_{mult}\frac{g}{t} - g_{offset}\right)^2 Kg, \tag{341}$$

where g_{mult} is the stiffness multiplier and t is the effective segment depth, i.e. half of the shell element thickness or brick depth associated with this segment. The multiplier g_{mult} can be set as large as necessary (e.g., 10^3) without decreasing the time-step scale factor (see CONTROL CARDS on page 62 - Card 6) because DYNA3D internally calculates the critical time step for all penalty method slide surfaces.

The non-linear penalty method and the master and slave surface stiffness scale factors S_m and S_s serve similar purposes, but function differently. While they both increase the effective penalty stiffness, the non-linear penalty method increases the stiffness on a local node-to-segment basis, as needed, while S_m and S_s increase it for all segments all the time. Note, both methods can be used simultaneously.

When the Lagrange formulation is chosen to enforce the contact constraint, a restoring force is again placed on thepenetrating node to return it to the surface, but is computed differently. This option computes the force by determining the predicted location of a node on the interface at the end of the time step, and computes the contact force required to place the node on the surface at the end of the time step. This method yields “exact” enforcement of the zero gap constraint. Two different approaches have been developed. When the master surface is a rigid material whose kinematics are prescribed, type 10 contact and Lagrange option 2 should be used. This method calculates the necessary forces via an coupled set of equations, and is very inexpensive. This option works very well for stamping problems where the die is rigid and has prescribed motion, and the work piece is deformable. Nodes in slidesurfaces that use the 2 Lagrange option should not be part of any other slidesurface definition. For all other cases or when overlapping 2 Lagrange slidesurfaces are desired, Lagrange contact option 3 should be used. In this case the constraint equations for the entire problem are assembled and solved via an iterative method (Zywicz and Puso, 1999). Since the exact contact forces are calculated at each time step, there is no interpenetration.

Although this feature costs slightly more than the penalty formulation (5% to 15% increase in overall computational cost), it has demonstrated excellent behavior in applications involving automatic contact, thin shell, and where large differences in mesh densities or material properties exist.

Nodes involved in Lagrange contact enforcement as well as in rigid wall definitions, nodal constraints, tied slidesurfaces, prescribed velocity and/or acceleration boundary conditions, or other kinematically imposed features may demonstrate some interpenetration or other undesirable behavior. (At present, the Lagrange contact algorithm does not account for the subsequent nodal movement from kinematically imposed options.) In most circumstances, the undesirable behavior can be eliminated by redefining the problem slightly. For example, a rigid wall can be replaced by a simple discretized object and either a new type 5 slidesurface, with Lagrange contact enforcement, or included in the previous slidesurface definition.

Both the non-linear penalty method and the Lagrange formulation are extremely useful with automatic contact in that they decrease or eliminate the amount of penetration. Because automatic contact uses a contact surface idealization that has a finite thickness, these approaches can prevent nodes from penetrating through the contact surface and causing the algorithm to fail.

4.29 TIE-BREAKING SHELL SLIDELINES

Define the number of tie-breaking shell slidelines, *NTBSL*, as specified on Control Card 7 in section 4.1 on page 62. First, input the following control card for all *NTBSL* tie-breaking shell slidelines.

Cards 1, . . . ,NTBSL

Columns		Quantity	Format	
1-5	(1-8)	Number of slave nodes in this slideline, N_s	I5	(I8)
6-10	(9-16)	Number of master nodes in this slideline, N_m	I5	(I8)

Following the definitions of all *NTBSL* control cards, define the following slideline card set for each tie-breaking shell slideline.

Card 1

Columns	Quantity	Format
1-10	Default effective plastic strain at failure, $\bar{\varepsilon}_f^p$	E10.0

Cards 2, . . . ,NSN+1

Columns		Quantity	Format	
1-5	(1-8)	Slave number EQ.0: the preceding slave number is incremented by 1	I5	(I8)
6-10	(9-16)	Node number	I5	(I8)
11-20	(17-26)	Plastic strain at failure, $\bar{\varepsilon}_f^p$ (optional)	E10.0	(E10.0)

Cards NSN+2, . . . , NSN+NMN+1

Columns		Quantity	Format	
1-5	(1-8)	Master number EQ.0: the preceding slave number is incremented by 1	I5	(I8)
6-10	(9-16)	Node number	I5	(I8)

Slidelines are defined by listing a set of nodes along the edge of a shell structure. One line of nodes is designated as the slave side, and the other line is designated as the master side. Nodes should be given in the order in which they appear along the surface. Nodes on the slave slideline may be given in order moving down the slideline in either direction, but nodes on the master slideline must be given in order such that the slave slideline lies to the left. *Tie-breaking shell slidelines must not cross.*

Tie-breaking shell slidelines may be used to tie shell edges together with a failure criterion on the joint. If the average volume-weighted effective plastic strain $\bar{\varepsilon}^p$ in the shell elements adjacent to a node exceeds the specified plastic strain at failure, $\bar{\varepsilon}^p_f$, then the tied slideline is released at that node. One default failure plastic strain is defined for the entire tie-breaking shell slideline, but this may be overridden on the slave node cards to define a unique failure plastic strain for each node.

Tie-Breaking Shell Slidelines may be used to simulate the effect of failure along a predetermined line, such as a seam or structural joint. When the failure criterion is reached in the adjoining elements, nodes along the slideline will begin to separate. As this effect propagates, the tied slideline will appear to “unzip,” thus simulating failure of the connection.

A more general (albeit more complex) fracture and failure modeling approach uses Tied Node Sets with Failure, as described in section 4.30 on page 382.

4.30 TIED NODE SETS WITH FAILURE

Define control cards for *NTNWF* Tied Node Sets with Failure as specified on Control Card 7 in section 4.1 on page 62.

Cards 1, . . . , NTNWF

Columns	Quantity	Format
1-5	Number of tied node constraints in this set, *NTNC*	I5
6-10	Maximum number of nodes tied at any constraint in this set, *NCMAX*	I5

Repeat the following group of cards to define *NTNWF* tied node data sets:

Define the following Constraint Set Default Card as the first card in each constraint set.

Card NTNWF+1

Columns	Quantity	Format
1-10	Default effective plastic strain at failure, $\bar{\varepsilon}_f^p$	E10.0

Repeat the following Constraint Definition Card(s) as necessary to define *NTNC* constraints in this set.

Cards NTNWF+2, . . . , NTNWF+NTNC

Columns		Quantity	Format	
1-10	(1-10)	Plastic strain failure, $\bar{\varepsilon}_f^p$ (optional)	E10.0	(E10.0)
11-15	(17-24)	First node to be tied in this constraint	I5	(I8)
16-20	(25-32)	Second node to be tied in this constraint	I5	(I8)
.	.	.	.	.
.	.	.	.	.
.	.	.	.	.
75-80	(57-64)	Twelfth (sixth) node to be tied in this constraint	I5	(I8)

Use additional cards as necessary, continuing with a format of 14I5 (or 10I8 for the “large” input option) on subsequent cards, until all nodes for this constraint have been defined.

A problem may contain several tied node sets with failure, as specified by $NTNWF$. One tied node set has $NTNC$ constraints, and each constraint may consist of from two to $NCMAX$ nodes. All constraints in one tied node set share a common default plastic strain at failure, $\bar{\varepsilon}_f^p$, but this may be overridden by giving a value for $\bar{\varepsilon}_f^p$ in the constraint definition.

Tied Node Sets with Failure apply only to shell elements. The specified nodes are tied together and are coincident until the volume-weighted effective plastic strain, averaged over all elements connected to nodes in a given constraint, exceeds the specified value. Once this failure criterion is exceeded, all nodes at that constraint are released to simulate the initiation of a crack or fracture.

To use this feature to simulate fracture and fragmentation of a plate or shell, all elements in the potential failure region should be generated to have unique nodes (i.e., no elements share nodes in common with other elements). These free elements are then tied together using Tied Node Sets with Failure at every corner, where nodes would be merged in a conventional model. Using this approach, a fracture may propagate through the plate as dictated by the analysis, and some estimate of the crack direction may be obtained. The fracture is required to move along element boundaries with this approach, however.

Tied Node Sets with Failure are similar to Tie-Breaking Shell Slidelines (described in section 4.29 on page 380), except that entire regions of individual shell elements may be tied together with this option and the fracture direction is not pre-defined. Tie-Breaking Shell Slidelines are more suited to a pre-defined potential fracture surface, and are somewhat less expensive and easier to define.

4.31 RIGID BODY MERGES

Define *NRBC* rigid body merge cards as specified on Control Card 4 in section 4.1 on page 62.

Columns	Quantity	Format
1-5	Master rigid body material number	I5
6-10	Slave rigid body material number	I5

The slave rigid body is merged into the master rigid body.

Two rigid materials are not permitted to have any nodes in common. If common nodes exist, define the two rigid materials as above to be merged into one rigid body for the analysis. This situation occurs infrequently, but may arise when rigid materials are used for solid elements, shell elements, and beam elements in close proximity in a model.

It is not necessary (or reasonable) to merge rigid materials which are completely separate and have no nodes in common.

4.32 EXTRA NODES FOR RIGID BODIES

Define one card set for each rigid body for which extra nodes are defined until *NRBEN* sets have been defined. *NRBEN* is specified on Control Card 7 in section 4.1 on page 62.

Card 1

Columns	Quantity	Format
1-5	Rigid body material number	I5
6-10	Number of extra nodes for this rigid material, *NEN*	I5

Cards 2, ... , NEN+1

Columns		Quantity	Format	
1-5	(1-8)	First extra node for this rigid material	I5	(I8)
6-10	(9-16)	Second extra node for this rigid material	I5	(I8)
11-15	(17-24)	Third extra node for this rigid material	I5	(I8)
.	.	.	.	.
.	.	.	.	.
.	.	.	.	.
45-50	(73-80)	Tenth extra node for this rigid material	I5	(I8)

Continue in this format until *NEN* extra nodes have been defined for this rigid material. Then, repeat both cards above until extra nodes have been defined for *NRBEN* rigid materials.

Extra nodes may be needed for rigid materials to facilitate the definition of a rigid body joint between two rigid materials, or to allow attachment of another structural member. Rigid body joints are described in section 4.34 on page 388.

4.33 DEFORMABLE-RIGID MATERIAL SWITCHING

Define NMSWCH groups of materials as specified on Control Card 7 in section 4.1 on page 68. Repeat the following input for each material group.

Card 1

Columns	Quantity	Format
1-10	Number of materials in a switching group, NMAT.	I10
11-20	The time at which a group of materials is merged and treated as a rigid body, TON.	E10.0
21-30	The time at which a group of materials is returned to their original material types, TOFF.	E10.0

Define NMAT material numbers in a group. Use as many cards as needed with 16 materials on a card.

Card 2, 3, ...

Columns	Quantity	Format
1-5	First material number in a group.	I5
6-10	Second material number in a group	I5

The material switching feature allows groups of materials to be treated as rigid bodies at their respective time interval during the analysis. Using this feature could improve computation efficiency considerably on parts of a model during a period when its change of deformation is negligible. The best examples for using this feature are container drop test and vehicle impacting roadside structures, as these problems often involve multiple impacts in a simulation. It would save significant computer time by treating the model as a rigid body between impacts.

The following restrictions apply to the use of this feature:

- Rigid materials can be included in the switching groups but rigid materials with assigned inertia properties cannot.
- No boundary conditions or prescribed velocities can be imposed upon any part of the switching groups.
- The stresses for solid elements in the switching groups are not rotated to keep pace with the motion during the rigid body phases. A proper stress transformation is done only before the individual group is about to be returned to their original material types.
- Rigid body phases of the switching groups cannot be overlapping if the groups share same materials.
- The first material in the material list for each group is treated as the master material. The rest of the materials in the list are merged into the master material.

4.34 RIGID BODY JOINTS

Define the number of joint definitions specified on Control Card 7 in section 4.34 on page 388.

Columns		Quantity	Format	
1-10	(1-10)	Relative penalty stiffness (default is 1.0)	E10.0	(E10.0)
11-15	(11-15)	Joint type EQ.1: Spherical EQ.2: Revolute EQ.3: Cylindrical EQ.4: Planar EQ.5: Universal EQ.6: Translational	I5	(I5)
16-20	(16-23)	Node n_1	I5	(I8)
21-25	(24-31)	Node n_2	I5	(I8)
26-30	(32-39)	Node n_3	I5	(I8)
31-35	(40-47)	Node n_4	I5	(I8)
36-40	(48-55)	Node n_5	I5	(I8)
41-45	(56-63)	Node n_6	I5	(I8)

The geometry of rigid body joints is shown in Figure 39. At each timestep, the relative penalty stiffness is multiplied by a function dependent on the time step size to give the maximum stiffness that will not destroy the stability of the solution. If the errors in the joint constraints are too large, the timestep must be reduced; simply increasing the relative stiffness will have no effect.

Node pairs n_1 and n_2 (n_3 and n_4, and n_5 and n_6) should be coincidental. For best performance, nodes n_1, n_3, and n_5 should be spaced as far apart as possible.

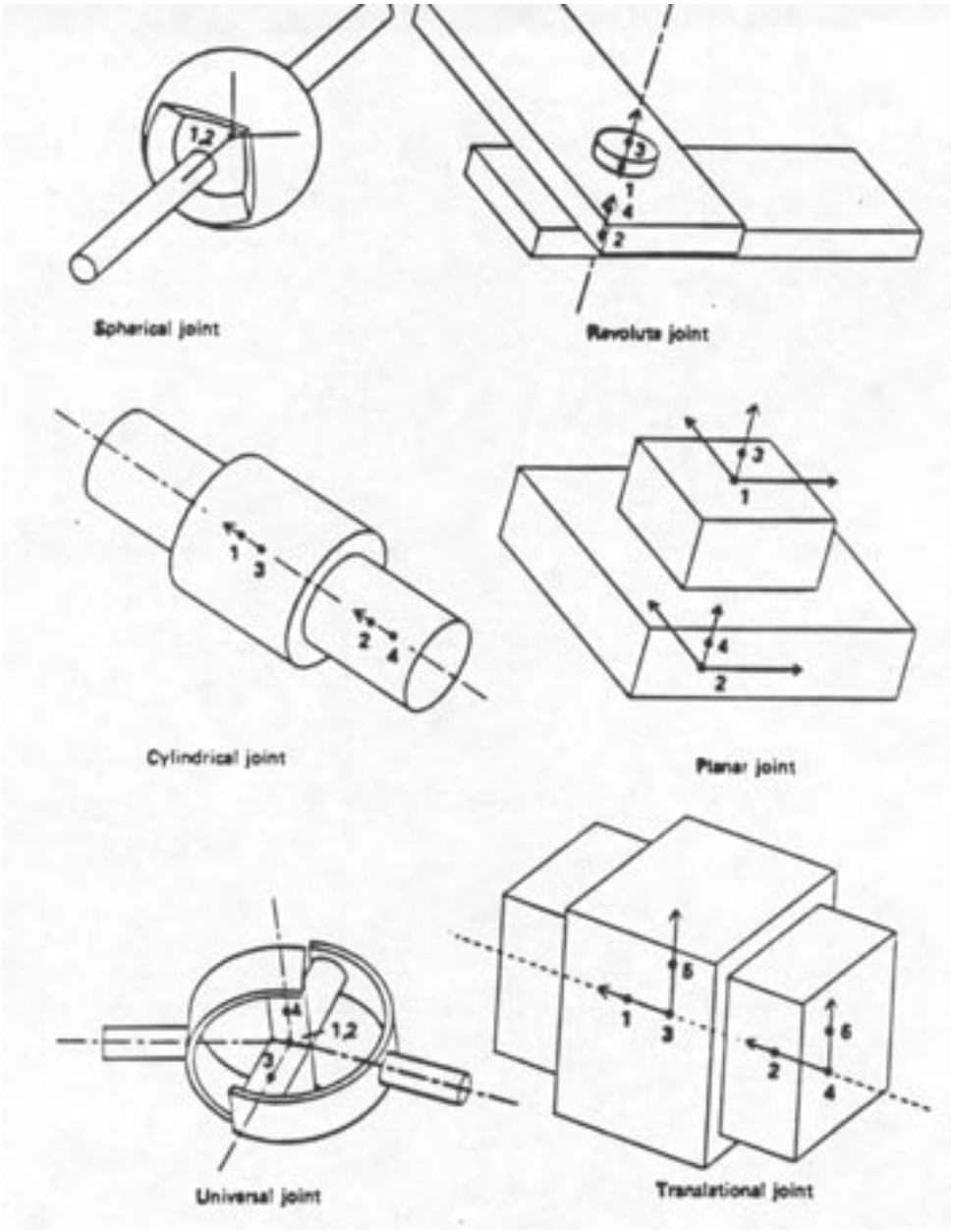

Figure 39 Rigid body joint geometry.

4.35 PRESCRIBED BASE ACCELERATIONS

Define nonzero “base acceleration” loads as specified on Control Card 5 in section 4.1 on page 62.

X-Direction Base Acceleration

Define this card only if a nonzero x-direction base acceleration is specified on Control Card 5.

Columns	Quantity	Format
1-5	Load curve number giving time variation	I5
6-15	Scale factor on x-acceleration EQ.0.0: default set to “1.0”	E10.0

Y-Direction Base Acceleration

Define this card only if a nonzero y-direction base acceleration is specified on Control Card 5.

Columns	Quantity	Format
1-5	Load curve number giving time variation	I5
6-15	Scale factor on y-acceleration EQ.0.0: default set to "1.0"	E10.0

Z-Direction Base Acceleration

Define this card only if a nonzero z-direction base acceleration is specified on Control Card 5.

Columns	Quantity	Format
1-5	Load curve number giving time variation	I5
6-15	Scale factor on z-acceleration EQ.0.0: default set to "1.0"	E10.0

Translational base accelerations allow body force loads, such as gravity, to be imposed on a structure. Conceptually, base acceleration may be thought of as accelerating the coordinate system in the direction specified, and thus the inertial loads acting on the model are of opposite sign. For example, if a cylinder were fixed to the x-y plane and extended in the positive z direction, then a positive z-direction base acceleration would tend to shorten the cylinder.

4.36 PRESCRIBED ANGULAR VELOCITIES

Define nonzero angular velocity components about the global axes as specified on Control Card 5 in section 4.1 on page 62.

ANGULAR VELOCITY ABOUT GLOBAL X-AXIS

Define this card only if a nonzero angular velocity component about the global x-axis is specified on Control Card 5.

Columns	Quantity	Format
1-5	Load curve number giving time variation	I5
6-15	Scale factor on angular velocity EQ.0.0: default set to "1.0"	E10.0

ANGULAR VELOCITY ABOUT GLOBAL Y-AXIS

Define this card only if a nonzero angular velocity component about the global y-axis is specified on Control Card 5.

Columns	Quantity	Format
1-5	Load curve number giving time variation	I5
6-15	Scale factor on angular velocity EQ.0.0: default set to “1.0”	E10.0

ANGULAR VELOCITY ABOUT GLOBAL Z-AXIS

Define this card only if a nonzero angular velocity component about the global z-axis is specified on Control Card 5.

Columns	Quantity	Format
1-5	Load curve number giving time variation	I5
6-15	Scale factor on angular velocity (default = 1.0)	E10.0

Body force loads due to the angular velocity are always calculated with respect to the deformed configuration, and act radially outward from the axis of rotation. Torsional effects arising from changes in angular velocity are not included. Angular velocity is assumed to have the units of radians per unit time.

The body force density $\boldsymbol{b}$ at a point P in the body is calculated from

$$\boldsymbol{b} = \rho(\mathbf{w} \times \mathbf{w} \times \boldsymbol{r}), \tag{342}$$

where ρ is the mass density, $\mathbf{w}$ the angular velocity, and $\boldsymbol{r}$ is a position vector from the origin to point P. Note that although the angular velocity may vary with time, the effects of angular acceleration are not included in this formulation.

This feature is useful for studying transient deformations of three-dimensional objects which are spinning about any axis of rotation through the global origin. Typical applications of this feature could include modeling the deformations of a tire spinning about an axle, or the impact of a foreign object on a satellite spinning rapidly about its own axis.

4.37 MOMENTUM DEPOSITION IN SOLID ELEMENTS

Card 1

Define momentum deposition data for the number of solid elements specified on Control Card 5 in section 4.1 on page 62.

Columns		Quantity	Format	
1-5	(1-8)	Solid element number to receive momentum	(I5)	(I8)
6-15	(9-18)	x-direction momentum	E10.0	(E10.0)
16-25	(19-28)	y-direction momentum	E10.0	(E10.0)
26-35	(29-38)	z-direction momentum	E10.0	(E10.0)
36-45	(39-48)	Deposition time	E10.0	(E10.0)

Momentum may be deposited in selected solid elements at a specified time during an analysis. This feature is useful for modeling impacts of a large body with many smaller bodies where only the momentum transfer is significant, and where detailed modeling of the collisions of the smaller bodies may lead to excessive cost. An example application of this feature would be the effect of dense blowing sand on a fast moving body, such as an automobile or low-flying aircraft.

4.38 DETONATION POINTS

Define one card for each high explosive detonation point specified on Control Card 5 in section 4.1 on page 62.

Columns	Quantity	Format
1-10	Lighting time for detonation point	E10.0
11-15	Material to be lit EQ.0: all H.E. materials are considered	I5
16-25	x-coordinate of detonation point	E10.0
26-35	y-coordinate of detonation point	E10.0
36-45	z-coordinate of detonation point	E10.0

During DYNA3D initialization, the lighting time of each element is computed using a simple programmed burn algorithm. The resulting point detonation is illustrated in Figure 40. The lighting time t_L for an element is computed based on the distance from the center of the element to the nearest detonation point l_d, the detonation velocity D, and the lighting time of that detonation point t_{det}, using

$$t_L = t_{det} + \frac{l_d}{D}. \tag{343}$$

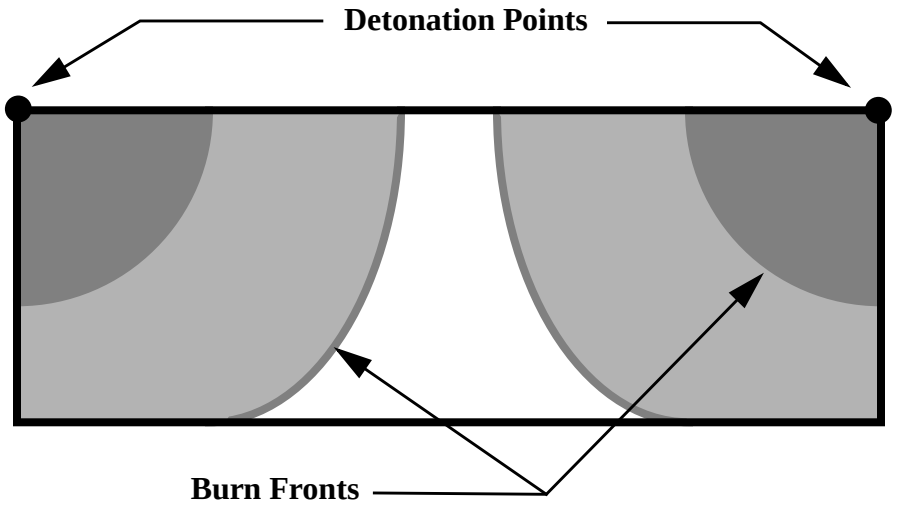

Figure 40
Point detonation for initiating high explosive burn.

4.39 SHELL-SOLID INTERFACES

Define the number of shell-solid interfaces specified on Control Card 7 in section 4.1 on page 62.

Card 1

Columns	Quantity	Format
1-5	Number of shell element nodes, *NSHLN*	I5
6-10	Number of solid element nodes tied to each shell node (maximum of eight)	I5

Card 2, . . . , NSHLN+1

Columns		Quantity	Format	
1-5	(1-8)	Shell element node, n_s	I5	(I8)
6-10	(9-16)	First solid element node, n_{b1}	I5	(I8)
11-15	(17-24)	Second solid element node, n_{b2}	I5	(I8)
.		.	.	
.		.	.	
.		.	.	
.		.	.	
41-45	(65-72)	Eighth solid element node, n_{b8}	I5	(I8)

The shell-solid interface is an *experimental* capability for coupling regions of 4-node shell elements to regions of solid elements. Since shell elements have 6 degrees-of-freedom per node (three translations and three rotations) and solid elements have only 3 degrees-of-freedom per node (three translations), a mismatch in degrees-of-freedom occurs along a shell-solid boundary. The approach followed in this option is to constrain nodes of the solid elements to lie along the shell fiber direction at the interface, thus transferring moments in the shell elements into spatially

varying stresses in the solid elements. The nodes of the solid elements are allowed to move along the tangent nodal fiber, and are constrained to move only along this fiber direction, as shown in Figure 41.

The solid element nodes must be specified in the order in which they occur along the shell fiber direction, but the fiber may be traversed in either the positive or negative direction.

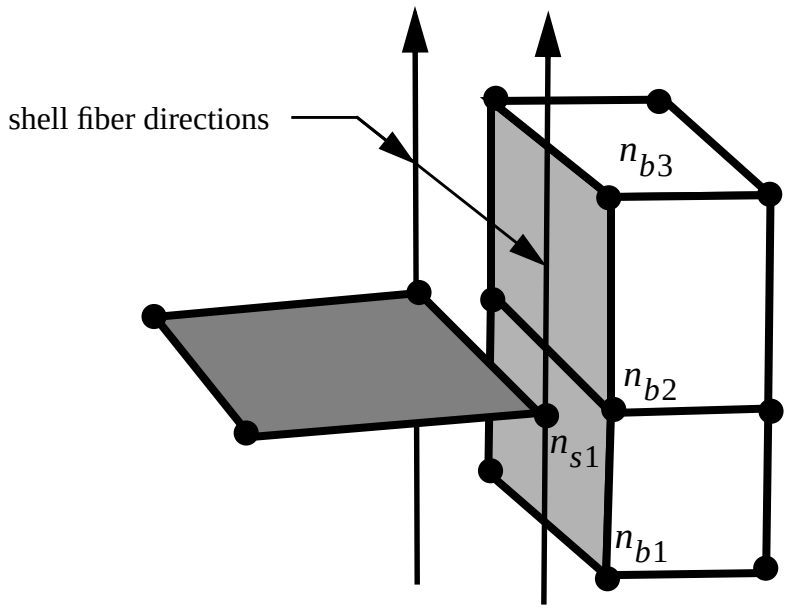

Figure 41
Shell-solid interface geometry and kinematics. Shell element node n_{s1} is associated with solid element nodes n_{b1}, n_{b2}, and n_{b3} in a shell-solid interface definition.

4.40 DISCRETE SPRINGS, DAMPERS, AND MASSES

Define discrete springs, dampers, and masses in this section if $INPSD = 1$ on Control Card 7 in section 4.1 on page 62. Discrete element input follows the general organization of the entire DYNA3D input file: first a control card defines the number of discrete element materials, discrete elements, and lumped nodal masses. Next, each discrete element material is defined by a Discrete Element Material Control Card and a Discrete Element Material Data Card. Then, discrete elements are defined on Discrete Element Data Cards, and discrete masses are specified on Lumped Mass Data Cards.

First, define the Discrete Element Control Card:

Card 1

Columns	Quantity	Format
1-5	Number of material definitions for discrete elements, $NDMAT$	I5
6-10	Number of discrete springs and dampers (discrete elements), $NUMELD$	I5
11-15	Number of discrete masses, $NUMMAS$	I5

Next, for each of the $NDMAT$ discrete element materials, define the Discrete Element Material Control Card and the Discrete Element Material Data Card as described below.

The Discrete Element Material Control Card is defined as:

Cards 2, 4, 6, . . .

Columns	Quantity	Format
1-5	Discrete element material number ($\leq NDMAT$)	I5
6-10	Discrete element material type:	I5
	Translational element material models: EQ.1: linear elastic EQ.2: linear viscous EQ.3: isotropic elastoplastic EQ.4: nonlinear elastic	

EQ.5: nonlinear viscous
EQ.6: general tabulated nonlinear

Rotational element material models:
EQ.21: linear elastic
EQ.22: linear viscous
EQ.23: isotropic elastoplastic
EQ.24: nonlinear elastic
EQ.25: nonlinear viscous
EQ.26: general tabulated nonlinear

The Discrete Element Material Data Card is defined as described below for each discrete element material type.

Cards 3, 5, 7, . . .

Discrete Element Material Type 1 and 21: (Linear Elastic)

Columns	Quantity	Format
1-10	Elastic stiffness (spring constant), k (force/displ. or torque/rotation)	E10.0

Discrete Element Material Type 2 and 22: (Linear Viscous)

Columns	Quantity	Format
1-10	Damping constant (viscosity), c (force/velocity or torque/angular velocity)	E10.0

Discrete Element Material Type 3 and 23: (Isotropic Elastoplastic)

Columns	Quantity	Format
1-10	Elastic stiffness, k (force/displ. or torque/rotation)	E10.0
11-20	Tangent stiffness, k_T (force/displ. or torque/rotation)	E10.0
21-30	Yield, F_Y (force or torque)	E10.0

Discrete Element Material Type 4 and 24: (Nonlinear Elastic)

Columns	Quantity	Format
1-10	Load curve number giving force vs. displacement or torque vs. rotation curve	E10.0

Element Material Type 5 and 25: (Nonlinear Viscous)

Columns	Quantity	Format
1-10	Load curve number giving force vs. velocity or torque vs. angular velocity curve	E10.0

Discrete Element Material Type 6 and 26: (General Tabulated Nonlinear)

Columns	Quantity	Format
1-10	Load curve number giving force vs. displacement or torque vs. rotation rotation for loading, LC_L	E10.0
11-20	Load curve number giving force vs. displacement or torque vs. rotation for loading, LC_U	E10.0
21-30	Plastic hardening parameter, β $(0 \le \beta \le 1)$	E10.0
31-40	Initial yield force or torque in tension ($F_{YT} > 0$)	E10.0
41-50	Initial yield force or torque in compression ($F_{YC} < 0$)	E10.0

Load curves define force (or torque) as a function of displacement (or rotation). The load curve points must be in order, starting with the most negative (compressive) displacement (or rotation) and ending with the most positive (tensile). The curves need not be symmetrical. The curve must not have a zero slope at any point; however, the slope may be made a small nonzero value if desired. The behavior of Discrete Element Material Type 6 is shown in Figure 42.

The displacement (or rotation) origin of the “unloading” curve is arbitrary, since it will be shifted as necessary as the element extends and contracts. On reverse yielding the “loading” curve will also be shifted along the displacement axis. The initial tensile and compressive yield forces (or torques) (F_{YT} and F_{YC}) define a range within which the element remains elastic (i.e. the “loading” curve is used for both loading and unloading). If at any time the force (or torque) in the element exceeds this range, the element is deemed to have yielded, and at all subsequent times the “unloading” curve is used for unloading.

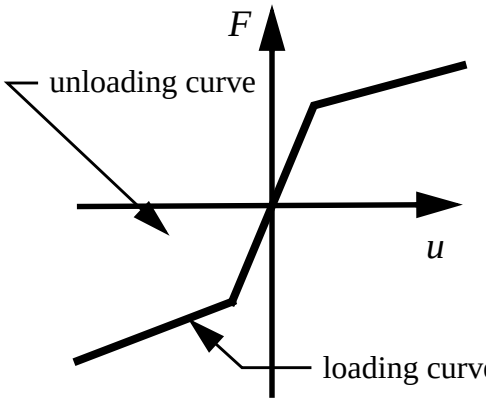

original loading and unloading curves

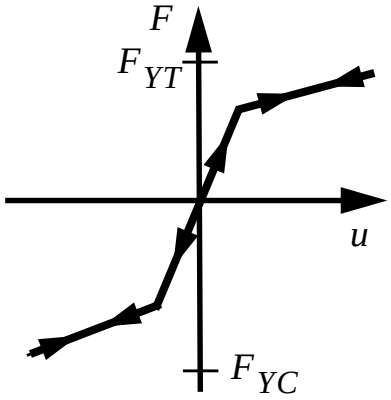

elastic behavior ($F_{YC} < F < F_{YT}$)

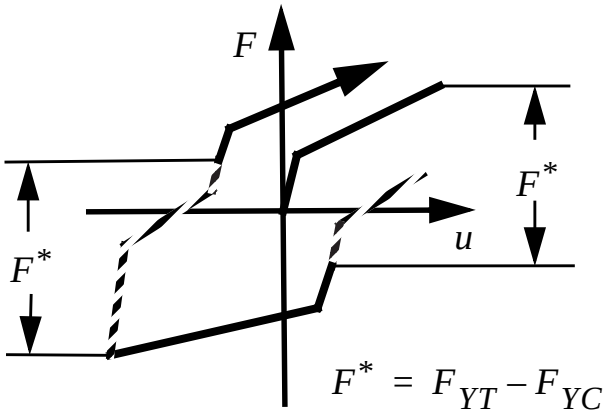

Plastic behavior ($\beta = 0$)

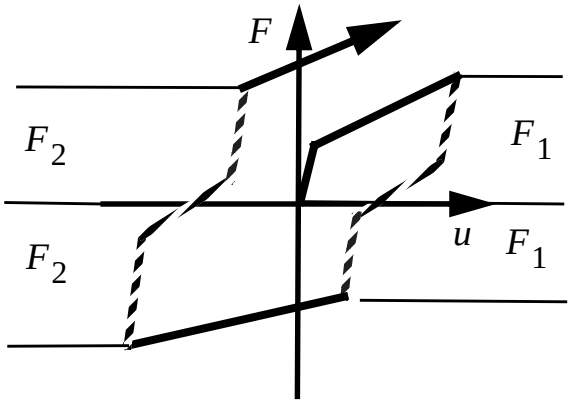

Plastic behavior ($\beta = 1$)

Figure 42:
Discrete Element Material Type 6: General Tabulated Nonlinear

The behavior of the model in the elastic range, the elastic-plastic (kinematic) mode, and the elastic-plastic (isotropic) mode is illustrated.

Define *NUMELD* Discrete Element Data Cards as specified on the Discrete Element Control Card.

Cards 2+2*NDMAT, . . . , 1+2*NDMAT+NUMELD

Columns		Quantity	Format	
1-5	(1-8)	Discrete element number	I5	(I8)
6-10	(9-16)	First node, n_1	I5	(I8)
11-15	(17-24)	Second node, n_2	I5	(I8)
16-20	(25-32)	Discrete element material number	I5	(I8)
21-30	(33-42)	Scale factor on computed force (default = 1.0)	E10.0	(E10.0)
31-32	(43-44)	Force calculation and direction option, $IOPT$	I2	(I2)
		If $IOPT = 0$, (default) no additional input required		
		If $IOPT = 1$		
33-42	(45-54)	First auxiliary node, an_1	E10.0	(E10.0)
43-52	(55-64)	Second auxiliary node, an_2	E10.0	(E10.0)
		If $IOPT = 2$		
33-42	(45-54)	Global x-direction component	E10.0	(E10.0)
43-52	(55-64)	Global y-direction component	E10.0	(E10.0)
53-62	(65-74)	Global z-direction component	E10.0	(E10.0)
		If $IOPT = 11$		
33-42	(45-54)	First auxiliary node, an_1	E10.0	(E10.0)
43-52	(55-64)	Second auxiliary node, an_2	E10.0	(E10.0)
		If $IOPT = 12$		
33-42	(45-54)	Global x-direction component	E10.0	(E10.0)
43-52	(55-64)	Global y-direction component	E10.0	(E10.0)
53-62	(65-74)	Global z-direction component	E10.0	(E10.0)

Define *NUMMAS* Lumped Mass Data Cards as specified on the Discrete Element Control Card.

Cards 2+2*NDMAT+NUMELD, . . . , 1+2*NDMAT+NUMELD+NUMMAS

Columns		Quantity	Format	
1-5	(1-8)	Node number,	I5	(I8)
6-15	(9-18)	Mass	E10.0	(E10.0)

Lumped nodal masses are added to any existing mass at a node.

Discrete elements (springs and dampers) may be imposed as one-dimensional translational or rotational elements between two nodes. Translational elements utilize the translational degrees of freedom to calculate the instantaneous relative vector between the two nodes. Rotational elements utilize the rotational degrees of freedom to construct the relative rotation vector between the two nodes, and, therefore, rotational elements can only be used with shell and beam elements.

Forces can be calculated based upon either the magnitude of the relative displacement/rotation vector with $IOPT = 0, 1, 2$ or the projected component of the relative displacement/rotation vector in the unit normal vector direction with $IOPT = 11, 12$. In all cases, the relative displacement and rotation vectors are calculated by subtracting the displacements or rotations of node 1 from node 2. Options $IOPT = 0, 1, 2$ are useful when modeling true one-dimensional translational spring behavior while options $IOPT = 11, 12$ permit orthotropic spring behavior to be defined. In both cases, the resultant force or torque is applied to the nodes parallel to the unit normal vector as discussed below.

The unit normal vector can be specified in three ways. When $IOPT = 0$, the unit normal vector parallels the vector that connects node 1 to node 2. It is recalculated at every time step. When $IOPT = 1, 11$, the unit normal vector is constructed by normalizing the vector that connects auxiliary node 1 to auxiliary node 2. The auxiliary nodes used to define the unit normal vector can be any nodes in the problem including the nodes that define the element. For rotational elements,

this option provides a convenient way to specify which components of the relative rotation vector should be used to define the “rotation”. When $IOPT = 2, 12$, the unit normal vector is specified in terms of its global coordinates.

Care should be used when using $IOPT = 1, 11$ and $IOPT = 2$. For translational elements positive (extensional) forces are applied in the direction of the unit normal vector at node 1. Thus, the unit normal vector should always point approximately from node 1 towards node 2 to obtain the correct force sign convention. *Reversing the definition will result in the force being applied in the wrong direction even though the sign of the element force is calculated correctly.* For rotational elements, although the forces are always applied in a consistent manner, the sign of the (relative) rotation depends upon the unit normal vector’s orientation. *Reversing the unit normal vector’s orientation will cause the (relative) rotation to switch signs.*

Discrete elements (springs and dampers) and lumped nodal masses provide a convenient method for imposing prescribed force-displacement relationships between two nodes. These features may be used alone to allow DYNA3D to solve lumped parameter spring-mass-damper models, or may be used in combination with a finite element model to represent a complex system.

Note that if discrete springs are connected to a rigid material for which rigid body inertial properties (section 4.41 on page 405) have been defined, it is possible in some circumstances to experience difficulties with the time step automatically chosen by DYNA3D. In most cases, simply altering the specified material density for the rigid material up to increase the time step or down to decrease the time step will provide the necessary user control without affecting anything else in the problem.

Internal forces in discrete elements may now be output to an ASCII file called `FORDIS`. This option is activated using the flag on Control Card 3 in section 4.1 on page 62.

4.41 RIGID BODY INERTIAL PROPERTIES

Define rigid body inertial properties for rigid materials as specified on Control Card 7 in section 4.1 on page 62. All requested data must be provided, and this data overrides other input data (such as nodal initial velocities) for nodes of rigid bodies.

Card 1

Columns	Quantity	Format
1-5	Material number of rigid body	I5
6-15	x-coordinate of center of mass	E10.0
16-25	y-coordinate of center of mass	E10.0
26-35	z-coordinate of center of mass	E10.0
36-45	Translational mass	E10.0

Rigid materials are defined using Material Type 20 as described in section 4.4 on page 92. Normally, each rigid material is considered a separate rigid body unless the Rigid Body Merge option (section 4.31 on page 384) has been used.

Card 2

Columns	Quantity	Format
1-10	Moment of inertia in the global x direction, I_{xx}	E10.0
11-20	Product of inertia in x-y direction, I_{xy}	E10.0
21-30	Product of inertia in x-z direction,I_{xz}	E10.0
31-40	Moment of inertia in the global y direction, I_{yy}	E10.0
41-50	Product of inertia in y-z direction,I_{yz}	E10.0
51-60	Moment of inertia in the global z direction, I_{zz}	E10.0

The mass moments of inertia are defined in the global coordinate system.

Card 3

Columns	Quantity	Format
1-10	Initial rigid body translational velocity in the x-direction	E10.0
11-20	Initial rigid body translational velocity in the y-direction	E10.0
21-30	Initial rigid body translational velocity in the z-direction	E10.0
31-40	Initial rigid body angular velocity about the x-axis (radians/time unit)	E10.0
41-50	Initial rigid body angular velocity about the y-axis	E10.0
51-60	Initial rigid body angular velocity about the z-axis	E10.0

Note that these initial velocities must be specified for any rigid body with inertial properties defined in this section. This data overrides nodal initial velocities specified in section 4.27 on page 350 for nodes of the rigid body. Initial velocity data for other nodes in the model is not affected.

Rigid body inertial properties are calculated by default from the geometry of the elements and the mass density ρ specified for the material. The Rigid Body Inertial Properties option allows the complete set of inertial properties to be specified directly for a rigid body. This approach is useful if the body has a spatially varying mass density which is not conveniently included in the material definitions, or if geometric approximations are made in the model which render the inertial properties calculated using the default procedure inaccurate.

Note: kinetic energy reported by DYNA3D may not properly account for the modified mass and moment of inertia of the rigid body, but actual computations use the modified values. Also, time step calculations for discrete springs and dampers connected to rigid bodies are based upon the original (as-input) material density. If undesirable time steps are selected by the code, modify the density specified for the rigid material until a suitable time step is achieved.

Useful tricks include defining the rigid material with a density such that the total mass is computed correctly, or with a very small density so that no significant contribution to kinetic energy is calculated from the rigid material.

4.42 NONREFLECTING BOUNDARY SEGMENTS

Define *NNRBS* nonreflecting boundary segments as specified on Control Card 7 in section 4.1 on page 62.

Columns		Quantity	Format	
1-5	(1-8)	Nonreflecting boundary segment number	I5	(I8)
6-10	(-)	Generation increment, k	I5	(omit)
11-15	(9-16)	Node n_1	I5	(I8)
16-20	(17-24)	Node n_2	I5	(I8)
21-25	(25-32)	Node n_3	I5	(I8)
26-30	(33-40)	Node n_4	I5	(I8)

Nonreflecting boundaries are only used with *solid* elements. Boundaries are defined as a collection of segments, and segments are equivalent to element faces on the boundary. Segments are defined by listing the corner nodes in either a clockwise or counterclockwise order. The first and last nonreflecting boundary segments must be explicitly defined. Gaps in intermediate segment numbers are filled by automatically generating segment definitions by adding the generation increment k to each node number of the previous segment.

Nonreflecting boundaries are used on the exterior boundaries of an analysis model of an infinite domain, such as a half-space, to prevent artificial stress wave reflections generated at the model boundaries from reentering the model and contaminating the results. Internally, DYNA3D computes an impedance matching function, in both normal and shear directions, for all nonreflecting boundary segments based on an assumption of *linear material behavior.* Thus, the finite element mesh should be constructed so that all significant nonlinear behavior is contained within the discrete analysis model.

4.43 TEMPERATURE INPUT OPTION I

Define one temperature card for each of the $NUMNP$ nodes if the thermal effects option is set to -9999 on Control Card 6 in section 4.1 on page 62.

Columns		Quantity	Format	
1-5	(1-8)	Node number, n_i	I5	(I8)
6-15	(9-18)	Temperature scale factor at this node, S_i	E10.0	(E10.0)
16-25	(19-28)	Base temperature, T_i^{base}	E10.0	(E10.0)
26-30	(29-36)	Load curve number giving time variation	I5	(I8)
31-35	(37-44)	Generation increment, k	I5	(I8)

Temperature data for missing nodes is generated using the specified node number increment, k. The temperature scale factor S_i and the base temperature T_i^{base} are linearly interpolated between the starting and ending values.

At any time t, the temperature at a node n_i is given by

$$T(t) = T_i^{base} + S_i f(t), \tag{344}$$

where T_i^{base} is the specified base temperature, S_i is the specified temperature scale factor, and $f(t)$ is the value of the specified load curve at the current time.

4.44 TEMPERATURE INPUT OPTION II

Define one temperature card for each of the $NUMNP$ nodes if the thermal effects option is set to -2 on Control Card 6 in section 4.1 on page 62.

Columns		Quantity	Format	
1-5	(1-8)	Node number	I5	(I8)
16-25	(19-28)	Temperature	E10.0	(E10.0)

Data for missing nodes is automatically generated by linearly interpolating from the endpoint values.

The reference temperature state is assumed to be a zero state with this option. One set of nodal temperatures is defined and held constant throughout the analysis.

4.45 ONE DIMENSIONAL SLIDELINES

Define $N1DSL$ one-dimensional slidelines as specified on Control Card 9 in section 4.1 on page 62. Repeat the following set of three cards for each one-dimensional slideline.

Define the One-Dimensional Slideline Control Card:

Columns	Quantity	Format
1-5	Number of slave nodes, NSN	I5
6-10	Number of master nodes, NMN	I5
11-20	External radius of rebar, R_o	E10.0
21-30	Compressive strength of concrete, f_c'	E10.0
31-40	Bond shear modulus, G	E10.0
41-50	Maximum shear displacement, u_{max}	E10.0
51-60	Exponent in damage curve, h_{dmg}	E10.0
61-70	Bond type flag, $IBOND$ EQ.0: elastic perfectly plastic GT.0: elastic-plastic with hardening	E10.0

Next, define the slave nodes as described below:

Cards 2, . . . , NSN+1

Columns		Quantity	Format	
1-5	(1-8)	Slave number EQ.0: the preceding slave number is incremented by 1	I5	(I8)
6-10	(9-16)	Node number	I5	(I8)

Omitted slave node definitions are automatically generated by incrementing the node numbers by

$$\frac{n_i - n_j}{s_i - s_j} \tag{345}$$

where s_i and s_j are the slave numbers on two successive cards, and n_i and n_j are their corresponding node numbers.

The master nodes are now defined as described below:

Cards NSN+2, . . . , NSN+NMN+1

Columns		Quantity	Format	
1-5	(1-8)	Master number EQ.0: the preceding slave number is incremented by 1	I5	(I8)
6-10	(9-16)	Node number	I5	(I8)

Omitted master node definitions are automatically generated by incrementing the node numbers by

$$\frac{n_i - n_j}{s_i - s_j} \tag{346}$$

where s_i and s_j are the master numbers on two successive cards, and n_i and n_j are their corresponding node numbers. The master nodes must be given in the order in which they appear as one moves along the slideline.

One-dimensional slidelines are useful for modeling the pullout of reinforcing bars from concrete structures. The present formulation was developed by Pelesson (1989). The concrete body is modeled using solid elements, and the reinforcing bars are modeled using truss or beam elements. The solid elements and beam elements should not have any nodes in common. A line of nodes along the intersection of solid elements is defined as the master line, and a line of nodes (connected by beam or truss elements) is defined as the slave line.

The bond between the reinforcing bars (beams) and concrete (solids) may be either elastic perfectly plastic ($IBOND = 0$) or elastic-plastic with strain hardening ($IBOND > 0$). In either case, a maximum allowable slip d_{max} is found from

$$d_{max} = u_{max} e^{-h_{dmg} D}, \tag{347}$$

where u_{max} and h_{dmg} are input parameters and D is a damage parameter to be discussed below. For the perfectly plastic bond model, the shear force at step $n + 1$ is found from

$$f_{n+1} = min(f_n - GA_s d, GA_s d_{max}), \tag{348}$$

where d is the nondimensional increment in slideline displacement (i.e., bond shear strain), A_s is the shear area of the concrete-bar bond, G is the bond shear modulus, and f_n is the bond shear force at the previous time step. For the elastic-plastic bond with hardening, the updated bond shear force is given by

$$f_{n+1} = f_n + \Delta f_{max}(1 - e^{-d/|d|}), \tag{349}$$

where

$$\Delta f_{max} = GA_s d_{max} - f_r. \tag{350}$$

The evolution of damage is related to the increment in shear force $\Delta f = f_{n+1} - f_n$ by

$$D_{n+1} = D_n + |d| - \frac{|f_{n+1} - f_n|}{GA_s}. \tag{351}$$

4.46 MASS PROPORTIONAL GENERALIZED RAYLEIGH DAMPING

Define *MDAMP* mass proportional damping definitions as specified in section 4.1 on page 62. Use one card for each definition.

Columns	Quantity	Format
1-10	Fraction of critical damping, *FCRTL*	E10.0
11-20	Frequency (rads/time) to be damped, *FREQ*	E10.0
21-30	Time at which mass proportional damping starts, *TMON*	E10.0
31-40	Time at which mass proportional damping ends, *TMOFF*	E10.0

Mass proportional damping is applied to all active nodes, and the damping factor, controlled by *FCRTL* and *FREQ*, can vary with analysis time. Mass proportional damping initiates when the analysis time reaches *TMON* of the first definition. When multiple and temporally varying damping coefficients are specified, the definitions must be defined in non-overlapping chronological order. The damping coefficient is assumed zero during periods in which *FCRTL* and *FREQ* are undefined.

This global damping capability is based on concepts from Rayleigh damping in linear analysis. In traditional Rayleigh damping, a global damping matrix $\mathbf{C}$ is constructed as a linear combination of the mass matrix $\mathbf{M}$ and stiffness matrix $\mathbf{K}$ as

$$\mathbf{C} = \alpha\mathbf{M} + \beta\mathbf{K}, \tag{352}$$

where α and β are damping mass proportional and stiffness proportional coefficients, respectively. During any time period, this approach can be used to introduce a specified fraction of critical damping at a selected frequency. The mass proportional damping coefficient α is related to *FCRTL* and *FREQ* by

$$\alpha = 2(FREQ)(FCRTL). \tag{353}$$

The stiffness proportional constant β may be specified by material to give additional flexibility in the introduction of viscous dissipation into the model. (See section 4.47 on page 414.)

Mass proportional damping yields a fraction of critical damping which decreases with increasing frequency, whereas stiffness proportional damping produces a fraction of critical damping which increases with frequency.

4.47 STIFFNESS PROPORTIONAL GENERALIZED RAYLEIGH DAMPING

Define stiffness proportional Rayleigh damping for *NDAMP* materials as specified in section 4.1 on page 62. Use one card for each material stiffness proportional damping definition.

Columns	Quantity	Format
1-5	Material number, n	I5
6-15	Stiffness proportional damping constant for this material, β_n	E10.0
16-25	Effective Young's modulus for damping computations, E_n	E10.0
26-35	Effective Poisson's ratio for damping computations, ν_n	E10.0

Stiffness proportional damping constants and effective elastic material parameters should be specified for materials where stiffness proportional damping is desired. Materials for which damping parameters are not defined will have zero stiffness proportional damping.

This global damping capability is based on concepts from Rayleigh damping in linear analysis. In traditional Rayleigh damping, a global damping matrix $\mathbf{C}$ is constructed as a linear combination of the mass matrix $\mathbf{M}$ and stiffness matrix $\mathbf{K}$ as

$$\mathbf{C} = \alpha\mathbf{M} + \beta\mathbf{K}, \tag{354}$$

where α and β are damping coefficients. This approach can be used to introduce a specified fraction of critical damping at two frequencies, since two parameters are available. The mass proportional damping coefficient α is specified in section 4.46 on page 413. The stiffness proportional constant β may be specified by material to give additional flexibility in the introduction of viscous dissipation into the model.

When used with nonlinear material models, the stiffness proportional damping is found using the isotropic elastic part of the material stiffness constructed using the elastic constants specified above. This approach prevents the amount of damping from varying with the material behavior (such as plastic yielding), and allows accurate computation of the degree of damping introduced into the model.

Mass proportional damping yields a fraction of critical damping which decreases with increasing frequency, whereas stiffness proportional damping produces a fraction of critical damping which increases with frequency.

4.48 MATERIAL INITIALIZATION FOR ROTATIONAL MOTION

Define *NMROT* materials or node range sets to have initial nodal velocities computed for rotational motion as specified on Control Card 9 in section 4.1 on page 62. Repeat the following group of cards for each material initialization set.

Card 1

Columns	Quantity	Format
1-10	x-component of angular velocity $\boldsymbol{w}$	E10.0
11-20	y-component of angular velocity $\boldsymbol{w}$	E10.0
21-30	z-component of angular velocity $\boldsymbol{w}$	E10.0
31-40	x-component of center of rotation point P	E10.0
41-50	y-component of center of rotation point P	E10.0
51-60	z-component of center of rotation point P	E10.0
61-65	Number of materials in set (or flag for nodal definition), *NUMMT* GT. 0: Number of materials in this set LT. 0: Node set defined by inclusive nodal pair	I5
66-70	Nodal velocity superposition flag, *IND* EQ. 0: Initial velocities are calculated from the prescribed rotational motion. EQ. 1: Initial velocities from the prescribed rotations are added to any previously defined initial velocities	I5

Define the following cards when prescribing rotational motion by material set.

Cards 2, . . .

Columns	Quantity	Format
1-5	First material to be initialized	I5
6-10	Second material to be initialized	I5

.	.	.
.	.	.
.	.	.
76-80	Sixteenth material to be initialized	I5

Continue on additional cards, sixteen materials per card, until all *NUMMT* materials have been listed.

Define the following card when prescribing rotational motion by inclusive nodal pairs.

Cards 2, . . .

Columns	Quantity	Format
1-5	First node in inclusive set to be initialized	I5
6-10	Last node in inclusive set to be initialized	I5

Materials are initialized for rotational motion by computing initial velocities from $\mathbf{v} = \boldsymbol{w} \times \mathbf{r}$ for all nodes of all elements using the listed materials or for all nodes, including the first and last nodes, using the nodal set. If static initialization is used (via either input from NIKE3D or dynamic relaxation in DYNA3D), $\mathbf{r}$ is evaluated using the *post-initialization* geometry. This feature is useful when using DYNA3D for the transient dynamic analysis of rotating machinery, such as the impact of a foreign object into a spinning fan.

The superposition flag *IND*, facilitates the initialization of simultaneous translational and rotational motions. When used, this option adds the nodal velocities components from the current rotational motion to the previously defined nodal velocities. Thus, a combined translation and rotational motion can be prescribed by defining the translation motion with the initial nodal conditions (see INITIAL CONDITIONS on page 350) and then superimposing the rotational motion on top of it. Alternatively, a local rotational motion may be prescribed about a point that itself is rotating in space. In this case two definitions would be required and the relative angular velocity should be specified.

4.49 BODY FORCE LOADS BY MATERIAL

Define *NMBDF* sets of materials to have body force loads applied as specified on Control Card 9 in section 4.1 on page 62. The first six cards define the desired body force load components and the corresponding load curves, and the remaining cards list the materials affected. Repeat the following group of cards for each material initialization set.

Card 1

Columns	Quantity	Format
1-5	Load curve number giving time variation for x-direction base acceleration EQ.0: no x-direction base acceleration body force	I5
6-15	Scale factor on x-direction base acceleration EQ.0.0: default set to "1.0"	E10.0

Card 2

Columns	Quantity	Format
1-5	Load curve number giving time variation for y-direction base acceleration EQ.0: no y-direction base acceleration body force	I5
6-15	Scale factor on y-direction base acceleration EQ.0.0: default set to "1.0"	E10.0

Card 3

Columns	Quantity	Format
1-5	Load curve number giving time variation for z-direction base acceleration EQ.0: no z-direction base acceleration body force	I5
6-15	Scale factor on z-direction base acceleration EQ.0.0: default set to "1.0"	E10.0

Card 4

Columns	Quantity	Format
1-5	Load curve number giving time variation for angular velocity about x-axis EQ.0: no body force due to angular velocity about x-axis	I5
6-15	Scale factor on angular velocity about x-axis EQ.0.0: default set to "1.0"	E10.0

Card 5

Columns	Quantity	Format
1-5	Load curve number giving time variation for angular velocity about y-axis EQ.0: no body force due to angular velocity about y-axis	I5
6-15	Scale factor on angular velocity about y-axis EQ.0.0: default set to "1.0"	E10.0

Card 6

Columns	Quantity	Format
1-5	Load curve number giving time variation for angular velocity about z-axis EQ.0: no body force due to angular velocity about z-axis	I5
6-15	Scale factor on angular velocity about z-axis EQ.0.0: default set to "1.0"	E10.0

Cards 7, . . .

Columns	Quantity	Format
1-5	Number of materials defined in this set, $NUMMAT$	I5
6-15	x-component of center of rotation point P	E10.0
16-25	y-component of center of rotation point P	E10.0
26-35	z-component of center of rotation point P	E10.0

Cards 8, . . .

Columns	Quantity	Format
1-5	First material to be initialized	I5
6-10	Second material to be initialized	I5
.	.	.
.	.	.
.	.	.
76-80	Sixteenth material to be initialized	I5

Continue on additional cards, sixteen materials per card, until all $NUMMAT$ materials have been listed.

Specify a load curve number of zero for body force load components which are not active.

Body force loads arising from base acceleration (gravity) or from rotational motion may be specified for a selected set of materials using this option. This capability is especially useful for static initialization of centrifugal stresses in rotating bodies or gravity stresses in soil prior to a transient dynamic analysis.

The angular velocity may be specified about any point $\boldsymbol{P}$ by prescribing non-zero components for $\boldsymbol{P}$. Thus, the local apparent velocity of a point located at position $\boldsymbol{R}$ is interpreted as $\boldsymbol{v} = \omega \times (\boldsymbol{R} - \boldsymbol{P})$.

This option may *not* be used in combination with the global body force options Prescribed Base Acceleration and Prescribed Angular Velocity. Those two options apply body force to the entire model instead of selectively by material.

This option is intended to work on disjoint parts, and slight inaccuracies may result if body forces are applied to only part of a monolithic structure. If body force loads by material are specified for a rigid body composed of multiple materials using the rigid body merge feature, then all materials composing that rigid body should be listed to receive body force loads.

4.50 CVS (MADYMO/ATB) COUPLING DATA

Define ellipsoids for coupling as defined on Control Card 4 in section 4.1 on page 62.

Card 1 - NMADEL

Specify *NMADEL* cards to define the ellipsoids for coupling.

Columns	Quantity	Format
1-5	Ordinal position of the ellipsoid in the MADYMO/ATB input	I5
6-10	DYNA3D material number of the corresponding rigid ellipsoid	I5

Define metrics to convert from CVS to DYNA3D, e.g. $Length_{CVS} \times metric = Length_{DYNA3D}$

Card NMADEL+1

Columns	Quantity	Format
1-10	Time metric Eq.0.0: default set to “1.0”	E10.0
11-20	Length metric Eq.0.0: default set to “1.0”	E10.0
11-20	Force metric Eq.0.0: default set to “1.0”	E10.0

When MADYMO is used as the CVS code, the ordinal position refers to the position of the ellipsoid definition in the COUPLING input section. When ATB is used as the CVS code, modifications must be made to the ATB source code to define a list of coupling ellipsoids and to implement the PVM interface as defined below.

This coupling option allows the CVS representation of the occupant to impact interior surfaces in the passenger compartment modeled in DYNA3D, and thus yields a more realistic simulation. In the current implementation of this coupling, during a time step the CVS program gives to DYNA3D the positions and orientations of each ellipsoid. DYNA3D then uses its contact algorithms to evaluate the total force and moment arising from impact between the ellipsoid and the occupant environment, and transmits this information back to the CVS code. To use this full coupling, the DYNA3D model should contain a geometric representation of the ellipsoids in the CVS model, and each ellipsoid should be defined as a separate DYNA3D rigid material.

4.51 AIR BAG GAS FLOW DEFINITIONS

Define *NUMAIR* air bag gas flow models as specified on Control Card 4. Define all *NUMAIR* control card sets first, then define segment definition cards as needed.

Card Sets1, ... , NUMAIR

Two control cards are needed for each air bag model.

Control Card 1

Columns	Quantity	Format
1-8	Number of segments (element surfaces) that define the air bag's exterior surface which fully encloses its volume, $NUMSEG$.	I8
9-16	Number of node or rigid material used to trigger gas flow into air bag.	I8
17-20	Trigger option, OPT: OPT.LT.0: Node number used. OPT.GT.0: Rigid material used. ABS(OPT).EQ.1: acceleration magnitude used. ABS(OPT).EQ.2: x-direction acceleration component used. ABS(OPT).EQ.3: y-direction acceleration component used. ABS(OPT).EQ.4: z-direction acceleration component used.	I4
21-30	Threshold acceleration magnitude, $A_{Threshold}$	E10.0
31-40	Minimum time to trigger, t_{min}. All accelerations before this time are ignored.	E10.0
41-50	Dwell time, t_{dwell}. The trigger acceleration must exceed the threshold acceleration $A_{Threshold}$ for a minimum of t_{dwell} before gas flow is triggered (initiated.)	E10.0
51-55	Load curve number giving the mass flow rate, $\dot{m}_{in}$, in to the air bag versus relative time. Time is specified relative to the trigger time.	I5
56-60	Load curve number giving the absolute temperature of incoming gas, T_{in}, versus relative time. Time is specified relative to the trigger time. Note, the residual air bag gas at initiation is presumed to be at the temperature corresponding to $T_{in}(t = 0)$.	I5
61-70	Absolute atmospheric pressure, P_{atm}.	E10.0
71-80	Effective gas constant, $\bar{R}$.	E10.0

Control Card 2

Columns	Quantity	Format
1-10	Constant coefficient of the effective constant-pressure specific heat, a.	E10.0
11-20	Linear coefficient of the effective constant-pressure specific heat, b.	E10.0
21-30	Effective exhaust area, D.	E10.0
31-35	Print interval, $Pint$. EQ.0: No information printed. GT.0: Step interval between prints of the air bag's relative pressure, volume, and temperature to the *hsp* file.	I5
36-40	Exhaust hole segment number, $NUMHOLE$. EQ.0: Exhaust area does not change with deformation. GT.0: Segment number used to scale exhaust area.	I5

SEGMENT DEFINITIONS

Card 1, ..., NUMSEG

For each of the $NUMAIR$ air bag models, define $NUMSEG$ segment definition cards.

Columns		Quantity	Format	
1-10	(-)	Segment number	I10	(omit)
11-15	(6-13)	Node n_1 (see Figure 33)	I5	(I8)
16-20	(14-21)	Node n_2	I5	(I8)
21-25	(22-29)	Node n_3	I5	(I8)
26-30	(30-37)	Node n_4	I5	(I8)

Each air bag is defined by a set of $NUMSEG$ segments (element faces) that enclose the entire air bag volume. The air bag is assumed to be simply connected and the node numbering convention, defined in Figure 28, must produce a normal vector, $\boldsymbol{n}$, which points outward from the enclosed air bag volume. During inflation, positive relative pressure produces nodal forces that act in the direction of instantaneous $\boldsymbol{n}$, i.e. outward from the bag's interior and normal to the segment faces in the current configuration.

Air bag inflation is triggered by the acceleration of either a node or a rigid material. For time greater than t_{min}, the current absolute value of the specified node or rigid material acceleration is compared to the threshold acceleration magnitude, $A_{Threshold}$. The value of OPT determines whether the controlling node/material's entire acceleration magnitude is used or just one of its acceleration components. The air bag's gas flow is initiated when the controlling node's or rigid material's acceleration exceeds $A_{Threshold}$ for the minimum time t_{Dwell}. If $t_{min} = 0$ and $t_{Dwell} = 0$, the air bag will begin to inflate the first time the threshold acceleration is exceeded.

The gas behavior is represented by an isentropic ideal gas relationship which assumes that uniform conditions exist inside the air bag. Gas is assumed to enter the air bag at the mass rate, $\dot{m}_{in}(t_r)$, and the temperature, $T_{in}(t_r)$, prescribed by the load curves. Here t_r is the relative time from the start of inflation, i.e. $t_r = 0$ when inflation initiates. The rate of gas mass that leaves the air bag is controlled by the relative pressure differential between the interior and exterior of the air bag and can be expressed as:

$$\dot{m}_{ex} = D\frac{mT}{V}\sqrt{\left(\frac{2C_p}{T}\right)\left[\left(\frac{P_{atm}}{P}\right)^{2/\gamma} - \left(\frac{P_{atm}}{P}\right)^{\frac{\gamma+1}{\gamma}}\right]} \tag{355}$$

where the air bag's internal pressure, volume, and mass are given by P, V, and m, respectively. The effective constant-pressure specific heat, C_p, is assumed to be linear in absolute temperature, T, and be given by

$$C_p = a + bT \tag{356}$$

where a and b are the effective constant and linear coefficients, respectively. Furthermore, the constant-volume specific heat, C_v, is defined to be

$$C_v = C_p - \bar{R} \tag{357}$$

with $\gamma = \dfrac{C_p}{C_v}$. The effective exhaust area D is given by

$$D = A_{ex}\sqrt{1-K} \tag{358}$$

where A_{ex} is the exhaust area and K is the head loss coefficient based upon the exit velocity.

Conservation of mass yields the first controlling differential equation for the rate of mass change, $\dot{m}$, occurring inside the air bag:

$$\dot{m} = \dot{m}_{in} - \dot{m}_{ex} \tag{359}$$

The second differential equation that governs temperature is derived from a standard rate equation of the first law for a control volume, i.e. conservation of energy. By assuming that the enthalpy of the incoming gas, h_{in}, is given by

$$h_{in} = \int_0^{T_{in}(t_r)} C_p dT \tag{360}$$

and the internal energy, u, is given by

$$u = \int_o^T C_v dT \tag{361}$$

then the rate of temperature change inside the air bag is expressed as

$$\dot{T} = \frac{\dot{m}_{in} T_{in} C_{p-in} - T\left[\dot{m} C_v + \dot{m}_{ex} C_p + m\bar{R}\frac{\dot{V}}{V}\right]}{mC_v} \tag{362}$$

Unless otherwise indicated by subscripts, all quantities pertain to the internal air bag variables. The instantaneous air bag volume, V, is obtained via

$$V = \int \frac{\boldsymbol{X}}{3} \bullet \boldsymbol{n} dA \ . \tag{363}$$

The surface integration is performed over all exterior surface segments using the current position vector, $\boldsymbol{X}$, and outward normal $\boldsymbol{n}$.

At initiation the current air bag volume, V_o, is calculated. Using the initial incoming gas temperature, T_o, defined as $T_o = T_{in}(t_r = 0)$, andV_o, the gas mass required to pressurize the air bag to atmospheric conditions, m_o, is calculated from

$$m_o = \frac{P_{atm} V_o}{T_o \bar{R}} \tag{364}$$

(For numerical reasons, a finite initial volume is required.) Using m_o and T_o for the initial conditions within the air bag, the two governing differential equations are integrated each step using an implicit, unconditionally stable, trapezoidal integration scheme. To ensure numerical accuracy,

integration error estimates are made at each time step. If the estimated error is greater than 0.001% of the current temperature or mass, the step is subdivided and the integration is performed again. This procedure ensures accurate results independent of the time step governing the global problem.

Deformation of the air bag's skin during inflation can substantially increase the exhaust orifice area, increasing $\dot{m}_{ex}$. To account for this behavior, the user can identify a specific segment whose relative area, $\frac{\alpha}{\alpha_o}$ (where α is the segment area), modulates the effective exhaust area A_{ex}. Although elements must completely enclose the entire air bag volume, the mechanical properties of the air bag hole(s) need not be the same as the other air bag elements.

The gas coefficients used, a and b, are effective quantities. They are obtained by appropriately averaging the contributions of all species present and then dividing the total quantities by the averaged molecular weight. Similarly, $\bar{R}$ is the universal gas constant, R, divided by the averaged molecular weight. Because effective gas properties are used, both single specie and poly species gases can be modeled.

For a complete description of the air bag formulation and implementation, see Kay and Zywicz (1994).

4.52 SLIDE SURFACE ACTIVATION/DEACTIVATION TIMES

Define *NUMSVT* activation/deactivation times for slide surfaces as specified on Control Card 4 in section 4.1 on page 62. Slide surface activation/deactivation times are not required for slide surfaces that remain active through out an analysis.

Card 1, ...,NUMSVT

Columns	Quantity	Format
1-5	Slide surface number to activate/deactivate	I5
6-15	Activation time during transient analysis (default $t = 0$)	E10.0
16-25	Deactivation time during transient analysis (default $t = 10^{20}$)	E10.0
26-35	Activation time during dynamic relaxation analysis (default $t = 0$)	E10.0
36-45	Deactivation time during dynamic relaxation analysis (default $t = 10^{20}$)	E10.0

Slide surfaces may be activated and deactivated during both the transient and dynamic relaxation portions of an analysis. This is an effective way to 1) simulate perforation, 2) alter contact attributes during an analysis, e.g. friction coefficients, or 3) minimize contact computational costs.

Slide surfaces are numbered in the order they are defined in the sliding interface definition section.

Care must be used when activating/deactivating slide surfaces of type 1, 2, 6, 7, 8, or 9. Surfaces of these types must be activate at the start of the analysis. Furthermore, these slide surfaces should not be deactivated during the dynamic relaxation portion of an analysis and then reactivated during the transient portion of an analysis.

4.53 DELAMINATION ELEMENTS

Define delamination elements in this section if $DELAM > 0$ on Control Card 4 in section 4.1 on page 62. Delamination element input follows the general organization of the entire DYNA3D input file: first the Delamination Element Control Section defines the number of delamination elements, number of material models, and sets optional delamination element default values. Next, each delamination element material model and associated parameters are specified in the Delamination Element Material Model Section. Then, the connectivity for all delamination elements is given in the Delamination Element Connectivity Section. All parameter input is keyword based, and delamination element connectivity is specified as free-formatted, space-delimited input.

The keyword and associated parameters are prescribed follow the same convention used to define the analysis control cards (see section 4.2 on page 73) and override any values defined previously.

Delamination Element Control Section

First, define the Delamination Element Control Section parameters. This section must be terminated with the **endfree** keyword.

elements *delam*	Number of delamination element
materials *ndeld*	Number of delamination element materials
tsmin *tsmin*	Default minimum timestep size for delamination element deletion (default value 0.0)
endfree	End keyword input

Delamination Element Material Model Section

Second, define *ndeld* delamination element material models. Each model definition begins with the keyword **material** and ends with the keyword **endfree**. Note, not all keywords are active for all material model types and that all model parameters need not be defined to fully specify the traction-displacement relationship.

material *number* — Begin definition of delamination material number *number.* Note, *number* need not be inclusive between 1 and *ndeld*. For example, the delamination material numbers might range from $nmmat + 1$ to $nmmat + ndeld$, where $nmmat$ is the number of conventional material definitions in the problem.

endfree — End keyword input

Note: This section is also used to define cohesive element material models.

eta η — Linear viscosity coefficient for material type 2. (Default 0.0)

g1 G_1 — Mode I toughness or fracture energy. (Units: *energy/crack area)*

g2 G_2 — Mode II toughness or fracture energy. (Units: *energy/crack area)*

k1b K_1 — Mode I stiffness. (Units: *stress/length)*

k2b K_2 — Mode II stiffness. (Units: *stress/length)*

model *model* — Material model type:
Eq.1: Original SNL model
Eq.2: Single internal damage variable model

s1cr S_1^{cr} — Mode I critical stress. (Units: *stress)*

s2cr S_2^{cr} — Mode II critical stress. (Units: *stress)*

tsmin *tsmin* — Minimum timestep size for delamination element deletion. This value overrides the global value for this material model. (default value 0.0)

u1cr U_1^{cr} — Mode I critical displacement. (Units: *length)*

u2cr U_2^{cr} Mode II critical displacement (Units: *length)*

u1max U_1^{max} Mode I maximum displacement. (Units: *length)*

u2max U_2^{max} Mode II maximum displacement (Units: *length)*

Note, for each mode, either the critical displacement or critical stress and either the maximum displacement or toughness need be specified. The remaining terms will be internally calculated. Also, $U_1^{max} > U_1^{cr}$ and $U_2^{max} > U_2^{cr}$.

Delamination Element Connectivity Section

Define *delam* delamination element definitions. Each definition consists of the following free-formatted, space-delimited data set. The element definitions may be specified in any order, i.e., they are independent of the actual delamination element number.

Quantity	Format
Delamination element number	Integer
Delamination material number	Integer
Node n_1	Integer
Node n_2	Integer
Node n_3	Integer
.	.
.	.
Node n_7	Integer
Node n_8	Integer

Delamination elements should be defined using the same ordering convention used for solid 6-node and 8-node elements (see Figure 28). In addition, the shell elements connected by the delamination element must reside on opposite faces, as in Figure 43, and connect two and only two shell elements.

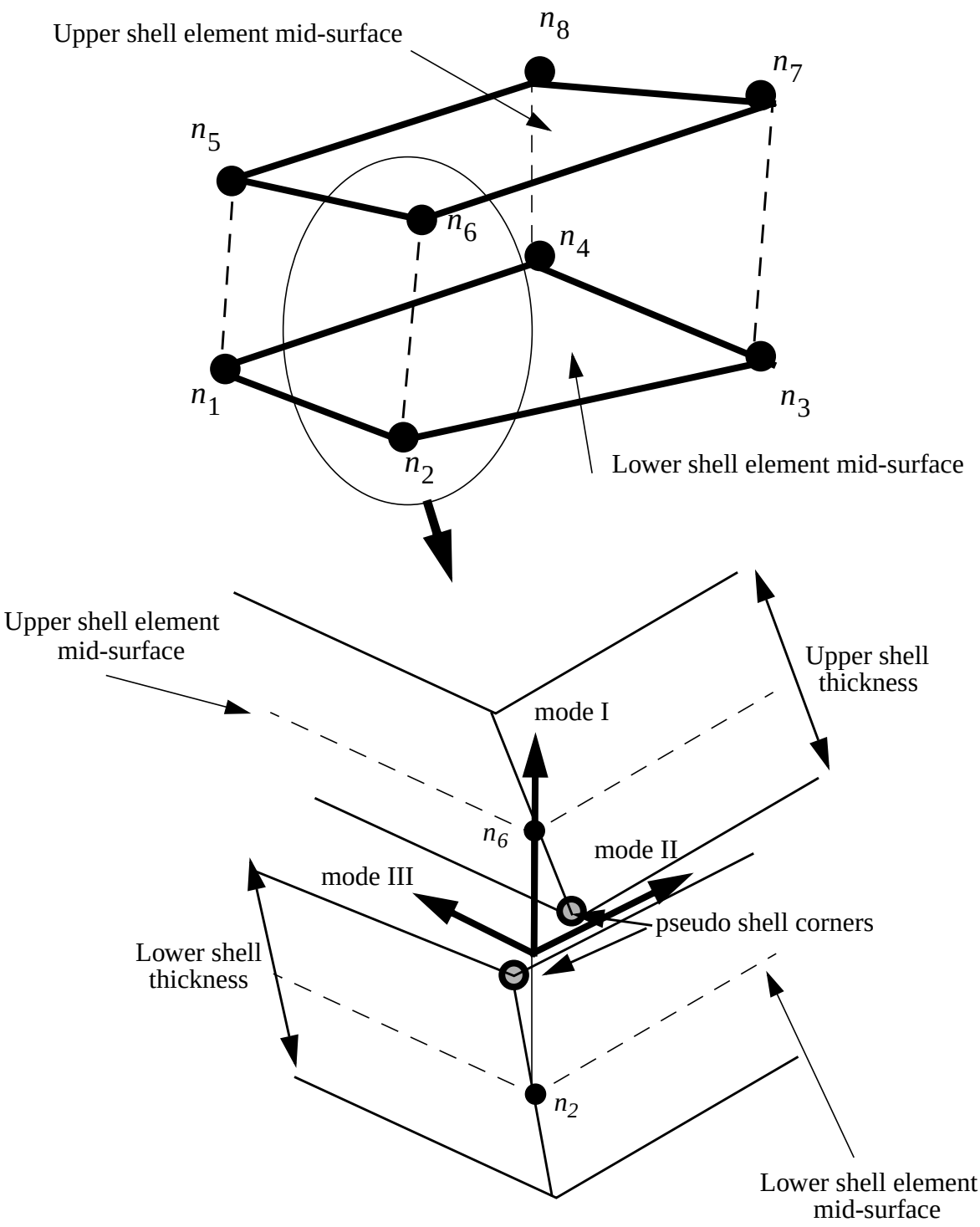

Figure 43
DYNA3D delamination element geometry and local delamination coordinate system.

Delamination elements are used to simulate cohesion or interlaminar forces between “parallel”, but offset, pairs of stacked shell elements. The original element formulation and implementation in DYNA3D was developed by Reedy, et. al. (1997, 1996). In it, delamination elements employ traction-displacement relationships to generate nodal forces and moments based upon the projected displacements of the shell element corners (see Figure 43) in opening (mode I) and inplane shear (mode II) directions. The instantaneous local mode I direction is established by connecting the adjacent nodes. The mode II and III directions are orthogonal to the mode I direction and point essentially along the mid-surface edges. The total modal displacements, $\boldsymbol{u}=(u_I, u_{II}, u_{III})^t$ are obtained by integrating the differences in the projected corner velocities with time.

Delamination and Cohesive Element’s Traction-Displacement Concepts

Although the delamination or cohesive element’s mode I (u_I) displacement corresponds to the traditional fracture mechanics opening mode, i.e., mode I, the delamination element’s displacement modes II and III represent orthogonal components of the traditional inplane shear mode, i.e., fracture mechanic’s mode II. Consequently, it is convenient to define the effective mode II displacement $\bar{u}_{II}$ by

$$\bar{u}_{II} = \sqrt{u_{II} + u_{III}} \tag{365}$$

when considering damage.

The traction-displacement laws relate the modal displacement vector $\boldsymbol{u}$ to the local surface traction vector $\boldsymbol{t}$ as

$$\boldsymbol{t} = \boldsymbol{K}(\boldsymbol{d})\boldsymbol{u} \tag{366}$$

Here $\boldsymbol{K}$, the stiffness matrix, initially has the form

$$\boldsymbol{K} = \begin{bmatrix} K_1 & 0 & 0 \\ 0 & K_2 & 0 \\ 0 & 0 & K_2 \end{bmatrix} \tag{367}$$

and $\boldsymbol{d}$ represents the vector of internal damage variables. The critical stress at which damage initiates under pure mode I loading, S_1^{cr}, is given by $S_1^{cr} = K_1 \times u_I$. Similarly, the critical stresses at damage initiation under pure mode II is given by $S_2^{cr} = K_2 \times u_{II}$.

Figure 44 shows the traction-displacement relationship for pure mode I and II loadings for models 1 and 2. The toughness or energy dissipated in pure mode I or mode II loading is given by G_1 and G_2. During unloading, the current secant stiffness is used. When $u_1 < 0$, the full K_1 is employed.

Model 1, SNL's original relationship, employs two internal damage variables, d_1 and d_2, to scale the mode I and II stiffnesses as

$$\boldsymbol{K} = \begin{bmatrix} K_1 \times d_1 & 0 & 0 \\ 0 & K_2 \times d_2 & 0 \\ 0 & 0 & K_2 \times d_2 \end{bmatrix} \tag{368}$$

and generate a bi-linear response under pure mode I or mode II loading. The damage variables initially start at 1 and progress to 0 and are based upon u_I and $\bar{u}_{II}$, respectively. Consequently, G_1 and G_2 are related to the critical tractions and maximum displacements via

$$G_1 = \frac{S_1^{cr} \times U_1^{max}}{2} \text{ and } G_2 = \frac{S_2^{cr} \times U_2^{max}}{2}, \tag{369}$$

respectively. When $d_1 > \frac{1}{2}$ and $d_2 > \frac{1}{2}$, the damage variables evolve independently and damage in one mode does not influence the behavior in the other mode. However, when either d_1 and d_2, decrease below 1/2, both d_1 and d_2, are set to the minimum of value d_1 and d_2 and the damage evolution and response becomes coupled.

Model 2, developed within a thermodynamic framework (for example, see Govindjee, 1995), uses the single damage variable *d* to evolve damage in both mode I and II simultaneously. The damage surface, expressed in terms of the traction components**,** is given by

$$\phi = \sqrt{t_1 \frac{(|t_I| + t_I)}{2} + \left(\frac{S_1^{cr}}{S_2^{cr}}\right)^2 (t_{II}^2 + t_{III}^2)} + \frac{S_1^{cr}}{X} - \frac{\eta}{\Delta t}\Delta d \tag{370}$$

$$X = Exp\left(\frac{d}{U_1^{max}}\right) \tag{371}$$

Here Δt and Δd denote the present time step size and current increment in damage, respectively, and η is the viscosity in pure mode I loading. (The effective viscosity in pure mode II loading is given by $\eta\,(S_1^{cr} U_1^{max}) / (S_2^{cr} U_2^{max})$.) The damage variable *d* is required to evolve such that $\Delta d \times \phi = 0$ and $\Delta d \geq 0$ for all times. The complete model consists of equations (366), (368)-(371), and d_1 and d_2, defined as

$$d_1 = \begin{cases} \dfrac{S_1^{cr}}{(S_1^{cr} + U_1^{max} K_1 (X - 1))} & u_I \geq 0 \\ 1 & u_I < 0 \end{cases} \tag{372}$$

$$d_2 = \frac{S_2^{cr}}{(S_2^{cr} + U_2^{max} K_2 (X - 1))} \tag{373}$$

Note, U_1^{max} and U_2^{max} do not have the exact same physical meaning as they do in model 1.

Under pure mode I or II loading, the traction-displacement response appears bi-linear with a small tail that asymptotes to zero. When $\eta > 0$, rate effects increase the area under the curve and elongate the tail region. Note, the model can be run without rate effects by simply specifying $\eta = 0$

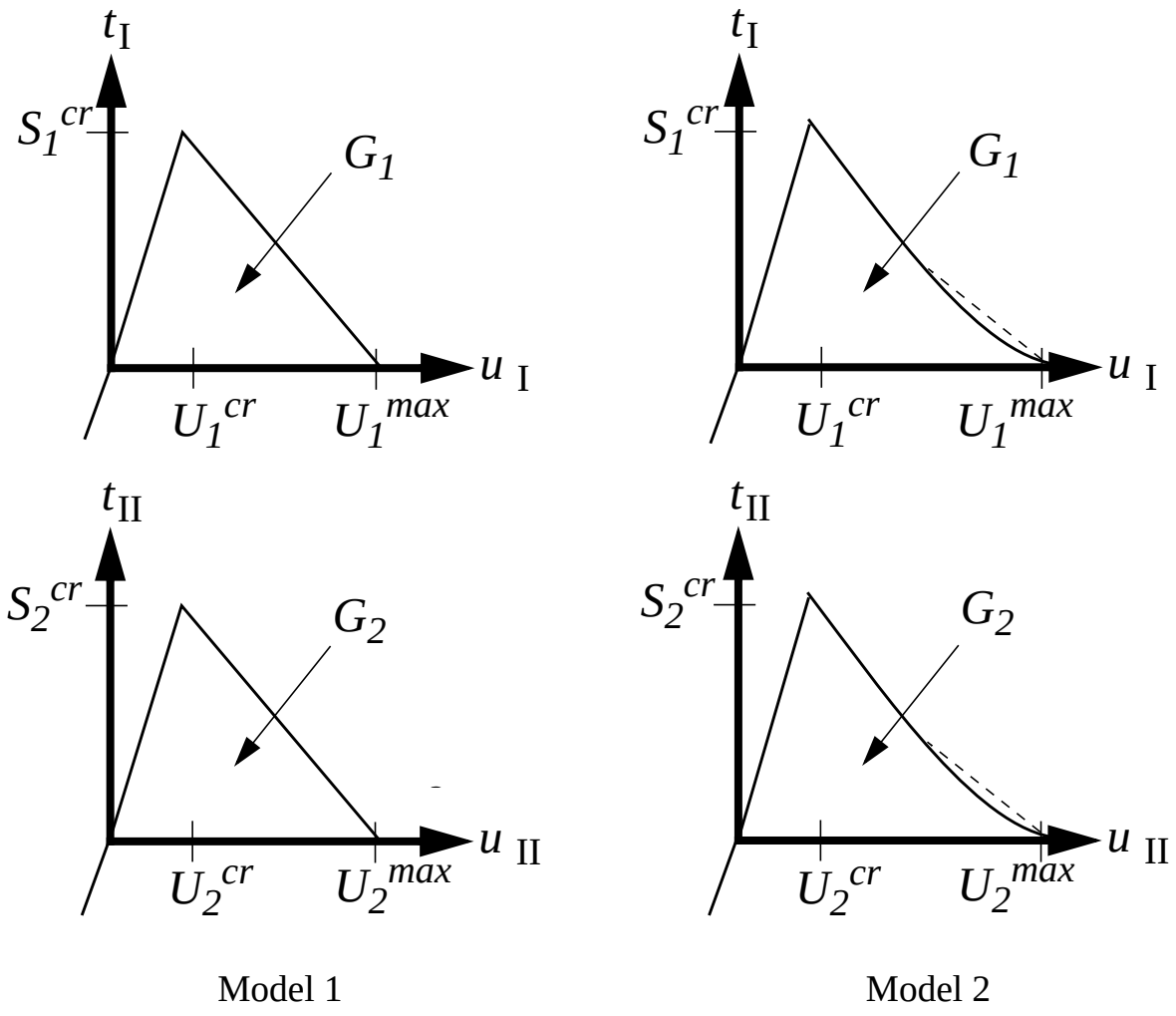

Figure 44:Traction-displacement behavior for models 1 and 2 under pure mode I and II loadings.

Delamination and cohesive elements remain active in the calculation until one of the damage variables reaches a critical level (model 1: d_1 or d_2 equal zero, model 2: $X = 10^6$), either of the associated shell elements are deleted from the calculation (for example, due to element failure), or the element time-step size falls below *tsmin*. In order to prevent the associated shell or hex elements from penetrating each other, slide surfaces should be define. When using automatic contact or conventional slidesurface with the “thickness” option, local deformation sometimes causes the shell elements to contact and the delamination element to fail prematurely. The slidesurface option *thicsl* is helpful in eliminating this artificial behavior, e.g. $thicsl = 0.9$.

Delamination and cohesive elements are included in the state plot files as additional brick elements. To avoid conflicts, both the element and material numbers maybe renumbered as described in the `hsp` file. The three traction components (*I, II,* and *III*) and the mode *I* and *II* internal damage variables (*d)* are element averaged and outputted as the *x, y, z, xy,* and, if active, *yz,* stress components, respectively.

4.54 COHESIVE ELEMENTS

Define cohesive elements in this section if $NUMCOH > 0$ on Control Card 4 in section 4.1 on page 62. Cohesive element input follows the general organization of the entire DYNA3D input file: first the Cohesive Element Control Section defines the number of cohesive elements, number of material models, and sets optional cohesive element default values. Next, each cohesive element material model and associated parameters are specified in the Cohesive Element Material Model Section. Then, the connectivity for all cohesive elements is given in the Cohesive Element Connectivity Section. All parameter input is keyword based, and cohesive element connectivity is specified as free-formatted, space-delimited input.

Cohesive and delamination elements
The keyword and associated parameters are prescribed follow the same convention used to define the analysis control cards (see section 4.2 on page 73) and override any values defined previously.

Cohesive Element Control Section

First, define the Delamination Element Control Section parameters. This section must be terminated with the **endfree** keyword.

elements *numcoh*	Number of cohesive element
materials *ncohd*	Number of cohesive element materials
tsmin *tsmin*	Default minimum timestep size for cohesive element deletion (default value 0.0)
endfree	End keyword input

Cohesive Element Material Model Section

Second, define *ncohd* cohesive element material models. Each model definition begins with the keyword **material** and ends with the keyword **endfree**. Note, not all keywords are active for all material model types and that all model parameters need not be defined to fully specify the traction-displacement relationship.

material *number*	Begin definition of cohesive material number *number.* Note, *number* need not be inclusive between 1 and *ncohd*. For example, the cohesive material numbers might range from $nmmat + 1$ to $nmmat + ncohd$, where $nmmat$ is the number of conventional material definitions in the problem.
endfree	End keyword input

Cohesive elements and delamination elements have common traction-displacement material laws. Thus, the input parameters are exactly the same as that listed for delamination elements (see, Delamination Element Material Model Section on page 430).

Cohesive Element Connectivity Section

Define *numcoh* cohesive element definitions. Each definition consists of the following free-formatted, space-delimited data set. The element definitions may be specified in any order, i.e., they are independent of the actual delamination element number.

Quantity	Format
Cohesive element number	Integer
Cohesive material number	Integer
Node n_1	Integer
Node n_2	Integer
Node n_3	Integer
.	.
.	.
Node n_7	Integer

Node n_8	Integer

Cohesive elements should be defined using the same ordering convention used for solid 6-node and 8-node elements (see Figure 28). In addition, the hex elements connected by the delamination element must reside on opposite faces, as in Figure 45, and connect two and only two hex elements. The upper and lower cohesive element nodes should be coincidental initially.

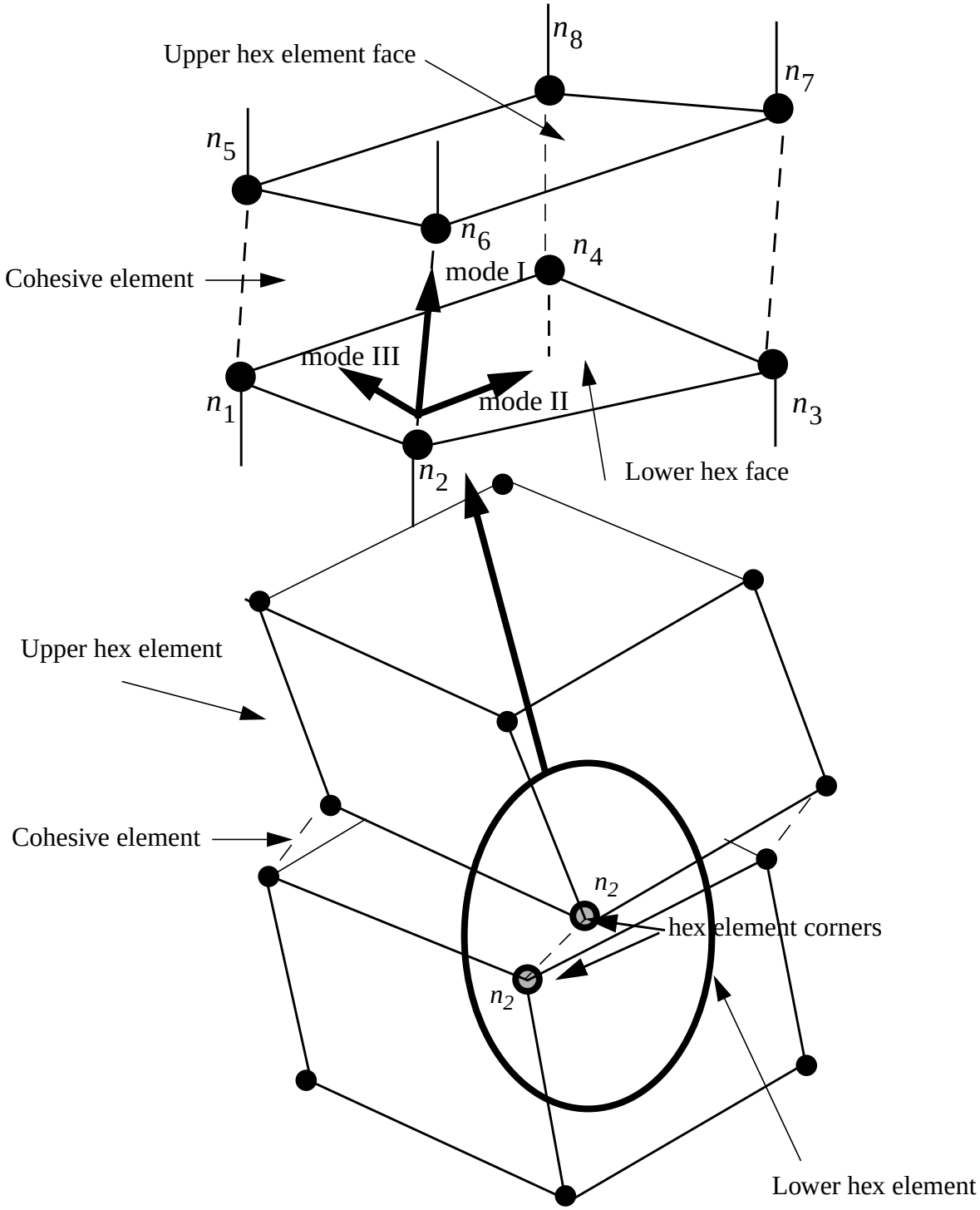

Figure 45
DYNA3D cohesive element geometry and local delamination coordinate system.

Cohesive elements are used to simulate cohesion or interlaminar forces between “parallel”hex elements. Cohesive elements employ traction-displacement relationships to generate nodal forces based upon the projected displacements of the hex element corners (see Figure 43) in opening (mode I) and inplane shear (mode II) directions. The instantaneous local mode I direction is established by connecting the adjacent nodes. The mode II and III directions are orthogonal to the mode I direction and point essentially along the mid-surface edges. The total modal displacements, $\boldsymbol{u}=(u_I, u_{II}, u_{III})^t$ are obtained by integrating the differences in the projected corner velocities with time.

Cohesive elements and delamination elements share common traction-displacement laws and kinematic idealizations. For a detailed description of these, see Delamination and Cohesive Element’s Traction-Displacement Concepts on page 433.

5.0 RESTART INPUT FORMAT

The following sections describe the format of the DYNA3D restart input file. The procedure for initiating a DYNA3D restart analysis is described in section 3.4 on page 56.

The specification of a restart input file is optional when restarting an analysis which was terminated before the termination time specified in the initial input file. If no changes to the model or analysis parameters are desired, the restart may be initiated by omitting the restart input file and specifying only the restart dump file (or the running restart file) which contains the desired starting point data. DYNA3D will then resume execution and continue until the termination time specified in the original input file.

A restart input file is required when restarting a run which completed normally (to, for example, increase the termination time), when changes to the model or analysis parameters are desired, or when stress initialization files for NIKE3D or DYNA3D are to be generated. A restart input file may be used to:

- change the termination time,
- change the time interval between writes of time history plot data,
- change the time interval between writes of state plot data,
- delete sliding interfaces,
- delete materials,
- delete solid, beam, shell, or thick shell elements,
- reset the time step scale factor,
- reset the interval between restart or running restart dumps,
- change the global rigid-body translational velocity,
- change the definitions of rigid walls.

If a restart input file is used, it should be specified along with the appropriate restart dump file (or running restart file) on the DYNA3D command line used to initiate the restart. The restart input file must contain cards 1, 2, and 3

Changes made at a restart will be reflected in all subsequent restart dumps.

After a restart, the familied files for the state plot database, time history database, and restart dump files will retain their original names (by default) and will continue with numbering according to the original sequence. This allows convenient plotting of the entire analysis results using only one family of plot database files.

5.1 TITLE CARD

Card 1

Columns	Quantity	Format
1-72	Heading or problem title	12A6
76-80	Format option for node numbers Input “large” if node numbers exceed 99999.	A5

Note that in the following input description, column numbers and format descriptors in parenthesis apply to the “large” input format option.

5.2 RESTART CONTROL

Card 2

Columns	Quantity	Format
1-10	New termination time EQ.0.0: termination time remains unchanged	E10.0
11-20	New time interval between writes of time history plot data EQ.0.0: interval remains unchanged	E10.0
21-30	New time interval between writes of state plot data EQ.0.0: interval remains unchanged	E10.0
31-35	Number of sliding interfaces to be deleted (maximum of 48)	I5
36-40	Number of materials to be deleted	I5
41-45	Number of solid element blocks to be deleted	I5
46-50	Number of beam element blocks to be deleted	I5
51-55	Number of 4-node shell element blocks to be deleted	I5
56-60	Number of 8-node thick shell element blocks to be deleted	I5

Note that sliding interfaces and materials to be deleted are simply listed, but elements to be deleted are specified in blocks, or groups of elements. Groups are defined by giving the first and last element numbers of a consecutive sequence of elements to be deleted.

Card 3

Columns	Quantity	Format
1-10	New time step scale factorE10.0 LT.0.0: restart the job with a fixed time step; the absolute value of the new scale factor is used as the constant time step. EQ.0.0: time step scale factor remains unchanged. GT.0.0: define the new time step factor.	
11-15	Number of changed translational boundary condition codes	I5
16-20	Number of materials for stress initialization, *NMSI*. This feature causes DYNA3D to generate stress initialization files for DYNA3D and then terminates. EQ. *NMSI*: number of materials to initialized. EQ. -1: all materials will be initialized.	I5
21-25	Number of time steps between restart dumps. EQ.0: no change	I5
26-30	Number of time steps between running restart dumps EQ.0: no change	I5
31-35	New global rigid-body translation velocity is specified, *NVEL* EQ.0: no change EQ.1: change	I5
36-40	Number of rigid walls to be redefined, *NNUMRW* EQ.0: no change	I5
41-46	Generate stress initialization files for NIKE3D. This feature causes DYNA3D to generate stress initialization files for NIKE3D and then terminates. EQ. 0: no files generated. EQ. 1: generate files and terminate.	I5

Card 4 ... 3+Nfree

Free format keywords and options are optionally specified on cards 4 to 3+Nfree. Control card keywords (see section 4.2 on page 73), if present, are specified first the same way they are specified in the main input deck. Next, keyword based options (see section 4.3 on page 88), if desired, are prescribed. **Only keywords that alter run time parameters should be specified.** For example, it is permissible to change the number of SMP threads, termination time, plot state interval, or time-step scale factor. However, the number of nodes, elements, prescribed velocities, etc. should not be altered; such modifications will result in an abnormal termination!

5.3 DELETED SLIDING INTERFACES

Skip this section if there are no sliding interfaces to be deleted at restart.

Columns		Quantity	Format	
1-5	(1-8)	Number of first sliding interface to be deleted	I5	(I8)
6-10	(9-16)	Number of second sliding interface to be deleted	I5	(I8)
10-15	(17-24)	Number of third sliding interface to be deleted	I5	(I8)
.	.	.	.	
.	.	.	.	
.	.	.	.	
.	.	.	.	

Currently, a maximum of 48 sliding interfaces may be deleted at restart. Each card may include up to 16 sliding interfaces, or 10 if large format is used. This should not be a serious limitation in most situation.

5.4 DELETED MATERIALS

Skip this section if there are no materials to be deleted at restart.

Columns		Quantity	Format	
1-5	(1-8)	Material number of first material to be deleted	I5	(I8)
6-10	(9-16)	Material number of second material to be deleted	I5	(I8)
10-15	(17-24)	Material number of third material to be deleted	I5	(I8)
.	.	.	.	
.	.	.	.	
.	.	.	.	
.	.	.	.	

When a material is deleted, all elements associated with that material are also deleted. There is no limit to the number of materials which may be deleted. Each card may include up to 16 material numbers, or 10 if large format is used. Deleting materials is a way of deleting a group of elements which all share the same material number, and may be more convenient than listing the elements individually if the element numbers are not contiguous.

5.5 DELETED SOLID ELEMENT BLOCKS

Skip this section if there are no solid elements to be deleted at restart.

Columns		Quantity	Format	
1-5	(1-8)	First solid element of first block to be deleted	I5	(I8)
6-10	(9-16)	Last solid element of first block to be deleted	I5	(I8)
10-15	(17-24)	First solid element of second block to be deleted	I5	(I8)
16-20	(25-32)	Last solid element of second block to be deleted	I5	(I8)
.	.	.	.	
.	.	.	.	
.	.	.	.	
.	.	.	.	

All solid elements with numbers between the first and last numbers of each block are deleted. Each card may include up to 16 element numbers (8 blocks), or 8 (4 blocks) if large format is used.

5.6 DELETED BEAM ELEMENT BLOCKS

Skip this section if there are no beam elements to be deleted at restart.

Columns		Quantity	Format	
1-5	(1-8)	First beam element of first block to be deleted	I5	(I8)
6-10	(9-16)	Last beam element of first block to be deleted	I5	(I8)
10-15	(17-24)	First beam element of second block to be deleted	I5	(I8)
16-20	(25-32)	Last beam element of second block to be deleted	I5	(I8)
.	.	.	.	
.	.	.	.	
.	.	.	.	
.	.	.	.	

All beam elements with numbers between the first and last numbers of each block are deleted. Each card may include up to 16 element numbers (8 blocks), or 8 (4 blocks) if large format is used.

5.7 DELETED SHELL ELEMENT BLOCKS

Skip this section if there are no shell elements to be deleted at restart.

Columns		Quantity	Format	
1-5	(1-8)	First shell element of first block to be deleted	I5	(I8)
6-10	(9-16)	Last shell element of first block to be deleted	I5	(I8)
10-15	(17-24)	First shell element of second block to be deleted	I5	(I8)
16-20	(25-32)	Last shell element of second block to be deleted	I5	(I8)
.	.	.	.	
.	.	.	.	
.	.	.	.	
.	.	.	.	

All shell elements with numbers between the first and last numbers of each block are deleted. Each card may include up to 16 element numbers (8 blocks), or 8 (4 blocks) if large format is used.

5.8 DELETED THICK SHELL ELEMENT BLOCKS

Skip this section if there are no deleted thick shell elements.

Columns		Quantity	Format	
1-5	(1-8)	First thick shell element of first block to be deleted	I5	(I8)
6-10	(9-16)	Last thick shell element of first block to be deleted	I5	(I8)
10-15	(17-24)	First thick shell element of second block to be deleted	I5	(I8)
16-20	(25-32)	Last thick shell element of second block to be deleted	I5	(I8)
.	.	.	.	
.	.	.	.	
.	.	.	.	
.	.	.	.	

All thick shell elements with numbers between the first and last numbers of each block are deleted. Each card may include up to 16 element numbers (8 blocks), or 8 (4 blocks) if large format is used.

5.9 CHANGED BOUNDARY CONDITIONS

Skip this section if there are no nodal boundary condition codes to be changed at restart.

Columns		Quantity	Format	
1-5	(1-8)	Node number	I5	(I8)
6-10	(9-13)	New translational boundary condition code	F5.0	(F5.0)
11-15	(14-18)	New rotational boundary condition code	F5.0	(F5.0)

Nodal boundary condition codes are described in section 4.7 on page 306. Changed boundary condition codes offer flexibility in modeling. For example, one might apply forces to a panel to establish a tensile preload using the dynamic relaxation initialization option, and then restart and change the boundary conditions on boundary nodes to fixed to simulate a clamped prestressed plate. Changed boundary conditions can also be used to simulate some aspects of structural failure.

Boundary condition codes may be changed for nodes on rigid or deformable bodies.

5.10 MATERIAL NUMBERS FOR STRESS INITIALIZITION

Skip this section if *NMSI* equals 0 or -1.

Cards 1, 2, . . . , NMSI

Columns	Quantity	Format
1-5	Old material number	I5
6-10	New material number	I5

Stress initialization is performed only for elements of materials that have a prescribed old material number.

Note that material numbers may be changed from their values in the restart file (i.e. old material numbers) to their values in the new input file, provided that the constraints explained in section 2.20 on page 38 are not violated.

When $NMSI = -1$, a one to one correspondence is established between all old and new material numbers. If fewer new material numbers exist than old material numbers, the extraneous element data will be ignored.

5.11 CHANGED GLOBAL TRANSLATIONAL VELOCITY

Skip this section if $NVEL = 0$.

Columns	Quantity	Format
1-10	New X-translational rigid-body velocity	E10.0
11-20	New Y-translational rigid-body velocity	E10.0
21-30	New Z-translational rigid-body velocity	E10.0

The global rigid-body translational velocity of all nodes and rigid bodies in an analysis may be changed on restart. The change is made by adding the difference between the new rigid-body velocity and the current rigid-body velocity to each node and rigid body in the problem. The current rigid-body velocity is defined as the mass averaged velocity of all nodes and rigid materials in the problem. It may differ from the rigid-body velocities reported in the status query (section 3.3 on page 54) since it excludes all contributions from moving rigid walls. Both the new rigid-body velocity and current rigid-body velocity (before the change) are included in the restart's printed output file.

This feature, coupled with the ability to redefine rigid walls (section 5.12 on page 458), is extremely useful when simulating multiple sequential impacts.

5.12 CHANGED RIGID WALLS

Skip this section if $NNUMRW = 0$.

Card 1

Columns		Quantity	Format	
1-5	(1-8)	Number of rigid wall to be redefined	I5	(I8)
6-15	(9-18)	x-coordinate of point P (must be on rigid wall)	E10.0	(E10.0)
16-25	(19-28)	y-coordinate of point P	E10.0	(E10.0)
26-35	(29-38)	z-coordinate of point P	E10.0	(E10.0)
36-45	(39-48)	x-coordinate of point Q (must be in space)	E10.0	(E10.0)
46-55	(49-58)	y-coordinate of point Q	E10.0	(E10.0)
56-65	(59-68)	z-coordinate of point Q	E10.0	(E10.0)
66-70	(69-73)	Moving rigid wall option, $IMSWF$ EQ.0: rigid wall is fixed in space EQ.1: rigid wall has mass m_{wall} and initial velocity v_0	I5	(I5)
71-75	(74-78)	Stick condition option, $ISTICK$ EQ.0: frictionless sliding after contact EQ.1: no sliding after contact	I5	(I5)
76-80	(79-80)	Finite size rigid wall option, $LIMIT$ EQ.0: rigid wall extends to infinity EQ.1: size and orientation is defined	I5	(I2)

The geometry of rigid wall definitions is shown in Figure 34. Point P is at the origin of the rigid wall local coordinate system, and therefore must lie on the rigid wall surface. Point Q is a point in space, and the rigid wall normal vector $\boldsymbol{n}$ is defined as a vector from P to Q. This normal vector must point towards the impacting body. If $LIMIT = 1$, the dimensions of the rigid wall plane l_x and l_y (as specified on the next card) are measured from the origin at point P.

After impact, two friction options are available for rigid walls. If $ISTICK = 0$, then the wall is frictionless, and no resistance is provided to transverse motion in the plane of the wall. If $ISTICK = 1$, then sufficient friction is provided to prevent any transverse motion of the contacting body in the plane of the wall.

The slave nodes associated with the redefined rigid-wall can not be changed.

Card 1 + LIMIT

Define this card only if $LIMIT = 1$.

Columns	Quantity	Format
1-10	x-coordinate of point R	E10.0
11-20	y-coordinate of point R	E10.0
21-30	z-coordinate of point R	E10.0
31-40	Length of $\boldsymbol{x}_l$ edge, l_x (see Figure 34) EQ.0.0: extends from negative to positive infinity	E10.0
41-50	Length of $\boldsymbol{y}_l$ edge, l_y EQ.0.0: extends from negative to positive infinity	E10.0

Note that l_x and l_y cannot both be zero if the finite rigid wall option is active ($LIMIT = 1$).

Card 1+LIMIT+IMSWF

Define this card only if $IMSWF = 1$.

Columns	Quantity	Format
1-10	Total mass of rigid wall, m_{wall}	E10.0
11-20	Initial velocity of rigid wall, v_0, in direction of normal vector, $\boldsymbol{n}$	E10.0

6.0 MATERIAL MODEL DRIVER

6.1 OVERVIEW

This section describes a Material Model Driver which is incorporated into DYNA3D. The Material Model Driver allows plotting of the stress-strain response predicted by a material model under a given load path. This feature is particularly useful when fitting complex material models to experimental data, or when using a complex model for the first time. The interactive graphics plotting capability of the Material Model Driver allows the simulated material stress-strain behavior to be easily compared with actual material test results or theoretical predictions.

The material model driver works with any DYNA3D material model, including both solid and shell element material models, and computes the stress history corresponding to a given strain history without including the effects of dynamic response. The dynamic equations of motion are not used by the material model driver, and therefore the material behavior is simulated independent of inertial effects. These inertial effects would be present and complicate the interpretation of the results if a “one-element” problem were used to demonstrate the material model behavior. Rate dependence in the constitutive model is included, so realistic strain rates must be used with the Material Model Driver for rate-dependent materials.

6.2 INPUT DEFINITION

The Material Model Driver is invoked by setting the total number of beam, shell, and solid elements to zero in a standard DYNA3D input file (described in Chapter 4 of this manual). The number of load curves should be set to nine, and the termination time should be set to the desired length of the simulation. The complete state dump interval is interpreted as the time step to be used in the Material Model Driver run. This value should be chosen in conjunction with the strain vs. time description in the load curves to yield realistic strain increments at each step of the simulation. Plotting information is saved at every step of a Material Model Driver simulation.

The remainder of the input file should be as specified in Chapter 4 up through the material model definition. Do not include section properties for shell elements! Immediately after the material definition, nine load curves describing the strain path should be defined. These nine curves describe the time history of the displacement gradient components shown in Table 1, where x, y, and z

represent three orthogonal coordinate directions and u, v, and w represent displacement fields in those directions, respectively. Note that if a rate-dependent model is used, then the “time” in the Material Model Driver corresponds to physical time and must yield realistic strain rates. If a rate-independent material model is used, then “time” is really a nonphysical quasi-time used to parameterize the strain history, and any convenient scale may be used (such as Driver time step size of 1.0 and a termination time equal to the number of steps desired).

The Material Model Driver supports material models for both solid and shell elements. The choice of solid element vs. shell element material model is indicated on the Material Control Card. For shell element material models, the input value of ε_{zz} is not used since it is not an independent variable in the plane stress constitutive formulation used in shell elements.

Load Curve Number	Component Definition
1	$\frac{\partial u}{\partial x}$
2	$\frac{\partial v}{\partial y}$
3	$\frac{\partial w}{\partial z}$
4	$\frac{\partial u}{\partial y}$
5	$\frac{\partial v}{\partial x}$
6	$\frac{\partial u}{\partial z}$
7	$\frac{\partial w}{\partial x}$
8	$\frac{\partial v}{\partial z}$
9	$\frac{\partial w}{\partial y}$

Table 1 - Load Curve Definitions

The strain rate, or rate of deformation in a finite strain context, is found by taking the symmetric part of a finite difference time derivative of the components specified by the load curves. For example, if the above components are considered to form a tensor $\boldsymbol{S}$, then a tensor $\boldsymbol{L}$ at time t_k (corresponding to step k) is calculated from

$$\boldsymbol{L}(t_k) = \frac{\boldsymbol{S}(t_k) - \boldsymbol{S}(t_{k-1})}{(t_k - t_{k-1})} \quad , \tag{374}$$

and then the rate of deformation $\boldsymbol{d}$ is found from

$$\boldsymbol{d} = \frac{1}{2}(\boldsymbol{L} + \boldsymbol{L}^T) \tag{375}$$

and the spin is found from:

$$\boldsymbol{w} = \frac{1}{2}(\boldsymbol{L} - \boldsymbol{L}^T) \, . \tag{376}$$

In a small strain context, load curves 1-6 may be used to specify strain time histories, and load curves 7-9 simply defined as zero throughout the duration of the simulation. *All nine load curves must be defined in all cases, and must be defined over the entire time interval of the simulation.* The small strain interpretation of the load curve quantities is given in Table 2.

Load Curve Number	Small Strain Interpretation
1	ε_{xx}
2	ε_{yy}
3	ε_{zz}
4	ε_{xy}
5	ε_{yx}
6	ε_{xz}
7	ε_{zx}
8	ε_{yz}
9	ε_{zy}

Table 2: Small Strain Load Curve Definitions

6.3 INTERACTIVE COMMANDS

The Material Model Driver contains an integral plotting package to allow immediate display of simulation results. After reading the input file and completing the calculations, DYNA3D gives a command prompt to the terminal. A summary of the available interactive commands is given in this section. An on-line help package is available by typing **help** at the prompt. Refer to the notational conventions described in section 2.1 on page 9.

- **ASCL** - scale all abscissa data by f. default is $f = 1$.
- **OSCL** - scale all ordinate data by f. default is $f = 1$.
- **ASET** - *amin omax* - set minimum and maximum values on abscissa to *amin* and *amax*, respectively. If *amin*=*amax*=0, scaling is automatic.
- **OSET** - *omin omax* - set minimum and maximum values on ordinate to *omin* and *omax*, respectively. If *omin*=*omax*=0, scaling is automatic.
- **GRID** - tmds or graphics display will be overlayed by a grid of orthogonal lines
- **NOGRID** - tmds or graphics displays will not be overlayed by a grid of orthogonal lines
- **LOGO** - puts LLNL logo on all plots (default). Retyping this command removes the logo.
- **TV** *n* - use tmds *n* or graphics device *n*, where *n* is the monitor or device number
- **TV** - *n1 n2 n3* - (LLNL only) use color tmds with monitor numbers *n1*, *n2*, and *n3* for red, green, and blue channels, respectively.
- **PLOTS box** *ann* - (LLNL only) create a plotfile for box number *ann* that contains a record of the tmds display
- **CLASS** *lev* - (LLNL only) reset classification level of hardcopy output from default unclassified to: proglev, pard, adp, confidnt, srd, or system. This command must precede the plots command if used.
- **RJET** *n* - (LLNL only) send a copy of the fr80 file to rjet *n*
- **TIME** *c* - plot component *c* versus time
- **CROSS** *c1 c2* - plot component *c1* versus *c2*
- **PRINT** - print plotted time history data in file "pamper." Only data plotted after this command is printed. File name can be changed with the “FILE” command. The “pampers” file contains 2-column ASCII data suitable for plotting with other software.
- **FILE** *name* - change pampers filename to *name*.

- **RDLC** *m n r1 z1 ... rn zn* - redefine load curve *m* using *n* coordinate pairs (*r1,z1),(r2,z2),...,(rn,zn*)
- **CONTINUE** - reanalyze material model
- **ECOMP** - display component numbers on the tmds or graphics display. The component numbers are also shown in Table 3.
- **CHGL** *n* - change label for component *n*. Program will prompt for new label.
- **QUIT, END, T** - exit the material model driver

Component	Quantity	Component	Quantity
1	x-stress	12	3rd principal deviatoric stress
2	y-stress	13	maximum shear stress
3	z-stress	14	1st principal stress
4	xy shear stress	15	2nd principal stress
5	yz shear stress	16	3rd principal stress
6	zx shear stress	17	$ln(v/v_0)$
7	effective plastic strain	18	relative volume
8	pressure	19	$v_0/v - 1$
9	effective stress	20	1st history variable
10	1st principal deviatoric stress	21	2nd history variable
11	2nd principal deviatoric stress	22	3rd history variable

Table 3: Element Components for interactive graphics display.

7.0 EXAMPLES

This chapter presents several large-scale DYNA3D simulations of actual engineering problems, and gives two brief examples illustrating the use of the Material Model Driver described in Chapter 6. The DYNA3D Examples Manual (Lovejoy and Whirley, 1990) describes ten tutorial examples in more detail, and includes the INGRID mesh generation files and TAURUS post-processing commands used in each analysis.

7.1 NOSE CONE IMPACT

This example shows an analysis of a nose cone designed by Sandia National Laboratories in Livermore to limit the impact force transmitted to the aft section. An oblique impact event was simulated as described in (Chiesa and Callabresi, 1981).

The initial mesh, containing 6074 nodes and 4356 solid elements, is shown in Figure 46. The nose cone is made of steel, with a yield strength of 0.0048 Mbar and a tangent modulus of 0.0138 Mbar. The mass of the aft section was included by using a high density material in the top rows of elements. This is an interesting problem due to the importance of the slide surfaces and contact, which are essential in computing a realistic deformed geometry. The tied interfaces were used for convenience in the design of the mesh, as they allowed regions of different mesh refinement to be tied together. The sliding interfaces permit the collapse of the voids between ribs in the nose piece. The locations of the slide surfaces are shown in Figure 47.

Comparisons with experimental data reported in (Chiesa and Callabresi, 1981) showed excellent agreement with the calculation. A sequence of deformed shapes at 3000 μs intervals is shown in Figure 48. At 15,000 μs, the peak deformation is reached and the nose cone begins to rebound.The final shape obtained in the experiment was very close to the final computed shape. The computed force deflection curve plotted by TAURUS is compared to that obtained from the experiment in Figure 49. Only minor discrepancies exist, and the importance of the slide surfaces in modeling force spikes due to void closure is evident.

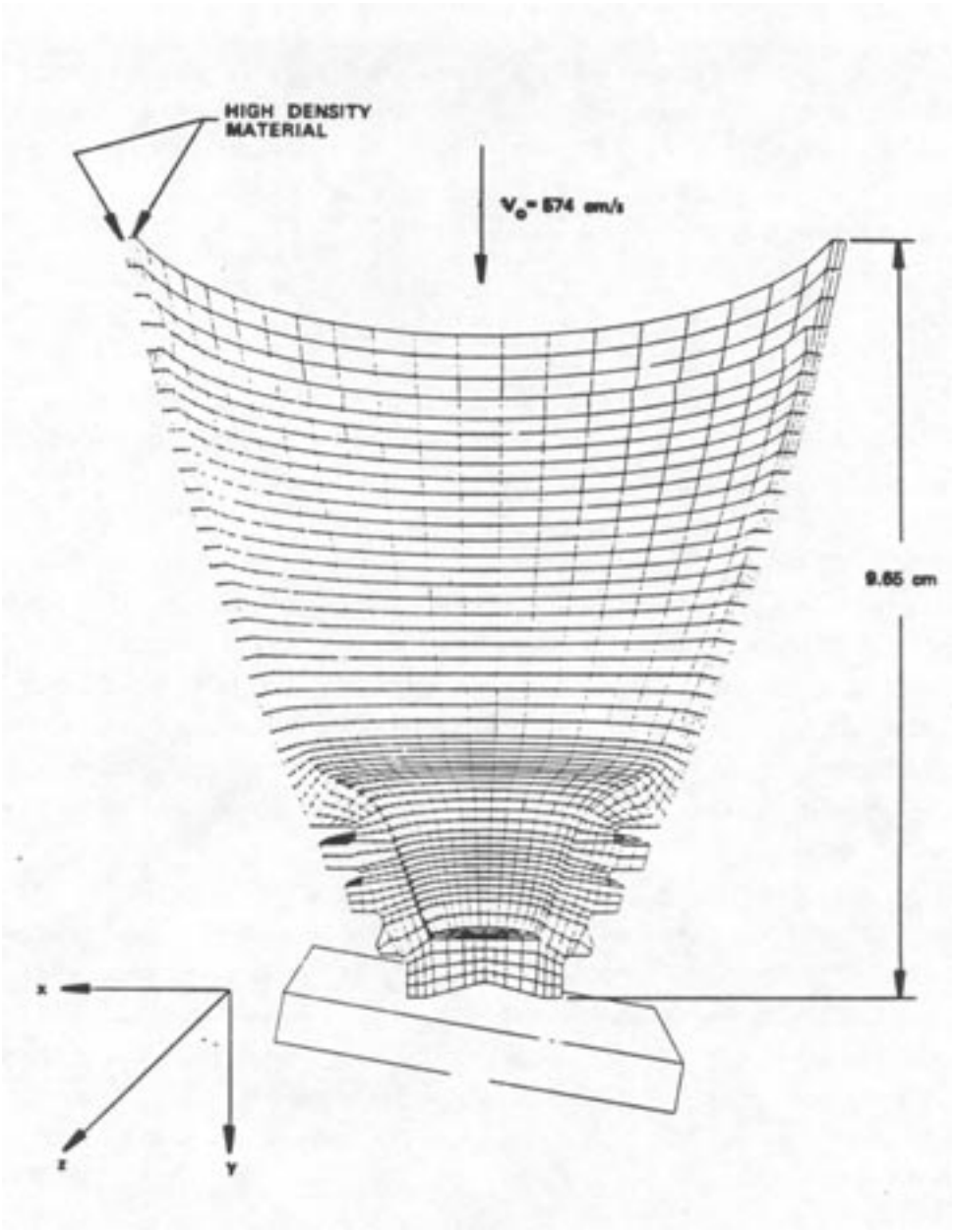

Figure 46
Initial mesh of steel node cone.

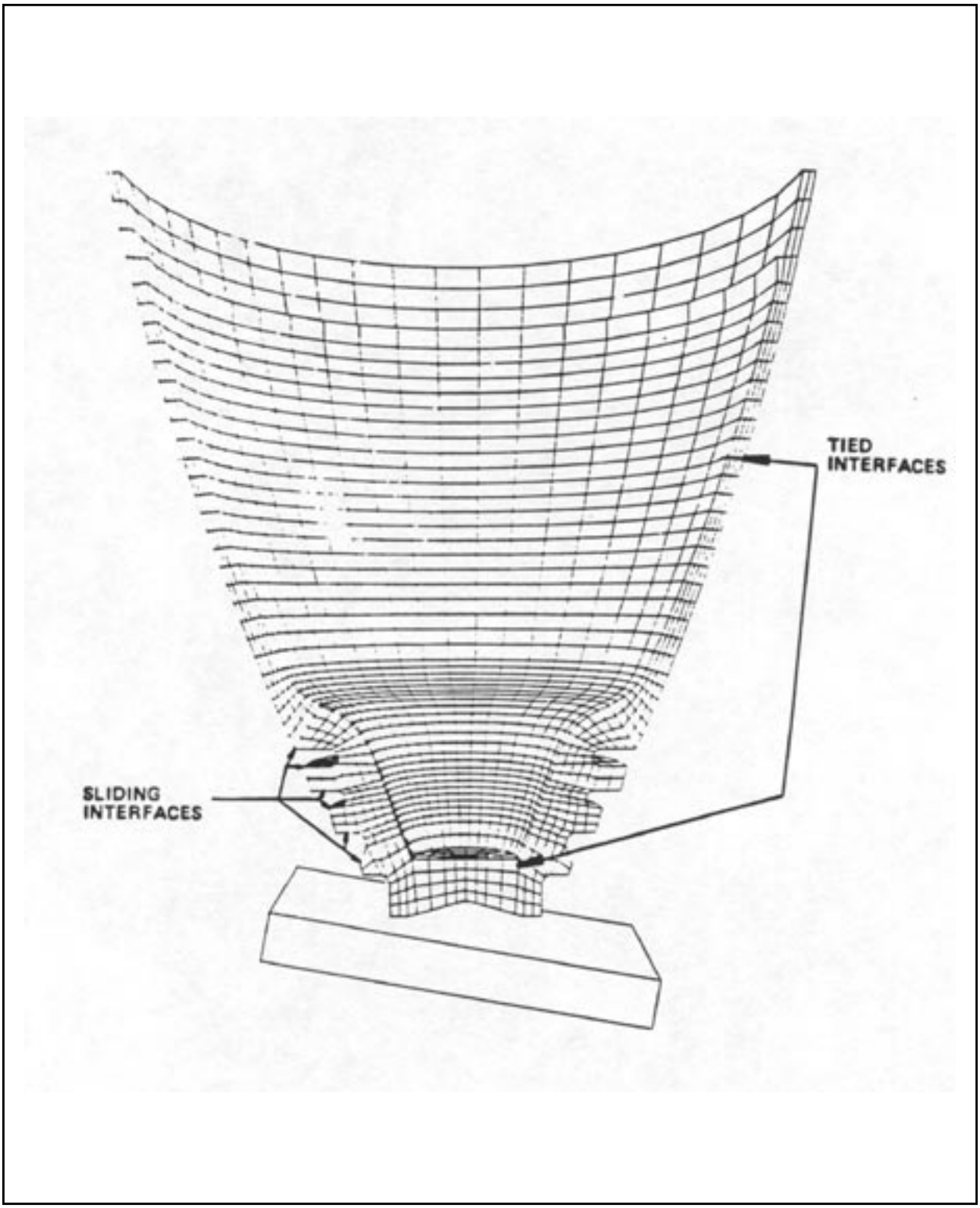

Figure 47
Location of tied and sliding interfaces.

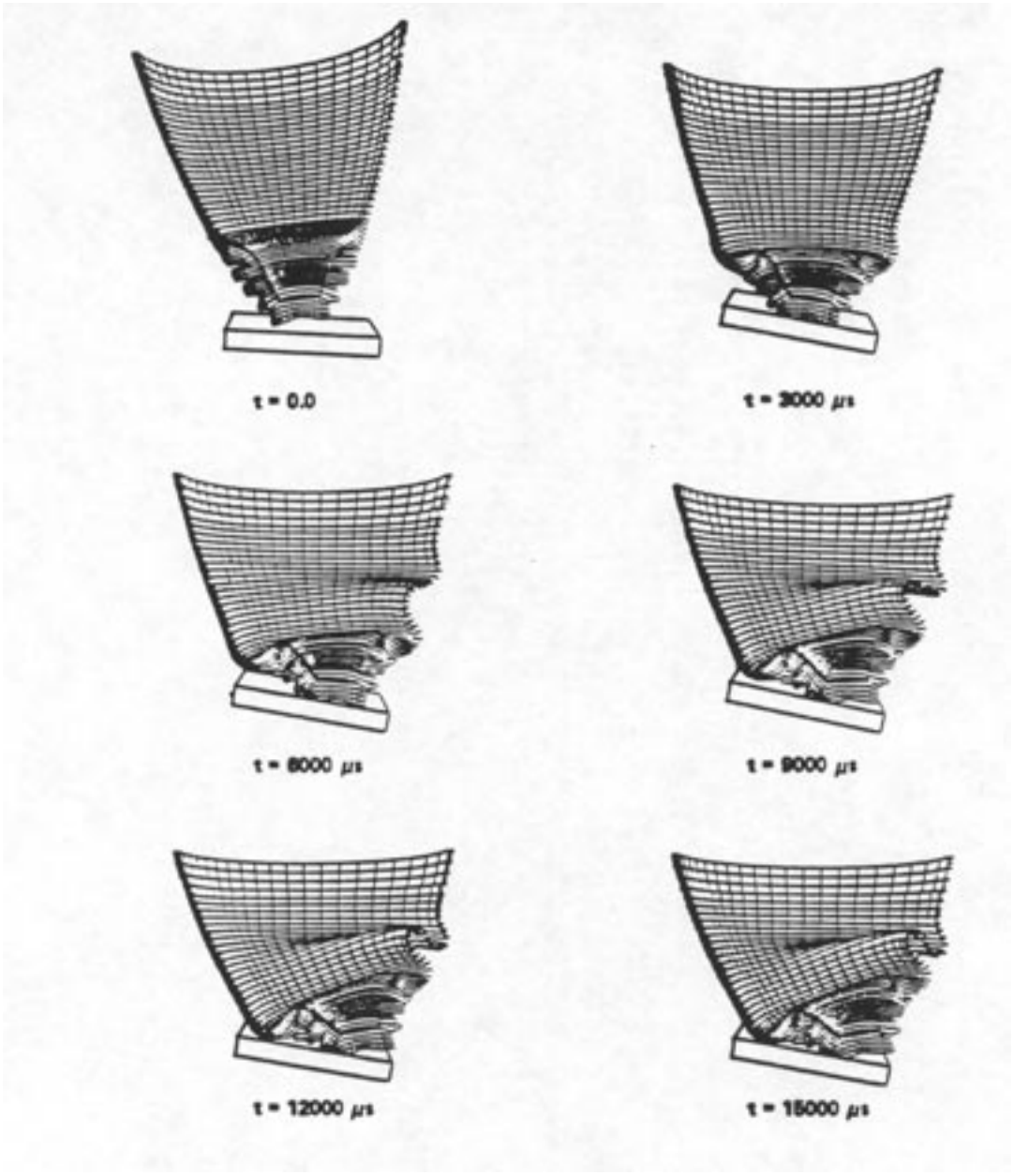

Figure 48
Sequence of deformed shapes after impact. Note closure of voids in nose region.

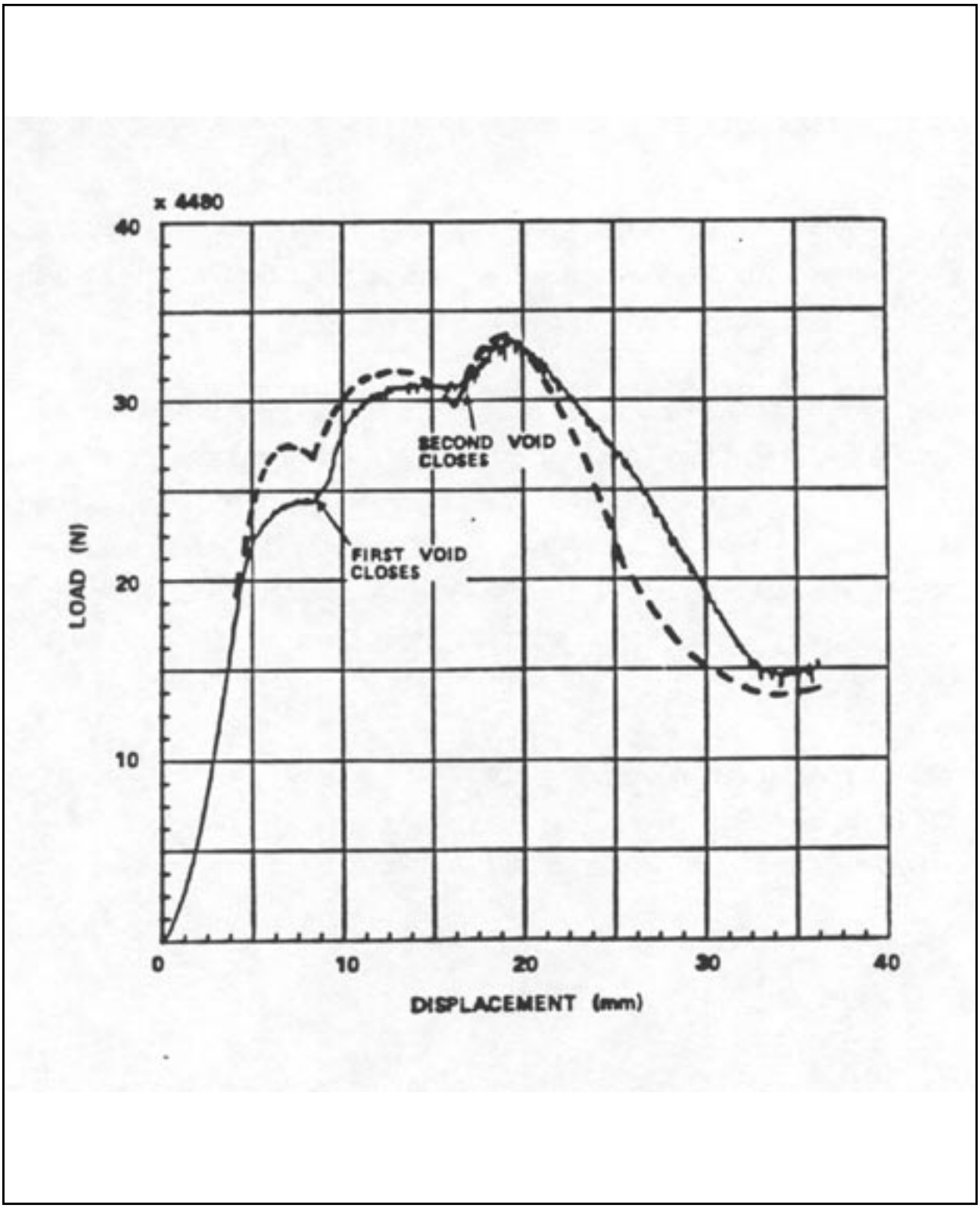

Figure 49
Computed (___) and experimental (---) force-displacement curve for the steel nose cone. The steps in the curves correspond to void closures.

7.2 OBLIQUE IMPACT OF ROD

This example presents the simulation of a long aluminum rod impacting a rigid surface. The rod is 30.5 cm long, 0.658 cm in diameter, and is made of aluminum. The rod impacts the target at an angle of 10 degrees and at a velocity of 20,170 cm/sec.

The computational model of the rod uses only solid elements. The material behavior is simulated using the Steinberg-Guinan model (Material Type 11) with the properties given in (Steinberg and Guinan, 1978). The target is modeled using the Rigid Wall option in DYNA3D to save the cost of discretizing the rigid target. The initial mesh is shown in Figure 50.

A sequence of deformed shapes is shown in Figure 51, and a close-up view of the mesh at 300 μs is shown in Figure 52. The final shape from the experiment is compared to that predicted by DYNA3D in Figure 53. The computed shapes agree well with experimental profiles, supplied by J. Zukas at the Ballistics Research Laboratory, up to approximately 600 μs. At later times the agreement is fair, but the experimental results tended to show more curvature in the rod than did the computational predictions. Some factors which may have led to these discrepancies include:

- coarse zoning,
- inaccurate material properties,
- rigid wall approximation to armor plate,
- lack of interface friction.

Even considering these approximations, the overall qualitative prediction of the rod behavior is quite good.

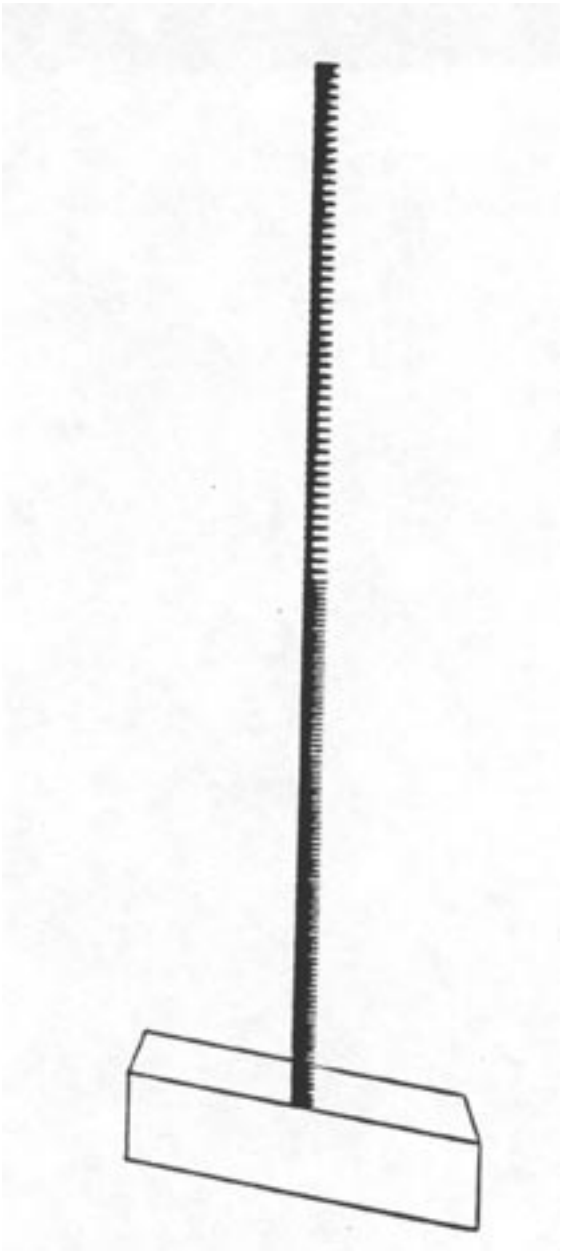

Figure 50
Calculational mesh for oblique rod impact problem.

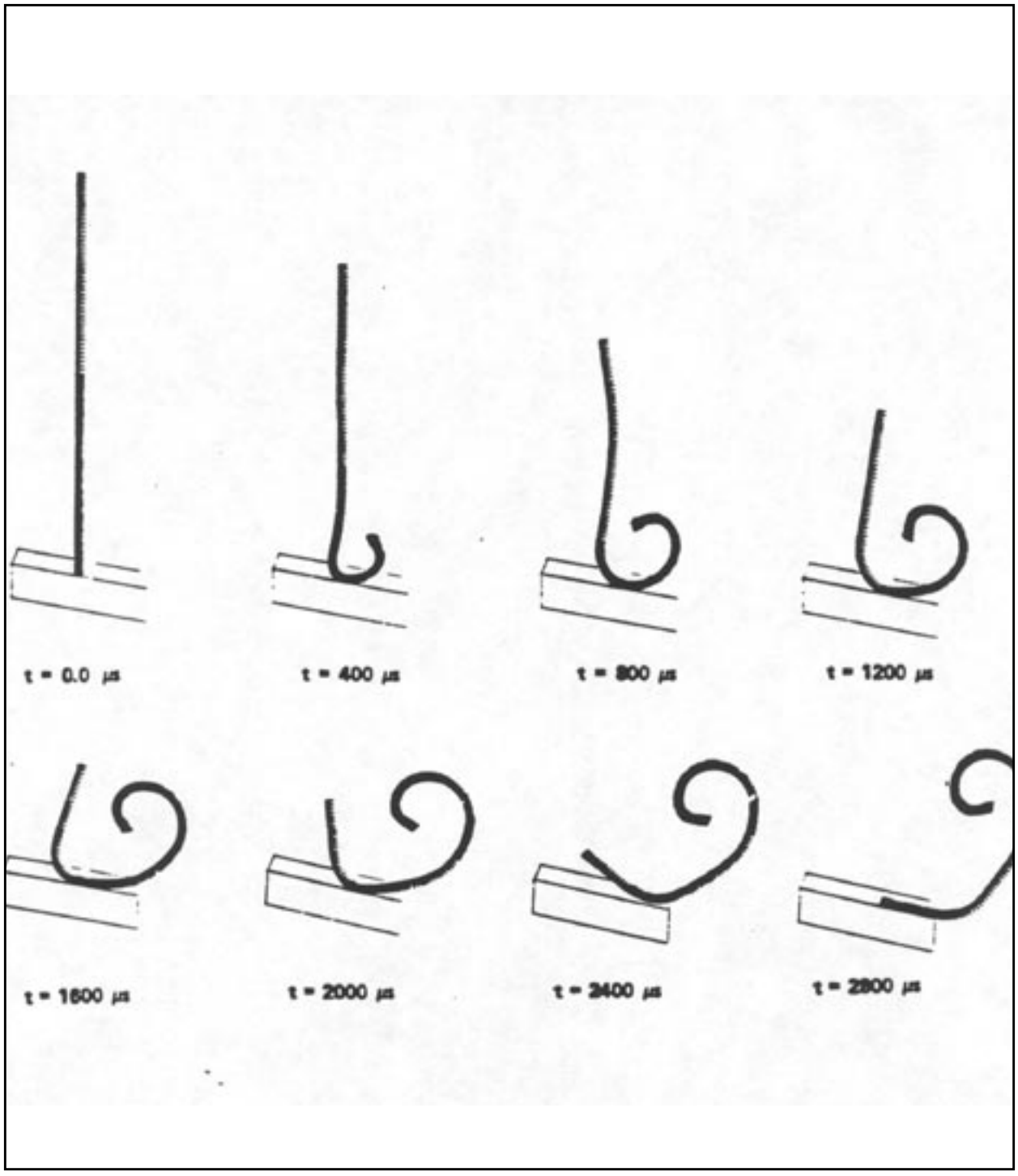

Figure 51
Deformed shapes of rod impacting oblique rigid wall.

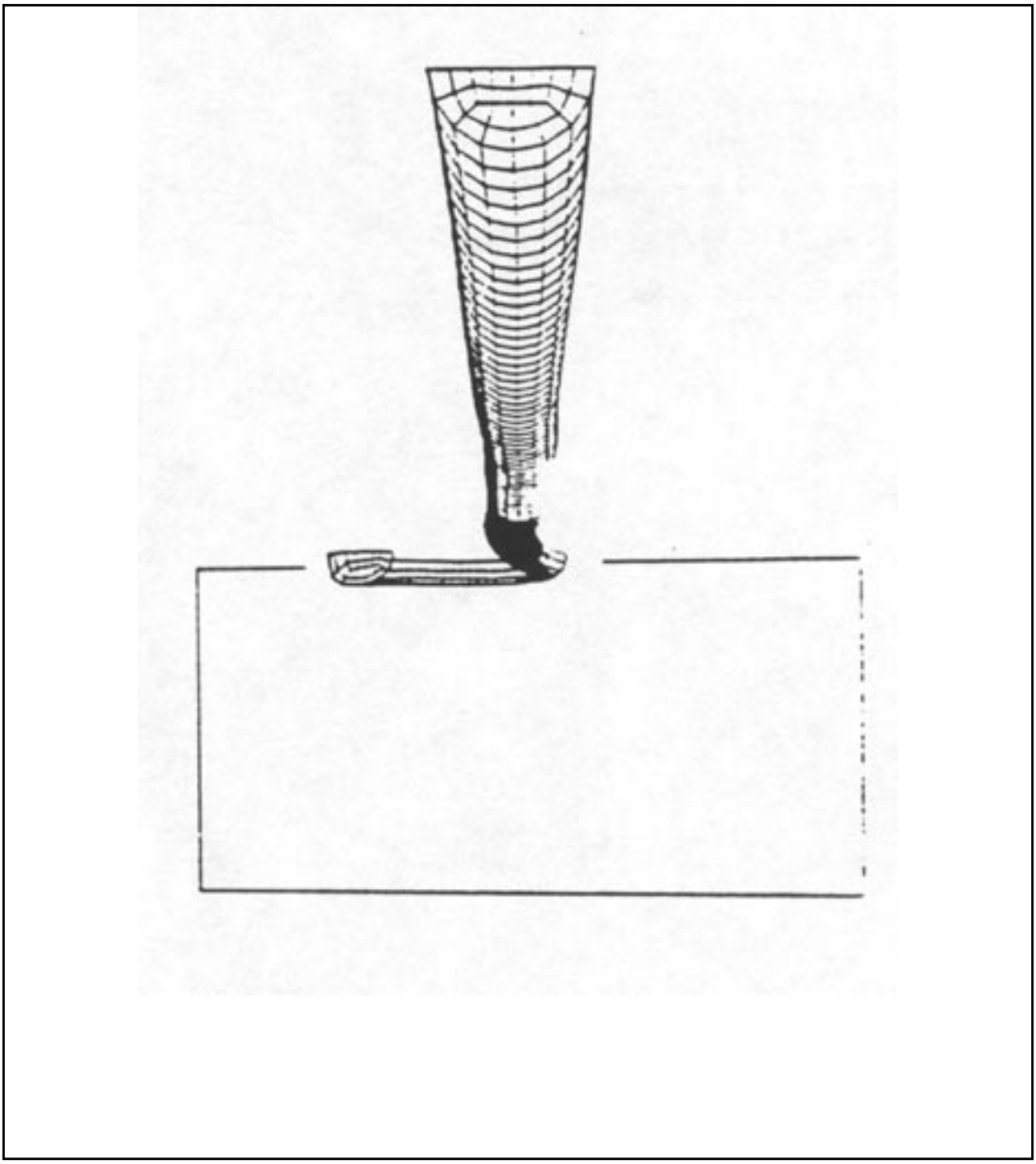

Figure 52
Plan view of rod at 300 μs.

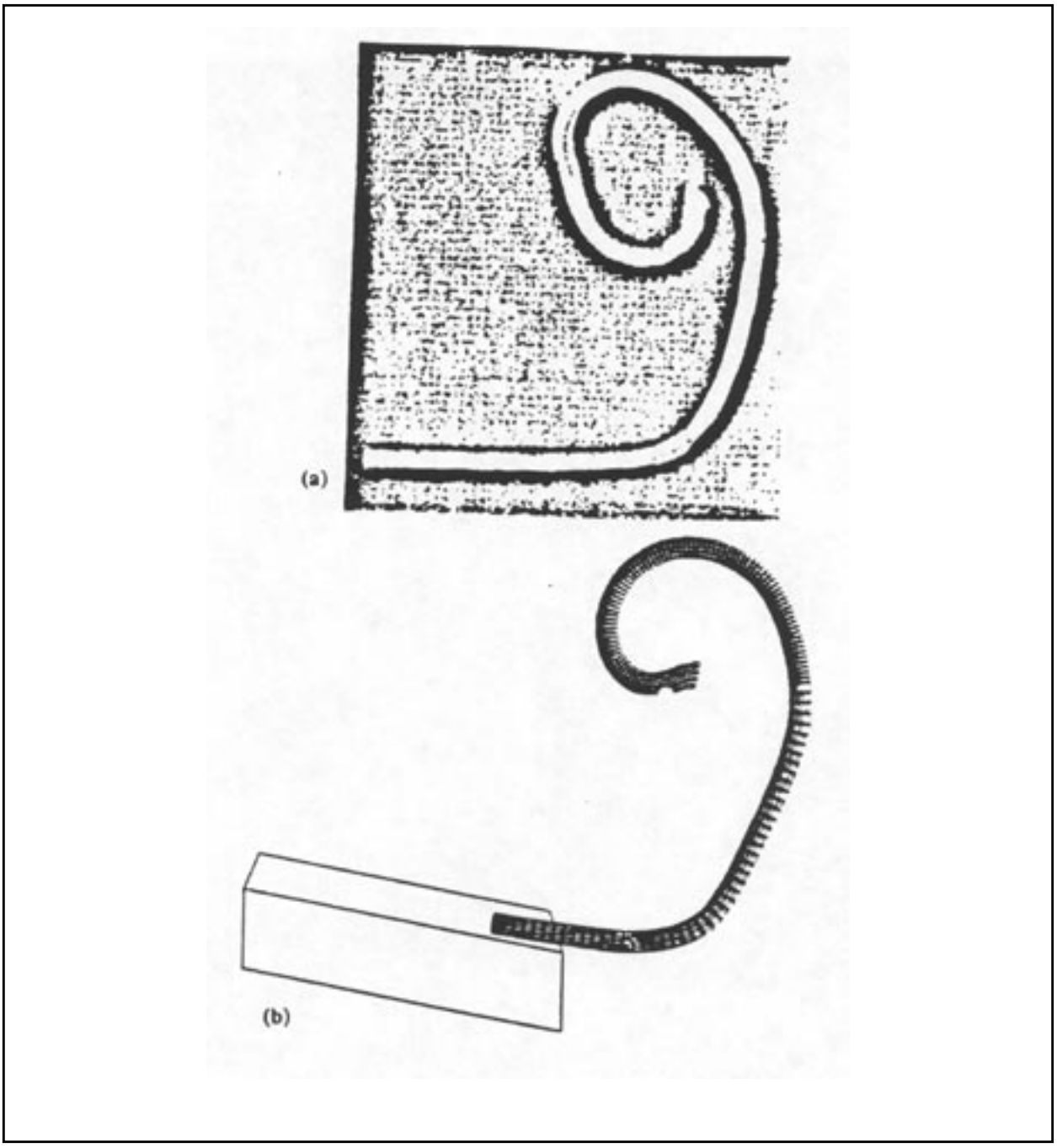

Figure 53
Final profiles: (a) experiment and (b) computed.

7.3 FRAME MEMBER IMPACT

This example illustrates the deformation and collapse of a mild steel rail under impact loading. The geometry definitions of a mild steel frame member dynamically crash tested by Suzuki were provided in (Igarashi, 1985) and discussed in (Benson, et. al, 1986). Frame members are attached to a sled that accelerates to 30 km/hr before impact into a fixed barrier, as shown in Figure 54. Experimental output ceases at 35ms when the sled impacts a bumper that stops its motion. Force time histories are obtained by load cells at the frame-barrier interface, and movies record the deformation history.

Preliminary calculations have been performed on coarsely meshed members to study the feasibility of this type of explicit simulation using DYNA3D. Figure 55 shows a close-up view of the initial mesh with 1600 shell elements. Figure 56 shows the cross section of the 1000mm beam, which is fabricated by spot welding along the flange.

Although the spot welds were not modeled in detail, such modeling may be important in capturing the details of the force histories. Deformed shapes are plotted at 10 μs intervals in Figure 57. The overall deformed shape is predicted quite well, but a more refined mesh must be used to resolve the highly localized buckling. Although the peak force was accurately predicted, the width of the force pulse was under-predicted.

Since the peak force occurs almost immediately and decays rapidly, the interesting part of the force time history occurs early in the event (well before 5 ms). Thus, simulations of 5 ms duration can be done very cheaply, and parameter studies are quite feasible with only modest computer requirements.

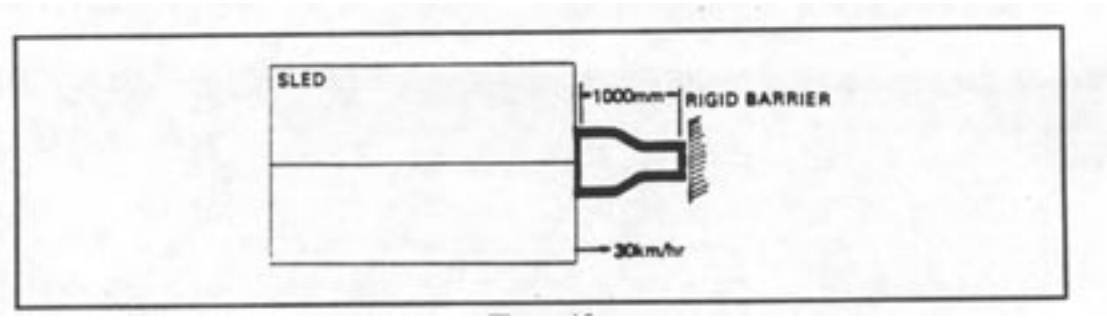

Figure 54
Finite element model of sled test.

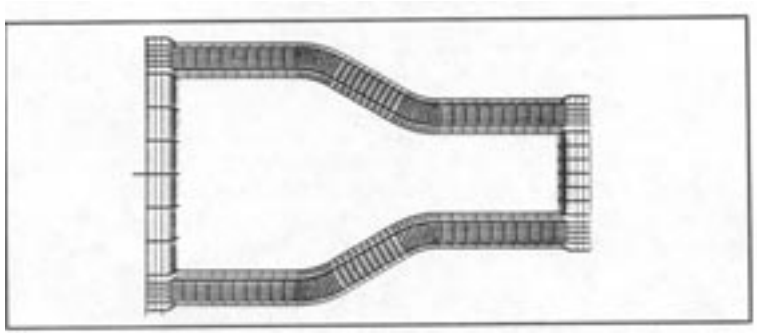

Figure 55
Close-up view of the finite element mesh. The mesh contains 1600 shell elements.

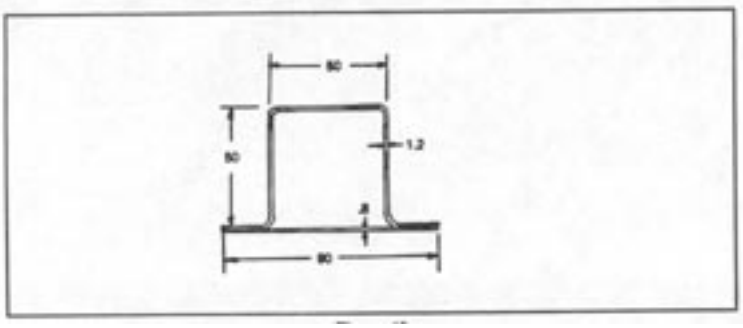

Figure 56
Cross section of frame member. All dimensions are in millimeters.

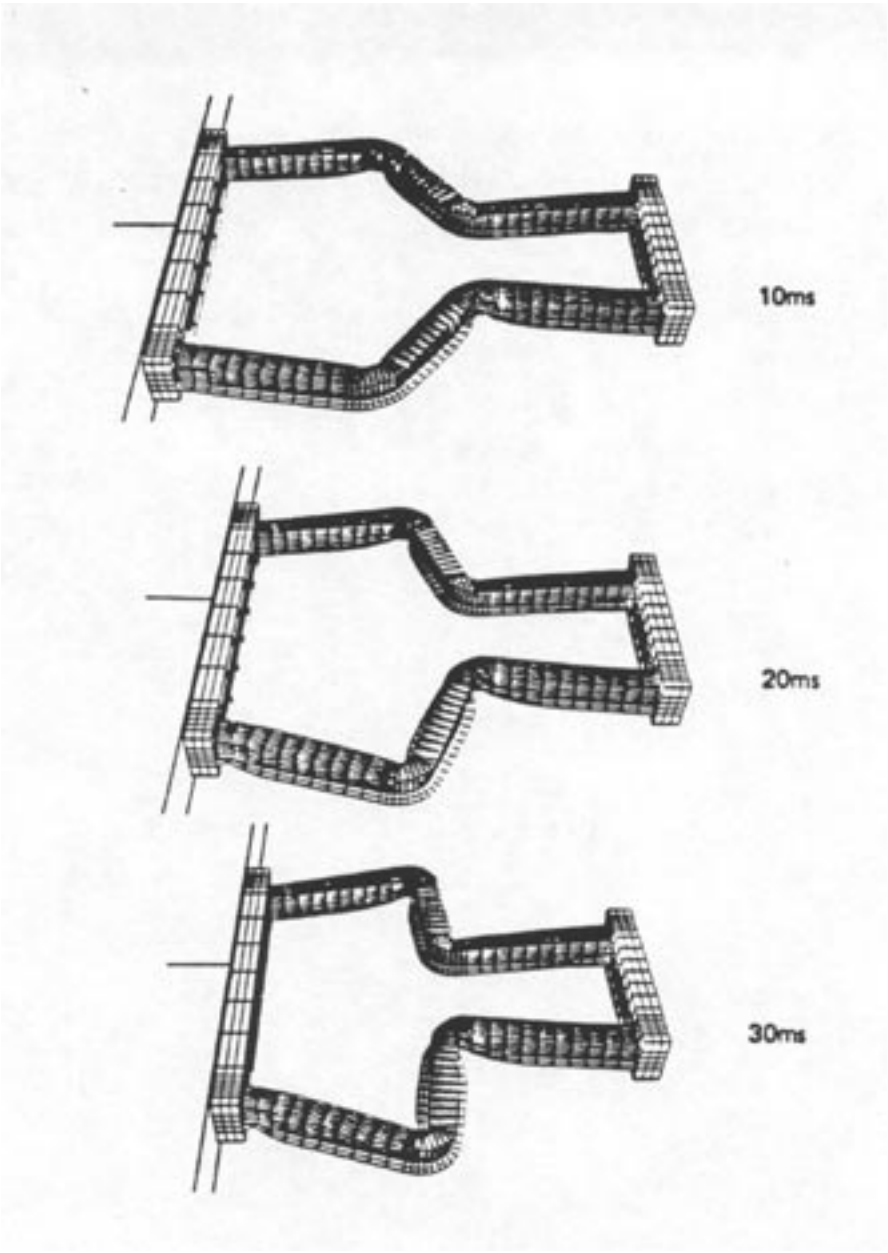

Figure 57
Deformed shapes at 10 ms output intervals.

7.4 Material Model Driver Example 1

The first example is a simple linear elastic material (Material Type 1) subjected to uniaxial strain. The plots were interactively generated using the **CROSS** command (as described in section 6.3 on page 464), and show the Cauchy stress vs. infinitesimal strain curves generated by the Material Model Driver. For this example, a Young's modulus of 30×10^6 psi and a Poisson's ratio of 0.25 were used. From Figure 58, it is easily verified that the slope of the line is $\lambda + 2G = 3.6 \times 10^7$, where λ is the Lame parameter and G is the shear modulus. Figure 59 shows the transverse Cauchy stresses plotted against axial strain, and the slope is seen to be λ, as expected. Thus, this simple example has illustrated the agreement between elasticity theory and the DYNA3D elastic material model for the case of uniaxial strain.

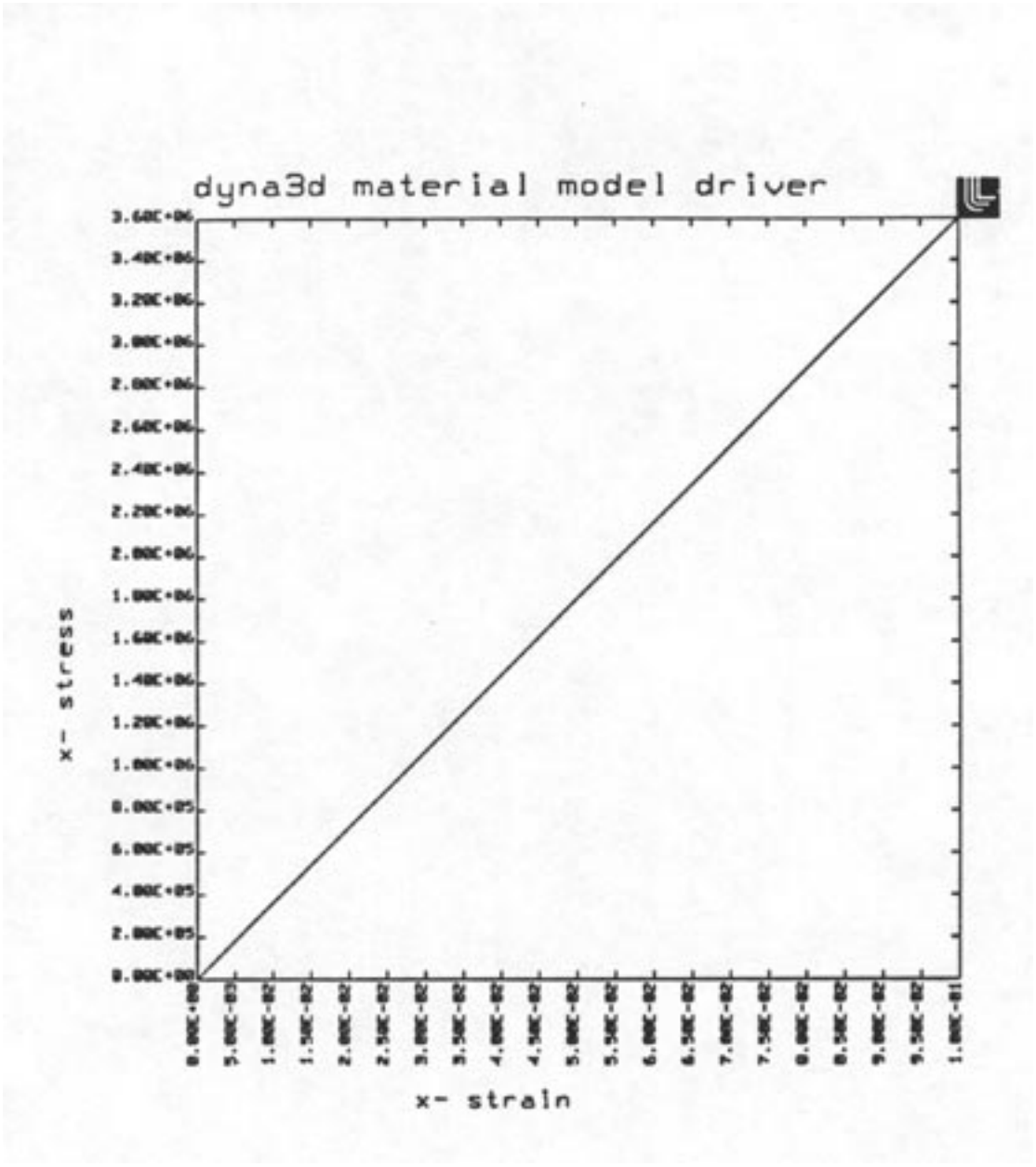

Figure 58
Linear elasticity stress-strain curve in uniaxial tension: σ_{xx} vs. ε_{xx}

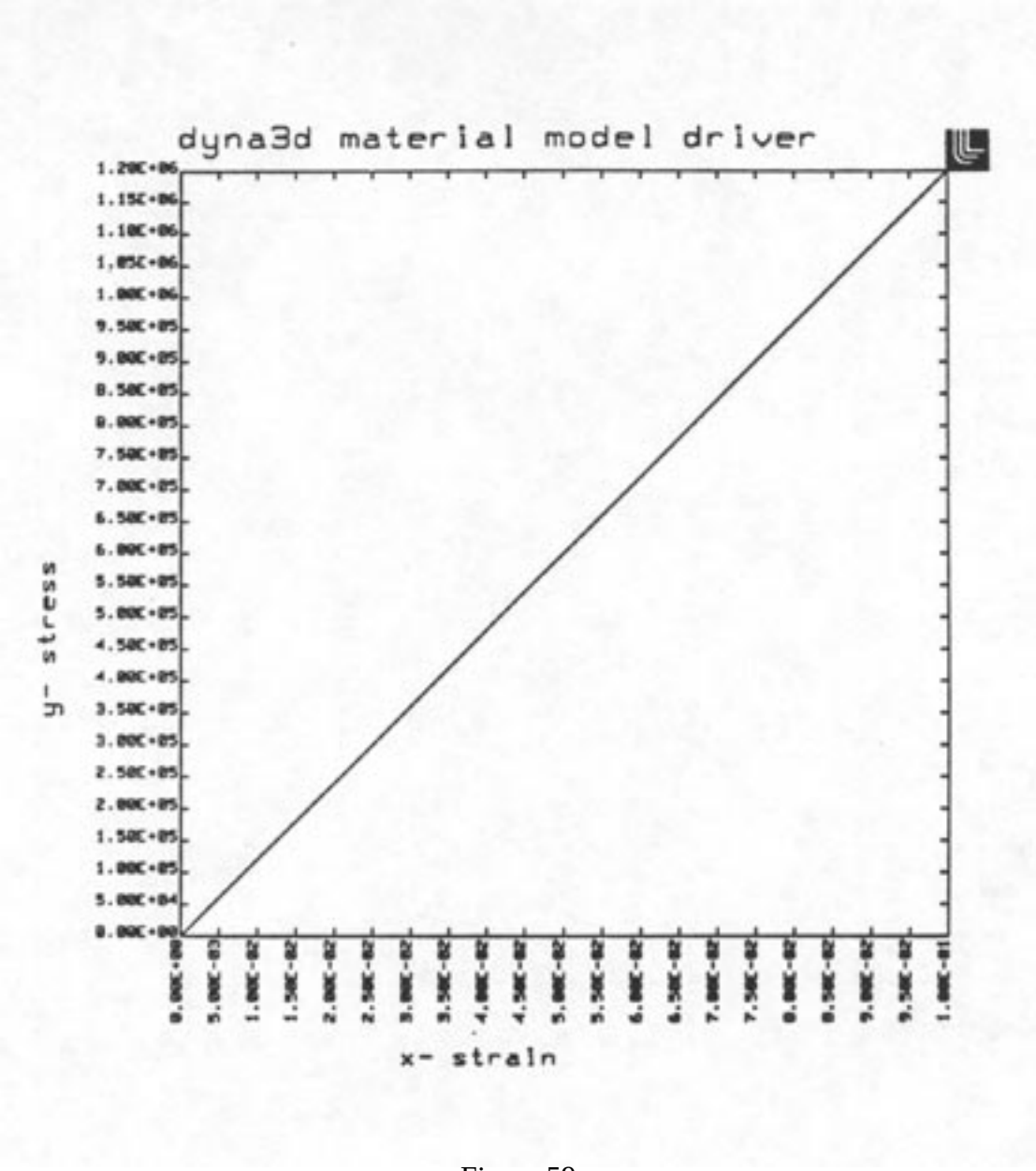

Figure 59
Linear elasticity stress-strain curve in uniaxial strain: σ_{yy} vs. ε_{xx}

7.5 Material Model Driver Example 2

The second example considers a geologic material represented by the Soil and Crushable Foam model (Material Type 5) in DYNA3D. The parameter values and pressure-volume are taken from an actual soil model used for production calculations, and are given below.

The prescribed strain history is a shear deformation in the x - y direction, increasing linearly from zero to a strain of 5% at a time of 100. Superimposed on this shear deformation is a volumetric compaction starting at a time of 50.0, and increasing linearly to a volumetric strain of -0.03 at a time of 100. Thus, the first half of the simulation illustrates the material response at zero pressure, while the second half of the simulation shows the effect of increasing pressure on the shear behavior. Figure 60 shows the resulting plot of shear stress vs. pressure, and Figure 61 shows the pressure-volume behavior predicted by the model. Figure 62 directly shows the influence of pressure on the shear stress-shear strain curve. Clearly, plots such as these can be easily correlated with experimental data to determine the appropriate parameters for a DYNA3D material model.

Parameter	Value
shear modulus	6.70×10^5
bulk modulus	4.20×10^6
a_0	9.90×10^6
a_1	3.50×10^3
a_2	0.30
pressure cutoff	-5.70×10^2

Relative Volume	Pressure
0.0	0.0
-4.0×10^{-3}	2.9×10^{3}
-1.0×10^{-2}	8.7×10^{3}
-1.6×10^{-2}	1.8×10^{4}
-2.0×10^{-2}	2.5×10^{4}
-2.6×10^{-2}	3.5×10^{4}
-3.0×10^{-2}	4.1×10^{4}
-3.7×10^{-2}	5.3×10^{4}
-4.0×10^{-2}	5.8×10^{4}

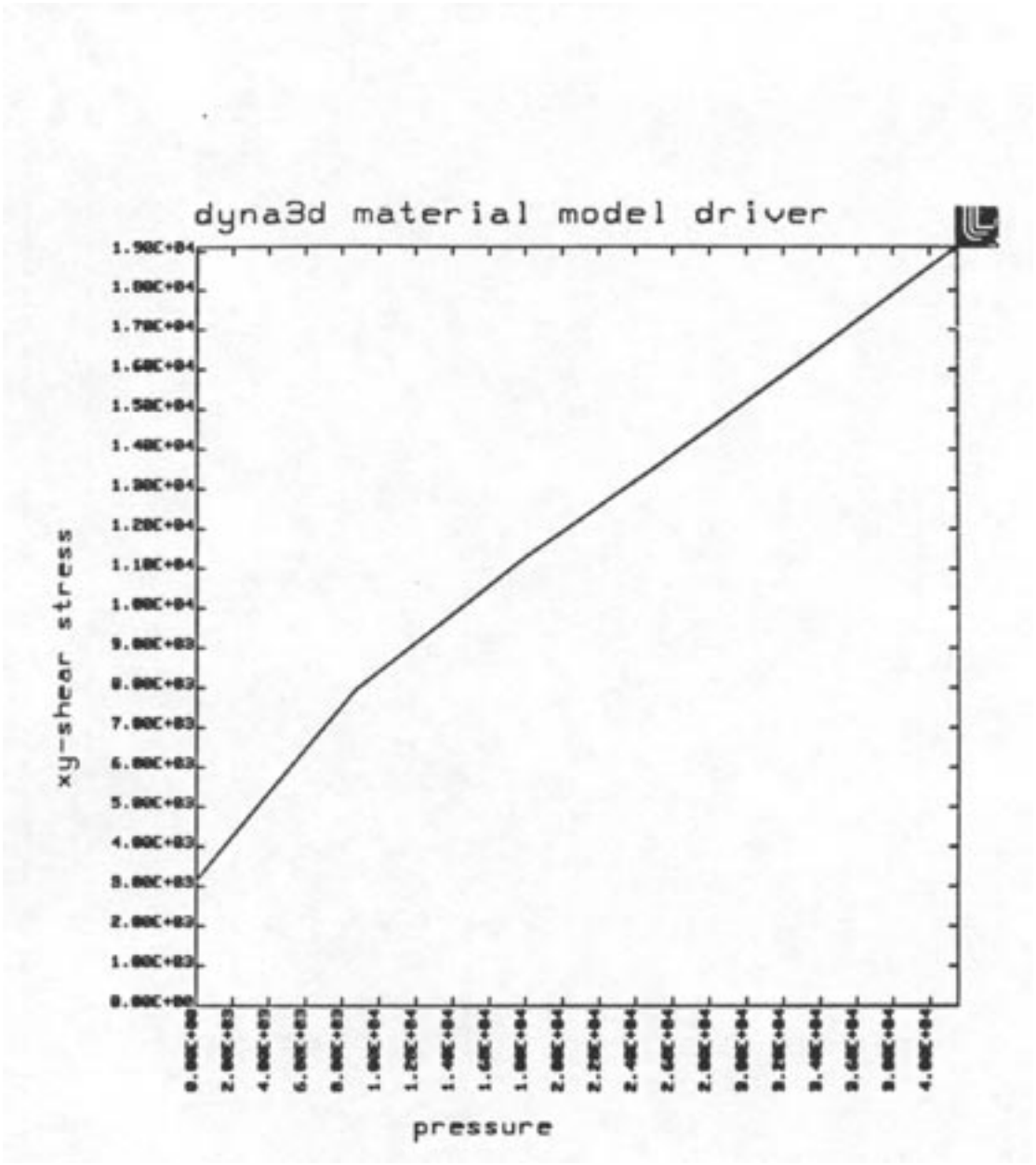

Figure 60
Soil and crushable foam model: σ_{xy} vs. p

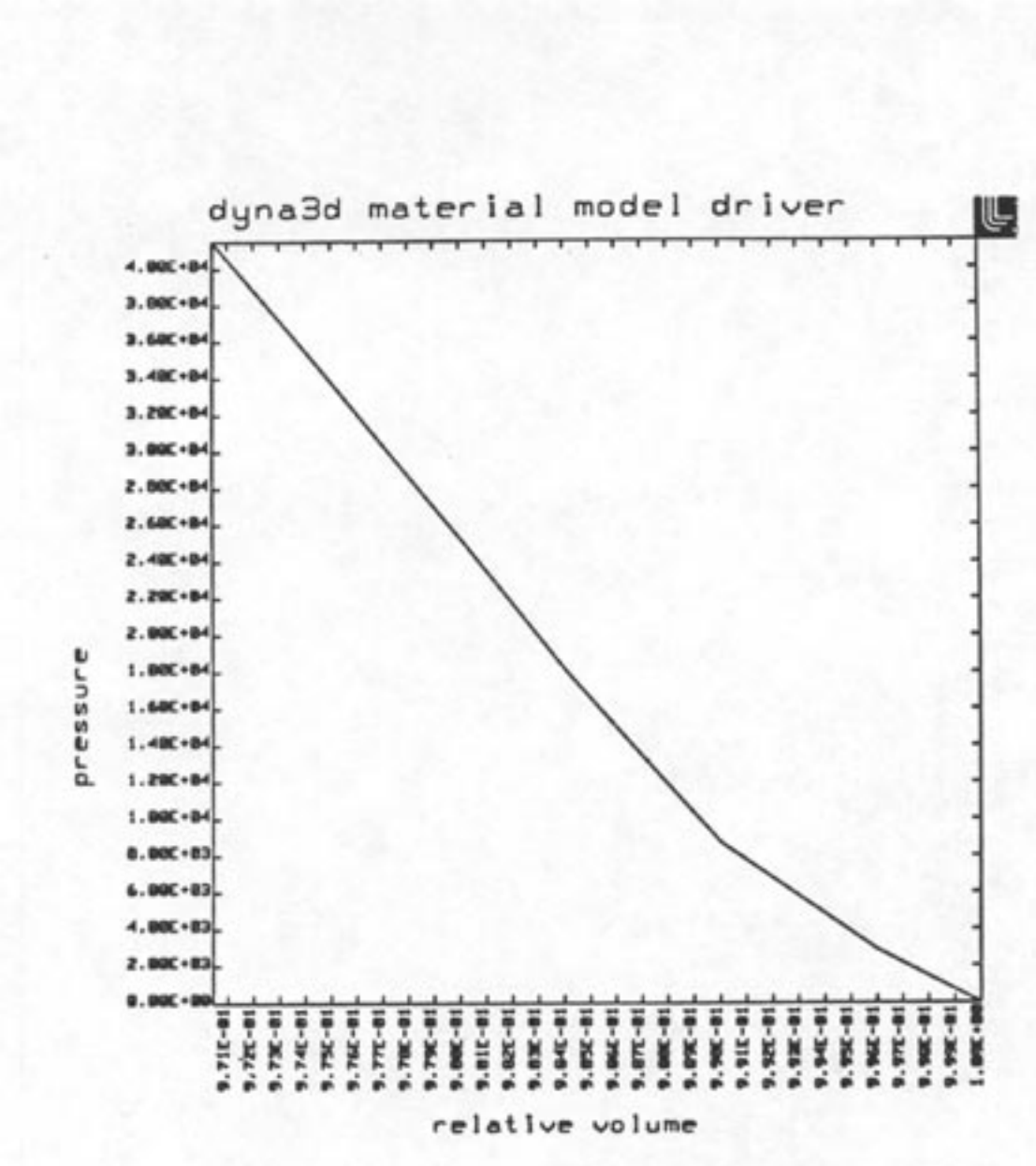

Figure 61
Soil and crushable foam model: p vs. relative volume v

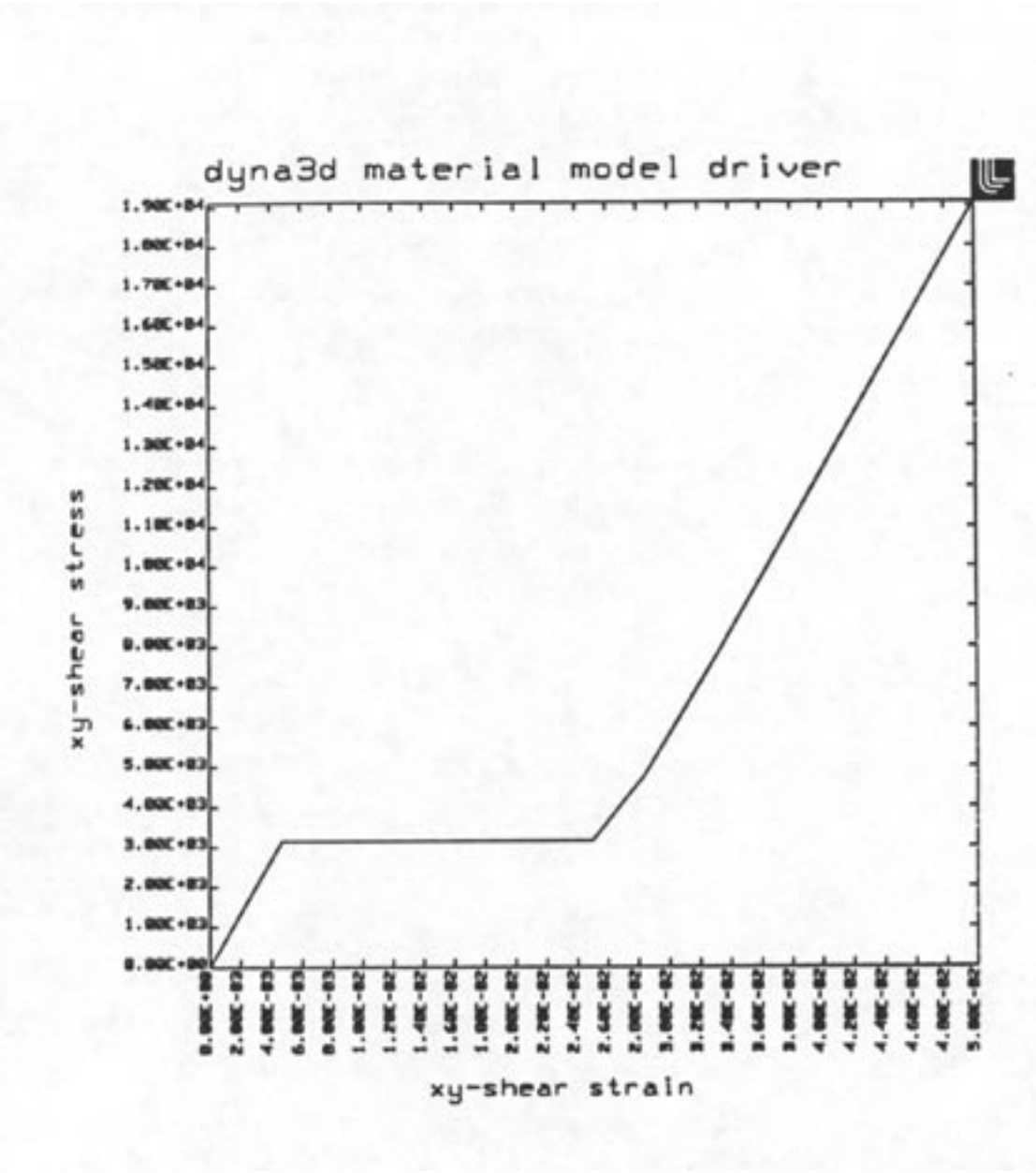

Figure 62
Soil and crushable foam model: σ_{xy} vs. γ_{xy}

ACKNOWLEDGEMENTS

The authors first wish to acknowledge the many suggestions and requests from the DYNA3D user community. Collaborative feedback from analysts and researchers, both inside LLNL and in industry, continues to be invaluable in contributing to this manual and to the continuing evolution of DYNA3D.

In particular, thanks to Mr. Mike Burger (LLNL), Mr. Doug Faux (LLNL), and Dr. Len Schwer (SE&CS) for their day-to-day feedback and suggestions for the improvement of DYNA3D. Thanks also to all of the LLNL engineering analysts, whose discussions, experiences, and frustrations have shaped the continuing development of DYNA3D.

The authors also acknowledge the following who contributed directly to the development of new features in this version of DYNA3D: Dr. Sanjay Govindjee (material type 36), Dr. Len Schwer and Ms. Yvonne Murray (material 37), Dr. Doug Bammann, Dr. Mike Chiesa and SNLL coworkers (materials 38, 39).

The following collaborators are also recognized for sharing feedback and suggestions on their applications of DYNA3D: Mr. Javaid Nazir, Mr. Carl Berner, and Mr. Stuart Kari (Boeing); Dr. Tom Moyer (NKF Engineering); Dr. Tom Vasko (UTRC) and Dr. Ken Brown (CASA); Dr. Mike Kleinburger (NHTSA); Mr. Nigel Barry and Mr. Alan Tanner (BAe); Dr. Tom Khalil (GM); Mr. Bill DePorter (FMC Corporation); Dr. Alan Pifko (Grumman); Dr. Brett Lewis (APTEK); Mr. Stan Challener and Mr. Ian Bush (Frazer-Nash).

The authors also wish to acknowledge their colleagues in the Methods Development Group at LLNL. Dr. Jerry Goudreau, Dr. Mark Christion, Dr. Brad Maker, and Mr. Don Dovey all provided ideas, technical insight, and continuous encouragement throughout our work.

Finally, the authors wish to again acknowledge Dr. John Hallquist for his initial work on the DYNA3D code and his contributions to the field of computational mechanics.

REFERENCES

1. Adley, M.D., Berger, R.P., Cargile, J.D., and White, H.G.,"Three-Dimensional Projectile Penetration Into Curvilinear Geologic/Structural Targets: User's Guide for PENCRV3D V2.0,"U.S. Army Corps of Engineers Instruction Report SL-99-1, **1999**.

2. Bammann, D. J., "Modeling Temperature and Strain Rate Dependent Large Deformation of Metals," *Applied Mechanics Reviews,* Vol. 43, pp. 312-319, **1990**.

3. Bammann, D. J., Johnson, J. C., and Chiesa, M. L., "A Strain Rate Dependent Flow Surface Model of Plasticity," Sandia National Laboratories, Report SAND90-8227, **1990**.

4. Bammann, D. J., Chiesa, M. L., McDonald, A., Kawahara, W. K., Dike, J. J., and Revelli, V. D., "Prediction of Ductile Failure in Metals," in *Failure Criteria and Analysis in Dynamic Response,* H. E. Lindberg, ed., ASME AMD Vol. 107, pp. 7-12, November, **1990**.

5. Bammann, D. J., Chiesa, M. L., Horstemeyer, M. F., and Weingarten, L, I., "Failure in Ductile Materials Using Finite Element Methods," in Structural Crashworthiness and Failure, N. Jones and T. Wierzbicki, eds, Elsevier Applied Science Publishers, **1993**.

6. Bathe, K. J., and Dvorkin, E. N., "A Continuum Mechanics Based Four-Node Shell Element for General Nonlinear Analysis," *International Journal for Computer-Aided Engineering and Software,* Vol. 1, pp. 77-88, **1984**.

7. Bazeley, G.P., W.K. Cheung, R.M. Irons, and O.C. Zienkiewicz, "Triangular Elements in Plate Bending-Conforming and Nonconforming Solutions in Matrix Methods and Structural Mechanics," *Proc. Conf. on Matrix Methods in Structural Analysis,* Rept. AFFDL-R-66-80, Wright Patterson AFB, pp. 547-576, **1965**.

8. Belytschko, T.B. and A.H. Marchertas, "Nonlinear Finite Element Method for Plates and its Application to the Dynamic Response of Reactor Fuel Subassemblies," *ASME J. Pressure Vessel Tech.*, pp. 251-257, **1974**.

9. Belytschko, T.B., L. Schwer, and M.J. Klein, "Large Displacement Transient Analysis of Space Frames," *Int. J. Num. Meth. Eng.*, 11, pp. 65-84, **1977**.

10. Belytschko, T.B. and C.S. Tsay, "Explicit Algorithms for Nonlinear Dynamics of Shells," AMD-Vol.48, ASME, pp. 209-231, **1981**.

11. Belytschko, T.B., and C. S. Tsay, "A Stabilization Procedure for the Quadrilateral Plate Element with One-Point Quadrature," *Int. J. Num. Meth. Eng.*, 19, pp. 405-419, **1983**.

12. Belytschko, T.B. and C.S. Tsay, "Explicit Algorithms for Nonlinear Dynamics of Shells," *Comp. Meth. Appl. Mech. Eng.,* 43, pp. 251-276, **1984**.

13. Belytschko, T.B., H. Stolarski, and N. Carpenter, "A C^0 Triangular Plate Element with One-Point Quadrature," *Int. J. Num. Meth. Eng.*, 20, pp. 787-802, **1984**.

14. Benson, D. J. and J.O. Hallquist, "A Simple Rigid Body Algorithm for Structural Dynamics Program," *Int. J. Num. Meth. Eng.*, 22, **1986**.

15. Benson, D.J. and J.O. Hallquist, "A Single Surface Contact Algorithm for the Postbuckling Analysis of Shell Structures,**"** *Computer Methods in Applied Mechanics and Engineering*, Vol. 78, pp. 141-163**, 1990**.

16. Benson, D. J., Hallquist, J. O., Igarashi, M., Shimomaki, K., and Mizuno, M., "The Application of DYNA3D in Large Scale Crashworthiness Calculations," Proc. of the ASME Int. Computers in Engineering Conference, Vol. 1, pp. 311-317, **1986**.

17. Burton, D.E. et al., "Physics and Numerics of the TENSOR Code," University of California, Lawrence Livermore National Laboratory, Report UCID-19428, July, **1982**.

18. Chang, F.K. and K.Y. Chang, "Post-Failure Analysis of Bolted Composite Joints in Tension or Shear-Out Mode Failure," *J. of Composite Materials*, 21, pp. 809-833, **1987a**.

19. Chang, F.K. and K.Y. Chang, "A Progressive Damage Model for Laminated Composites Containing Stress Concentration," *J. of Composite Materials*, 21, pp. 834-855, **1987b**.

20. Chen, W. F., and Baladi, G. Y., *Soil Plasticity: Theory and Implementation*, Elsevier, New York, **1985**.

21. Chiesa, M. and M. Callabresi, "Nonlinear Analysis of a Mitigating Steel Nose Cone," *Computers and Structures*, Vol. 13, p. 295, **1981**.

22. Cochran, S.G. and J. Chan, "Shock Initiation and Detonation Models in One and Two Dimensions," University of California, Lawrence Livermore National Laboratory, Rept. UCID-18024, **1979**.

23. Danielson, K.T., and Adley, M.D., "A Meshless Treatment of Three-Dimensional Penetrator Targets for Parallel Computation," Computational Mechanics, Vol. 25, **2000**.

24. Desai, C. S., and Siriwardane, H. J., *Constitutive Laws For Engineering Materials With Emphasis On Geologic Materials*, Prentice-Hall, Chapter 10, **1984**.

25. Dilger, W. H., Koch, R., and Kowalczyk, R., "Ductility of Plain and Confined Concrete Under Different Strain Rates," ACI Journal, January-February, **1984**.

26. Dobratz, B.M., "LLNL Explosives Handbook, Properties of Chemical Explosives and Explosive Simulants," University of California, Lawrence Livermore National Laboratory, Rept. UCRL-52997, **1981**.

27. Dovey, D. J., and Spelce, T. E., ''GRIZ: Finite Element Analysis Results Visualization for Unstructured Grids - User Manual,'' University of California, Lawrence Livermore National Laboratory, UCRL Report, October, **1993**.

28. Engelmann, B. E., and Hallquist, J. O., "NIKE2D: A Nonlinear, Implicit, Two-Dimensional Finite Element Code for Solid Mechanics - User Manual," University of California, Lawrence Livermore National Laboratory, UCID Report, **1991**.

29. Engelmann, B. E., and Whirley, R. G., "A New Explicit Shell Element Formulation for Impact Analysis," in Computational Aspects of Impact and Penetration, Elme Press, **1991**.

30. Engelmann, B. E., and Whirley, R. G., "A New Elastoplastic Shell Element Formulation for DYNA3D," Proceedings of the 1990 DYNA3D User Group Conference, Bournemouth, England, September, **1990**.

31. Engelmann, B. E., Whirley, R. G., and Goudreau, G. L., "A Simple Shell Element Formulation for Large-Scale Elastoplastic Analysis," in *Analytical and Computational Models of Shells,* ASME CED Vol. 3, December, **1989**.

32. Flanagan, D.P. and T. Belytschko, "A Uniform Strain Hexahedron and Quadrilateral and Orthogonal Hourglass Control," *Int. J. Numer. Meths. Eng.*, 17, pp. 679-706, **1981**

33. Fahrenthold, E., ''A Continuum Damage Model for Fracture of Brittle Solids Under Dynamic Loading,'' ASME Journal of Applied Mechanics, Vol. 58, pp. 904-909, December, **1991**.

34. Fung Y-C.: *Biomechanics: Mechanics Properties of Living Tissues*. Springer-Verlag, New York, 1981.

35. Ginsberg, M. and J. Johnson, "Benchmarking the Performance of Physical Impact Simulation Software on Vector and Parallel Computers," *Applications Track of Supercomputing,* IEEE monograph, Computer Society Press, March, **1989**.

36. Giroux, E.D. "HEMP User's Manual," University of California, Lawrence Livermore National Laboratory, Rept. UCRL-51079, **1971**.

37. Goudreau, G.L. and J.O. Hallquist, "Recent Developments in Large Scale Finite Element Lagrangian Hydrocode Technology," *J. Comp. Meths. Appl. Mechs. Eng.*, 30, **1982**.

38. Govindjee, S., Kay, J.G., and Simo, J.C., "Anisotropic Modeling and Numerical Simulation of Brittle Damage in Concrete," *Int. J. Num. Meth. Eng*, 38, **1995**

39. Hallquist, J.O. "A Procedure for the Solution of Finite Deformation Contact-Impact Problems by the Finite Element Method," University of California, Lawrence Livermore National Laboratory, Rept. UCRL-52066, **1976**.

40. Hallquist, J.O. "A Numerical Procedure for Three-Dimensional Impact Problems," *American Society of Civil Engineers,* Preprint 2956, **1977**.

41. Hallquist, J.O. "A Numerical Treatment of Sliding Interfaces and Impact," in: K.C. Park and D.K. Gartling (eds.), *Computational Techniques for Interface Problems,* AMD Vol. 30, ASME, New York, **1978**.

42. Hallquist, J.O. "Theoretical Manual for DYNA3D," University of California, Lawrence Livermore National Laboratory, Rept. UCID-19401, **1982**.

43. Hallquist, J.O., D.J. Benson, and G.L. Goudreau, "Implementation of a Modified Hughes-Liu Shell into a Fully Vectorized Explicit Finite Element Code," *Proceedings of the International Symposium on Finite Element Methods for Nonlinear Problems,* University of Trondheim, Trondheim, Norway, **1985**.

44. Hallquist, J.O., G.L. Goudreau, and D.J. Benson, "Sliding Interfaces with Contact-Impact in Large Scale Lagrangian Computations," *Comp. Meths. Appl. Mech. Eng.*, 51, pp. 107-137, **1985**.

45. Hallquist, J.O. and D.J. Benson, "A Comparison of an Implicit and Explicit Implementation of the Hughes-Liu Shell," *Finite Element Methods for Plate and Shell Structures,* T.J.R. Hughes and E. Hinton, Editors, pp. 394-431, Pineridge Press Int., Swanea, U.K., **1986**.

46. Hill, R., *The Mathematical Theory of Plasticity,* Clarendon Press, Oxford, **1950**.

47. Hughes, T.J.R. and W.K. Liu, "Nonlinear Finite Element Analysis of Shells: Part I. Three-Dimensional Shells," *Comp. Meths. Appl. Mechs.*, 27, 331-362, **1981a**.

48. Hughes, T.J.R. and W.K. Liu, "Nonlinear Finite Element Analysis of Shells: Part II. Two-Dimensional Shells," *Comp. Meths. Appl. Mechs.*, 27, 167-181, **1981b**.

49. Hughes, T.J.R. W.K. Liu and I. Levit, "Nonlinear Dynamics Finite Element Analysis of Shells," *Nonlinear Finite Element Analysis in Struct. Mech.*, Eds. W. Wunderlich, E. Stein, and K.J. Bathe, Springer-Verlag, Berlin, pp. 151- 168, **1981**.

50. Igarashi, M., Private Communication, Suzuki Motor Co., Ltd., Hamamatsu, Japan, May, **1985**.

51. Isenberg, J., Vaughn, D. K., and Sandler, I., "Nonlinear Soil-Structure Interaction," EPRI Report MP-945, Weidlinger Associates, December, **1978**.

52. Johnson, G.R. and W. H. Cook, "A Constitutive Model and Data for Metals Subjected to Large Strains, High Strain Rates and High Temperatures," Presented at the Seventh International Symposium on Ballistics, the Hague, The Netherlands, April, **1983**.

53. Keeler, S. P., "Understanding Sheet Metal Formability," Parts IV and VI, *Machinery Magazine*, May and July, **1968**.

54. Kenchington, G.J., "A Non-Linear Elastic material Model for DYNA3D," Proceedings of the DYNA3D Users Group Conference, September, **1988**, published by Boeing Computer Services (Europe) Limited.

55. Kennedy, J. M., Belytschko, T., and Lin, J. I., "Recent Developments in Explicit Finite Element Techniques and Their Application to Reactor Structures," *Nuclear Engineering and Design,* Vol. 97, **1986**.

56. Key, S.W. "HONDO - A Finite Element Computer Program for the Large Deformation Dynamic Response of Axisymmetric Solids," Sandia National Laboratories, Albuquerque, N.M., Rept. 74-0039, **1974**.

57. Krieg, R.D. and S.W. Key, "Implementation of a Time Dependent Plasticity Theory into Structural Computer Programs," Vol. 20 of *Constitutive Equations in Viscoplasticity: Computational and Engineering Aspects*, American Society of Mechanical Engineers, New York, N.Y., pp. 125-137, **1976**.

58. Lee, E.L. and C.M. Tarver, "Phenomenological Model of Shock Initiation in Heterogenous Explosives,: PHYS. Fluids, Vol. 23, p. 2362, **1980**.

59. Logan, R. W., "Incorporating Non-quadratic and Crystallographic Yield Surfaces into Finite Element Codes," University of California, Los Alamos National Laboratory, Report LA-CP-88-186, **1988**.

60. Logan, R. W., “Implementation of a Pressure and Rate Dependent Forming Limit Diagram Model into NIKE and DYNA,” University of California, Lawrence Livermore National Laboratory, Report UCRL-ID-105760, **1991**.

61. Lovejoy, S. C., and Whirley, R. G., “DYNA3D Example Problem Manual,” University of California, Lawrence Livermore National Laboratory, Report UCRL-MA-105259, October, **1990**.

62. Maker, B. N., Ferencz, R. M., and Hallquist, J. O., “NIKE3D: A Nonlinear, Implicit, Three-Dimensional Finite Element Code for Solid and Structural Mechanics - User’s Manual, University of California, Lawrence Livermore National Laboratory, Report UCRL-MA-105268, January, **1991**.

63. Malvar, L.J., Crawford, J.E., Wesevich, J.W., and Simon, D., “A New Concrete Material Model for DYNA3D,” Defense Nuclear Agency Contract Report DNA001-91-C-0059, **1996**.

64. Maudlin, P.J., Davidson, R.F., and Henninger, R.J., “Implementation and Assessment of the Mechanical-Threshold-Stress Model Using the EPIC2 and pINON Computer Codes,” University of California, Los Alamos National Laboratory, Report LA-11895-MS, **1990**.

65. Moor, E., University of California, Lawrence Livermore National Laboratory, Private Communication, April, **1991**.

66. Obergefell, L. A., Gardner, T. R., Kaleps, I., and Fleck, J. T., ‘‘Articulated Total Body Model Enhancements - Volume 2: User’s Guide,’’ Harry G. Armstrong Aerospace Medical Research Laboratory, Wright-Patterson Air Force Base, Ohio, Report AAMRL-TR-88-043, **1988**.

67. Oliver, J., “A Consistent Characteristic Length of Smeared Cracking Models,” *Int. J. Num. Meth. Eng*., 28, pp. 461-474, **1989**.

68. Pelesson, D., Private communication, GA Technologies, P. O. Box 85608, San Diego, CA., **1989**.

69. Puso MA and Weiss JA: “Finite element implementation of anisotropic quasilinear viscoelasticity.” *ASME J. Biomech Engng*, January, **1997**.

70. Reedy, E.D., Mello, F.J., and Guess, R.R., “Modeling the Initiation and Growth of Delaminations in Composite Structures,” *J. of Comp. Mats*., **31,** 812-831, **1997**.

71. Reedy, E.D., and Mello, F.J., “Modeling Delamination Growth in Composites”, Proc. of Symp. on Durability and Damage Tolerance of Composites, ASME 1996 International Mechanical Engineering Congress and Exposition, Atlanta, Georgia, **1997**.

72. Sackett, S.J., “Geological/Concrete Model Development,” Private Communication, **1987**.

73. Sandler, I.S. and D. Rubin, “An Algorithm and a modular subroutine for the cap model,” *Int. J. Numer. Analy. Meth. Geomech.*, 3, pp. 173-186, **1979**.

74. Schwer, L. E., **“**Viscoplastic Augumentation of the Smooth Cap Model,” *Nuclear Engineering and Design*, 150, pp. 215-233, **1994**.

75. Schwer, L. E., and Murray, Y., **"**A Three-Invariant Smooth Cap Model with Mixed Hardening,'' *International Journal for Numerical and Analytical Methods in Geomechanics*, 18, pp. 657-688, **1994**.

76. Shapiro, A. B., "TOPAZ3D - A Three Dimensional Finite Element Heat Transfer Code," University of California, Lawrence Livermore National Laboratory, Report UCID-20484, **1985**.

77. Shapiro, A. B., and Edwards, A. L., "TOPAZ2D Heat Transfer Code Users Manual and Thermal Property Data Base," University of California, Lawrence Livermore National Laboratory, Report UCRL-ID-104558, May, **1990**.

78. Simo, J. C., J.W. Ju, K.S. Pister and R.L. Taylor, "An assessment of the cap model: Consistent return algorithms and rate-dependent extension,: *J. Eng. Mech.*, Vol. 114, No. 2, pp. 191-218, **1988**.

79. Simo, J. C., J.W. Ju, K.S. Pister and R.L. Taylor, "Softening Response, Completeness Condition, and Numerical Algorithms for the Cap Model," *Int. J. Numer. Analy. Meth. Eng.*, **1990**.

80. Simo, J.C., and Wong, K. K., "Unconditionally Stable Algorithms for rigid Body Dynamics That Exactly Preserve Energy and Momentum," *Int. J. Num. Meth. Eng.*, **31**, pp. 19-52, **1991**

81. Speicher, S. J., and Brode, H. L., Pacific-Sierra Research Corporation, Report PSR-1630, April, **1987**.

82. Steinberg, D.J. and M.W. Guinan, "A High-Strain-Rate Constitutive Model for Metals," University of California, Lawrence Livermore National Laboratory, Rept. UCRL-80465, **1978**.

83. Spelce, T., and Hallquist, J. O., "TAURUS: An Interactive Post-Processor for the Analysis Codes NIKE3D, DYNA3D, TOPAZ3D, and GEMINI, University of California, Lawrence Livermore National Laboratory, Report UCRL-MA-105401, May, **1991**.

84. Stillman, D. W. and J. O. Hallquist, "INGRID: A Three-Dimensional Mesh Generator for Modeling Nonlinear Systems," University of California, Lawerence Livermore National Laboraotry, Rept. UCID-20506, **1985**.

85. TNO Road-Vehicles Research Institute, ''MADYMO User's Manual 3D, Version 5.0,'' July, **1992**.

86. Weiss JA, Maker BN, Govindjee S: "Finite element implementation of incompressible, transversely isotropic hyperelasticity." *Computer Methods in Applied Mechanics and Engineering* 135:102-128, **199**6.

87. Whirley, R. G., J.O. Hallquist and G.L. Goudreau, "An Assessment of Numerical Algorithms for Plane Stress and Shell Elastoplacity on Supercomputers," Engineering Computations, Vol. 6, No. 2, June, **1989**.

88. Whirley, R. G., "Elastoplastic Shell Analysis in DYNA3D," *Engineering Research and Development Report FY89,* University of California, Lawrence Livermore National Laboratory, Report UCRL-53868-89, June, **1990**.

89. Whirley, R. G., and Engelmann, B. E., “An Implementation of Hill’s Theory of Normal Anisotropic Plasticity for Explicit Shell Analysis”, University of California, Lawrence Livermore National Laboratory, UCID Report, **1991**.

90. Whirley, R. G., and Engelmann, B. E., “Large-Scale Nonlinear Finite Element Analysis - Explicit Aspects”, *Control and System Dynamics*, C. T. Leondes, ed., **1991a**

91. Whirley, R. G., and Engelmann, B. E., ‘‘Recent Developments in DYNA3D for Impact Problems,’’ *Nuclear Engineering and Design*, Vol. 138, pp. 11-22, **1992**.

92. Whirley, R. G., and Engelmann, B. E., ‘‘Automatic Contact in DYNA3D for Vehicle Crashworthiness Analysis,’’ *Proceedings of the ASME Winter Annual Meeting, Symposium on Crashworthiness and Occupant Protection*, **1993**.

93. Whirley, R. G., and Engelmann, B. E., ‘‘An Automatic Contact Algorithm in DYNA3D for Impact Analysis,’’ *Nuclear Engineering and Design*, accepted for publication. **1993a**.

94. Wilkins, M.L., R.E. Blum, E. Cronshagen, and P. Grantham, "A Method for Computer Simulation of Problems in Solid Mechanics and Gas Dynamics in Three Dimensions and Time," University of California, Lawrence Livermore National Laboratory, Rept. UCRL-51574, **1974**.

95. Woodruff, J.P., "KOVEC User's Manual," University of California, Lawrence Livermore National Laboratory, Rept. UCRL-51079, **1973**.

96. Zemansky, M.W., Heat and Thermodynamics -An Intermediate Textbook, 5-th Edition, McGraw Hill, New York, **1951**.

97. Zywicz, E., and Puso, M.A., “A General Predictor-Corrector Solver for Explicit Finite-Element Contact,” *Int. J. Num. Meth. Eng.*, **44**, 439-459, **1999**.

98. Zywicz, E., “DYNA3D Material Model 50: A Progressive Composite Damage Model,” University of California, Lawrence Livermore National Laboratory, Rept. UCRL-ID-128518, **1997**.